MARCH 1988

LIDS-TH-1757

Research Supported By:

NASA Ames and Langley Research Centers Grant NASA/NAG-2-297

General Electric Corporate Research and Development Center

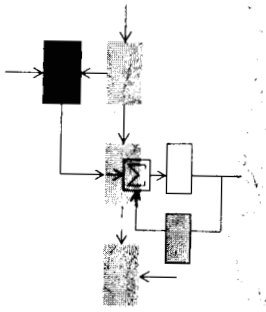

DESIGN FOR PERFORMANCE ENHANCEMENT IN FEEDBACK CONTROL SYSTEMS WITH MULTIPLE SATURATING NONLINEARITIES

Petros Kapasouris

Laboratory for Information and Decision Systems

MASSACHUSETTS INSTITUTE OF TECHNOLOGY, CAMBRIDGE, MASSACHUSETTS 02139

MARCH 1988 LIDS-TH-1757

DESIGN FOR PERFORMANCE ENHANCEMENT IN FEEDBACK CONTROL SYSTEMS WITH MULTIPLE SATURATING NONLINEARITIES

By

PETROS KAPASOURIS

This report is based on the unaltered thesis of Petros Kapasouris submitted in partial fulfillment of the requirements for the Degree of Doctor of Philosophy at the Massachusetts Institute of Technology in February 1988. The research was conducted at the M.I.T. Laboratory for Information and Decision Systems with support provided by NASA Ames and Langley Research Centers under grant NASA/NAG-2-297, and by the General Electric Corporate Research and Development Center.

Laboratory for Information and Decision Systems
Massachusetts Institute of Technology
Cambridge, MA. 02139

DESIGN FOR PERFORMANCE ENHANCEMENT IN FEEDBACK CONTROL SYSTEMS WITH MULTIPLE SATURATING NONLINEARITIES

by
Petros Kapasouris

B.S., Electrical Engineering, University of Connecticut
(1982)
S.M., Electrical Engineering, Massachusetts Institute of Technology
(1984)

Submitted to the Department of
ELECTRICAL ENGINEERING AND COMPUTER SCIENCE
in partial fulfillment of the requirements for the degree of

DOCTOR OF PHILOSOPHY

at the
MASSACHUSETTS INSTITUTE OF TECHNOLOGY
February 1988

Signature of Author: .....
Department of Electrical Engineering and Computer Science
February, 1988

Certified by: .....
Michael Athans
Thesis Supervisor

Accepted by: .....
Arthur C. Smith, Chairman
Committee on Graduate Students

Design for Performance Enhancement in Feedback Control Systems with Multiple Saturating Nonlinearities

by
Petros Kapasouris

Submitted to the Department of Electrical Engineering and Computer Science on February 1, 1987 in partial fulfillment of the requirements for the degree of Doctor of Philosophy.

ABSTRACT

In this thesis a systematic control design methodology is introduced for multi-input/multi-output systems with multiple saturations. The methodology can be applied to stable and unstable open loop plants with magnitude and/or rate control saturations and to systems in which state limitations are desired. This new methodology is a substantial improvement over previous heuristic single-input/single-output approaches.

The idea is to introduce a supervisor loop so that when the references and/or disturbances are sufficiently small, the control system operates linearly as designed. For signals large enough to cause saturations, the control law is modified in such a way to ensure stability and to preserve, to the extent possible, the behavior of the linear control design.

Key benefits of this methodology are: the modified compensator never produces saturating control signals, integrators and/or slow dynamics in the compensator never windup, the directional properties of the controls are maintained, and the closed loop system has certain guaranteed stability properties.

The advantages of the new design methodology are illustrated by numerous simulations, including the multivariable longitudinal control of modified models of the F-8 (stable) and F-16 (unstable) aircraft.

Furthermore new stability results and new performance criteria are introduced which characterize how saturations can affect negatively the performance of the feedback system.

Thesis Supervisor: Dr. Michael Athans
Title: Professor of Systems Science and Engineering.

ACKNOWLEDGEMENTS

First, I would like to thank my thesis supervisor, Professor Michael Athans. Without his guidance and support the results of this research would not be possible. I feel very fortunate not only to have had the opportunity to learn from him, as a student, but also to have associated with him as a person. I strongly believe that he is one of the best supervisors one could possibly have.

Next, I am grateful to my thesis readers, Professors Gunter Stein, Lena Valavani, John Tsitsiklis and H. Austin Spang III. Their experience and helpful comments proved to be of extreme importance for this research.

In addition, I would like to thank my colleagues at M.I.T. for their friendship and for the countless constructive(and destructive) arguments. The experience and knowledge that I gain from the association with them is priceless. I am grateful to Alex Gioulekas, Dan Grunberg, Ioannis Kyratzoglou, Richard Lamaire, David Milich, Jason Papastavrou, Brett Ridgely, Tony Rodriguez, Jeff Shamma, Petros Voulgaris and Jim Walton. I appreciate the help of Fifa Monserrate and Lisa Babine, their cheerful attitude made M.I.T. a better place. Also, I would like to thank Jane Maloof for always being considerate and helpful.

Finally, I would like to thank my family for their encouragement and the strong support they gave me over my endless academic years.

This research was conducted at the M.I.T. Laboratory for Information and Decision Systems with support provided by the General Electric Corporate Research and Development Center, and by the NASA Ames and Langley Research Centers under grant NASA/NAG 2-297.

TABLE OF CONTENTS

CHAPTER 3. MATHEMATICAL PRELIMINARIES

CHAPTER 4 CONTROL STRUCTURE WITH THE OPERATOR EG

CHAPTER 5 CONTROL STRUCTURE WITH THE OPERATOR RG

CHAPTER 6 COMPARISONS

CHAPTER 7 RATE SATURATION, RATE/MAGNITUDE AND STATE LIMITERS

LIST OF FIGURES

CHAPTER 2. ANALYSIS

CHAPTER 3. MATHEMATICAL PRELIMINARIES

CHAPTER 4. CONTROL SYSTEM FOR STABLE PLANTS

CHAPTER 5. CONTROL SYSTEM FOR UNSTABLE PLANTS

CHAPTER 6. COMPARISONS

CHAPTER 7. RATE SATURATION, RATE/MAGNITUDE AND STATE LIMITERS

LIST OF TABLES

CHAPTER 1
INTRODUCTION

1.1 Overview

1.1.1 Problem Definition

Almost every physical system has maximum and minimum limits or saturations on its control signals. These limits may be on the magnitude and/or the rate of the controls. In addition, certain states of the plant should not exceed predefined limits for safety considerations.

A common standard in designing a control system is to linearize the plant, ignore the bounds on the controls and/or the specified limits on the states, and then design the controller for the resulting linear time-invariant plant. At the end, engineering intuition and extensive simulations are used, and the linear controller is adjusted and modified to cope with stability and performance problems due to saturations. In this research, the linear design methodology is retained, but the control saturations and any desired limits on the states are explicitly included in the design process.

When a control system is designed for a linear plant and then control saturations are introduced, the closed loop system loses some of the key properties that the linear closed loop system had. The two most serious problems that occur with the introduction of multiple saturations to the otherwise linear closed loop system are those of *stability* and *performance degradation.*

Often closed loop *stability* is not preserved in the presence of one or more saturations. For example, it is well known that global closed loop stability cannot be achieved for unstable

plants with saturating actuators. The introduction of saturation nonlinearities in the closed loop system causes the reference and disturbance inputs to impact the global stability of the system. In the linear case, stability is independent of the size of exogenous inputs. In a system with saturations, large reference and/or disturbance signals can cause instabilities. Thus, given a plant and a compensator, the designer should be concerned with the size and directions of disturbances and references so that the closed loop system will remain stable in the presence of these exogenous signals.

For multivariable systems, a different major problem that arises (because of saturations) is the fact that control saturations alter the direction of the control vector. For example, let us assume that there are m control signals with m saturation elements. Each saturation element operates on its input signal independently of the other saturation elements; as we shall show in the analysis chapter, this can disturb the direction of the applied control vector. Consequently, erroneous controls can occur, causing degradation with the performance of the closed loop system over and above the expected fact that output transients will be "slower".

Another performance degradation occurs when a linear compensator with integrators is used in a closed loop system and the phenomenon of reset-windup appears. During the time of saturation of the actuators, the error is continuously integrated even though the controls are not what they should be. The integrator, and other slow compensator states, attain values that lead to larger controls than the saturation limits. This leads to the phenomenon known as reset-windup, resulting in serious deterioration of the performance (large overshoots and large settling times.) Many attempts have been made to address this problem for SISO systems, but a general design process has not been formalized. No research has been found in the literature that addresses and solves the reset-windup problem for MIMO systems. In practice, the saturations are ignored in the first stage of the control design process, and then the final controller is designed using ad-hoc modifications and extensive simulations.

A common classical remedy was to reduce the bandwidth of the control system so that

control saturation seldom occurred. Thus, even for small commands and disturbances, one intentionally degraded the possible performance of the system (longer settling times etc.). Although reduction in closed-loop bandwidth by reduction in the loop gain is an "easy" design tool, it clearly is not necessarily the best that could be done. Hence, a new design methodology is desirable which will generate transients consistent with the actuation levels available, but which maintains the rapid speed of response for small exogenous signals (reference commands and disturbances).

The main question is then: what effects do saturating actuators introduce to the closed loop system, and how can one design controllers such that the problems that they introduce are solved to the extent possible.

1.1.2 Contributions of Thesis

As explained in the previous section, input saturations are common to most physical systems and their effects are not small enough to neglect. This research brings new advances in the theory concerning the analysis and a new methodology for the design of control systems with multiple saturations.

In the *analysis* part, with a **new stability result** one can specify the sizes of the exogenous disturbances and/or references so that in the presence of those exogenous signals the closed loop system remains stable. All the current stability results give bounds on the control signals to maintain stability. The designer, does not have any direct access to the control signals but has knowledge of the disturbances and can define entirely the reference signals. This is why our stability result is relevant in design.

In the analysis part it is also shown how saturations can degrade the performance of the system. As was discussed in the previous section, in addition to integrator windups in MIMO

systems, the direction of the control signals is very important. Saturations can alter the direction of the control signals and thus effect the performance negatively. In the analysis part the performance of the nonlinear system is examined and new performance criteria are introduced.

In the *design* part, a **systematic methodology is introduced** to design control systems with multiple saturations. The idea is to design a linear control system ignoring the saturations and when necessary to modify that linear control law. When the exogenous signals are small, and they do not cause saturations, the system operates linearly as designed. When the signals are large enough to cause saturations, the control law is then modified in such a way to preserve ("mimic") to the extent possible the responses of the linear design. Our modification to the linear compensator is introduced at the error (Error Governor) and/or the reference signals (Reference Governor).

The methodology can be applied to stable and unstable open loop plants with magnitude and/or rate control saturations and to systems in which state limitations are desired. The main benefits of the methodology are that it leads to controllers with the following properties:

(a) The signals that the modified compensator produces **never cause saturation**. The nonlinear response mimics the shape of the linear one with the difference that its speed of response may be, as expected, slower. Thus the output of the compensator (the controls) are not altered by the saturations.

(b) Possible integrators or slow dynamics in the compensator **never windup**. That is true because the signals produced by the modified compensator never exceed the limits of the saturations.

(c) For closed loop systems with stable plants **finite gain stability** is guaranteed for any reference and/or disturbance. For closed loop systems with unstable plants **BIBO stability** is guaranteed for any reference. A set of disturbances is given such that any disturbance from that set will not violate the BIBO stability of the closed loop system.

(d) The **on-line computation** required to implement the control system **is minimal** and realizable in most of today's microprocessors.

The main disadvantage of our new design methodology is due to its severe off-line computational requirements. Effectively, one must conduct and store a high-dimensional surface whose dimension is that of either the dynamic compensator for stable plants or of the compensator and the plant for unstable plants. The algorithms are straight-forward, but they can demand a significant amount of CPU time (off-line) for high-dimensional applications.

Another shortcoming for unstable plants is that the state variables of the plant are needed in real time for the implementation of the logic.

1.2 Previous Research and Related Literature

1.2.1 Analysis of Control Systems with Multiple Saturations

In recent years complete linear multivariable analysis and design methodologies for feedback control has been developed. Such methodologies are the LQR, LQG, LQG/LTR, H_2 [1]-[5] and the H_∞ [6]. These methodologies, especially the LQG/LTR, have been applied to many specific examples in process control, aerospace systems and elsewhere. The designs were successful as far as the performance of the linear closed loop system was concerned [7]-[10]. However, major problem that one can observe in many of those linear designs is the size of the controls and the potential saturation problem. From the research indicated above, one can conclude that having saturations in the linear control system can be a problem of great importance to control engineers.

As far as the theory is concerned, a great amount of work has been done on the stability

of SISO systems with sector nonlinearities. If the saturation is considered as a sector nonlinearity, there are stability criteria as the Popov and Circle criteria [11]-[14] that can be exploited. An extension for MIMO systems is the Multiloop circle criterion [15]. Of course, Lyapunov stability theory is always applicable [16] and [17]. The problem with most of these stability criteria is that they give bounds on specific signals in the control system, but it is not known what kind of commands or disturbances will cause those signals to exceed the bounds. Hence, they cannot be used directly to influence the design methodology.

1.2.2 Design of Control Systems with Multiple Saturations

One way to design controllers for systems with bounded controls, would be to solve an optimal control problem; for example, the time optimal control problem or the minimum energy problem etc. The solution to such problems usually leads to a bang-bang feedback controller [18]. Even though the problem has been solved completely in principle, the solution to even the simplest systems requires good modelling, is difficult to calculate open loop solutions, or the resulting switching surfaces are complicated to work with. For these reasons, in most applications the optimal control solution is not used.

Because of the problems with optimal control results, other design techniques have been attempted. Most of them are based on solving the Lyapunov equation and getting a feedback which will guarantee global stability when possible or local stability otherwise [19]-[22]. The problem with these techniques is that the solutions tend to be unnecessarily conservative and consequently the performance of the closed loop system may suffer. For example, when global stability is guaranteed, it is often required that the final open loop system is strictly positive-real with all the limitations that such systems possess.

Attempts to solve the reset windup problems when integrators are present in the forward loop, have been made for SISO systems [23]-[28]. Most of these attempts lead to controllers

with substantially improved performance but not well understood stability properties. As part of this research, an initial investigation was made on the effects on performance of the reset windups for MIMO systems [29] showing potential for improving the performance of the system. A simple case study was also recently conducted on the effects of saturations to MIMO systems where potential for improvement in the performance was demonstrated [30].

There also exists a theory for general nonlinear control systems [31]-[34] which either does not include hard nonlinearities such as saturations or the theory is general and, perhaps, too conservative to use in practice.

One can see that many engineers have tried to solve the problems that saturation introduces in many different ways, and that there are many bits and pieces of results that can be very useful. The bottom line is that *there does not exist a systematic methodology for designing MIMO control systems* for systems with multiple saturations and engineers still use ad-hoc methods to resolve the problems that saturations introduce.

1.3 Organization of Thesis

In addition to the introductory chapter this thesis is organized in 7 chapters (chapter 2 to chapter 8). Chapter 2 contains the analysis of systems with saturations, which includes stability and performance analysis. Chapter 3 is the introduction to the design methodology with mathematical preliminaries and all the tools that are needed for the design methodology. Chapter 4 introduces the design methodology for control systems with stable plants including the control structure, the properties of the control system and some numerical examples. Chapter 5 introduces the control design for systems with unstable plants, including the control structure, the properties of the new control system and a numerical example. In Chapter 6 the new design methodology is compared with some ad-hoc extensions of SISO antiwindup techniques to MIMO systems. Chapter 7 discusses the case where rate and/or magnitude

saturation are present and the case where state limitations are introduced. Finally, chapter 8 contains concluding remarks and directions for future research in this area.

CHAPTER 2
ANALYSIS

2.1 Introduction

This chapter contains the analysis of control systems with multiple magnitude saturations at the control signals. It involves the analysis of the stability and performance of such systems.

In the stability part, one of the existing methods, the multiloop circle criterion, will be described and its usefulness and its limitations will be analyzed. Then a new stability result will be developed that yields bounds on the exogenous signals, i.e. references and disturbances, such that the closed loop system remains BIBO stable when signals within those bounds are applied.

In the performance part, an analysis will be given on why and how the multiple saturations affect the direction of the control vector and consequently, the performance of the control system. Then performance objectives will be defined for the nonlinear system. The goal is to "mimic", to the extent possible, the responses of the control system without the saturations (linear system) even when the saturations are present.

Without loss of generality one can assume that each element $u_i(t)$ of the control vector $\mathbf{u}(t) = [\, u_1(t) \ldots u_p(t)]^T$ has saturation limits ± 1 and the saturation operator can be defined as follows:

$$\text{sat}(u_i(t)) = \begin{cases} 1 & u_i(t) \geq 1 \\ u_i(t) & -1 \leq u_i(t) \leq 1 \\ -1 & u_i(t) \leq -1 \end{cases} \tag{2.1}$$

Figure 2.1 shows the closed loop system with the saturation element at the controls. The compensator **K**(s) is designed using linear control system techniques and it is assumed that the closed loop system without the saturations (the linear system) is stable with "good" properties.

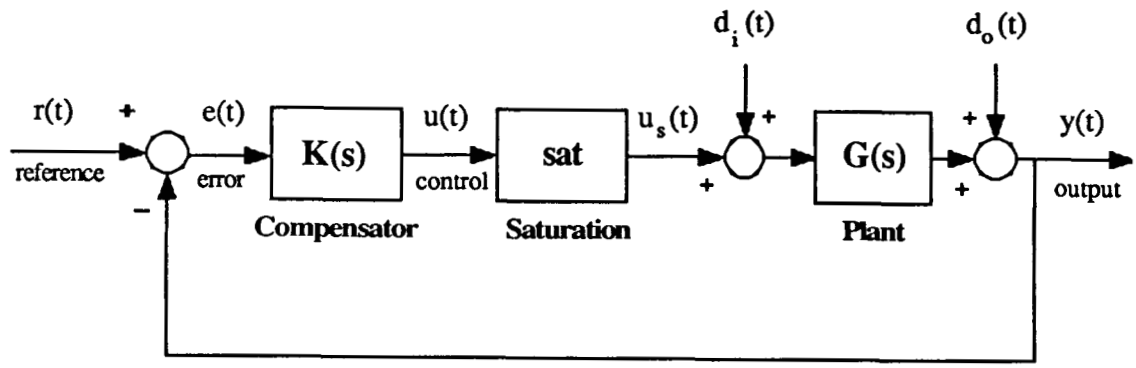

Figure 2.1: The closed loop system

The analysis results will be introduced for square systems, i.e. $\mathbf{v}(t), \mathbf{u}(t), \mathbf{y}(t) \in \mathbf{R}^m$. Similar results can be proven for nonsquare systems by following the same techniques as the ones that will be described in this chapter.

2.2 Stability

2.2.1 Saturation as Sector Nonlinearity

Since the system of concern (shown in figure 2.1) has a linear part (**G**(s)**K**(s)) and a nonlinear part (saturations) one can take advantage of the special structure and use available

stability criteria such as the circle and multiloop criteria. The circle criterion can be used for SISO systems if the saturation is to be taken as a sector nonlinearity. Similarly, the multiloop criteria can be used for multiple saturations.

A continuous function $f: \mathbb{R} \rightarrow \mathbb{R}$ with $f(0) = 0$ is said to belong to the sector $[a,b]$, $a < b$ if

$$a \leq \frac{f(x)}{x} \leq b \qquad \forall\, x \neq 0 \tag{2.2}$$

Consider the saturation in one of the channels of the controls $u_i(t)$. The sector that contains the saturation is defined by the slopes [1,0]. Many times it is difficult or impossible to prove global stability by using the whole sector. In such a case, local stability can be proven if the sector nonlinearity belongs in a smaller sector [1,a] where $a > 0$.

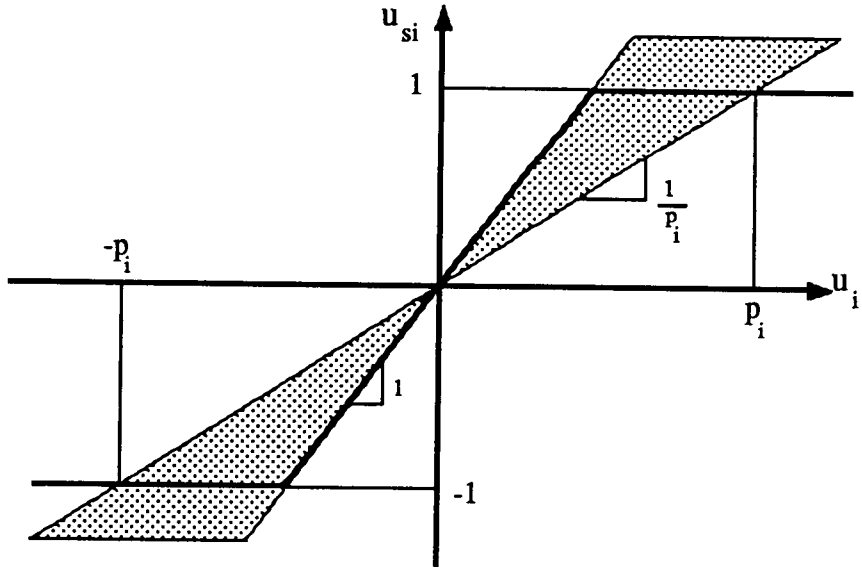

Figure 2.2: Saturation element as a sector nonlinearity in a $(1,1/p_i)$ sector.

If one assumes that the controls to the plant are always less than p_i ($|u_i(t)| \leq p_i$), then one can say that the saturation belongs in a sector $[1,1/p_i]$. Figure 2.2 shows part of the saturation inside the sector $[1,1/p_i]$. The problem then becomes how to find what kind of references and disturbances will force the controls to remain bounded ($|u_i(t)| \leq p_i$).

2.2.2 Existing Stability Theory

There exists an extensive theory on the stability of nonlinear systems, e.g. the Lyapunov stability theory [16],[17]. Most of the theory can be applied to general nonlinear systems and it is too conservative for the saturation case. For sector nonlinearities some more specific stability criteria as the Popov, the circle and the multiloop circle criteria are applicable. Here only the multiloop criterion will be stated, the proof is given in [15]. The Popov and circle criteria give results similar in nature to those obtained via the multiloop circle criterion.

In the multiloop circle criterion each sector for each of the saturations is defined by a center and a radius. More specifically, assume that the closed loop system is defined by a linear system $\mathbf{T}(s)$ (i.e. $\mathbf{K}(s)\mathbf{G}(s)$) connected with a nonlinearity $f(\bullet)$ as shown in figure 2.3. For this research the nonlinearity $f(\bullet)$ will be a diagonal matrix with saturations $f_i(u_i(t))$ corresponding to each control $u_i(t)$. Each saturation belongs to a sector as in figure 2.2 with the following center C_i and radius R_i.

$$C_i + R_i = 1 + \frac{\varepsilon}{2} \tag{2.3}$$

$$C_i - R_i = \frac{1}{p_i} - \frac{\varepsilon}{2} \qquad (2.4)$$

where $\varepsilon > 0$, and ε can be arbitrarily small.

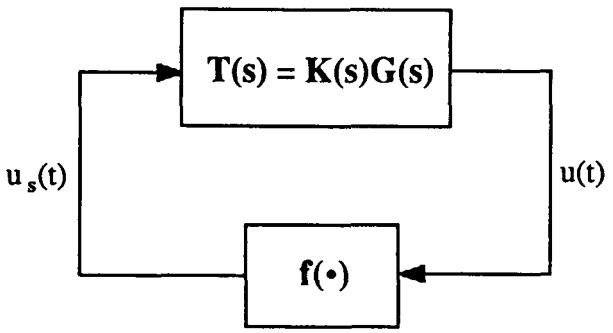

Figure 2.3: Closed loop system for stability analysis.

The multiloop circle criterion states that the closed loop system is extended L_2 stable if :

1. The closed loop system is stable if the nonlinearities are replaced by their centers C_i
2. The following is true for all frequencies.

$$\bar{\sigma}_{max} [\mathbf{R}\, \mathbf{T}(j\omega)\, [\mathbf{I} + \mathbf{C}\, \mathbf{T}(j\omega)]^{-1}] \leq 1 \qquad \forall\, \omega \qquad (2.5)$$

where **C** and **R** are matrices with diagonal elements C_i and R_i respectively.

If $C_i = 1$ and $R_i = 0$ then condition 2 of the multiloop circle criterion is the same as condition 1 which corresponds to having a linear gain of I rather than a sector nonlinearity. The sector with $C_i = 1/2$ and $R_i = 1/2$ will include the whole saturation element and if the conditions of the criterion are met then the closed loop system will be extended L_2 stable. If global

stability cannot be proven then a smaller sector has to be chosen (i.e. $[1,1/p_i]$ where $p_i < \infty$) and p_i has to be small enough (it is known that one exists, $p_i = 1$) so that the conditions of the criterion are met. Thus, the multiloop circle criterion can be used to define p_i for L_2 stability. Effectively by defining the p_i, the bounds in the controls for each channel are defined.

Even though control bounds p_i can be defined by using the multiloop circle criterion, one does not know what kind of exogenous signals (references and disturbances) will violate these control bounds. As was previously stated, the objective is to define exogenous signals to insure that the bounds in the controls are not violated.

2.2.3 New Stability Results

The objective here is to find the relationship between bounds in the references and disturbances and bounds in the controls. Assume that the relationship of the controls and the saturated controls is given by the following

$$\mathbf{u_s}(t) = \begin{bmatrix} u_{s1}(t) \\ \cdots \\ u_{sm}(t) \end{bmatrix} = \text{sat}(\mathbf{u}(t)) = \mathbf{f}(\mathbf{u}(t)) = \begin{bmatrix} f_1(u_1(t)) \\ \cdots\cdots \\ f_m(u_m(t)) \end{bmatrix} \tag{2.6}$$

For analysis purposes, once all the p_i's are fixed, one can replace each saturation element $f_i(u_i(t))$ by a linear gain $C_i(p_i)$ and an additive signal $u'_i(t)$. Then, each saturated control is given by

$$u_{si}(t) = C_i(p_i)u_i(t) + u'_i(t) \tag{2.7}$$

Define the matrix $\mathbf{C(p)}$ and the vector $\mathbf{u'}(t)$ as follows:

$$\mathbf{C(p)} = \begin{bmatrix} C_1(p_1) & 0 \\ 0 & C_m(p_m) \end{bmatrix} \qquad \mathbf{u'}(t) = \begin{bmatrix} u'_1(t) \\ \cdot \cdot \cdot \\ u'_m(t) \end{bmatrix} \tag{2.8}$$

Then, in compact form

$$\mathbf{u_s}(t) = \mathbf{C(p)u}(t) + \mathbf{u'}(t) \tag{2.9}$$

The substitution given in eq. (2.9) is not a linearization; it is an exact modelling, where the signal $u'_i(t)$ captures the difference between the $u_{si}(t)$ and the output of the linear gain $C_i(\mathbf{p})$. Notice in the substitution given in eq. (2.9) the $\mathbf{u'}(t)$ signals depend on the choice of $\mathbf{C(p)}$. Figure 2.4 shows the closed loop system with the substitution of eq. (2.9).

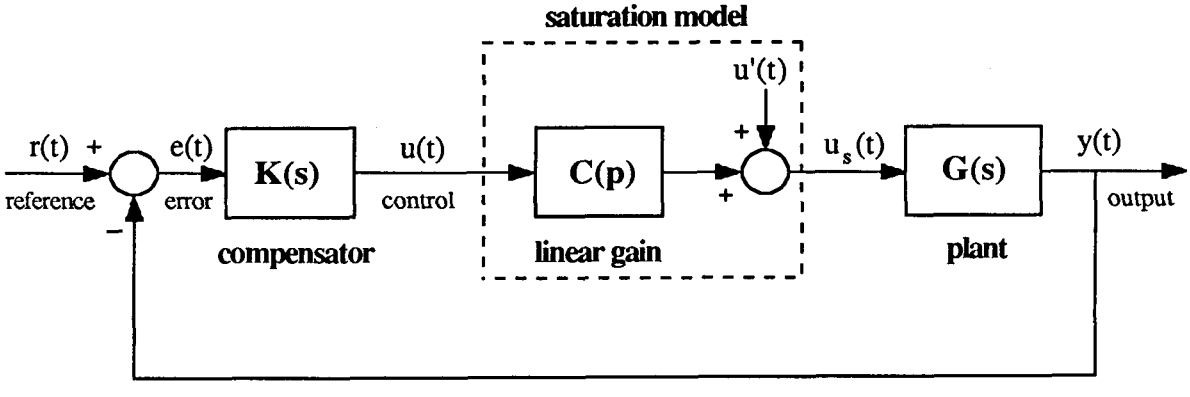

Figure 2.4: The closed loop system with the saturation modeled as a linear gain and an additive signal

If $|u_i(t)| \leq p_i \ \forall t$, i, then each saturation is a sector nonlinearity in the $[1/p_i, 1]$ sector.With

the linear gain $\mathbf{C(p)}$, instead of the saturation, the closed loop system becomes linear and thus easier to analyze. $\mathbf{C(p)}$ can be chosen to be any linear gain with elements $C_i(\mathbf{p})$ in the sector $[1/p_i, 1]$. Under this model each $u'_i(t)$ is an L_∞ signal with the following bound.

$$\|u'_i(t)\|_\infty \le \max_{1\le q\le p_i} |\, C_i(q)q-1 \,|, \quad \frac{1}{p_i} \le C_i(p_i) \le 1, \quad p_i \ge 1 \tag{2.10}$$

The problem now is to ensure that $|u_i(t)| \le p_i \ \forall t$, i. From the following theorem one can get L_∞ bounds for the references r(t) such that, when the references belong to the specified subset of L_∞ space, the closed loop system shown in figure 2.1 is BIBO stable.

Theorem 2.1:

With zero initial conditions the closed loop system shown in figure 2.1 with $\mathbf{d_I}(t) = 0$ and $\mathbf{d_o}(t) = 0$ will have a bounded output for references that satisfy the following condition for some $\mathbf{C(p)}$ and p_i's.

$$\begin{bmatrix} \|h_{11}\|_1 \ldots\ldots \|h_{1m}\|_1 \\ \ldots\ldots\ldots\ldots \\ \|h_{m1}\|_1 \ldots\ldots \|h_{mm}\|_1 \end{bmatrix} \begin{bmatrix} \|r_1\|_\infty \\ \ldots \\ \|r_m\|_\infty \end{bmatrix} + \begin{bmatrix} \|q_{11}\|_1 \ldots\ldots \|q_{1m}\|_1 \\ \ldots\ldots\ldots\ldots \\ \|q_{m1}\|_1 \ldots\ldots \|q_{mm}\|_1 \end{bmatrix} \begin{bmatrix} \|u'_1\|_\infty \\ \ldots \\ \|u'_m\|_\infty \end{bmatrix} \le \begin{bmatrix} p_1 \\ \ldots \\ p_m \end{bmatrix} \tag{2.11}$$

where

$$\mathbf{H}(s) = \begin{bmatrix} h_{11}(s) \ldots\ldots, h_{1m}(s) \\ \ldots\ldots\ldots\ldots \\ h_{m1}(s) \ldots\ldots h_{mm}(s) \end{bmatrix} = [\,\mathbf{I}+\mathbf{K}(s)\mathbf{G}(s)\mathbf{C}(p)]^{-1}\mathbf{K}(s) \tag{2.12}$$

$$\mathbf{Q}(s) = \begin{bmatrix} q_{11}(s) \ldots\ldots q_{1m}(s) \\ \ldots\ldots\ldots\ldots \\ q_{m1}(s) \ldots\ldots q_{mm}(s) \end{bmatrix} = [\mathbf{I}+\mathbf{K}(s)\mathbf{G}(s)\mathbf{C}(p)]^{-1}\mathbf{K}(s)\mathbf{G}(s) \tag{2.13}$$

$$\|h_{ij}\|_1 = \int_0^\infty |h_{ij}(t)|\,dt \qquad \|q_{ij}\|_1 = \int_0^\infty |q_{ij}(t)|\,dt \tag{2.14}$$

where $h_{ij}(t)$ and $q_{ij}(t)$ are the impulse responses of $h_{ij}(s)$ and $q_{ij}(s)$ respectively, and

$$\|r_i\|_\infty = \sup_t |r_i(t)| \tag{2.15}$$

Proof:

By using the saturation model given in eq. (2.7) one can compute the control $\mathbf{u}(t)$ by

$$\mathbf{u}(t) = \begin{bmatrix} u_1(t) \\ \ldots \\ u_m(t) \end{bmatrix} = \begin{bmatrix} \sum_{j=1}^{m} \int_0^t h_{1j}(t-\tau)\, r_j(\tau)\, d\tau \\ \ldots\ldots\ldots\ldots\ldots \\ \sum_{j=1}^{m} \int_0^t h_{mj}(t-\tau)\, r_j(\tau)\, d\tau \end{bmatrix} + \begin{bmatrix} \sum_{j=1}^{m} \int_0^t q_{1j}(t-\tau)\, u'_j(\tau)\, d\tau \\ \ldots\ldots\ldots\ldots\ldots \\ \sum_{j=1}^{m} \int_0^t q_{mj}(t-\tau)\, u'_j(\tau)\, d\tau \end{bmatrix} \tag{2.16}$$

By using the triangle inequality one can bound the controls u_i as shown in eqs. (2.17)-(2.21).

$$|u_i(t)| \le \left| \sum_{j=1}^{m} \left[\int_0^t h_{ij}(t-\tau)\, r_j(\tau)\, d\tau \right] \right| + \left| \sum_{j=1}^{m} \left[\int_0^t q_{ij}(t-\tau)\, u'_j(\tau)\, d\tau \right] \right| \tag{2.17}$$

$$|u_i(t)| \le \sum_{j=1}^{m} \int_0^t |h_{ij}(t-\tau)|\, |r_j(\tau)|\, d\tau + \sum_{j=1}^{m} \int_0^t |q_{ij}(t-\tau)|\, |u'_j(\tau)|\, d\tau \tag{2.18}$$

$$|u_i(t)| \le \sum_{j=1}^{m} \int_0^t |h_{ij}(t-\tau)|\, \|r_j(\tau)\|_\infty d\tau + \sum_{j=1}^{m} \int_0^t |q_{ij}(t-\tau)|\, \|u'_j(\tau)\|_\infty d\tau \tag{2.19}$$

$$\|u_i(t)\|_\infty \le \sum_{j=1}^{m} \int_0^\infty |h_{ij}(\tau)|\, d\tau\, \|r_j(t)\|_\infty + \sum_{j=1}^{m} \int_0^\infty |q_{ij}(\tau)|\, d\tau\, \|u'_j(t)\|_\infty \tag{2.20}$$

$$\|u_i(t)\|_\infty \le \sum_{j=1}^{m} \|h_{ij}\|_1\, \|r_j\|_\infty + \sum_{j=1}^{m} \|q_{ij}\|_1\, \|u'_j\|_\infty \tag{2.21}$$

In order for the control to belong in a sector it is required that the controls are bounded.

$$\begin{bmatrix} \|u_1(t)\|_\infty \\ \cdots\cdots \\ \|u_m(t)\|_\infty \end{bmatrix} \le \begin{bmatrix} p_1 \\ \cdots \\ p_m \end{bmatrix} \tag{2.22}$$

$$\|u_i(t)\|_\infty \le \sum_{j=1}^{m} \|h_{ij}\|_1\, \|r_j\|_\infty + \sum_{j=1}^{m} \|q_{ij}\|_1\, \|u'_j\|_\infty \le p_i \tag{2.23}$$

$$\begin{bmatrix} \|h_{11}\|_1 \ldots\ldots \|h_{1m}\|_1 \\ \ldots\ldots\ldots\ldots \\ \|h_{m1}\|_1 \ldots\ldots \|h_{mm}\|_1 \end{bmatrix} \begin{bmatrix} \|r_1\|_\infty \\ \ldots \\ \|r_m\|_\infty \end{bmatrix} + \begin{bmatrix} \|q_{11}\|_1 \ldots\ldots \|q_{1m}\|_1 \\ \ldots\ldots\ldots\ldots \\ \|q_{m1}\|_1 \ldots\ldots \|q_{mm}\|_1 \end{bmatrix} \begin{bmatrix} \|u'_1\|_\infty \\ \ldots \\ \|u'_m\|_\infty \end{bmatrix} \leq \begin{bmatrix} p_1 \\ \ldots \\ p_m \end{bmatrix} \quad (2.24)$$

////

One can use this result to define a control limit **p** and a bound on the references $\|\mathbf{r}(t)\|_\infty$ such that for every **r**(t) within the predefined bounds the controls will never exceed the limit **p** and thus the closed loop system will be BIBO stable. In theorem 2.1 there are many different combinations of $\|r_i(t)\|_\infty$ that can satisfy the inequality (2.11). In a specific design the control engineer should evaluate the references and choose the best $\|r_i(t)\|_\infty$.

Corollary 2.1:

With zero initial conditions the controls in the closed loop system shown in figure 2.1 will never saturate ($|u_i(t)| \leq 1\ \forall i, t$) if the reference **r**(t) is such that

$$\begin{bmatrix} \|h_{11}\|_1 \ldots\ldots \|h_{1m}\|_1 \\ \ldots\ldots\ldots\ldots \\ \|h_{m1}\|_1 \ldots\ldots \|h_{mm}\|_1 \end{bmatrix} \begin{bmatrix} \|r_1\|_\infty \\ \ldots \\ \|r_m\|_\infty \end{bmatrix} \leq \begin{bmatrix} 1 \\ \ldots \\ 1 \end{bmatrix} \quad (2.25)$$

where $\|h_{ij}\|_1$ are defined as in theorem 2.1 with $\mathbf{C(p)} = \mathbf{I}$

Proof:

The proof of this corollary it follows from theorem 2.1 when $p_i = 1$, $\forall i$. In such a case $u'_i(t) = 0$, $\forall i$ and then the corollary 2.1 follows from theorem 2.1.

////

The result of corollary 2.1 is not conservative, because if

$$\sum_{j=1}^{m} \|h_{ij}\|_1 \, \|r_j\|_\infty = 1 \quad \text{for some } i, \tag{2.26}$$

then there exists a reference signal $\mathbf{r}(t)$ that if applied will lead to a control $u_i(t) = 1$. To be more specific consider the following reference signal

$$\mathbf{r}(t) = [\, r_1(t) \cdot \cdot \cdot \cdot \cdot r_m(t)]^T \quad \text{where} \quad r_j(t) = \text{sign}(h_{ij}(t)), \ \forall j \tag{2.27}$$

By using the reference specified in eq. (2.27) the following is true.

$$u_i(t) = \sum_{j=1}^{m} \|h_{ij}\|_1 \, \|r_j\|_\infty = 1 \tag{2.28}$$

Now that the simple problem with the references being the only exogenous signal has been solved, let us try to find out what happens when input and output disturbances are present. Assume that input disturbances $\mathbf{d_i}(t)$ and output disturbances $\mathbf{d_o}(t)$ are entering the system as shown in the following equations (see also figure 2.1)

$$\mathbf{u_s}(t) = \mathbf{f}(\mathbf{u}(t)) + \mathbf{d_i}(t) \tag{2.29}$$

$$\mathbf{y}(t) = \mathbf{G}(s)\mathbf{u_s}(t) + \mathbf{d_o}(t) \tag{2.30}$$

Then the following corollary incorporating the input and output disturbances can be proven.

Corollary 2.2:

With zero initial conditions, the closed loop system shown in figure 2.1 will remain BIBO stable for references and disturbances that satisfy the following condition for some C(p) and p_i's.

$$\begin{bmatrix} \|h_{11}\|_1 \cdot \|h_{1m}\|_1 \\ \cdots\cdots\cdots \\ \|h_{m1}\|_1 \cdot \|h_{mm}\|_1 \end{bmatrix} \begin{bmatrix} \|r_1\|_\infty + \|d_{o1}\|_\infty \\ \cdots\cdots\cdots \\ \|r_m\|_\infty + \|d_{om}\|_\infty \end{bmatrix} + \begin{bmatrix} \|q_{11}\|_1 \cdot \|q_{1m}\|_1 \\ \cdots\cdots\cdots \\ \|q_{m1}\|_1 \cdot \|q_{mm}\|_1 \end{bmatrix} \begin{bmatrix} \|u'_1\|_\infty + \|d_{i1}\|_1 \\ \cdots\cdots\cdots \\ \|u'_m\|_\infty + \|d_{im}\|_1 \end{bmatrix} \leq \begin{bmatrix} p_1 \\ \cdots \\ p_m \end{bmatrix} \qquad (2.31)$$

where h_{ij} and q_{ij} are defined as in theorem 2.1, and d_{oj} and d_{ij} are the components of the output disturbance vector $\mathbf{d_o}(t)$ and input disturbance vector $\mathbf{d_i}(t)$, respectively.

Proof:

The proof of corollary 2.2 follows from theorem 2.1. It should be pointed out that the input disturbances enter the loop at the controls, which is the same point where the $\mathbf{u}'(t)$ signals enter the loop. Similarly, the output disturbances enter the loop at the same point as the references. Thus it is clear why the proof of this corollary follows from theorem 2.1.

////

From corollary 2.2 one can see that for BIBO stability there is a tradeoff between the disturbances $\mathbf{d_i}(t)$, $\mathbf{d_o}(t)$ that can be rejected and the references $\mathbf{r}(t)$ that can be followed. For example, in eq. (2.30) the $\|r_i(t)\|_\infty$ and $\|d_{oi}(t)\|_\infty$ enter the equation in a similar manner and the only constraint that one can obtain is upon $\|r_i(t)\|_\infty + \|d_{oi}(t)\|_\infty$.

From the theorem and the corollaries given in this section one can define L_∞ bounds for the references and/or disturbances so that the output of the system remains bounded in the presence of exogenous signals that belong in the set defined by the L_∞ bounds. The results of this section will be used in chapter 5 for the stability analysis of the new design methodology which is presented there.

2.3 Performance

The purpose of this section is to analyze the performance problems in a system with saturations and to *define performance objectives.*

There are well developed methods for defining performance criteria and for designing linear closed loop systems which meet the performance requirements. It would then be desirable, whenever the closed loop system operates in the linear region, to meet the a priori performance constraints (because it easy to define them and easy to design control systems satisfying these constraints). When the system operates in the nonlinear region new performance criteria have to be defined and new ways of achieving the desired performance must be developed.

There are two major problems that multiple saturations can introduce to the performance of the system: (a) the reset windup problem, and (b) the fact that multiple saturations change the direction of the controls.

When the linear compensator contains integrators and/or slow dynamics reset windups can occur. Whenever the controls are saturated the error is continuously integrated and this can lead to large overshoots in the response of the system. It is obvious that if the states of the compensator were such that the controls would never saturate, then reset windups would never appear. See references [26] and [27] for additional discussion of the reset windup problem.

Almost every current design methodology for linear systems inverts the plant and replaces the open loop system with a desired design loop. The inversion is done through the controls with signals at specific frequencies and directions. The saturations alter the direction and frequency of the control signal and thus interfere with the inversion process. The main problem is that although both the compensator and the plant are multivariable highly coupled systems, the saturations operate as SISO systems. Each saturation operates on its input signal *independently* from the other saturation elements.

To see exactly what happens assume as an example that in a two input system the control signal at some time t_0 is $\mathbf{u'}_1 = [\,3 \quad 1.1\,]^T$ the saturated signal will be $\mathbf{u'} = [\,1 \quad 1\,]^T$. Notice that the direction of the $\mathbf{u'}_1$ signal at time t_0 is altered. In fact, any input control signal $\mathbf{u} = [\,u_1 \quad u_2\,]^T$ will be transformed through the saturation to $\mathbf{u}_s = [\,1 \quad 1]^T$ if $u_1 \geq 1$ and $u_2 \geq 1$. Figure 2.5 shows an illustration of four different control directions $\mathbf{u'}_1, \mathbf{u'}_2, \mathbf{u''}_1, \mathbf{u''}_2$ which are mapped at only two directions $\mathbf{u'}$ and $\mathbf{u''}$.

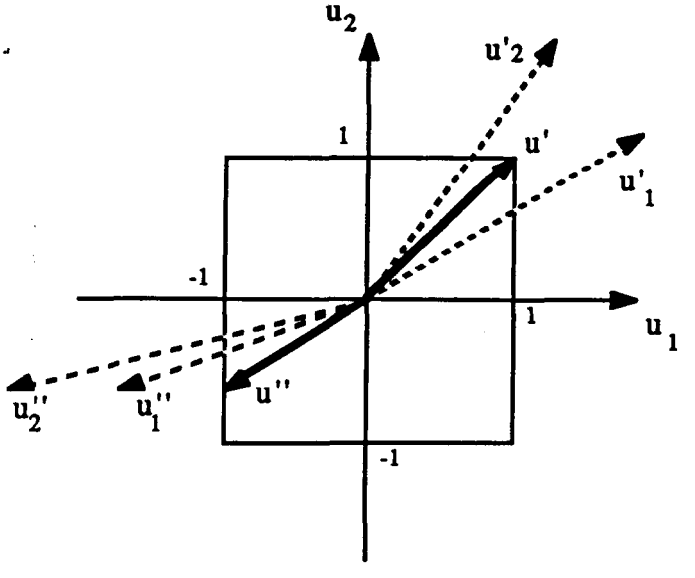

Figure 2.5: Examples of control directions at the input of the saturation $\mathbf{u'}_1, \mathbf{u'}_2, \mathbf{u''}_1, \mathbf{u''}_2$ and at the output of the saturation $\mathbf{u'}, \mathbf{u''}$.

Since the saturations can alter the direction of the control signals, and in effect disturb the compensator/plant inversion process, the logical question to ask is, under what conditions the linearly designed compensator that inverts (or partially inverts) the linear plant also inverts the plant when the saturations are present. To understand the issues let us consider an algebraic system.

2.3.1 The Algebraic System Example

Consider the algebraic system in figure 2.6. Both **K** and **G** are real matrices with $\mathbf{K} = \mathbf{G}^{-1}$. The problem is how to find the **K** matrices that inverts the matrix **G** with the saturation element sat(**u**). The elements of figure 2.6 are defined as follows

$$\mathbf{G}: \mathbf{u_s} \in \mathbb{R}^m \rightarrow \mathbf{y} \in \mathbb{R}^m, \text{ assume } \mathbf{G}^{-1} \text{ exists} \tag{2.32}$$

$$\mathbf{K}: \mathbf{e} \in \mathbb{R}^m \rightarrow \mathbf{u} \in \mathbb{R}^m \tag{2.33}$$

where $\mathbf{u_s}$, **y**, **e**, **u** are vectors with u_{si}, y_i, e_i, u_i as their i^{th} component respectively.

$$u_{si} = \text{sat}(u_i) = \begin{cases} 1 & \text{when} \quad u_i > 1 \\ u_i & \text{when} \quad |u_i| \le 1 \\ -1 & \text{when} \quad u_i < -1 \end{cases} \tag{2.34}$$

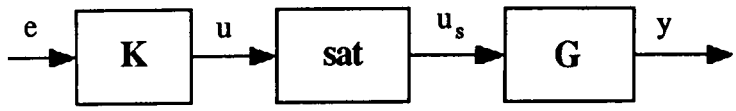

Figure 2.6: The algebraic system

The output **y** in figure 2.6 is given by the following

$$\mathbf{y} = \mathbf{G}\,\mathrm{sat}(\mathbf{Ke}) \tag{2.35}$$

$$\mathbf{G}^{-1}\mathbf{y} = \mathrm{sat}(\mathbf{Ke}) \tag{2.36}$$

$$\mathbf{G}^{-1}\mathbf{y} = \mathrm{sat}(\mathbf{G}^{-1}\mathbf{e}) \tag{2.37}$$

For the matrix $\mathbf{K} = \mathbf{G}^{-1}$ to invert **G** in the system shown in figure 2.6, one can choose a scaling λ for every input vector **e** such that

$$\mathbf{u} = \mathbf{K}\lambda\mathbf{e} = \mathbf{G}^{-1}\lambda\mathbf{e} \quad \text{and} \quad |u_i| \le 1 \tag{2.38}$$

Then from eq. (2.37) the following is true

$$\mathbf{y} = \mathbf{G}\,\mathrm{sat}(\mathbf{G}^{-1}\lambda\mathbf{e}) = \mathbf{G}\mathbf{G}^{-1}\lambda\mathbf{e} = \lambda\mathbf{e} \tag{2.39}$$

The modification shown in eq. (2.39) keeps the direction of the output **y** the same as the one of the input **e** and the only difference is a scaling of λ in the output **y**. Because of the nonlinear element sat(**u**) it is impossible to find **K** to invert **G** for all the inputs $\mathbf{e} \in \mathbb{R}^{\mathbf{m}}$. The scaling λ is necessary so at least the direction of the output y is preserved and is the same as the input direction **e**.

The main problem in this simple algebraic problem is that the sat(**u**) element alters the direction of the **u** vector while transforming it to the $\mathbf{u_s}$ vector. In addition, the nonlinear mapping of sat(**u**) is not invertible. For example, assume that $\mathbf{u}, \mathbf{u_s} \in \mathbb{R}^2$, then the vector $[2 \quad 1]^T$ is transformed to $[1 \quad 1]^T$ altering the direction, and the vector $[3 \quad 1]^T$ is transformed again to $[1 \quad 1]^T$, so the noninvertibility is apparent.

2.3.2 Performance Definition

After the analysis in the algebraic problem let us try to analyze the performance problem in the dynamic system. The system in question is the original closed loop system shown in figure 2.1 where the compensator and the plant are dynamic systems. Problems in performance can occur for the following two reasons: (a) the multiple saturations change the control vector direction and/or (b) the compensator has integrators or slow dynamics so that windups can occur.

Let us assume for a second that the reference and/or the error were such that the controls in the closed loop system never saturate. Then, if the compensator was designed to invert or partially invert the plant the inversion process would not be disturbed. At the same time the integrators and slow dynamics of the compensator would never windup.

To solve the performance problem let us assume that two nonzero operators are added to the system. The first operator O_1 is applied to the error signals and for convenience purposes it will be called **Error Governor (EG)** and the second operator O_2 is applied in the reference signals and it will be called **Reference Governor (RG)**.

$$\mathbf{u} = \mathbf{K}O_1\mathbf{e} \tag{2.40}$$

$$\mathbf{e} = O_2\mathbf{r} - \mathbf{y} \tag{2.41}$$

The two nonzero operators can be chosen, *if possible*, so that the control $\mathbf{u}(t)$ never saturates, i.e. $\|\mathbf{u}(t)\|_\infty \leq 1$, for any reference and/or disturbances. It is also desired that the $O_1\mathbf{e}$ and $O_2\mathbf{r}$ signals are "close" to the $\mathbf{e}(t)$ and $\mathbf{r}(t)$ signals respectively. In Chapters 3-5 the two operators will be defined in detail. Figure 2.7 shows the closed loop system with the two added operators.

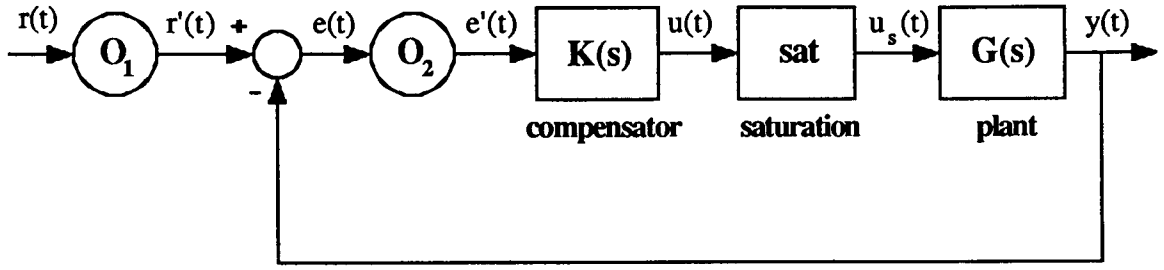

Figure 2.7: General structure for the control system

Effectively, with the introduction of the EG and RG operators, the saturation is transferred from the controls to other points in the loop where it makes the control analysis and design process easier.

As was discussed previously, the selection of the EG and RG is such that the controls will never saturate; and if, for example, the compensator was designed to invert or partially invert the plant, then the inversion process will not be distorted by the saturation and ***GsatK*** *will remain linear and equal to* ***GK***. In the closed loop system with the operators O_1 and O_2 the compensator will never cause windups. The integrators and slow dynamics of the compensator will never cause the controls to exceed the limits of the saturation and thus *windups never occur.*

2.4. Concluding Remarks

In this chapter certain issues about the stability and the performance of a control system with multiple saturations were discussed.

As far as the stability is concerned, a new stability criterion was introduced where L_∞ reference and disturbance spaces were defined so that for any exogenous signal (reference or disturbance) in those spaces the closed loop system will remain BIBO stable.

As far as the performance is concerned, at first, the performance problems that saturations introduce were analyzed. These problems can be integrator windups and the control direction alteration by the multiple saturations. To solve these problems new performance objectives were introduced. The idea is to somehow prevent the controls from saturating so that the compensator can invert or partially invert the plant as designed.

The introduction of the two operators, the Error Governor (EG) and the Reference Governor (RG), will address these stability and performance concerns; in chapters 3-5, it will be shown how to design those two operators in detail.

CHAPTER 3
MATHEMATICAL PRELIMINARIES

3.1 Introduction

This chapter is an introduction to the new design methodology. Some necessary mathematical preliminaries will be given and two basic problems will be introduced. The two basic problems will be solved and their solution will lead to the design of the two operators that were introduced in chapter 2, i.e. the Error Governor (EG) and the Reference Governor (RG).

The design of the operator EG involves the design of a time-varying gain such that the outputs of a linear system remain bounded. The design of the operator RG involves the design of a time-varying rate such that the outputs of a linear system remain bounded.

3.2 Preliminaries

Consider the following linear time invariant system

$$\dot{x}(t) = Ax(t) \qquad A \in \mathbb{R}^{nxn},\ x(t) \in \mathbb{R}^{n} \qquad (3.1)$$

$$x(0) = x_0 \qquad (3.2)$$

$$y(t) = Cx(t) \qquad C \in \mathbb{R}^{mxn},\ y(t) \in \mathbb{R}^{m} \qquad (3.3)$$

$$y(x_0,t) = Ce^{At}x_0 \qquad (3.4)$$

where e^{At} is the state transition matrix (matrix exponential) for A

In the rest of this section certain definitions and facts will be presented. These definitions

and facts will be used for the design of the operators EG and RG.

Definition 3.1:

The scalar-valued function g(x) is defined as follows:

$$g(\mathbf{x}_0): \mathbb{R}^n \rightarrow \mathbb{R}, \quad g(\mathbf{x}_0) = \|y(\mathbf{x}_0,t)\|_\infty \tag{3.5}$$

This function $g(\mathbf{x}_0)$ is not necessarily differentiable at all points in $\mathbb{R}^n$. One can easily see the possibility of having a nondifferentiable $g(\mathbf{x}_0)$ when $\|y_i(\mathbf{x}_0,t)\|_\infty = |y_j(\mathbf{x}_0,t')|$, where $t \neq t'$ and/or $i \neq j$. In figure 3.1 three responses are shown which correspond to a fictitious system with three initial conditions. For the initial condition $\mathbf{x}_0$ the system has a response with the maximum value occurring at times t_1 and t_2. Then, for a small deviation in the initial condition, $\mathbf{x}_0 + \mathbf{v}$, the maximum in the response occurs at time t_1 and for another small deviation in the initial condition, $\mathbf{x}_0 - \mathbf{w}$, the response has its maximum value at t_2. For such a system it is obvious why the $g(\mathbf{x}_0)$ may not be differentiable at $\mathbf{x}_0$.

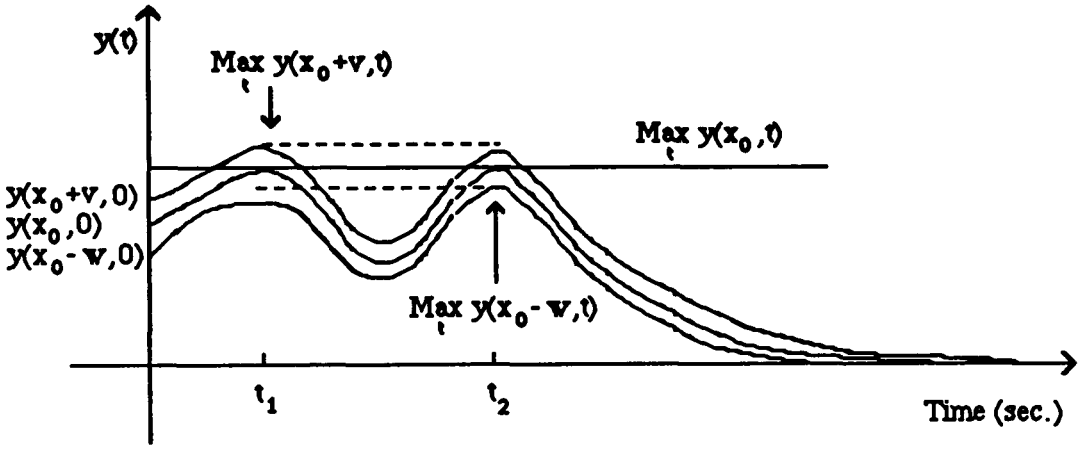

Figure 3.1: Output response of a hypothetical system for three different initial conditions.

Definition 3.2:

The Jacobian matrix of g(x) is defined as follows:

$$Dg(x) = \left[\frac{\partial g(x)}{\partial x_1} \quad \frac{\partial g(x)}{\partial x_2} \cdots\cdots\cdots \frac{\partial g(x)}{\partial x_n} \right] \tag{3.6}$$

where each $x \in \mathbb{R}^n$ is given by

$$x = \left[x_1 \quad x_2 \quad \cdots\cdots\cdots \quad x_n \right]^T \tag{3.7}$$

Theorem 3.1:

Let $\lambda_i(A)$ be an observable mode of (A,C) and let the multiplicity of $\lambda_i(A)$) be n_i. The function g(x) is finite $\forall x \in \mathbb{R}^n$ if and only if

a) $\mathrm{Re}(\lambda_i(A)) \leq 0$, $\forall i$, and

b) The modes $\lambda_i(A)$ with $\mathrm{Re}(\lambda_i(A)) = 0$ and $n_i > 1$ have independent eigenvectors (i.e. the order of the Jordan blocks associated with the eigenvalues of A with $\mathrm{Re}(\lambda_i(A)) = 0$ and $n_i > 1$ is 1.).

Proof:

Let **P** be the similarity transformation matrix that transforms **A** to the Jordan form as follows

$$\mathbf{A_J = PAP^{-1}}$$

Since A_J is in Jordan form, every entry of the $e^{\mathbf{A_J}t}$ matrix is of the form $t^k e^{(\alpha_i + j\omega_i)t}$ where $\lambda_i = \alpha_i + j\omega_i$ and λ_i is an eigenvalue of $\mathbf{A_J}$. If $\alpha_i < 0$, then $t^k e^{(\alpha_i + j\omega_i)t} < \infty \; \forall k$. If $\alpha_i = 0$, then $t^k e^{j\omega_i t} < \infty$ only if $k = 0$, and consequently the order of the Jordan block associated with the eigenvalue $j\omega_i$ is 1.

$\Leftarrow$

If the assumptions a) and b) of the theorem are satisfied, then $e^{\mathbf{A_J}t}$ and $e^{\mathbf{A}t}$ are bounded; consequently, $\mathbf{y(x_0,t) = Ce^{At}x_0}$ is bounded and $g(\mathbf{x}) < \infty$, $\forall \mathbf{x} \in \mathbf{R^n}$.

$\Rightarrow$

If $g(\mathbf{x}) < \infty$, then $\mathbf{y(x_0,t) = Ce^{At}x_0}$ is bounded; consequently, the observable modes of **(A,C)** have to satisfy assumptions (a) and (b) of the theorem.

////

Systems that satisfy conditions (a) and (b) of theorem 3.1 are called **neutrally stable**. Note that if **[A,C]** is unobservable and if, because of the unobservability, there is an unstable pole/zero cancellation, then all the assumptions of theorem 3.1 are met and $g(\mathbf{x})$ will be finite. Because $g(\mathbf{x})$ will be used eventually for designing control systems, there are other obvious reasons that unstable pole/zero cancellations are not allowed.

Theorem 3.2:

Let $g(\mathbf{x})$ be as in Definition 3.1 and assume that $g(\mathbf{x}) < \infty$, $\forall \mathbf{x} \in \mathbb{R}^n$. Then $g(\mathbf{x})$ is continuous.

Proof:

Given an $\varepsilon > 0$, $\forall\ \mathbf{x_0}, \mathbf{v_0} \in \mathbb{R}^n$, $\exists\ \mathbf{w_0} \in \mathbb{R}^n$

$$\|w_0\|_\infty = \frac{\varepsilon}{\max\limits_t (\sigma_{max}(Ce^{At}))} = \delta$$

such that if $| \mathbf{x_0} - \mathbf{v_0} | \le \delta$, then $\mathbf{v_0} = \mathbf{x_0} + \mathbf{w_0}$

and since $g(\mathbf{x}) < \infty$, $\max\limits_t (\sigma_{max}(Ce^{At}))$ is finite and thus $\delta > 0$, $\forall \mathbf{x} \in \mathbb{R}^n$

$$| g(\mathbf{x_0}) - g(\mathbf{v_0}) | = | \| y(\mathbf{x_0},t) \|_\infty - \| y(\mathbf{v_0},t) \|_\infty |$$

$$= | \| Ce^{At}\mathbf{x_0} \|_\infty - \| Ce^{At}\mathbf{v_0} \|_\infty |$$

$$| g(\mathbf{x_0}) - g(\mathbf{v_0}) | = | \| Ce^{At}\mathbf{x_0} \|_\infty - \| Ce^{At}\mathbf{x_0} + Ce^{At}\mathbf{w_0} \|_\infty | \le$$

$$| \| Ce^{At}\mathbf{x_0} \|_\infty - \| Ce^{At}\mathbf{x_0} \|_\infty + \| Ce^{At}\mathbf{w_0} \|_\infty | = \| Ce^{At}\mathbf{w_0} \|_\infty$$

$$| g(\mathbf{x_0}) - g(\mathbf{v_0}) | \le \| Ce^{At}\mathbf{w_0} \|_\infty \le \max\limits_t (\sigma_{max}(Ce^{At})) \ \| w_0 \|_\infty \le \varepsilon$$

then $\forall \varepsilon > 0$, $\exists \delta > 0$, such that, $\forall \mathbf{x_0}, \mathbf{v_0} \in \mathbb{R}^n$ with $|\mathbf{x_0} - \mathbf{v_0}| \le \delta$, then $|g(\mathbf{x_0}) - g(\mathbf{v_0})| \le \varepsilon$

////

Definition 3.3: The set $\mathbf{P_g}$ is defined as:

$$\mathbf{P_g} = \{ [\mathbf{x},\mathbf{v}] : \mathbf{x} \in \mathbb{R}^n, \mathbf{v} \in \mathbb{R}, \mathbf{v} \ge g(\mathbf{x}) \} \tag{3.8}$$

From this definition we see that $\mathbf{P_g}$ is the interior of the graph of the function $g(\mathbf{x})$ in

$\mathbb{R}^{n+1}$, as shown in figure 3.2.

Definition 3.4: $\mathbf{B}_{A,C}$ is the set of all $x \in \mathbf{R}^n$ with $0 \le g(x) \le 1$, i.e.

$$\mathbf{B}_{A,C} = \{x: \ 0 \le g(x) \le 1\} \tag{3.9}$$

Suppose that the system (3.1)-(3.4) has an initial condition $x_0 \in \mathbf{B}_{A,C}$. From this definition we see that for such an initial condition the output of the system, y(t), will satisfy $\|y(t)\|_\infty \le 1$.

Theorem 3.3:

The set $\mathbf{P}_g$ as it is defined in Definition 3.3 is a convex cone.

Proof:

$\mathbf{P}_g$ is a cone.

$\mathbf{P}_g$ is a cone if $w_1 \in \mathbf{P}_g$ and $c \in \mathbf{R}^+$ then $cw_1 \in \mathbf{P}_g$.

If $[x_1,v_1] \in \mathbf{P}_g$ and $c \in \mathbf{R}^+$ then since $v_1 \ge g(x_1) \Rightarrow cv_1 \ge cg(x_1)$

$cg(x_1) = g(cx_1) \Rightarrow cv_1 \ge g(cx_1)$ which imply that $[cx_1,cv_1] \in \mathbf{P}_g$ and $\mathbf{P}_g$ is a cone.

$\mathbf{P}_g$ is convex.

$\forall\ [x_1,v_1], [x_2,v_2] \in \mathbf{P}_g$, given ρ such that $0 \le \rho \le 1$

if $[x_1,v_1], [x_2,v_2] \in \mathbf{P}_g$ then $\rho[x_1,v_1]$ and $(1-\rho)[x_2,v_2] \in \mathbf{P}_g$ because $\mathbf{P}_g$ is a cone

since $\rho v_1 \ge g(\rho x_1)$ and $(1-\rho)v_2 \ge g((1-\rho)x_2) \Rightarrow \rho v_1+(1-\rho)v_2 \ge g(\rho x_1)+g((1-\rho)x_2)$

since $g(\rho x_1)+g((1-\rho)x_2) \ge g(\rho x_1+ (1-\rho)x_2) \Rightarrow \rho v_1+ (1-\rho)v_2 \ge g(\rho x_1+ (1-\rho)x_2)$

Then $[\ \rho x_1+ (1-\rho)x_2, \rho v_1+ (1-\rho)v_2] \in \mathbf{P}_g$.

So a convex combination of two points in the set is also in the set and consequently

$\mathbf{P_g}$ is convex.

////

One might expect that $\mathbf{P_g}$ would be a convex cone from the linearity ($g(\alpha x) = \alpha g(x)$)of the system (3.1)-(3.4). Because $\mathbf{P_g}$ is a cone and $g(x)$ defines its boundary we will refer to $g(x)$ as a conic function.

Corollary 3.1:

$\mathbf{B_{A,C}}$ is a symmetric, closed and convex set.

Proof:

The proof of this corollary follows from Definitions 3.1- 3.5 and theorems 3.1-3.2. Note that the set $\mathbf{B_{A,C}}$ is symmetric with respect to the origin. This is true because $\|y(x_0,t)\|_\infty = \|y(-x_0,t)\|_\infty$ and consequently $g(x_0) = g(-x_0)$. Also, note that because $\mathbf{P_g}$ is a convex cone, then $\mathbf{B_{A,C}}$ is a closed convex set.

////

Theorem 3.4:

Define e_i to be an eigenvector of $\mathbf{A}$ and $\eta(\mathbf{C})$ to be the null space of $\mathbf{C}$.

If $e_i \notin \eta(\mathbf{C})\ \forall\ i$ then $\mathbf{B_{A,C}}$ is bounded.

Equivalently, if the pair $[\mathbf{A},\mathbf{C}]$ is observable then $\mathbf{B_{A,C}}$ is bounded.

Proof:

If $\mathbf{e}_i \notin \eta(\mathbf{C})\ \forall i$, then $y(\mathbf{x}_0,t)\neq 0\ \forall \mathbf{x}_0$, and since $y_i(c\mathbf{x}_0,t) = cy_i(\mathbf{x}_0,t)\ \forall\ c\in \mathbf{R}, i \Rightarrow$ $g(c\mathbf{x}_0) = 1$ for some scalar c $\forall \mathbf{x}_0$, So $\mathbf{B}_{A,C}=\{\mathbf{x}_0: g(\mathbf{x}_0) \leq 1\}$ is bounded.

////

If the pair [A,C] is not observable then $\mathbf{B}_{A,C}$ will not be bounded. Specifically, if $\mathbf{e}_i \in \eta(\mathbf{C})$ for some i then $c\mathbf{e}_i \in \mathbf{B}_{A,C}$ $\forall$scalar c.

Figure 3.2 gives a visualization of the function $g(\mathbf{x}_0)$ and the sets $\mathbf{B}_{A,C}$ and $\mathbf{P}_g$ in $\mathbb{R}^n$ and $\mathbb{R}^{n+1}$ respectively.

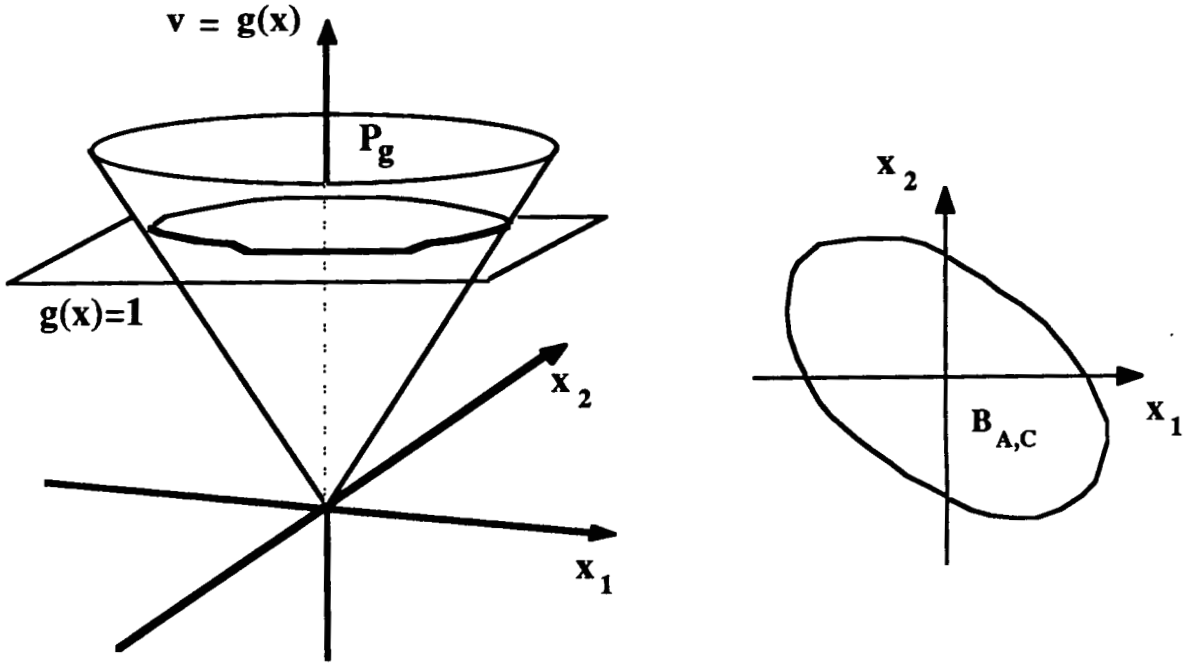

Figure 3.2: Visualization of the function g(x) and the sets $\mathbf{P}_g$ and $\mathbf{B}_{A,C}$.

Definition 3.5 [17]: The upper right Dini derivative is defined as

$$D^{+}f(t_0) = \lim_{t \to t_0^{+}} \sup \frac{f(t)-f(t_0)}{t-t_0} \tag{3.10}$$

Definitions of the lower right, upper left and lower left Dini derivatives are given in reference [17]. In the sequel only the upper right Dini derivative will be used as in definition 3.5. The $D^{+}f(t_0)$ is finite at t_0 if the function f satisfies the Lipschitz condition locally around t_0 [17]. Note that the function g(**x**) defined by Definition 3.1 satisfies the Lipschitz condition locally if the conditions of Theorem 3.1 are met. This is obvious because g(**x**) is a conic function.

Theorem 3.5 [17]:

Suppose that f(t) is continuous on (a,b), then f(t) is nonincreasing on (a,b) iff $D^{+}f(t) \leq 0$ for every $t \in (a,b)$.

Proof:

The proof of this theorem is given in reference [17].

////

In the following example we will illustrate the set $\mathbf{B}_{A,C}$ and an approximate $\mathbf{B}_{A,C}$ set, $\mathbf{B'}_{A,C}$, for a given linear time invariant system.

Example:

Consider the following model

$$\dot{\mathbf{x}}(t) = \begin{bmatrix} -2.6093 & 1.4180 \\ -7.1476 & 1.5213 \end{bmatrix} \mathbf{x}(t) + \begin{bmatrix} -29.8308 & 2.989 \\ -68.7543 & 10.8387 \end{bmatrix} \mathbf{u}(t) \quad (3.11)$$

$$\mathbf{y}(t) = \begin{bmatrix} -1 & 1 \\ 2 & -1 \end{bmatrix} \mathbf{x}(t) \quad (3.12)$$

To compute the set $\mathbf{B}_{A,C}$ for this system, it suffies to compute the output $\mathbf{y}(t)$ with $\mathbf{u}(t) = 0$ for different initial conditions, $\mathbf{x}_i$, on the unit circle. With $\mathbf{y}(\mathbf{x}_i,t)$ we compute $g(\mathbf{x}_i) = \|\mathbf{y}(\mathbf{x}_i,t)\|_\infty$. The boundary of $\mathbf{B}_{A,C}$ is then given by the points $\mathbf{v}_i = \mathbf{x}_i/g(\mathbf{x}_i)$. This follows from the linearity of the unforced system with respect to the initial condition. The $\mathbf{B}_{A,C}$ set for this system is shown in Figure 3.3.

The system has two poles at **-.544±j2.422.** and no finite transmission zeros. The pair [A,C] is observable and hence it follows from theorem 3.1 that the function $g(\mathbf{x})$ is bounded. Consequently, the $\mathbf{B}_{A,C}$ set is closed. In addition, the $\mathbf{B}_{A,C}$ set, as expected, is a symmetric and convex set.

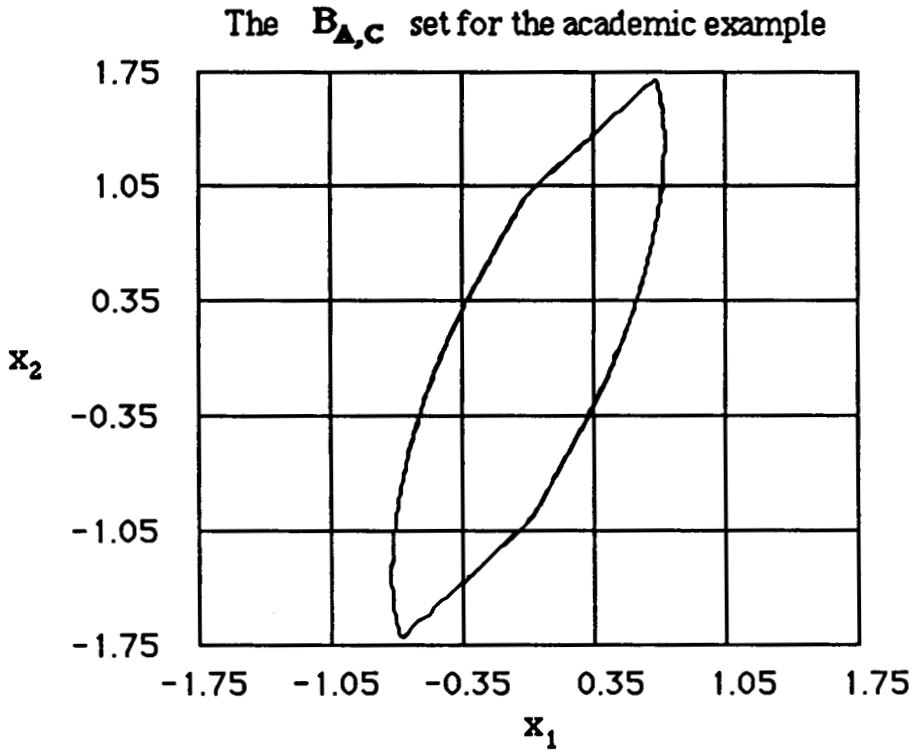

Figure 3.3: The $\mathbf{B}_{A,C}$ set for the example.

The exact calculation of this set could be difficult for higher order systems and in such a case an approximation of that set can be used. For this particular example the $\mathbf{B}_{A,C}$ set can be easily approximated by an ellipse that includes the whole set. Figure 3.4 shows the actual $\mathbf{B}_{A,C}$ with its ellipse approximation $\mathbf{B'}_{A,C}$. The $\mathbf{B'}_{A,C}$ is given by the following

$$\mathbf{B}_{A,C}=\left\{x\in\mathbf{R}^2,\ x=\begin{bmatrix}x_1 & x_2\end{bmatrix}^T : \frac{3.5\,x_1-\sqrt{-6.47\,x_1^2+4.08}}{2}\le x_2\le \frac{3.5\,x_1+\sqrt{-6.47\,x_1^2+4.08}}{2}\right\} \quad (3.13)$$

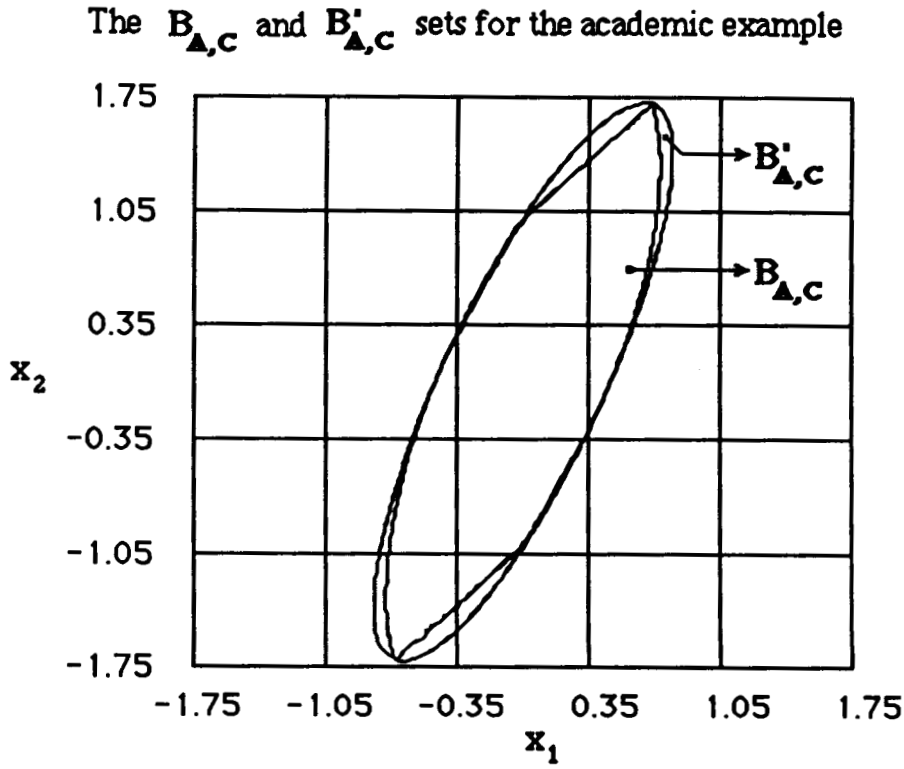

Figure 3.4: The $B_{A,C}$ set and an approximation of it $B'_{A,C}$ for the example.

One can do better approximations of this particular $B_{A,C}$ but the point here is not to find the best approximation but to see the effects of an approximation in a particular example. In the sequel the system (3.11)-(3.12) will be used as a compensator in a closed loop control system. The $B_{A,C}$ and the $B'_{A,C}$ will be used in a new control methodology (will be described in chapters 4 and 5) and the effects of this approximation will be discussed.

3.3. Design of a Time-Varying Gain such that the Outputs of a Linear System are Bounded

Assume that a linear system is defined by the following equations

$$\dot{\mathbf{x}}(t) = \mathbf{A}\mathbf{x}(t)+\mathbf{B}\mathbf{u}(t) \qquad \mathbf{A}\in\mathbb{R}^{nxn},\ \mathbf{B}\in\mathbb{R}^{nxm} \qquad (3.14)$$

$$\mathbf{y}(t) = \mathbf{C}\mathbf{x}(t) \qquad \mathbf{C}\in\mathbb{R}^{mxn} \qquad (3.15)$$

and also assume that the linear system is **neutrally stable**. Then, if one were to construct the function g(**x**) (definition 3.1) for the system (3.14)-(3.15) for **B** = 0, the following is true; g(**x**) $< \infty$, $\forall \mathbf{x}\in\mathbb{R}^n$. This follows from theorem 3.1.

The goal here, is to keep the outputs of the linear system (3.14)-(3.15) bounded (i.e. $|y_i(t)| \le 1$, $\forall$ t, i) for any input **u**(t). To achieve our goal, consider the following system with a time-varying scalar gain $\lambda(t)$

$$\dot{\mathbf{x}}(t) = \mathbf{A}\mathbf{x}(t) + \mathbf{B}\lambda(t)\mathbf{u}(t) \qquad (3.16)$$

$$\mathbf{y}(t) = \mathbf{C}\mathbf{x}(t) \qquad (3.17)$$

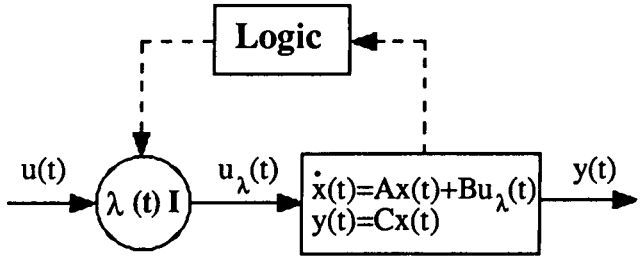

Figure 3.5: The basic system for calculating $\lambda(t)$.

Figure 3.5 shows the basic system and the location of the time-varying gain $\lambda(t)$. In this framework a basic problem can be defined.

***The Basic Problem*:**

At time t_0, find the maximum gain $\lambda(t_0)$, $0 \le \lambda(t_0) \le 1$, such that $\forall u(t)$, $t > t_0$ $\exists$ $\lambda(t)$, $t > t_0$ such that the output will satisfy $|y_i(t)| \le 1 \; \forall \; i$, $t > t_0$.

A solution to this problem can be obtained by using a function $g(\mathbf{x})$ given in definition 3.1 and by using a set $\mathbf{B}_{A,C}$ given in definition 3.4. To be more specific, for the system (3.16)-(3.17), with $\mathbf{u}(t) = 0$, one can define $g(\mathbf{x})$ as in eqs. (3.18)-(3.19). The function $g(\mathbf{x})$ is finite because the system (3-16)-(3-17) is neutrally stable (theorem 3.1).

$$g(\mathbf{x}_0): \; \mathbf{R}^n \rightarrow \mathbb{R}, \quad g(\mathbf{x}_0) = \|y(\mathbf{x}_0,t)\|_\infty \tag{3.18}$$

$$\mathbf{x}(0) = \mathbf{x}_0 \tag{3.19}$$

$$\mathbf{B}_{A,C} = \{\mathbf{x} : \; g(\mathbf{x}) \le 1\} \tag{3.20}$$

By defining $g(\mathbf{x})$ and $\mathbf{B}_{A,C}$ as in eqs. (3.18)-(3.20) one can construct $\lambda(t)$ as follows:

Construction of λ(t):

For every time t choose λ(t) as follows

a) if $\mathbf{x}(t) \in \text{Int}\mathbf{B}_{A,C}$ then $\lambda(t) = 1$ (3.21)

b) if $\mathbf{x}(t) \in \text{Bd}\mathbf{B}_{A,C}$ then choose the largest λ(t) such that (3.22)

$$0 \le \lambda(t) \le 1 \tag{3.23}$$

$$\lim_{\varepsilon \to 0} \sup \frac{\mathbf{g}(\mathbf{x}(t)+\varepsilon[\mathbf{A}\mathbf{x}(t)+\mathbf{B}\lambda(t)\mathbf{u}(t)]) - \mathbf{g}(\mathbf{x}(t))}{\varepsilon} \le 0 \tag{3.24}$$

or for the points where g(x) is differentiable choose the largest λ(t) such that

$$0 \le \lambda(t) \le 1 \tag{3.25}$$

$$\mathbf{D}\mathbf{g}(\mathbf{x}(t))[\mathbf{A}\mathbf{x}(t) + \mathbf{B}\lambda(t)\mathbf{u}(t)] \le 0 \tag{3.26}$$

where Dg(x(t)) is the Jacobian matrix of g(x(t)) as in definition 3.2.

c) if $\mathbf{x}(t) \notin \mathbf{B}_{A,C}$ then choose λ(t), $0 \le \lambda(t) \le 1$ such that the expression in 3.24 is minimum.

In the construction of λ(t) if $\mathbf{x}(t_0) \notin \mathbf{B}_{A,C}$ then the basic problem cannot be solved because there exists a $\mathbf{u}(t_0)$ for $t > t_0$ (i.e. $\mathbf{u}(t) = 0$) where it will lead to $\|\mathbf{y}(\mathbf{x}(t_0),t)\|_\infty > 1$. In such a case, the best that can be done is to find λ(t) such that the states x(t) will be driven into $\mathbf{B}_{A,C}$ as soon as possible.

With the λ(t) defined as above let us examine some properties of the system (3.16)-(3.17). To be more specific it will be shown that

(a) There is always exists a λ(t) that satisfies all the constraints in the construction of λ(t).

(b) If λ(t) is constructed as it was specified above and $\mathbf{x}(t_0) \in \mathbf{B}_{A,C}$, then $\mathbf{x}(t) \in \mathbf{B}_{A,C}$ $\forall t > t_0$ and for all u(t).

(c) the construction of $\lambda(t)$ solves the basic problem when that is possible (i.e. $\mathbf{x}(t) \in \mathbf{B}_{A,C}$ for all t).

Theorem 3.6:

For the system given in eqs. (3.16)-(3.17) the following is always true $\forall \mathbf{x} \in \mathbb{R}^n$.

$$\lim_{\varepsilon \to 0} \sup \frac{g(\mathbf{x}(t)+\varepsilon[\mathbf{A}\mathbf{x}(t)]) - g(\mathbf{x}(t))}{\varepsilon} \leq 0 \qquad (3.27)$$

and at the points where $g(\mathbf{x})$ is differentiable

$$Dg(\mathbf{x})\,\mathbf{A}\mathbf{x} \leq 0 \qquad \forall \mathbf{x} \in \mathbb{R}^n \qquad (3.28)$$

where $Dg(\mathbf{x}(t))$ is the Jacobian matrix of $g(\mathbf{x}(t))$ as in definition 3.2.

Proof:

Assume that the inequality (3.27) is not true for some $\mathbf{x}(t) = \mathbf{x}_0$. If the $\mathbf{x}_0$ is used as an initial condition to the $\dot{\mathbf{x}}(t) = \mathbf{A}\mathbf{x}(t)$ system then because of theorem 3.5 $\exists t'>0$ such that $g(\mathbf{x}(t')) > g(\mathbf{x}(t))$. But $g(\mathbf{x}_0) = \|\mathbf{C}\mathbf{x}(t)\|_\infty$ so this is a contradiction. Therefore, inequality (3.27) is true $\forall \mathbf{x} \in \mathbf{R}^n$.

////

The construction of $\lambda(t)$ is always possible because of theorem 3.6, namely one can choose $\lambda(t) = 0$ $\forall t$ and the inequality (3.24) is always true.

Lemma 3.1:

In the system (3.16)-(3.17) if $\mathbf{x}_0 \in \mathbf{B}_{A,C}$ and $\lambda(t)$ is constructed as it was described above, then $\mathbf{x}(t) \in \mathbf{B}_{A,C}$ for all t and for all $\mathbf{u}(t)$.

Proof:

The proof of this Lemma follows from the construction of $\lambda(t)$.

////

Theorem 3.7:

For the system (3.16)-(3.17) with $\lambda(t)$ constructed as above the following is always true

if $\mathbf{x_0} \in \mathbf{B}_{A,C}$ then $\|y(t)\|_\infty \leq 1$ $\forall$input $\mathbf{u}(t)$

if $\mathbf{x_0} \notin \mathbf{B}_{A,C}$ then $\|y(t)\|_\infty \leq g(\mathbf{x_0})$ $\forall$input $\mathbf{u}(t)$

Proof:

If $\mathbf{x_0} \in \mathbf{B}_{A,C}$, then

The construction of $\lambda(t)$ guarantees that $\mathbf{x}(t) \in \mathbf{B}_{A,C}$ $\forall t$. (see Lemma 3.1). It is also true that for any state $\mathbf{x}(t) \in \mathbf{B}_{A,C}$ $\|\mathbf{Cx}(t)\|_\infty \leq 1$. If $\|\mathbf{Cx}(t)\|_\infty > 1$ and $\mathbf{x}(t)$ is used as an initial condition in the system the following will be true, $g(\mathbf{x}(t)) > 1$ and $\mathbf{x}(t) \notin \mathbf{B}_{A,C}$ which is a contradiction. Since $\mathbf{y}(t) = \mathbf{Cx}(t)$ and $\mathbf{x}(t) \in \mathbf{B}_{A,C}$ $\forall t$ then $\|y(t)\|_\infty \leq 1$ $\forall$input $\mathbf{u}(t)$.

If $\mathbf{x_0} \notin \mathbf{B}_{A,C}$, then $g(\mathbf{x_0}) > 1$ and from the construction of $\lambda(t)$ $g(\mathbf{x}(t)) < g(\mathbf{x_0})$ ($g(x)$ is decreasing by theorem 3.5). Thus $\|y(t)\|_\infty \leq g(\mathbf{x}(t)) \leq g(\mathbf{x_0})$.

////

Theorem 3.8:

At every time t_0, if $\mathbf{x}(t_0) \in \mathbf{B}_{A,C}$ then the time-varying gain $\lambda(t_0)$ is the maximum possible such gain that $0 \leq \lambda(t_0) \leq 1$ and $\forall \mathbf{u}(t)$, $t > t_0$ $\exists$ $\lambda(t)$, $t > t_0$ such that the output $|y_i(t)| \leq 1$ $\forall$ i, $t > t_0$. If $\mathbf{x}(t_0) \notin \mathbf{B}_{A,C}$ then such a gain $\lambda(t_0)$ does not exist.

Proof:

If $\mathbf{x}(t_0) \in \mathbf{B}_{A,C}$, then

from the construction of $\lambda(t)$, at any time t_0 the maximum gain $\lambda(t_0)$ is chosen such that $0 \leq \lambda(t_0) \leq 1$ and $\mathbf{x}(t) \in \mathbf{B}_{A,C} \forall t > t_0$. If a greater gain $\lambda(t_0)$ is used then $g(\mathbf{x}(t_0)$ will be increasing (see theorem 3.5) and $\mathbf{x}(t) \notin \mathbf{B}_{A,C} \forall t > t_0$; consequently there exists $\mathbf{u}(t)$ (i.e. $\mathbf{u}(t) = 0$ $t \geq t_0$) where $\|\mathbf{y}(t)\|_\infty > 1$.

If $\mathbf{x}(t_0) \notin \mathbf{B}_{A,C}$, then there exists $\mathbf{u}(t)$ (i.e. $\mathbf{u}(t)=0$ $t \geq t_0$) where $\|\mathbf{y}(t)\|_\infty > 1$ and thus for any $\lambda(t_0)$ the basic problem does not have a solution.

////

The solution to the basic problem which was given above assumed that $\lambda(t)$ is a scalar. A similar solution can be obtained if a time-varying diagonal matrix $\Lambda(t)$ is employed.

$$\Lambda(t) = \begin{bmatrix} \lambda_1(t) & & 0 \\ & \ddots & \\ 0 & & \lambda_m(t) \end{bmatrix} \tag{3.32}$$

The construction of $\Lambda(t)$ and all the properties that were described previously can easily be extended for the matrix case.

Similar analysis can be done for systems with a feedforward term from the controls to the outputs. Consider the system defined by the following equations

$$\dot{\mathbf{x}}(t) = \mathbf{A}\mathbf{x}(t)+\mathbf{B}\mathbf{u}(t) \qquad \mathbf{A} \in \mathbf{R}^{n \times n},\ \mathbf{B} \in \mathbf{R}^{n \times m} \tag{3.33}$$

$$\mathbf{y}(t) = \mathbf{C}\mathbf{x}(t) + \mathbf{D}\mathbf{u}(t) \qquad \mathbf{C} \in \mathbb{R}^{m \times n},\ \mathbf{D} \in \mathbb{R}^{m \times m} \tag{3.34}$$

One can introduce a time-varying gain $\lambda(t)$ so that for any input $\mathbf{u}(t)$ the output $\mathbf{y}(t)$ remain bounded. A similar basic problem can be defined as for the case where $\mathbf{D} = 0$. The construction of $\lambda(t)$ then is modified as follows

Construction of $\lambda(t)$ for the system with a feedforward term (D matrix):

For every time t choose $\lambda(t)$ as follows

a)The largest $\lambda(t)$ such that $\|\mathbf{C}\mathbf{x}(t) + \mathbf{D}\lambda(t)\mathbf{u}(t)\|_\infty \le 1$

b) if $\mathbf{x}(t) \in \mathrm{Bd}\mathbf{B}_{\mathbf{A},\mathbf{C}}$ then choose the largest $\lambda(t)$ such that (3.35)

$$0 \le \lambda(t) \le 1 \tag{3.36}$$

$$\lim_{\varepsilon \to 0} \sup \frac{g(\mathbf{x}(t)+\varepsilon[\mathbf{A}\mathbf{x}(t)+\mathbf{B}\lambda(t)\mathbf{u}(t)]) - g(\mathbf{x}(t))}{\varepsilon} \le 0 \tag{3.37}$$

or for the points where $g(\mathbf{x})$ is differentiable choose the largest $\lambda(t)$ such that

$$0 \le \lambda(t) \le 1 \tag{3.38}$$

$$Dg(\mathbf{x}(t))[\mathbf{A}\mathbf{x}(t)+\mathbf{B}\lambda(t)\mathbf{u}(t)] \le 0 \quad \forall t > 0 \tag{3.39}$$

where $Dg(\mathbf{x}(t))$ is the Jacobian matrix of $g(\mathbf{x}(t))$ as it is given in definition 3.2.

c) if $\mathbf{x}(t) \notin \mathbf{B}_{\mathbf{A},\mathbf{C}}$ then choose $\lambda(t)$, $0 \le \lambda(t) \le 1$ such that the expression in (3.37) is minimum.

When a feedforward term ($\mathbf{D}$ matrix) is present, part (a) of the construction of $\lambda(t)$ is different. Because of the feedforward term one can drive $\|\mathbf{y}(t)\|_\infty > 1$ at every time t just with the controls. The constraint (a) in the construction of $\lambda(t)$ prevents the "large" controls from entering into the system and consequently causing $\|\mathbf{y}(t)\|_\infty > 1$.

3.4 Design of a Time-Varying Rate such that the Outputs of a Linear System are Bounded

Assume that a linear system is defined by the following equations

$$\dot{\mathbf{x}}(t) = \mathbf{A}\mathbf{x}(t) + \mathbf{B}\mathbf{r}(t) \qquad \mathbf{A} \in \mathbb{R}^{n \times n}, \mathbf{B} \in \mathbb{R}^{n \times m} \qquad (3.40)$$

$$\mathbf{y}(t) = \mathbf{C}\mathbf{x}(t) \qquad \mathbf{C} \in \mathbb{R}^{m \times n} \qquad (3.41)$$

The goal here, again, is to keep the outputs of the linear system bounded (i.e. $|y_i(t)| \leq 1 \; \forall$ t, i) for any $\mathbf{r}(t)$. In section 3.3 a time-varying gain was introduced and this problem was solved completely. Here a time-varying-rate will be introduced and a different solution will be obtained. One can modify the inputs to the system $\mathbf{r}(t)$ to $\mathbf{r}_\mu(t)$ with a time-varying rate operator, such that for any input $\mathbf{r}(t)$ the system output $\mathbf{y}(t)$ remains bounded. The new system can be defined as follows (also shown in figure 3.6).

$$\dot{\mathbf{x}}(t) = \mathbf{A}\mathbf{x}(t) + \mathbf{B}\mathbf{r}_\mu(t) \qquad (3.42)$$

$$\dot{\mathbf{r}}_\mu(t) = \mu(t)\,(\,\mathbf{r}(t) - \mathbf{r}_\mu(t)\,) \qquad (3.43)$$

$$\mathbf{y}(t) = \mathbf{C}\mathbf{x}(t) \qquad (3.44)$$

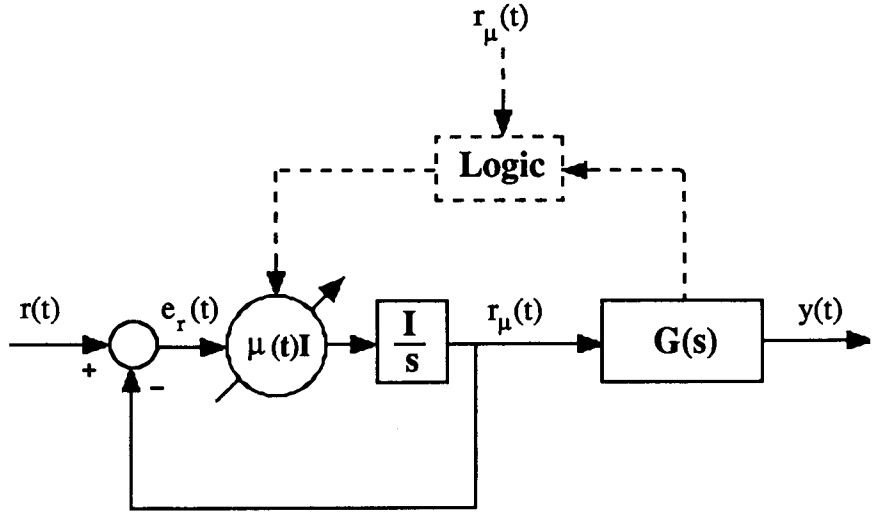

Figure 3.6: The basic system for calculating $\mu(t)$.

Now a basic problem for this case can be defined.

***The Basic Problem*:**

At time t_0 find, if possible, the maximum time-varying rate $\mu(t_0)$, $0 \leq \mu(t_0) \leq \infty$, such that $\forall r(t)$, $t > t_0$ $\exists$ $\mu(t)$, $t > t_0$ such that the output will satisfy $|y_i(t)| \leq 1$ $\forall$ i, $t > t_0$.

Define the following auxiliary system

$$\dot{\mathbf{x}}(t) = \mathbf{A}\mathbf{x}(t)+\mathbf{B}\mathbf{r}_\mu(t) \tag{3.45}$$

$$\dot{r}_\mu(t)=\mu(t)e_r(t) \tag{3.46}$$

$$\mathbf{y}(t) = \mathbf{C}\mathbf{x}(t) \tag{3.47}$$

and with $\mathbf{x}_a(t) = [\ \mathbf{x}(t) \quad r_\mu(t)\ ]^T$ one can obtain the following augmented system

$$\dot{x}_a(t) = A_a x_a(t) + B_a \mu(t) e_r(t) \qquad A_a \in R^{n+m \times n+m},\ B_a \in R^{n+m \times m} \tag{3.48}$$

$$y(t) = C_a x_a(t) \qquad C_a \in R^{m \times n+m} \tag{3.49}$$

The system (3.48)-(3.49) is similar to the system (3.16)-(3.17) if the $\lambda(t)$ is replaced by $\mu(t)$, the only difference is the fact that the $\mu(t) \in [0,\infty]$ whereas $\lambda(t) \in [0,1]$.

To obtain the solution to the basic problem we define a function $g(x)$ for the system (3.48)-(3.49) for $B_a = 0$ and a set $B_{A,C}$ as it was described in section 3.2.

$$g(x_{a0}):\ R^{n+m} \rightarrow R, \quad g(x_0) = \| y(x_{a0},t) \|_\infty \tag{3.50}$$

$$x_a(0) = x_{a0}, \tag{3.51}$$

$$B_{A,C} = \{ x:\ g(x) \leq 1 \} \tag{3.52}$$

For the function $g(x)$ to be finite for all $x \in R^n$ the original system (3.40)-(3.41) has to be such that the augmented system (3.48)-(3.49) is **neutrally stable**.

Construction of $\mu(t)$:

For every time t choose $\mu(t)$ as follows

a) if $\mathbf{x}_a(t) \in \text{Int}\mathbf{B}_{A,C}$ then $\mu(t) = \infty$ which implies that $\mathbf{r}(t) = \mathbf{r}_\mu(t)$ (3.53)

b) if $\mathbf{x}_a(t) \in \text{Bd}\mathbf{B}_{A,C}$ then choose the largest $\mu(t)$ such that (3.54)

$$0 \le \mu(t) \le \infty$$

$$\lim_{\varepsilon \to 0} \sup \frac{g\left(\mathbf{x}_a(t)+\varepsilon[\mathbf{A}_a\mathbf{x}_a(t)+\mathbf{B}_a\mu(t)\mathbf{e}_r(t)]\right) - g\left(\mathbf{x}_a(t)\right)}{\varepsilon} \le 0 \tag{3.55}$$

or for the points where g(x) is differentiable choose the largest $\mu(t)$ such that

$$0 \le \mu(t) \le \infty \tag{3.56}$$

$$Dg(\mathbf{x}_a(t))[\mathbf{A}_a\mathbf{x}_a(t)+\mathbf{B}_a\mu(t)\mathbf{e}_r(t)] \le 0 \quad \forall\, t > 0 \tag{3.57}$$

where $Dg(\mathbf{x}_a(t))$ is the Jacobian matrix of $g(\mathbf{x}_a(t))$ as in definition 3.2.

c) if $\mathbf{x}_a(t) \notin \mathbf{B}_{A,C}$ then choose $\mu(t)$, $0 \le \mu(t) \le \infty$ such that the expression (3.55) is minimum.

The proofs of the following theorems parallel those of section 3.3. By changing $\lambda(t)$ to $\mu(t)$, and $\mathbf{u}(t)$ to $\mathbf{e}_r(t)$ all the proofs are identical. The fact that $\lambda(t) \in [0,1]$ but $\mu(t) \in [0,\infty]$ is not important, for the proofs, because is not used in any of them.

Theorem 3.10:

For the system given in (3.48)-(3.49) and the given construction of $\mu(t)$ the following is always true $\forall x_a \in \mathbb{R}^{n+m}$.

$$\lim_{\varepsilon \to 0} \sup \frac{g(x_a(t)+\varepsilon[A_a x_a(t)]) - g(x_a(t))}{\varepsilon} \leq 0 \qquad (3.58)$$

and at the points where g(x) is differentiable

$$Dg(x_a)\, A_a x_a \leq 0 \qquad \forall x_a \in \mathbb{R}^{n+m} \qquad (3.59)$$

where $Dg(x_a(t))$ is the Jacobian matrix of $g(x_a(t))$ as in definition 3.2.

The construction of $\mu(t)$ is always possible because of theorem 3.10 , namely one can choose $\mu(t) = 0\ \forall t$ and the inequality (3.55) is always true.

Lemma 3.3:

In the system (3.48)-(3.49) if $x_{a0} \in \mathbf{B}_{A,C}$ and $\mu(t)$ is constructed as it was described above the states $x_a(t)$ of the system belong to $\mathbf{B}_{A,C}$ (i.e. $x_a(t) \in \mathbf{B}_{A,C}$) for all t and for all r(t).

Theorem 3.10:

For the system (3.48)-(3.49) with $\mu(t)$ constructed as above the following is always true

if $x_{a0} \in \mathbf{B}_{A,C}$ then $\|y(t)\|_\infty \leq 1$ $\forall$input r(t)

if $x_{a0} \notin \mathbf{B}_{A,C}$ then $\|y(t)\|_\infty \leq g(x_{a0})$ $\forall$input r(t)

Theorem 3.11:

At every time t_0, if $\mathbf{x_a}(t_0) \in \mathbf{B_{A,C}}$, then the time-varying gain $\mu(t_0)$ is the maximum possible such gain so that $0 \leq \mu(t_0) \leq \infty$, and $\forall \mathbf{r}(t)$, $t > t_0$ $\exists$ $\mu(t)$, $t > t_0$ such that the output $|y_i(t)| \leq 1$ $\forall$ i, $t > t_0$. If $\mathbf{x_a}(t_0) \notin \mathbf{B_{A,C}}$ then such a gain $\mu(t_0)$ does not exist.

3.5 Introduction to the New Design Methodology

In sections 3.3 and 3.4 two basic problems were solved. In section 3.3 it was shown how to design a time-varying gain $\lambda(t)$ so that the output of a linear system remains bounded. In chapter 4 the time-varying gain will be used as an Error Governor EG (as shown in figure 3.7) to significantly improve the performance of the closed loop system by keeping the controls $\mathbf{u}(t)$ bounded. In fact, the Error Governor will guarantee that the controls never saturate.

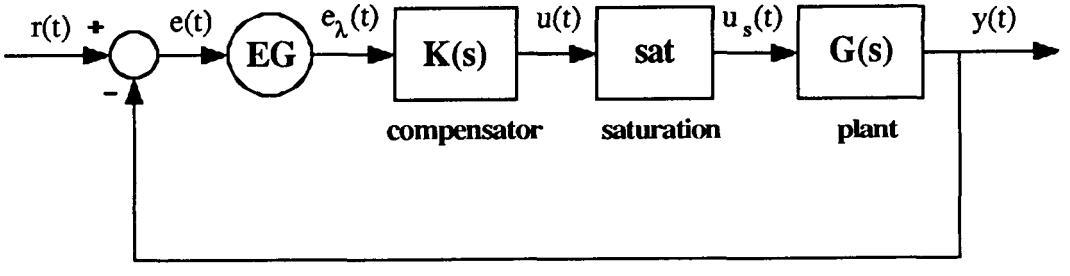

Figure 3.7: Control structure with the EG operator

Another control structure that also ensures that the control $\mathbf{u}(t)$ will never saturate is shown in figure 3.8. In chapter 5 the time-varying rate, introduced in section 3.4, will be used as a Reference Governor (RG). In chapter 5 we also present a third control structure which

utilizes both the EG and RG operators (not shown here).

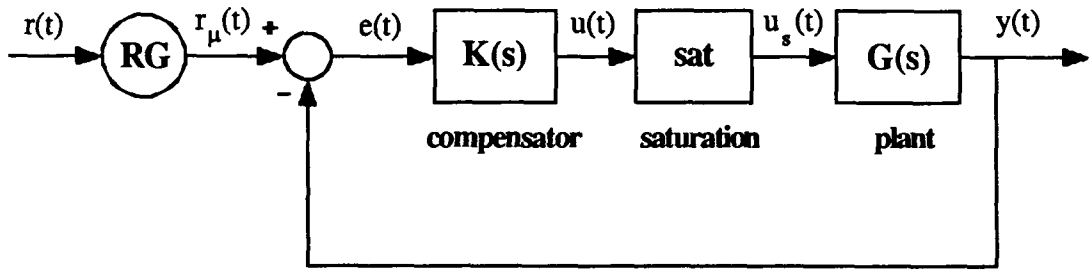

Figure 3.8: Control structure with the RG operator

Table 3.1 shows the potential applications of the different control structures. The intention here is not to give a complete description of the new design methodology but rather to give an overview on where one could use the control structures.

Table 3.1: Application of the control structures with the EG and RG operators

	Neutrally stable compensator	**Unstable compensator**
Stable plant	Control structure with EG Control structure with RG Control structure with RG and EG	Control structure with RG
Unstable plant	Control structure with RG Control structure with RG and EG	Control structure with RG

3.6 Concluding Remarks

In this chapter some necessary mathematical preliminaries were introduced which will be used to define the new design methodology. Two basic problems were posed and solved.

In the first problem, a time-varying gain was defined so that for any input in a linear system, if that input is multiplied by the time-varying gain, the output of the system will remain bounded.

In the second problem a time-varying rate was designed limiting the input rate such that for any input the output of the linear system remains bounded.

The solutions to these two problems will be the basis for the new design methodology which will be presented in chapters 4 and 5.

CHAPTER 4
CONTROL STRUCTURE WITH THE OPERATOR EG

4.1 Introduction

In section 2.3 (performance analysis) the need for an operator EG and/or an operator RG to achieve better control system performance was shown. In section 3.3, it was shown how to choose a time varying gain $\lambda(t)$, at the inputs of a linear time invariant system, such that the outputs of that system will remain bounded. In this chapter, we combine the results of sections 2.3 and 3.3 to obtain, a control structure with an EG operator (i.e. a time gain-varying gain). This structure will be introduced and analyzed. With the EG operator at the error signal, the system will remain unaltered (linear) when the references and disturbances are such that they don't cause saturation. For "large" reference and disturbance signals the operator EG will ensure that the controls will never saturate. This control structure is useful for feedback systems with stable open loop plants and neutrally stable linear compensators.

The new control structure has inherent good properties (stability, no reset windups etc.) which will be discussed and demonstrated in simulations of two examples. The examples chosen are an academic example (with pathological directional properties) and a model of the F8 aircraft longitudial dynamics.

4.2 Description of the Control Structure with the Operator EG

Consider a feedback control system with a linear plant $\mathbf{G}(s)$, a linear compensator $\mathbf{K}(s)$ and a magnitude saturation at the controls. The plant and the compensator are modelled by the following state space representations:

Plant:
$$\dot{\mathbf{x}}(t) = \mathbf{A}\mathbf{x}(t) + \mathbf{B}\mathbf{u}_s(t) \tag{4.1}$$
$$\mathbf{y}(t) = \mathbf{C}\mathbf{x}(t) \tag{4.2}$$

$$\mathbf{u_s}(t) = \text{sat}(\mathbf{u}(t)) \tag{4.3}$$

Compensator:

$$\dot{\mathbf{x}}_c(t) = \mathbf{A_c x_c}(t) + \mathbf{B_c e}(t) \tag{4.4}$$

$$\mathbf{u}(t) = \mathbf{C_c x_c}(t) \tag{4.5}$$

$$\mathbf{e}(t) = \mathbf{r}(t) - \mathbf{y}(t) \tag{4.6}$$

where $\mathbf{r}(t)$ is the reference, $\mathbf{u}(t)$ is the control and $\mathbf{y}(t)$ is the output signal.

The compensator can be thought of as an independent linear system with input $\mathbf{e}(t)$ (error signal) and output $\mathbf{u}(t)$ (control signal). The objective is to introduce a time-varying gain $\lambda(t)$ (EG operator) at the error, $\mathbf{e}(t)$, such that the control, $\mathbf{u}(t)$, will never saturate. Following the discussion of section 3.3 the gain, $\lambda(t)$, is injected at the error signal and the resulting compensator is given by

$$\dot{\mathbf{x}}_c(t) = \mathbf{A_c x_c}(t) + \mathbf{B_c}\lambda(t)\mathbf{e}(t) \tag{4.7}$$

$$\mathbf{u}(t) = \mathbf{C_c x_c}(t) \tag{4.8}$$

$$\mathbf{e}(t) = \mathbf{r}(t) - \mathbf{y}(t) \tag{4.9}$$

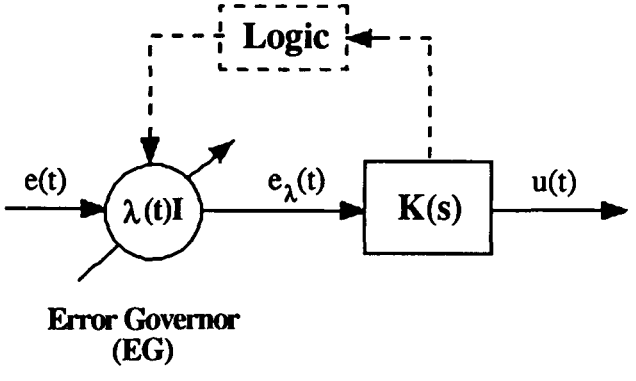

Figure 4.1: The basic system for calculating $\lambda(t)$.

In analogy to figure 3.5, figure 4.1 shows the basic system for computing $\lambda(t)$. A function $g(\mathbf{x})$ and a set $\mathbf{B_{A,C}}$ are defined and then the construction of $\lambda(t)$ follows in accordance

with the results presented in chapter 3.

$$g(x_0):\ g(x_0) = \|u(t)\|_\infty \tag{4.10}$$

where

$$\dot{x}_c(t) = A_c x_c(t); \qquad x_c(0)=x_0 \tag{4.11}$$

$$u(t) = C_c x_c(t) \tag{4.12}$$

$$B_{A,C} = \{x:\ g(x) \le 1\} \tag{4.13}$$

For g(x) to be finite, for all x, **the compensator has to be neutrally stable** (theorem 3.1). This is the reason why the operator EG is to be used only for feedback system with neutrally stable compensators. This is not an overly restrictive constraint because most compensators are usually neutrally stable. With finite g(x) the EG operator is given by

Construction of λ(t) :

For every time t choose λ(t) as follows

a) if $x_c(t) \in \text{Int}B_{A,C}$ then $\lambda(t) = 1$ (4.14)

b) if $x_c(t) \in \text{Bd}B_{A,C}$ then choose the largest λ(t) such that (4.15)

$$0 \le \lambda(t) \le 1$$

$$\lim_{\varepsilon \to 0} \sup \frac{g\left(x_c(t)+\varepsilon[A_c x_c(t)+B_c \lambda(t) e(t)]\right) - g\left(x_c(t)\right)}{\varepsilon} \le 0 \tag{4.16}$$

or for the points where g(x) is differentiable choose the largest λ(t) such that

$$0 \le \lambda(t) \le 1 \tag{4.17}$$

$$Dg(x_c(t))[A_c x_c(t)+B_c \lambda(t) e(t)] \le 0 \quad \forall\, t > 0 \tag{4.18}$$

where $Dg(x_c(t))$ is the Jacobian matrix of $g(x_c(t))$ as in definition 3.2.

c) if $x_c(t) \notin B_{A,C}$ then choose λ(t), $0 \le \lambda(t) \le 1$ such that the expression (4.16) is minimum.

From the results in section 3.3 it can be proven that if, at time t = 0, the compensator states, $\mathbf{x}_c(t)$, belong in the $\mathbf{B}_{A,C}$ set, then the EG operator exists and the signal $\mathbf{u}(t)$ remains bounded for any signal $\mathbf{e}(t)$. Hence, the controls will never saturate for any reference, any input disturbance, and any output disturbance.

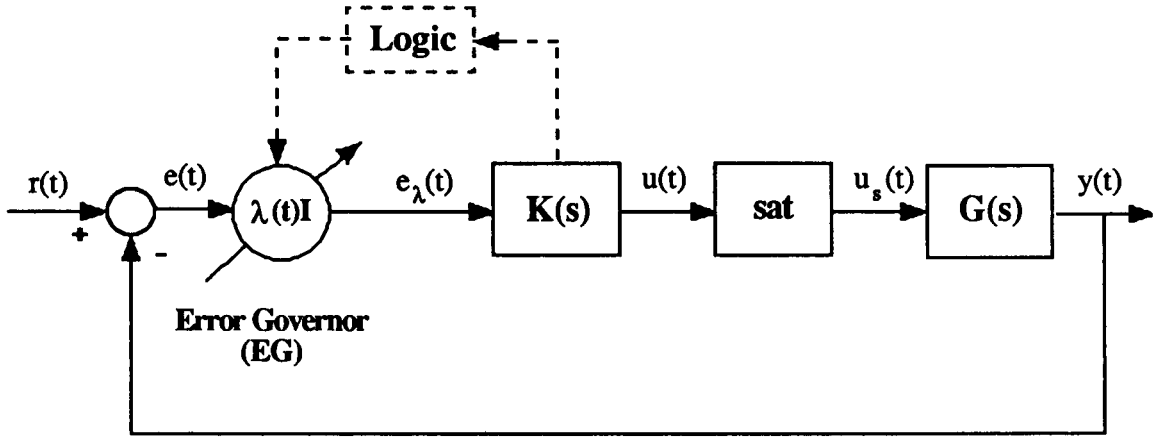

Figure 4.2: Control structure with the EG operator.

Figure 4.2 shows the control structure obtained with the operator EG at the error signal. With this control structure the feedback system will never suffer from the reset windup problems which occur when open loop integrators or "slow" poles are present. The reason for the absence of reset windups is that the Error Governor will prevent any states associated with integrators or the "slow" poles from reaching a value which will cause the controls to exceed the saturation limits.

Another important property of the new control structure, is that the saturation does not alter either the direction of the control vector or the magnitude of the controls. Thus, if the compensator inverts part of the plant the saturation does not alter the inversion process.

4.2.1 Stability Analysis for the Control System with the EG

When the plant is stable and the compensator includes the EG operator the following theorem can be proven.

Theorem 4.1:

The feedback system with a stable plant given by eqs. (4.1)-(4.3) and a compensator given by eqs.(4.7)-(4.9) is finite gain stable.

Proof:

$\exists r_0 \ni \|r\|_\infty \le r_0 \Rightarrow \|u\|_\infty \le 1$

if $\|r\|_\infty \le r_0$ then $\lambda(t) = 1$ and the linear system is stable, thus finite gain stable

$\exists y_0 \ni \|y\|_\infty \le y_0 \ \forall r(t)$ because G(s) is stable with bounded inputs

if $\|r\|_\infty > r_0$ then $\|y\|_\infty \le (\|r\|_\infty / r_0) y_0$ and $\|y\|_\infty \le (y_0/r_0)\|r\|_\infty$

Thus, for $k = (y_0/r_0)$ then $\|y\|_\infty \le k\|r\|_\infty$

////

Every stable system G(s) with bounded inputs is BIBO stable because the outputs are always bounded. The system in figure 4.1 is finite gain stable because in addition to being BIBO stable it is known that there exists a class of "small" inputs, $\|r(t)\|_\infty \le r_0$, for which the system remains linear.

For unstable plants one cannot guarantee closed loop stability because when $\lambda(t) = 0$ the system operates open loop. This is the reason why the control structure with the EG should be used for feedback systems with stable open loop plants (see table 3.1).

For stable plants the closed loop system remains finite gain stable in the presence of any input and/or output disturbance. This is true because the controls never saturate for any input and/or output disturbance. In addition, it is easy to see that the closed loop system will remain finite gain stable for any stable unmodelled dynamics. In fact, the controls will never saturate if the model is replaced by the "true" stable plant; thus, integrator windups and/or control direction problems cannot occur.

4.2.2 Computation of the Operator EG

In this section the actual computation of $\lambda(t)$ and some implementation issues will be discussed. There are two fundamentally different ways to compute $\lambda(t)$; in one method the computation is performed mostly **on-line** and in the other method most of the computation is performed **off-line**. As discussed previously, the time varying-gain was incorporated in the compensator model and the modified compensator was given by the following

$$\dot{\mathbf{x}}_c(t) = \mathbf{A}_c\mathbf{x}_c(t) + \mathbf{B}_c\lambda(t)\mathbf{e}(t), \qquad \mathbf{x}_c(t)\in \mathbb{R}^n, \mathbf{e}(t)\in \mathbb{R}^n \tag{4.19}$$

$$\mathbf{u}(t) = \mathbf{C}_c\mathbf{x}_c(t) \qquad \mathbf{u}(t)\in \mathbb{R}^n \tag{4.20}$$

Also assume that to implement the compensator a discrete difference equation, with integration step of Δt, which approximates the differential equation (4.19)-(4.20) is obtained. The model of the approximate discrete system is assumed to be the following

$$\mathbf{x}_c((n+1)\Delta t) = \mathbf{F}\mathbf{x}_c(n\Delta t) + \mathbf{G}\lambda(n\Delta t)\mathbf{e}(n\Delta t) \tag{4.21}$$

$$\mathbf{u}(n\Delta t) = \mathbf{C}_c\mathbf{x}_c(n\Delta t) \tag{4.22}$$

The objective here is to discuss the implementation of $\lambda(t)$ and its discrete time approximation $\lambda(n)$. The intention is not to give the "best" algorithm for computing or approximating $\lambda(t)$, but rather to give a feeling on what the issues are in constructing $\lambda(t)$. More research is needed to find efficient and computationaly robust algorithms.

First, a computation that is performed mostly **on-line** is possible and is given by the following steps.

STEP 1: Quantization of $\lambda(t)$:

At every time t_0, the time-varying gain $\lambda(t)$ is such that $0 \le \lambda(t) \le 1$. Because of

computational limitations one must quantitize the segment [0,1] with M points ($\lambda_1, \ldots, \lambda_M$).

STEP 2: Calculation of $\lambda(n\Delta t)$:

To compute $\lambda(n\Delta t)$ one has to compute $g(\mathbf{x})$. This computation of $g(\mathbf{x})$ can be done directly or indirectly. Form the definition of $g(\mathbf{x})$ (definition 3.1) one can conclude that the following is true:

$$g(\mathbf{x}(0)) = \|\mathbf{C}_c e^{\mathbf{A}_c t}\mathbf{x}_c(0)\|_\infty \approx \max_{n=1,2,\ldots} \|\mathbf{C}_c \mathbf{F}^n \mathbf{x}_c(0)\|_\infty \tag{4.23}$$

In the direct computation of $g(\mathbf{x})$ the $\mathbf{C}_c\mathbf{F}^n$ is stored and for any vector $\mathbf{x}_c(0)$ the function $g(\mathbf{x})$ can be computed. At every time $n_0\Delta t$, the error vector $\mathbf{e}(n_0\Delta t)$ and the states of the compensator $\mathbf{x}_c(n_0\Delta t)$ are known exactly. Then

- if $g(\mathbf{x}_c(n_0\Delta t)) < 1$ we set $\lambda(n_0\Delta t) = 1$.
- if $g(\mathbf{x}_c(n_0\Delta t)) = 1$ we compute the following quantity

$$z = \{g(\mathbf{F}\mathbf{x}_c(n_0\Delta t) + \mathbf{B}_c\lambda_i\mathbf{e}(n_0\Delta t)) - g(\mathbf{x}_c(n_0\Delta t))\} \tag{4.24}$$

The idea is to search (e.g. binary search) through all the λ_i's to find the maximum λ_i such that $z \le 0$. Then use that the max λ_i as $\lambda(n_0\Delta t)$.

- if $g(\mathbf{x}_c(n_0\Delta t)) > 1$ then search through all the λ_i's and use that λ_i which minimizes z as $\lambda(n_0\Delta t)$.

One can compute $g(\mathbf{x})$ indirectly. At every time $n_0\Delta t$ simulate the system (4.21)-(4.22) by using the vector $\mathbf{x}_c(n_0\Delta t)$ as an initial condition, the following input vector

$$\mathbf{e}(n\Delta t) = \begin{cases} \mathbf{e}(n_0\Delta t) & \text{for} \quad n = n_0 \\ \mathbf{0} & \text{for} \quad n > n_0 \end{cases} \tag{4.25}$$

and $\lambda(n_0\Delta t) = \lambda_i$, for some i.

We want the maximum, for all n, of $\|\mathbf{u}(n\Delta t)\|_\infty$ not to exceed the saturation limits. Thus, choose as $\lambda(n_0\Delta t)$ the maximum λ_i to satisfy that.

Most of the computations of $\lambda(t)$ in this thesis, for the simulations, were done on-line by computing $\lambda(t)$ indirectly as specified previously. By using parallel processing it seems possible to compute $g(\mathbf{x})$ directly even for systems with large number of states.

Another computation, performed mostly **off-line**, is possible and is given by following.

STEP 1: Computation of the function $g(\mathbf{x})$:

One can compute the function $g(\mathbf{x})$ using "brute force". Consider an n^{th} dimensional hypershere and define a quantization with N points $(\mathbf{x}_{c1}, \ldots, \mathbf{x}_{cN})$. Then by using $\mathbf{x}_{ci}$ as an initial condition, one can find $g(\mathbf{x}_{ci})$, for all i, as follows:

$$\dot{\mathbf{x}}_c(t) = \mathbf{A}_c\mathbf{x}_c(t), \qquad \mathbf{x}_c(0) = \mathbf{x}_{ci}, \tag{4.26}$$

$$\mathbf{u}(t) = \mathbf{C}_c\mathbf{x}_c(t) \tag{4.27}$$

$$g(\mathbf{x}_{ci}) = \|\mathbf{u}(t)\|_\infty \tag{4.28}$$

The function $g(\mathbf{x})$ is defined at N points and one can use approximation theory to obtain a closed form expression from N points on the n^{th} dimensional hypersphere [41],[42]. Sometimes it may be difficult to obtain a closed form expression for $g(\mathbf{x})$; in such a case, the $g(\mathbf{x}_i)$, for all i, can be stored and then for any other vector $v \in \mathbb{R}^n$ one can find the closest (in the Euclidean norm sense) collinear vector $\alpha\mathbf{x}_i$ to v and use $g(\alpha\mathbf{x}_i)$ as an approximation to $g(\mathbf{v})$. Since $g(\mathbf{x})$ is a cone the function is known for any vector collinear to $\mathbf{x}_i$, $(\alpha\mathbf{x}_i, \alpha \in \mathbb{R})$; Namely, $g(\alpha\mathbf{x}_i) = \alpha g(\mathbf{x}_i)$.

If the dimension of the compensator is large an approximate $g(\mathbf{x})$ should be considered. For example, in the sequel an ellipse is used to approximate $g(\mathbf{x})$ for the academic example in section 4.2.3.

More research is needed to determine how to choose the value of N so that the quantization points are "enough" and to determine smart ways to approximate g(**x**).

STEP 2: Quantization of $\lambda(t)$:

At every time t_0, the time-varying gain $\lambda(t)$ is such that $0 \le \lambda(t) \le 1$.Because of computational limitations one must quantize the segment [0,1] with M points $(\lambda_1, \ldots, \lambda_M)$.

STEP 3: Calculation of $\lambda(n\Delta t)$:

This is an on-line computation. At every time $n_0\Delta t$, the error vector $\mathbf{e}(n_0\Delta t)$ and the states of the compensator $\mathbf{x_c}(n_0\Delta t)$ are known exactly. Then

- if $g(\mathbf{x_c}(n_0\Delta t)) < 1$ then $\lambda(n_0\Delta t) = 1$.
- if $g(\mathbf{x_c}(n_0\Delta t)) = 1$ then compute the following quantity

$$z = \{g(\mathbf{F}\mathbf{x_c}(n_0\Delta t)+\mathbf{B_c}\lambda_i\mathbf{e}(n_0\Delta t)) - g(\mathbf{x_c}(n_0\Delta t))\} \qquad (4.29)$$

  The idea is to search (e.g. binary search) through all the λ_i's to find the maximum λ_i such that $z \le 0$. Then use the max λ_i as $\lambda(n_0\Delta t)$.
- if $g(\mathbf{x_c}(n_0\Delta t)) \ge 1$ then search through all the λ_i's and find the λ_i that minimizes z (eq. 4.29) and use it as $\lambda(n_0\Delta t)$.

Two methods for computing $\lambda(t)$ were described. Although, the methods were direct application of the theory and better methods may be possible, one can draw the following conclusions.

In the first method (**on-line** calculations) the computation of g(**x**) is very accurate. Thus if M is large the computation of $\lambda(t)$ is "almost" exact. This is true because the compensator is known exactly (no modelling errors). The implementation of the method is simple and for low order compensators the calculations are fairly fast. For large order compensators, if parallel processing is available, the on-line calculations can also be fast. More research is needed to

explore the applicability of this method.

In the second method (mostly **off-line** calculations) approximations were made for the calculation of g(**x**). For low order compensators it is possible to approximate g(**x**) very well by choosing large number N of points in $\mathbb{R}^n$; for large compensators this may not be possible so approximate g(**x**) are necessary (n dimensional ellipsoids for example). For this case the on-line computation is minimal, even for large M, and accurate.

4.2.3 Simulation of the Academic Example #1

The purpose of this example is to illustrate how the saturation can disturb the directionality of the controls and alter the compensator inversion of the plant. The "academic" plant **G**(s) has two zeros with low damping which the designed compensator **K**(s) cancels. In addition, the compensator does not have any integrators so the windup phenomenon is not expected to occur.

Consider the following state space representation of the plant **G**(s)

$$\dot{\mathbf{x}}(t) = \begin{bmatrix} -1.5 & 1 & 0 & 1 \\ 2 & -3 & 2 & 0 \\ 0 & .5 & -2 & 1 \\ 1 & -1.5 & 0 & -5 \end{bmatrix} \mathbf{x}(t) + \begin{bmatrix} 1 & 0 \\ 0 & 0 \\ 1 & 1 \\ 0 & 1.8 \end{bmatrix} \mathbf{u}_s(t) \qquad (4.30)$$

$$\mathbf{y}(t) = \begin{bmatrix} 0 & 2.4 & -3.1 & 1 \\ 1 & 6 & -.5 & -2.8 \end{bmatrix} \mathbf{x}(t) \qquad (4.31)$$

$$\mathbf{u}_s(t) = \text{sat}(\mathbf{u}(t)) \qquad (4.32)$$

Table 4.1 shows the poles and zeros of the plant **G**(s). Note the location and damping of the zeros.

Table 4.1 Poles and zeros of the plant

Poles

Real	Imaginary	Magnitude	Damping
-5.7678E-01	0.0000E-01	5.7678E-01	1.0000E+00
-2.2460E+00	0.0000E-01	2.2460E+00	1.0000E+00
-2.7222E+00	0.0000E-01	2.7222E+00	1.0000E+00
-5.9550E+00	0.0000E-01	5.9550E+00	1.0000E+00

Zeros

Real	Imaginary	Magnitude	Damping
-5.4404E-01	2.4228E+00	2.4831E+00	2.1909E-01
-5.4404E-01	-2.4228E+00	2.4831E+00	2.1909E-01

2 more infinite

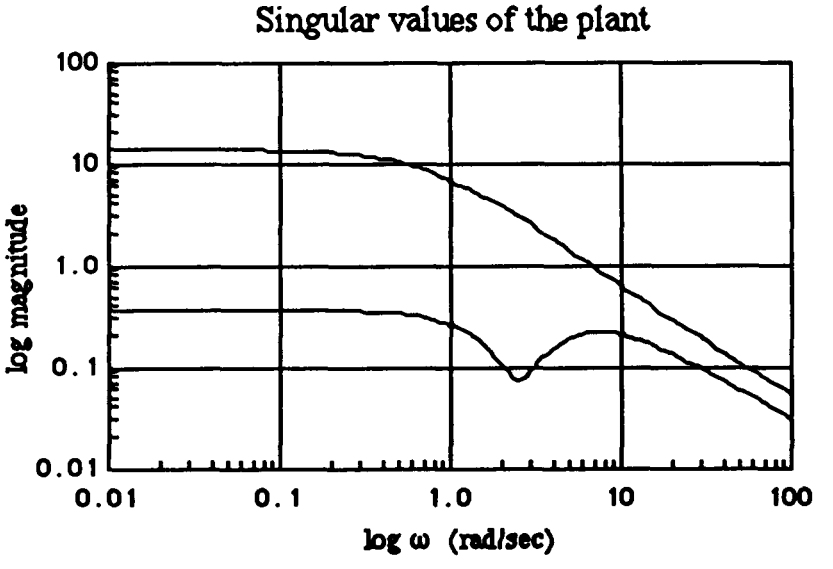

Figure 4.3: Singular values of the plant in the academic example #1.

Figure 4.3 shows the singular values of the open loop plant. Notice the effect of the two resonant zeros of the plant in the singular values at approximately 2.5 rad/sec. A compensator was designed to cancel the two resonant zeros of the plant. The compensator state space representation is given by the following model

$$\dot{\mathbf{x}}_c(t) = \begin{bmatrix} -2.6093 & 1.4180 \\ -7.1476 & 1.5213 \end{bmatrix} \mathbf{x}_c(t) + \begin{bmatrix} -29.8308 & 2.989 \\ -68.7543 & 10.8387 \end{bmatrix} \lambda(t)\, \mathbf{e}(t) \quad (4.33)$$

$$\mathbf{u}(t) = \begin{bmatrix} -1 & 1 \\ 2 & -1 \end{bmatrix} \mathbf{x}_c(t) \quad (4.34)$$

Table 4.2 shows the poles and zeros of the compensator **K**(s) when $\lambda(t) = 1$. The compensator has two states with poles at **-.544 ± j2.422**. The eigenvectors of the poles are collinear with the control direction of the transmission zero of the plant and thus, the compensator cancels the zeros of the plant.

Table 4.2 Poles and zeros of the linear compensator

Poles

Real	Imaginary	Magnitude	Damping
-5.4400E-01	2.4228E+00	2.4831E+00	2.1908E-01
-5.4400E-01	-2.4228E+00	2.4831E+00	2.1908E-01

Zeros

no finite zeros

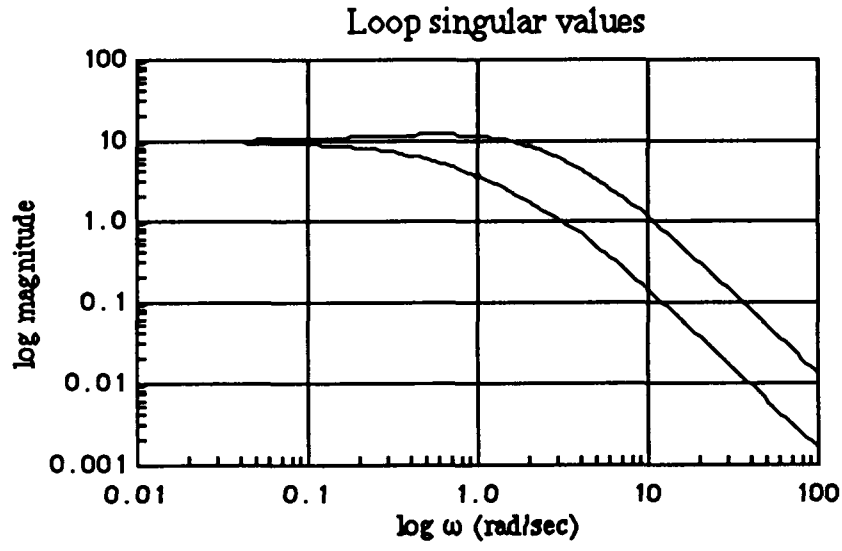

Figure 4.4: Singular values of the loop transfer function in the academic example #1.

Figure 4.4 shows the singular values of the **G(s)K(s)** transfer function matrix. Since the compensator cancels the poorly damped zero the antiresonance present in figure 4.3 is not present in figure 4.4. Also, the compensator is designed so that the singular values of the **G(s)K(s)** transfer function matrix are matched at low frequencies and thus, it is expected that the response of the system is similar for low frequency references in all directions. Integrators are not present in the loop and windup problems are not expected.

In this example, the saturation can disturb the cancellation of the plant zeros by the compensator. Since both the plant and the compensator are stable the control structure with the operator EG can be used to correct the problem. Figure 4.5 shows the closed loop system with the operator EG at the error signals and saturation limits at ± 1.

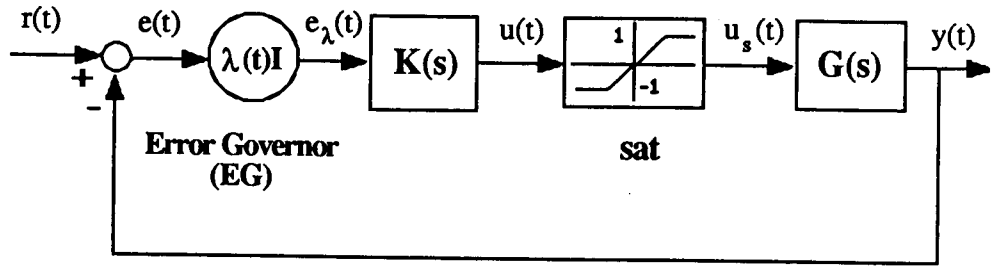

Figure 4.5: Closed loop system for the academic example #1 with the EG.

Three simulations were performed for the closed loop system shown in figure 4.5. These different simulations are as follows:

1) In the first simulation $\lambda(t) = 1$ and $\mathbf{u}(t) = \mathbf{u}_s(t)$. This is a simulation for a linear time invariant closed loop system and is referred to as the simulation for the *linear system.* It is assumed that the compensator **K**(s) was designed so that the linear system would have desirable responses.
2) In the second simulation $\lambda(t) = 1$ and $\mathbf{u}_s(t) = \text{sat}(\mathbf{u}(t))$. This is a simulation where the saturation element is added to the linear system without any other modification. This simulation is referred to as the simulation for the *system with saturation.*
3) In the third simulation $\mathbf{u}_s(t) = \text{sat}(\mathbf{u}(t))$, and $\lambda(t)$ was computed on-line by the method given in section 4.2.2. The computation was performed in approximately three hours using a Macintosh 512K. This type of simulation is referred to as the simulation of the *system with saturation and the EG.*

Figure 4.6 shows the state trajectory of the compensator states for the simulation of the linear system. Note that the states of the compensator do not remain within the $\mathbf{B}_{A,C}$ set so there is a potential for the controls to saturate.

Figures 4.7 and 4.8 show the linear response of the outputs $\mathbf{y}(t)$ and the controls $\mathbf{u}(t)$ respectively. The controls satisfy $\|\mathbf{u}(t)\|_\infty > 1$ at certain times and saturation is expected. It is assumed that the output responses meet the specifications. Thus, we would like the outputs to retain the relative shapes of figure 4.7 when we introduce the nonlinear saturations.

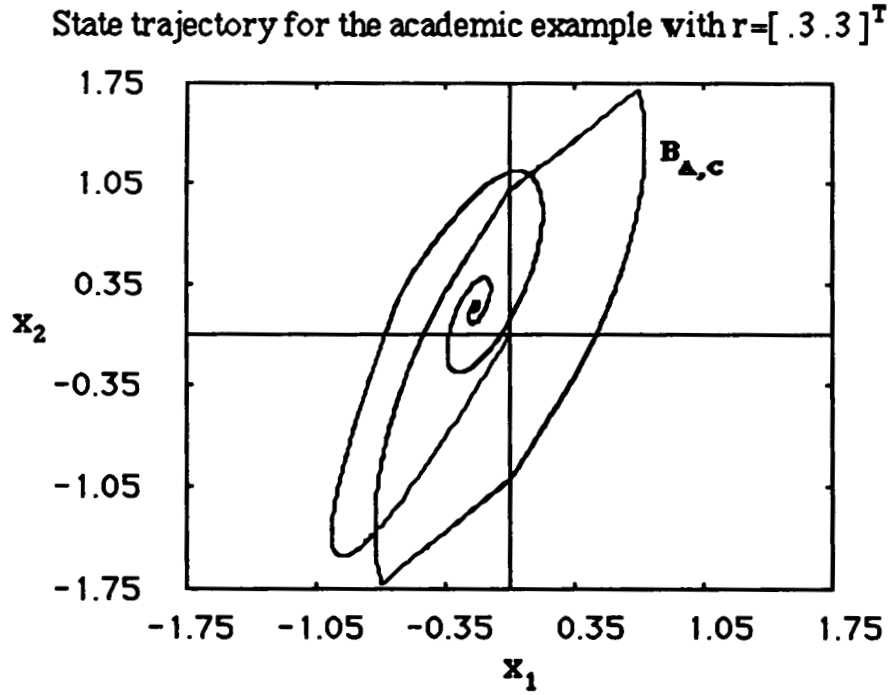

Figure 4.6: State trajectory of the compensator states in the linear system, ($\mathbf{r} = [.3 \quad .3]^T$).

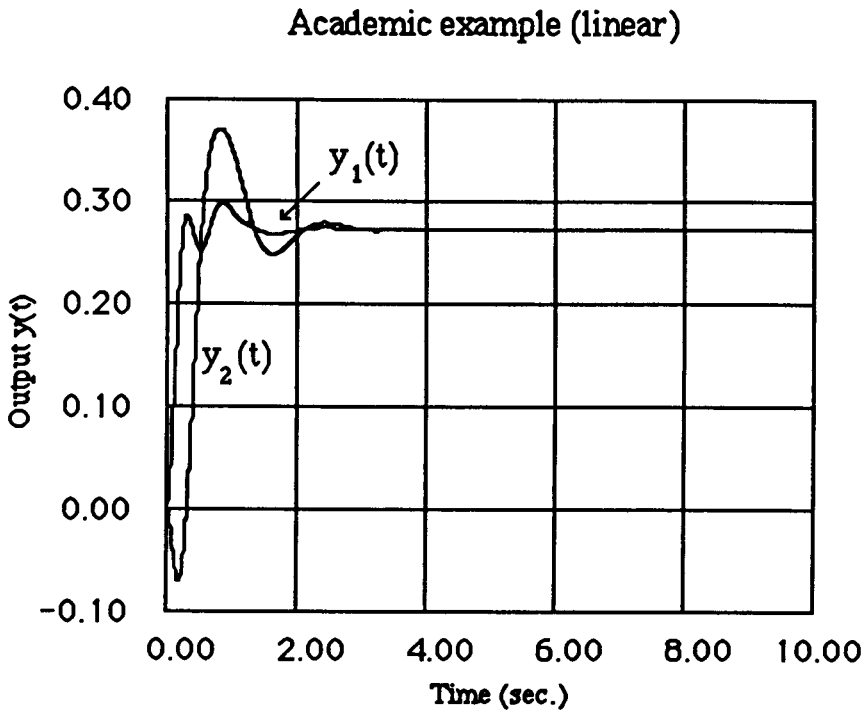

Figure 4.7: Output response for the linear system, ($\mathbf{r} = [.3 \quad .3]^T$).

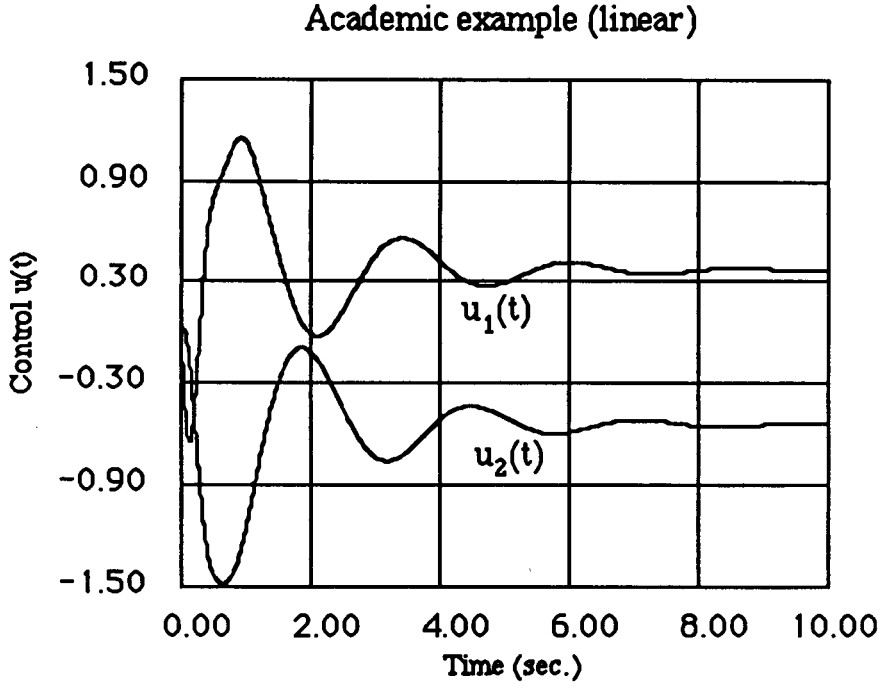

Figure 4.8: Controls in the linear system, ($\mathbf{r} = [.3 \quad .3]^T$).

Figure 4.9 shows the state trajectory of the compensator states for the simulation of the system with saturation, it is clear that he states of the compensator do not remain within the $B_{A,C}$ set. When the controls are saturated the direction of the controls is disturbed and the state trajectory changes dramatically (compare figures 4.6 and 4.9).

Figures 4.10 and 4.11 show the response of the outputs and the controls respectively. The controls have magnitude greater than one and consequently are saturating. In this example, when saturation occurs, the direction of the controls is altered in such a way that even though the original reference is $[\ .3 \quad .3]^T$, the control direction at saturation drives the system towards $[.3 \quad -.3]^T$ resulting in oscillatory behavior. The compensator does not have any integrators to cause windups and the problems in the performance of the system are solely due to the effects of the saturation upon the direction of the control vector.

Comparing the outputs, i.e. figures 4.7 and 4.10, we see that the shapes of the outputs in figure 4.10 do not match those desired and shown in figure 4.7. Thus, in this case the impact of saturation has produced an unacceptable output response.

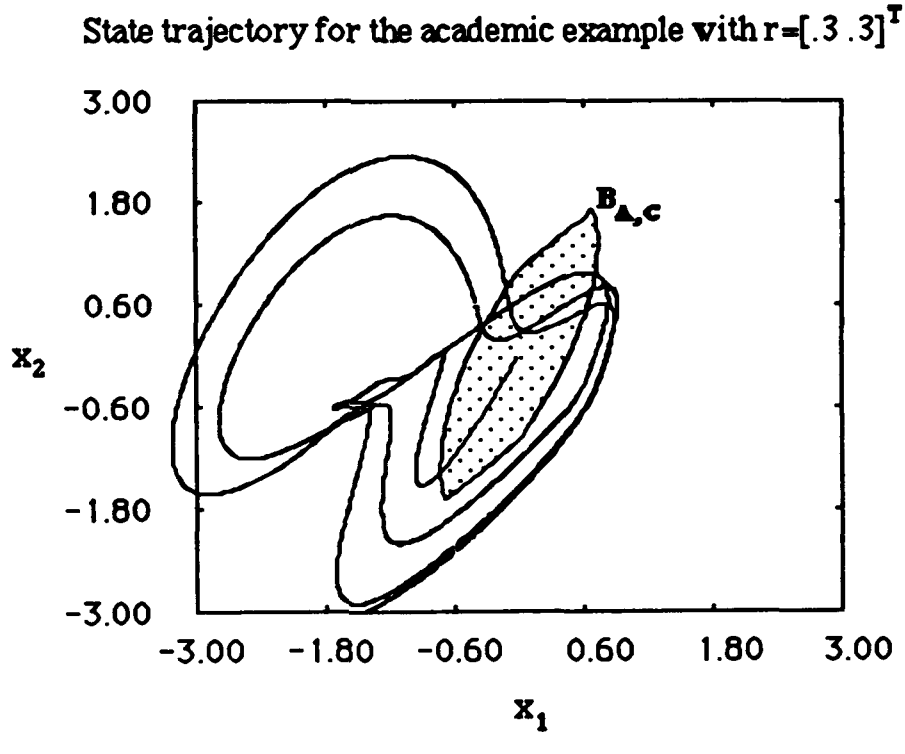

Figure 4.9: State trajectory of the compensator states in the system with saturation, ($\mathbf{r} = [.3 \quad .3]^T$).

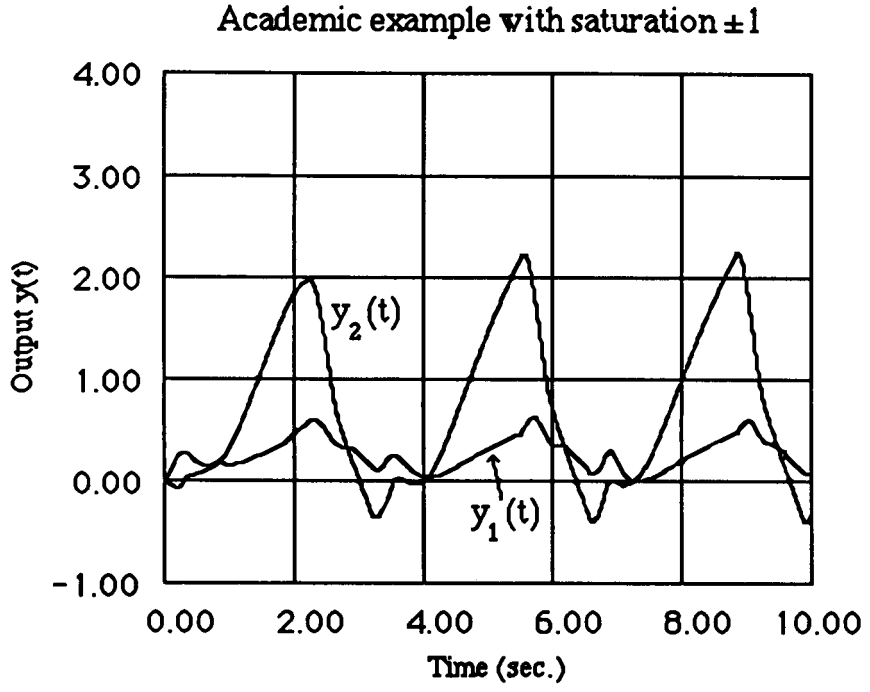

Figure 4.10: Output response for the system with saturation, ($\mathbf{r} = [.3 \quad .3]^T$).

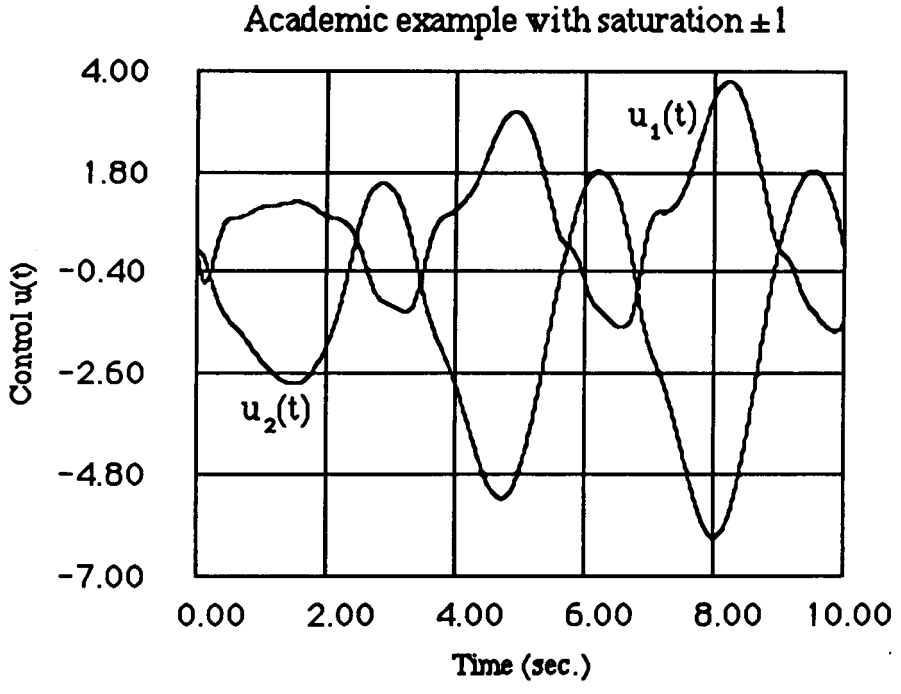

Figure 4.11: Controls in the system with saturation, ($\mathbf{r} = [.3 \quad .3]^T$).

Figure 4.12 shows the compensator state trajectory for the simulation of the system with saturation and the EG operator. The states of the compensator do remain within the $\mathbf{B}_{A,C}$ set so control saturation is not expected. In fact, the state trajectory remains on the boundary of the $\mathbf{B}_{A,C}$ set for a long period of time which implies that the controls will stay at their maximum level for a long period of time.

Figures 4.13 and 4.14 show the response of the outputs and the controls respectively. Note that the controls (the inputs to the saturation operator) do not cause saturation. Also note that when u_2 reaches the value of -1, the control u_1 is reduced to the appropriate level so that both controls will drive the output towards $[.3 \quad .3]^T$ as desired. In effect, it is like having a "smart multivariable saturation" instead of the SISO saturations in each channel. The net effect can be seen easier in the output responses. Comparison of figure 4.13 with figure 4.7, shows that the outputs have similar shapes (as desired), except that the outputs in figure 4.13 are "slower" because the control magnitudes are smaller than those in the linear case (compare figures 4.8 and 4.14).

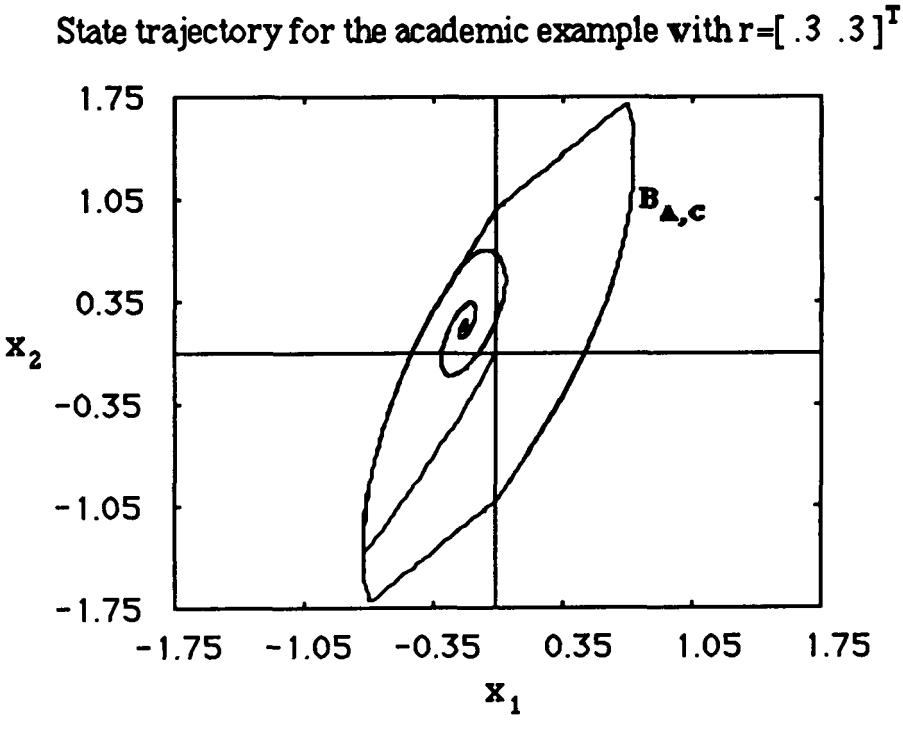

Figure 4.12: State trajectory of the compensator states in the system with saturation and the EG, ($\mathbf{r} = [.3 \quad .3]^T$).

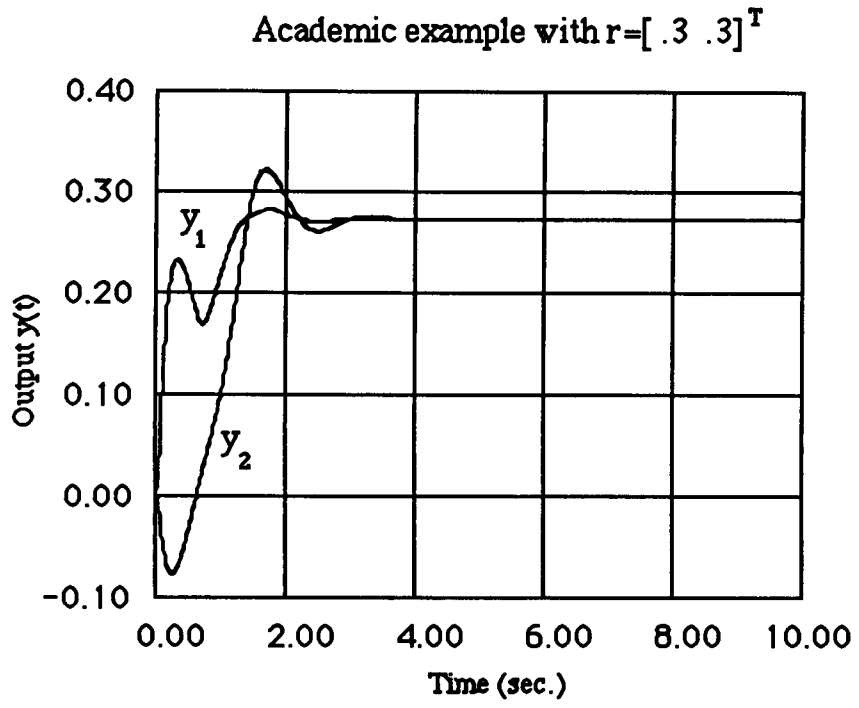

Figure 4.13: Output response for the system with saturation and the EG, ($\mathbf{r} = [.3 \quad .3]^T$).

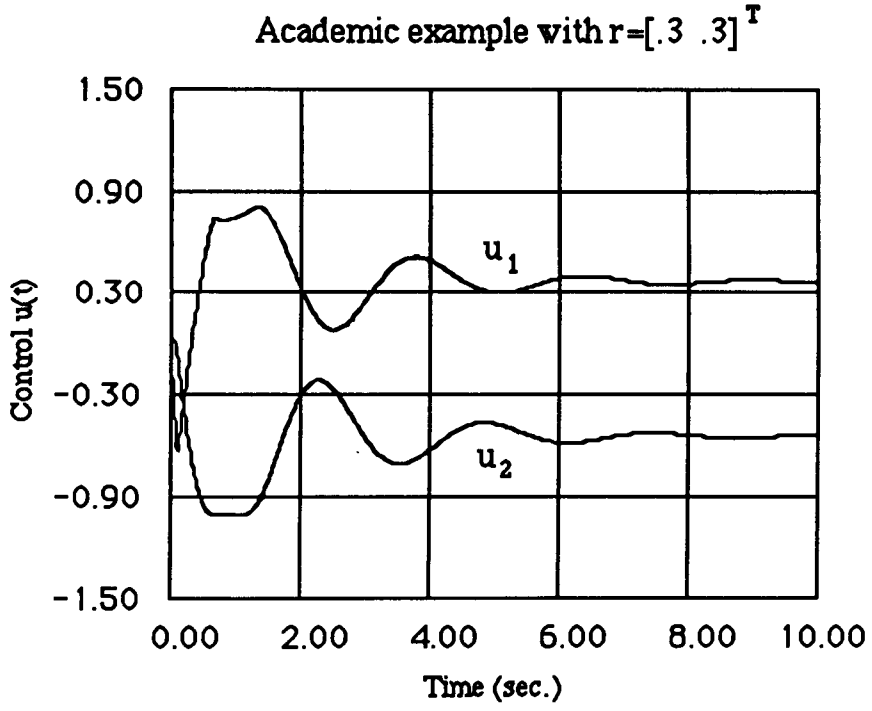

Figure 4.14: Controls in the system with saturation and the EG, ($\mathbf{r} = [.3 \quad .3]^T$).

Figure 4.15 shows the real-time behavior of the gain $\lambda(t)$, computed on-line with the method described in section 4.2.2, and used as the EG operator. At the beginning, $\lambda(t)$ is 1 and the system is linear. When the states of the compensator are such that they may lead the controls to saturate, $\lambda(t)$ becomes zero preventing the large errors to be driven by the compensator. The controls at the same time remain at their maximum possible level ($\|u(t)\|_\infty = 1$). Eventually, $\lambda(t)$ allows the compensator to accept more and more error, while at the same time the controls are kept at maximum level. At the end, $\lambda(t)$ becomes 1 and the system becomes linear time invariant again.

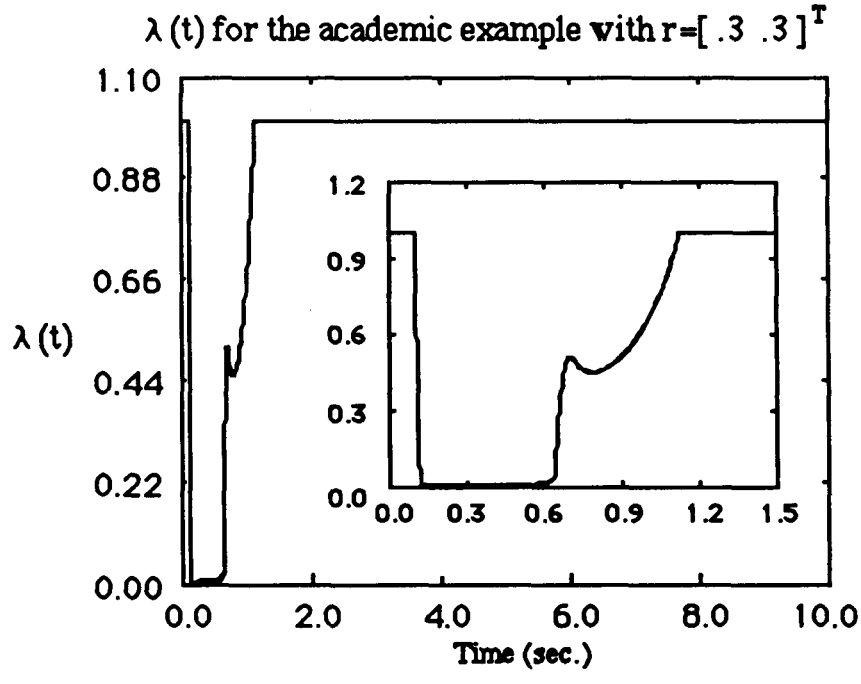

Figure 4.15: $\lambda(t)$ in the system with saturation and the EG, ($\mathbf{r} = [.3 \quad .3]^T$).
Insert: Blowup with $0 \le t \le 1.5$ sec.

Sometimes the exact $\mathbf{B}_{A,C}$ set is difficult to compute and to store in a closed form so approximations may be necessary, especially for compensators of large order. Consider an approximation for the $\mathbf{B}_{A,C}$ set, $\mathbf{B'}_{A,C}$, which is an ellipse given by eq. (3.13). Using this ellipse approximation the same simulation ($\mathbf{r} = [.3 \quad .3]^T$) was performed. Of course, the state

trajectories should not be expected to remain within the approximate $\mathbf{B'}_{A,C}$.

The $\mathbf{B'}_{A,C}$ here was computed off-line (see eq. (3.13)) and then the on-line computation (described in section 4.2.2) of $\lambda(t)$ was minimal. Using the Macintosh 512K the computation for this simulation required only a few minutes.

Figure 4.16 shows the approximate $\mathbf{B'}_{A,C}$ with the state trajectory of the compensator states for the system with saturation and the EG operator. Figure 4.17 shows the actual $\mathbf{B}_{A,C}$, the approximate $\mathbf{B'}_{A,C}$, and the state trajectory of the compensator states. The state trajectory does not remain inside $\mathbf{B}_{A,C}$ for all t and the controls are expected to saturate a bit. The amount that the controls will saturate and the amount that the state trajectory will go outside the $\mathbf{B}_{A,C}$ set depends on how good the approximation is.

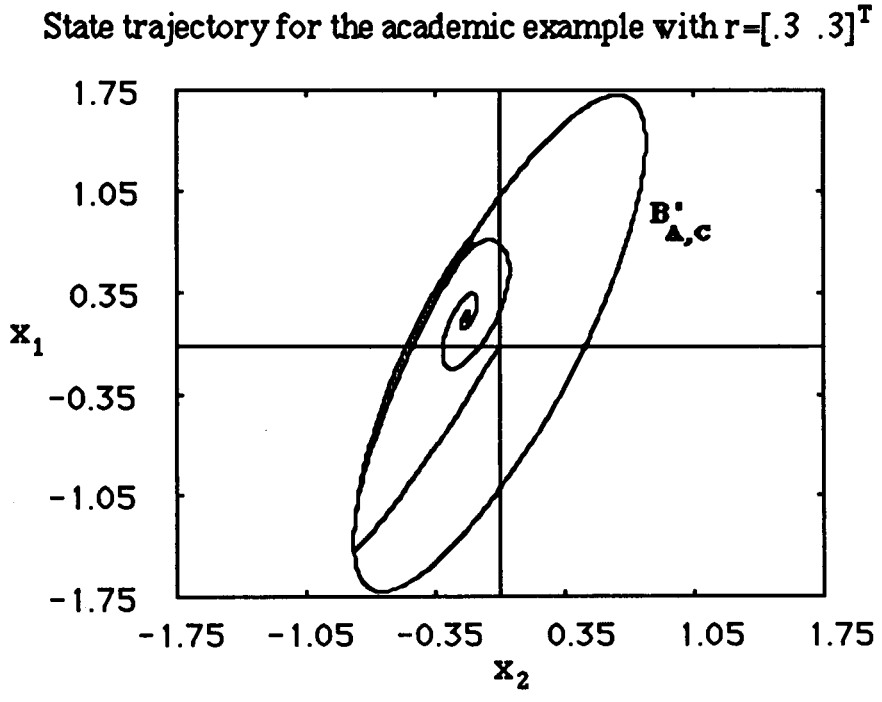

Figure 4.16: State trajectory of the compensator states in the system with saturation and EG using the approximate $\mathbf{B'}_{A,C}$ set, ($\mathbf{r} = [.3 \quad .3]^T$).

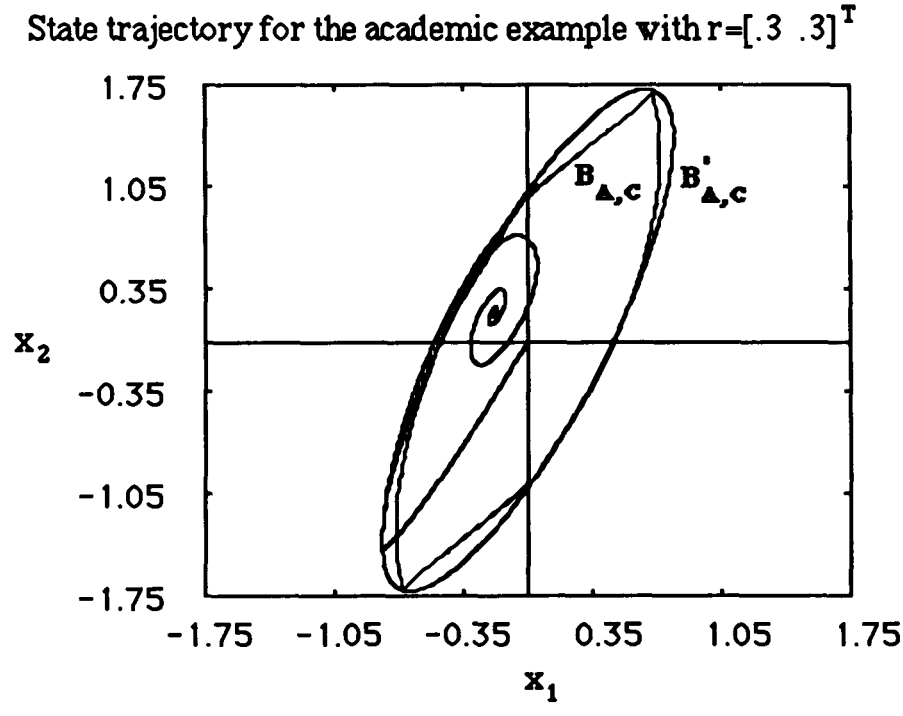

Figure 4.17: State trajectory of the compensator states in the system with saturation and EG using the approximate $\mathbf{B'}_{A,C}$ set, ($\mathbf{r} = [.3 \quad .3]^T$).

Figure 4.18 and figure 4.19 show the output response and the controls for the simulation with $\mathbf{r} = [.3 \quad .3]^T$. By comparing figures 4.13-4.14 with figures 4.18-4.19 one can see that the response of the system with the $\lambda(t)$ computed using the approximate $\mathbf{B'}_{A,C}$ is similar to the response when the actual $\mathbf{B}_{A,C}$ was used. Note that u_2 saturates for a small period of time ($\|u_2(t)\| \approx 1.08$). The amount that the controls exceed the saturation limits depends on how good the approximation of the $\mathbf{B}_{A,C}$ set is. Again, u_1 is reduced when the states of the compensator reach the boundary of $\mathbf{B'}_{A,C}$.

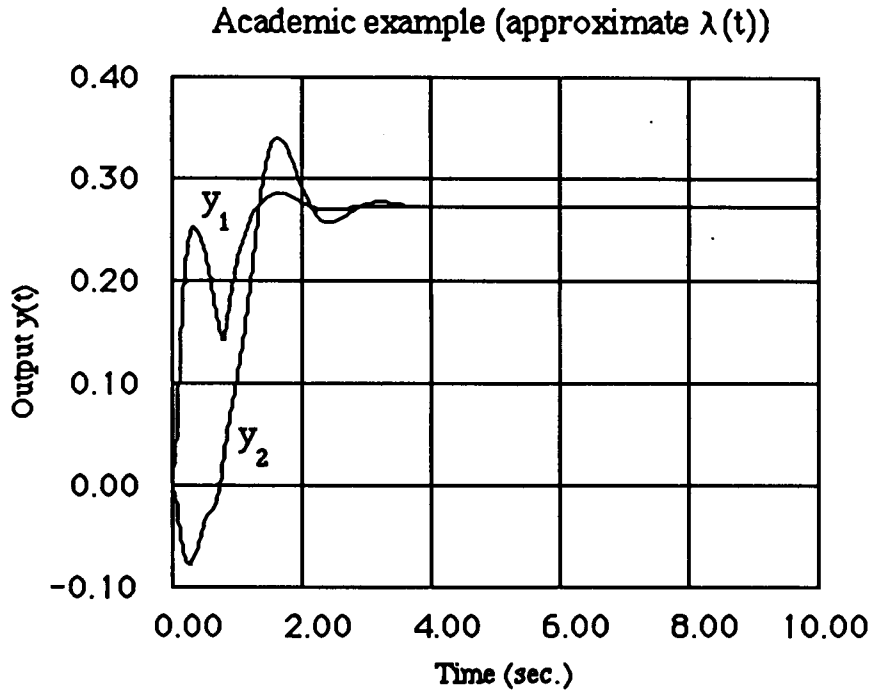

Figure 4.18: Output response for the system
with saturation and EG using the approximate $\mathbf{B'}_{A,C}$ set, ($\mathbf{r} = [.3 \quad .3]^T$).

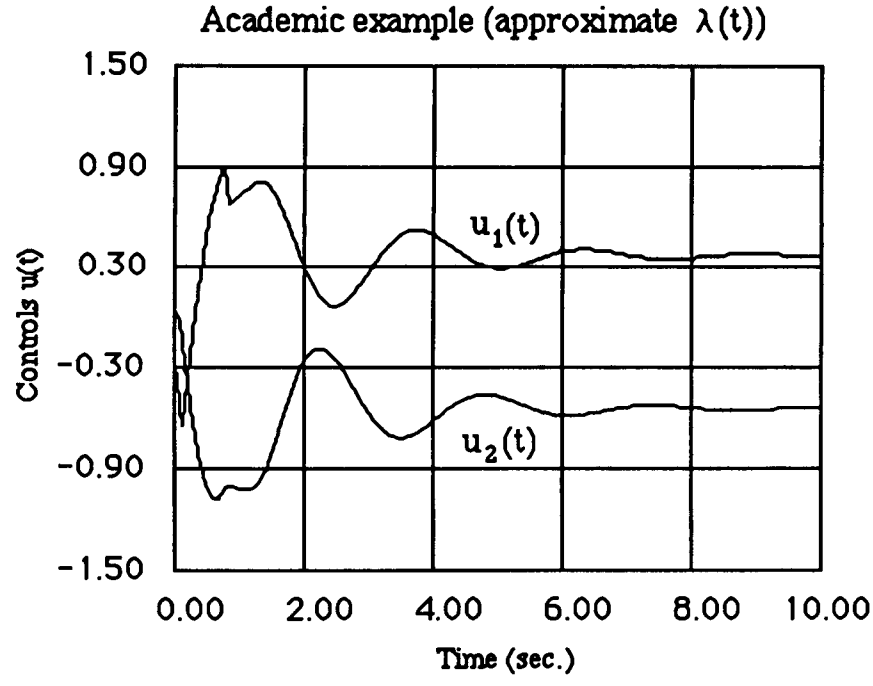

Figure 4.19: Output response for the system
with saturation and EG using the approximate $\mathbf{B'}_{A,C}$ set, ($\mathbf{r} = [.3 \quad .3]^T$).

For the same system, the academic example #1, another simulation was performed with reference $\mathbf{r} = [\,0 \quad 3]^T$.

Figures 4.20 and 4.21 show the outputs and the controls of the linear closed loop system. Again the linear system is assumed to meet all specifications. One can see that the oscillatory mode of the compensator does not show in the output because it is canceled by the plant. The controls do have oscillatory behavior and that is how the compensator cancels the resonant zeros of the plant. This cancellation process is what the multiple saturation prevents and the purpose of this simulation is to illustrate exactly that.

Figures 4.22 and 4.23 show the output and the controls of the system with saturation. It is clear from the responses that the saturation ruins the cancellation of the plant resonant zero from the compensator.

Figures 4.24 and 4.25 show the output and the controls of the system with saturation and the EG operator. By comparing figures 4.20 and 4.21 with figures 4.24 and 4.25 one can see that the response of the system with saturation and the EG is similar in nature (and slower) to the response of the linear system. In this case both u_1 and u_2 reached their maximum allowable value. When this happened, in both cases, the other control was adjusted in a special way to drive the output towards $[0 \quad 3]^T$.

Figure 4.26 shows the $\lambda(t)$ that resulted in the responses of figures 4.24 and 4.25 while figure 4.27 shows the state trajectory of the compensator states. The state trajectory "hit" the boundary of $\mathbf{B}_{A,C}$ twice and that is why $\lambda(t)$ in figure 4.26 was drastically decreased from unity twice, at about $t = 0$ and $t = 1$ seconds.

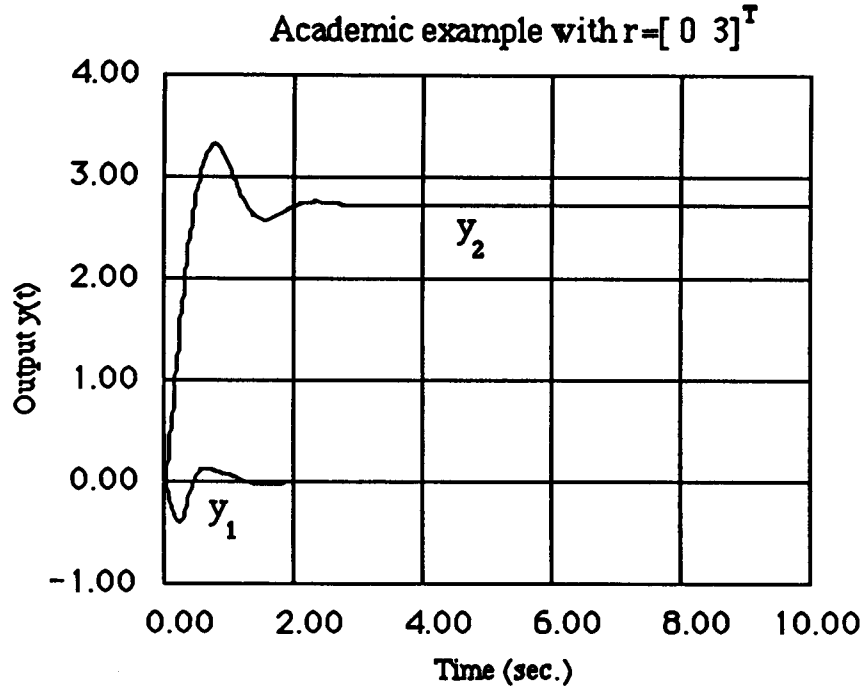

Figure 4.20: Output response for the linear system, ($\mathbf{r} = [0 \quad 3]^T$).

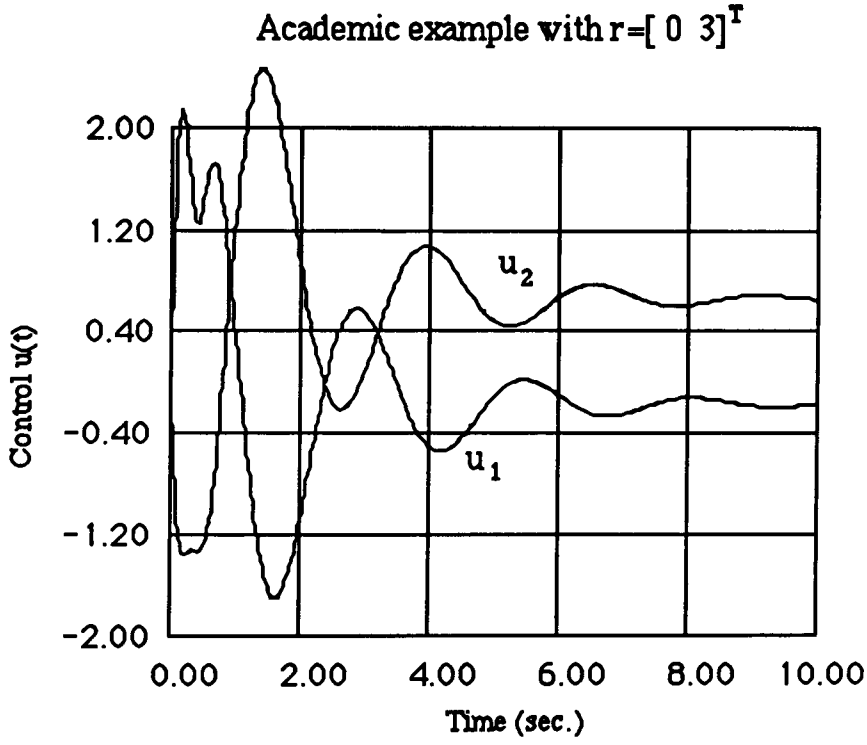

Figure 4.21: Controls in the linear system, ($\mathbf{r} = [0 \quad 3]^T$).

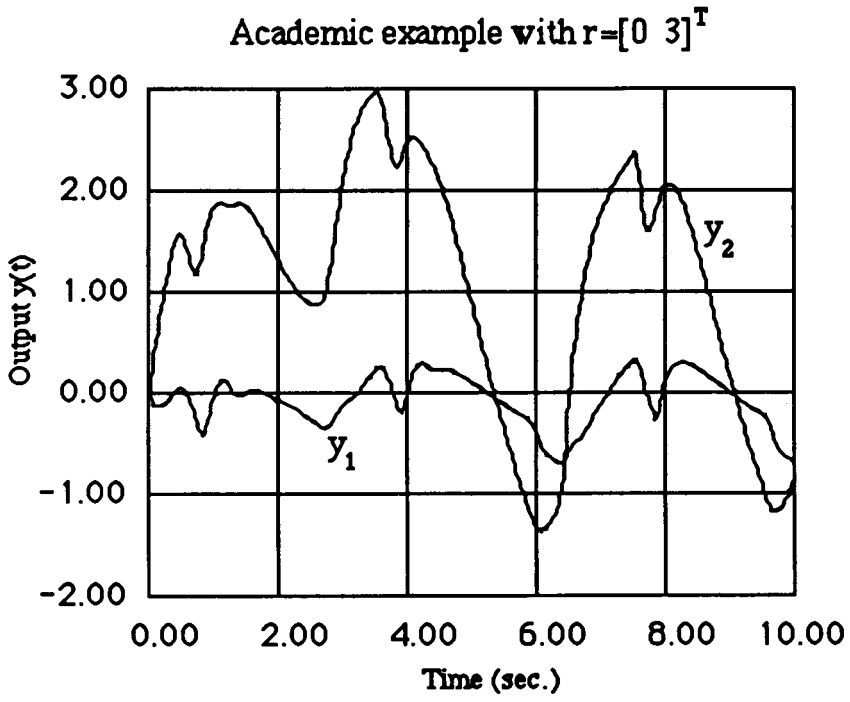

Figure 4.22: Output response for the system with saturation, ($\mathbf{r} = [0 \quad 3]^T$).

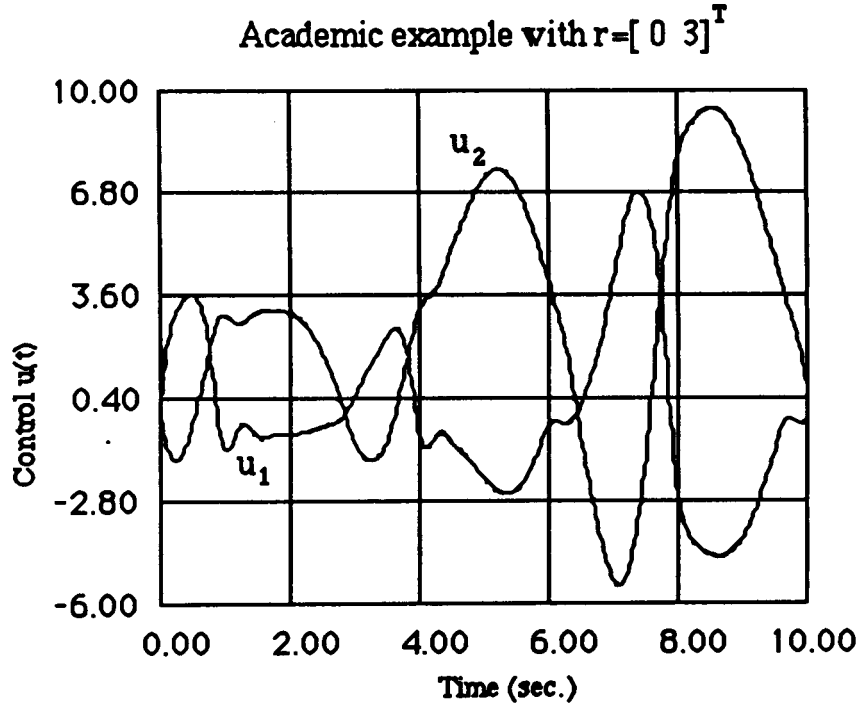

Figure 4.23: Controls in the system with saturation, ($\mathbf{r} = [0 \quad 3]^T$).

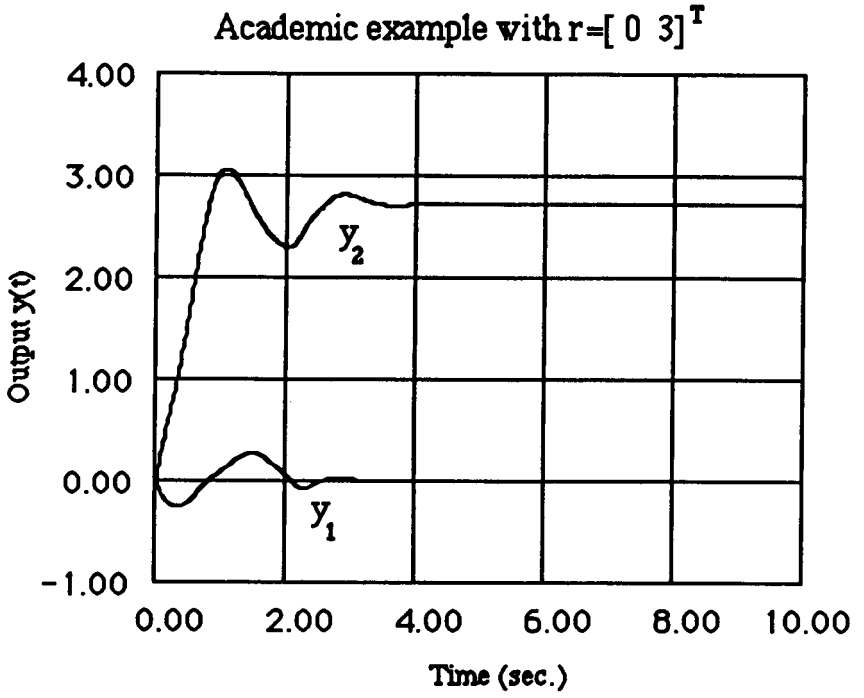

Figure 4.24: Output response for the system with saturation and the EG, ($\mathbf{r} = [0 \quad 3]^T$).

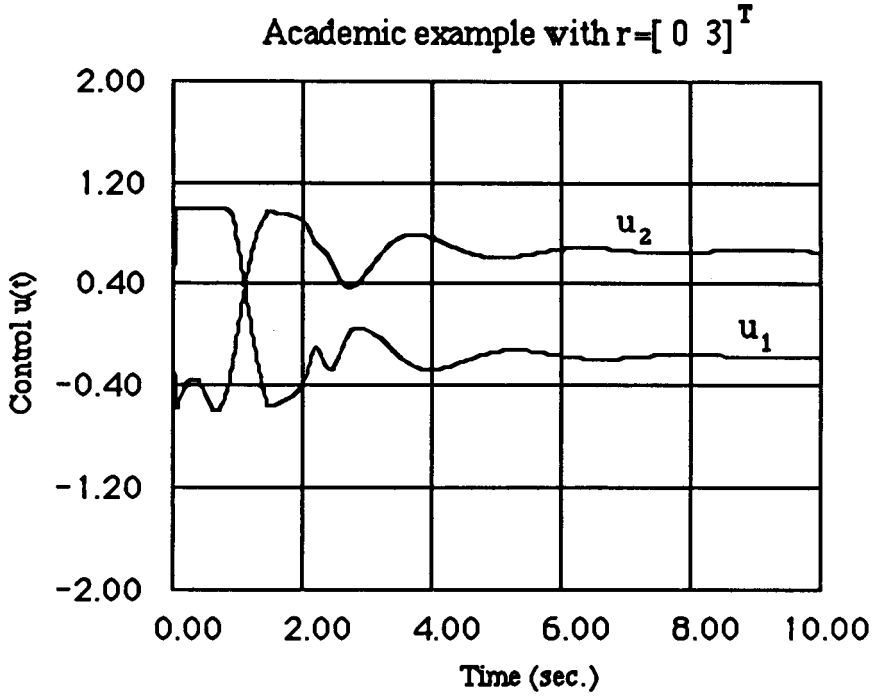

Figure 4.25: Controls in the system with saturation and the EG, ($\mathbf{r} = [0 \quad 3]^T$).

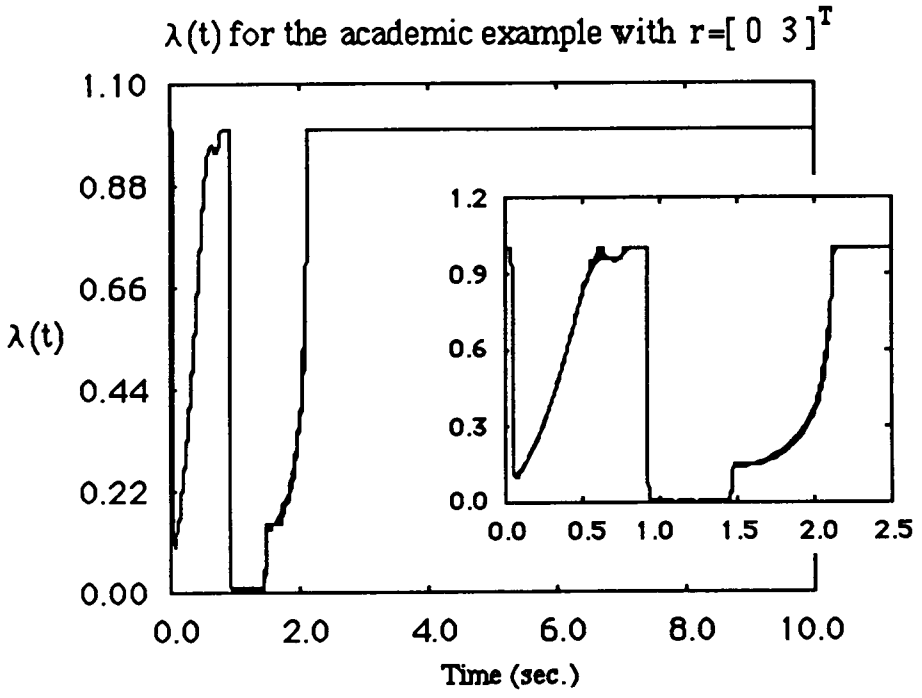

Figure 4.26: $\lambda(t)$ in the system with saturation and the EG, ($\mathbf{r} = [0 \quad 3]^T$).

Insert: Blowup with $0 \leq t \leq 2.5$ sec.

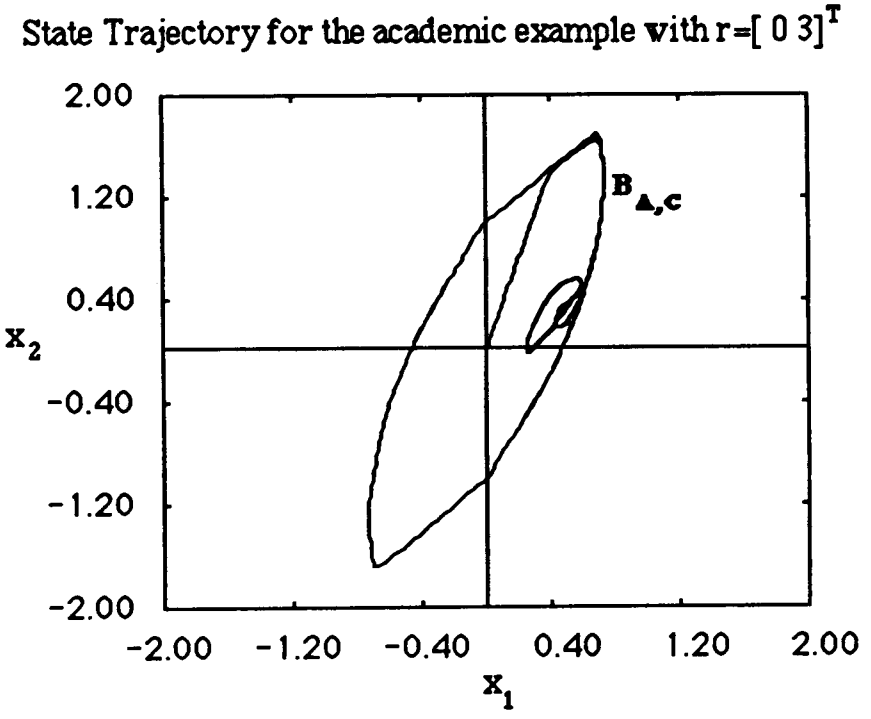

Figure 4.27: State trajectory of the compensator states for the system with saturation and the EG, ($\mathbf{r} = [0 \quad 3]^T$).

4.2.4 Simulation of a Model of the F8 Aircraft

The purpose of this example is to illustrate the effects of multiple saturations on the directions of the controls and consequently on the response of the control system and the integrator windup phenomenon. The simulation confirms our claim that the integrators in the control system with the EG never windup, and that the saturation does not effect the direction of the controls when the EG operator is used.

Consider a model of the longitudinal dynamics of the F8 aircraft. A flaperon has been added which does not exist in the F8 prototype. The state equations are given by

$$\dot{\mathbf{x}}(t) = \begin{bmatrix} -0.8 & -.0006 & -12 & 0 \\ 0 & -.014 & -16.64 & -32.2 \\ 1 & -.0001 & -1.5 & 0 \\ 1 & 0 & 0 & 0 \end{bmatrix} \mathbf{x}(t) + \begin{bmatrix} -19 & -3 \\ -.66 & -.5 \\ -.16 & -.5 \\ 0 & 0 \end{bmatrix} \mathbf{u}_s(t) \tag{4.35}$$

$$\mathbf{y}(t) = \begin{bmatrix} 0 & 0 & 0 & 1 \\ 0 & 0 & -1 & 1 \end{bmatrix} \mathbf{x}(t) \tag{4.36}$$

$$\mathbf{u}_s(t) = \text{sat}(\mathbf{u}(t)) \tag{4.37}$$

and in compact form

$$\dot{\mathbf{x}}(t) = \mathbf{A}\mathbf{x}(t) + \mathbf{B}\mathbf{u}_s(t) \tag{4.38}$$

$$\mathbf{y}(t) = \mathbf{C}\mathbf{x}(t) \tag{4.39}$$

where

$$\text{Controls } \mathbf{u}(t) = \begin{bmatrix} \delta_e(t) & \text{elevator angle (deg)} & \text{limit at } 25^\circ \\ \delta_f(t) & \text{flaperon angle (deg)} & \text{limit at } 25^\circ \end{bmatrix} \tag{4.40}$$

$$\text{Outputs } \mathbf{y}(t) = \begin{bmatrix} \theta(t) & \text{pitch angle (rad)} \\ \gamma(t) & \text{flight path angle (rad)} \end{bmatrix} \tag{4.41}$$

$$\text{States } \mathbf{x}(t) = \begin{bmatrix} q(t) & \text{pitch rate (rad/sec)} \\ v(t) & \text{forward velocity (ft/sec)} \\ \alpha(t) & \text{angle of attack (rad)} \\ \theta(t) & \text{pitch angle (rad)} \end{bmatrix} \tag{4.42}$$

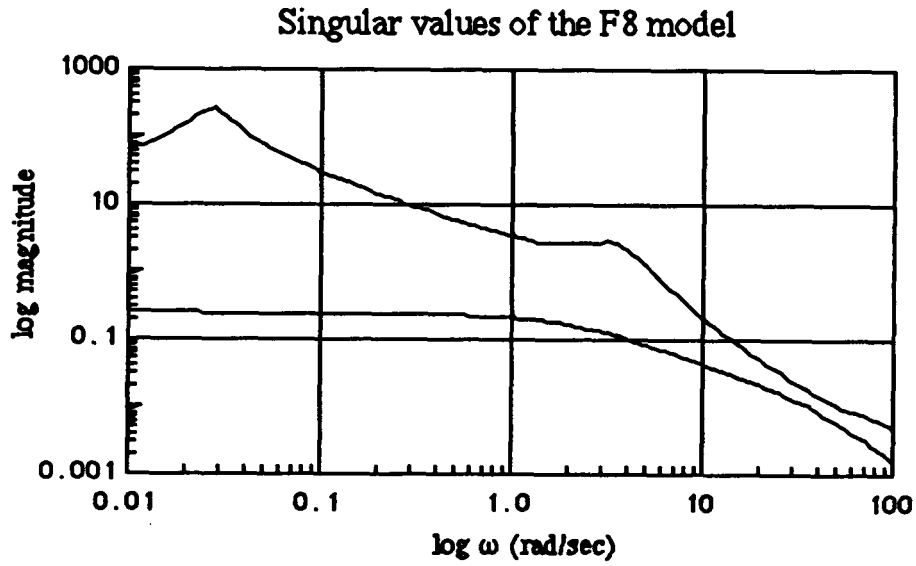

Figure 4.28: Singular values of the F8 model.

Figure 4.28 shows the singular values of the F8 linear model. The model has four stable poles and one transmission zero as it is shown in Table 4.3. Assume that a closed loop system has to be designed for the F8 model to follow pitch and flight path angle commands. Also

assume that zero steady state error is required for step commands. The control system to be designed, should be thought as a semi-realistic MIMO controller so as to test the new design methodology introduced in this section.

The design process is the following. First, linear control theory will be used to design the closed loop system. Then the linear compensator will be modified with the EG operator. Finally, simulations of the closed loop system will be performed to assess the benefits of the new design methodology.

Table 4.3 Poles and zeros of the F8 model

Poles

Real	Imaginary	Magnitude	Damping
-5.7744E-03	2.6425E-02	2.7049E-02	2.1348E-01
-5.7744E-03	-2.6425E-02	2.7049E-02	2.1348E-01
-1.1512E+00	3.4464E+00	3.6336E+00	3.1683E-01
-1.1512E+00	-3.4464E+00	3.6336E+00	3.1683E-01

Zeros

Real	Imaginary	Magnitude	Damping
-1.3900E-02	0.0000E-01	1.3900E-02	1.0000E+00
3 more infinite			

To obtain the required linear control system the saturation is ignored ($\mathbf{u}_s(t) = \mathbf{u}(t)$) and, two integrators were added at the controls. The augmented system (sixth order) is given by the following

$$\dot{\mathbf{x}}_a(t) = \mathbf{A}_a\mathbf{x}(t) + \mathbf{B}_a\mathbf{u}_a(t) \tag{4.43}$$

$$\mathbf{y}(t) = \mathbf{C}_a\mathbf{x}(t) \tag{4.44}$$

$$\mathbf{u}(t) = \frac{\mathbf{I}}{s}\mathbf{u}_a(t) \tag{4.45}$$

where

$$A_a = \begin{bmatrix} 0 & 0 \\ B & A \end{bmatrix} \qquad B_a = \begin{bmatrix} I \\ 0 \end{bmatrix} \qquad C_a = \begin{bmatrix} 0 & C \end{bmatrix}$$

Next, a linear compensator was designed for the augmented system to control the pitch angle and flight path angle. The LQG/LTR methodology was used to design the compensator which is computed as follows:.

$$K(s) = G[\, sI - A_a - B_a G - HC_a \,]^{-1} H \tag{4.46}$$

$$K_a(s) = \frac{I}{s} K(s) \tag{4.47}$$

where

$$H = \begin{bmatrix} -.844 & .819 \\ -11.54 & 13.47 \\ -.86 & .25 \\ -47.4 & 15 \\ 4.68 & -4.8 \\ 4.82 & .14 \end{bmatrix} \qquad G = \begin{bmatrix} -52.23 & -3.36 & 73.1 & -.0006 & -94.3 & 1072 \\ -3.36 & -29.7 & -2.19 & -.006 & 908.9 & -921 \end{bmatrix}$$

The LQG/LTR compensator K(s) has six poles and four transmission zeros as it shown in Table 4.4; note that it is stable and that cancels part of the F8 dynamics. From now on we assume that the $G(s)K_a(s)$ is the desired forward loop transfer matrix, and that we would like to mimic (to the extent possible) the transient response of this linear feedback system even in the presence of saturations. Figure 4.29 shows the singular values of the resulting loop transfer function matrix $G(s)K_a(s)$.

Table 4.4 Poles and zeros of the F8 linear compensator

Poles

Real	Imaginary	Magnitude	Damping
-1.3900E-02	0.0000E-01	1.3900E-02	1.0000E+00
-1.7507E+01	1.7683E+01	2.4884E+01	7.0357E-01
-1.7507E+01	-1.7683E+01	2.4884E+01	7.0357E-01
-1.4195E+01	2.5572E+01	2.9248E+01	4.8534E-01
-1.4195E+01	-2.5572E+01	2.9248E+01	4.8534E-01
-3.0585E+01	0.0000E-01	3.0585E+01	1.0000E+00

Zeros

Real	Imaginary	Magnitude	Damping
-1.3964E-02	0.0000E-01	1.3964E-02	1.0000E+00
-6.1540E-02	0.0000E-01	6.1540E-02	1.0000E+00
-9.6500E-01	3.3244E+00	3.4617E+00	2.7877E-01
-9.6500E-01	-3.3244E+00	3.4617E+00	2.7877E-01
2 more infinite			

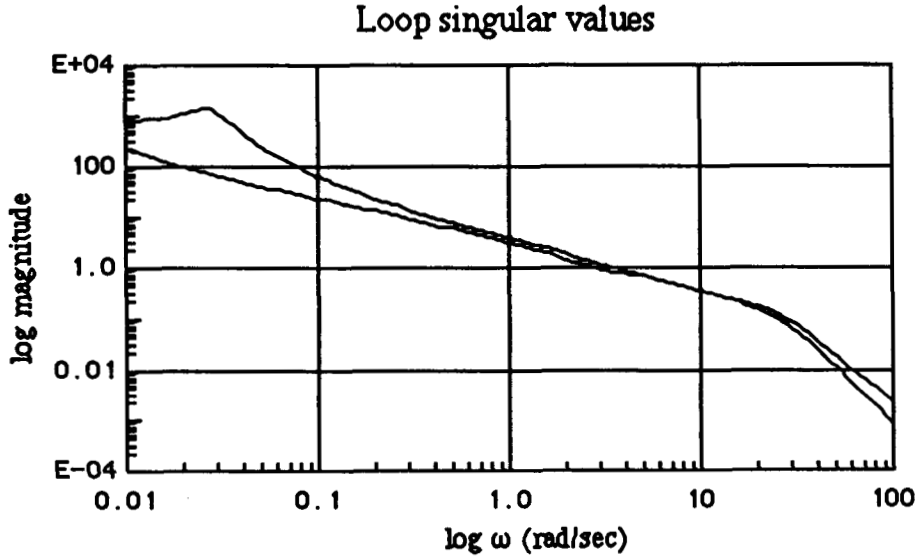

Figure 4.29: Singular values of the loop transfer function in the F8 closed loop system

To prevent control saturations, the Error Governor (the $\lambda(t)$ time-varying gain) is added to the feedback system at the error signal **e**(t). The construction of $\lambda(t)$ is possible because the compensator **K**(s) is neutrally stable and finite gain stability is guaranteed because in addition the plant **G**(s) is stable. Figure 4.30 shows the closed loop system for the F8 model with the EG operator.

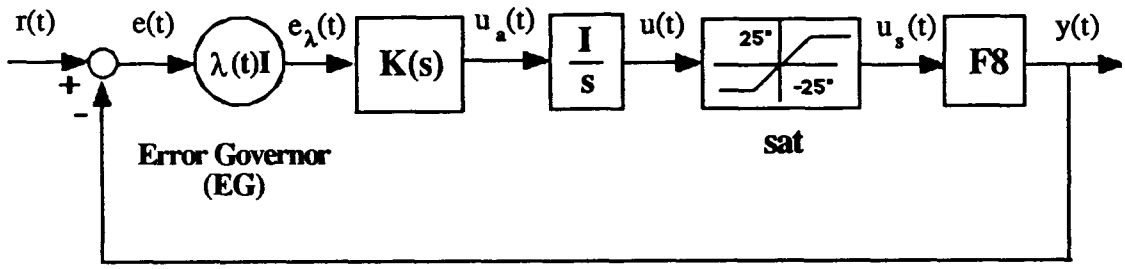

Figure 4.30: Closed loop system for the F8 example with the EG.

The result is a multivariable control system with integrators in the forward loop. In the presence of saturation, and without the EG operator, integrator windups would be expected and the direction of the control vector would be distorted.

Three different simulations were performed to evaluate the design methodology. The EG operator in these simulations was computed entirely on-line as discussed in section 4.2.2. The simulations were performed in the Macintosh 512K and the computation of the EG operator required approximately eight hours.

First, the closed loop system was simulated with reference vector $\mathbf{r} = [\ 10 \quad 10]^T$. Figures 4.31 and 4.32 show the linear output and control responses. As expected from the singular values of $G(s)\mathbf{K}_a(s)$, both outputs behave similarly and it is assumed that this type of an output response satisfies the posed constraints. Note that the controls have "impulsive" action at the beginning, and they violate the $\pm 25^\circ$ limit; thus saturation is expected.

Figures 4.33 and 4.34 show the outputs and controls of the system with saturation. From the oscillations in the output response it can be inferred that the integrators windup. In addition, the direction of the output is disturbed and the outputs are "not matched" any more (compare figures 4.31 and 4.33).

Figures 4.35 and 4.36 show the output and control responses of the system with saturation and the EG operator. Compare figures 4.31 and 4.35 and notice how the outputs are similar in shape (as it was desired), in addition to the fact that there are no integrator windups.

The output response has of course slower rise time, since we must use smaller controls, but the nature of the response is similar to the linear one. The controls $\mathbf{u}(t)$ in figure 4.36 never exceed the limits of the saturation; and when the flaperon $\delta_f(t)$ reaches 25° the elevator $\delta_e(t)$ remains almost constant until $\delta_f(t)$ unsaturates. The direction of the controls during that period of time is such that drives the plant output towards the command $[10 \quad 10]^T$. The system behaves like having "a smart multivariable saturation".

Figure 4.37 shows the $\lambda(t)$ that was computed with the method described in sections 4.2.1 and 4.2.3. Note that the error is almost completely "turned-off" at about .05 seconds. The gain $\lambda(t)$ then increases slowly towards unity and the system operates linearly again.

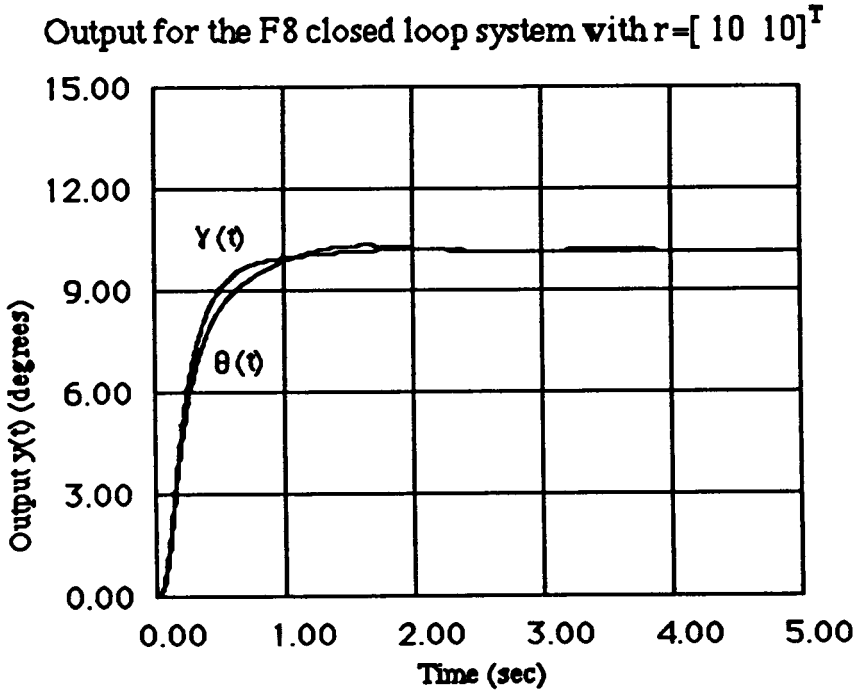

Figure 4.31: Output response for the F8 linear system, ($\mathbf{r} = [\ 10\ \ 10\ ]^T$).

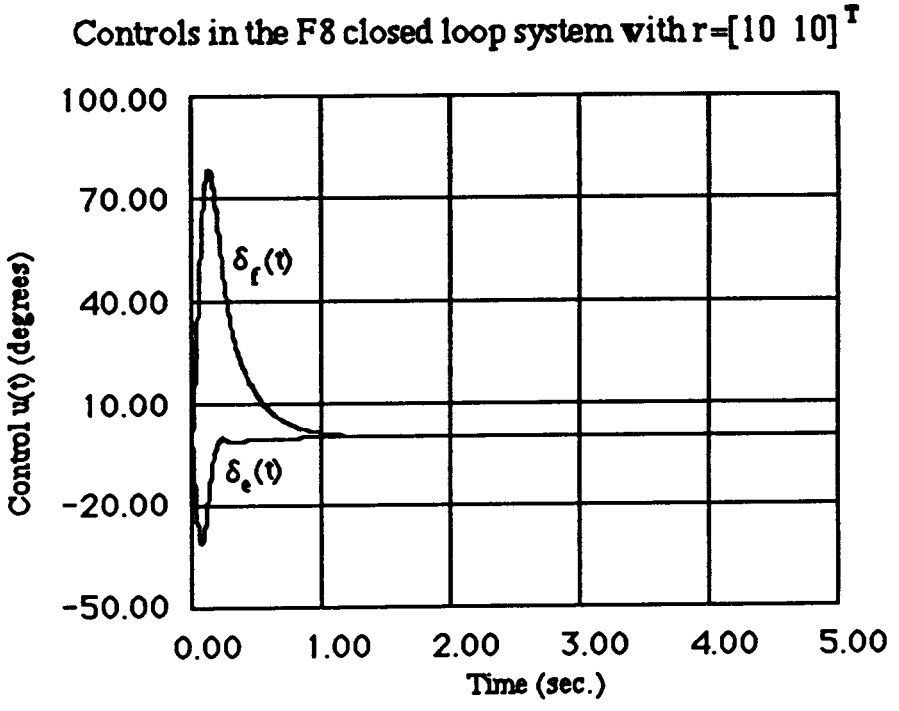

Figure 4.32: Controls in the F8 linear system, ($\mathbf{r} = [\ 10\ \ 10\ ]^T$).

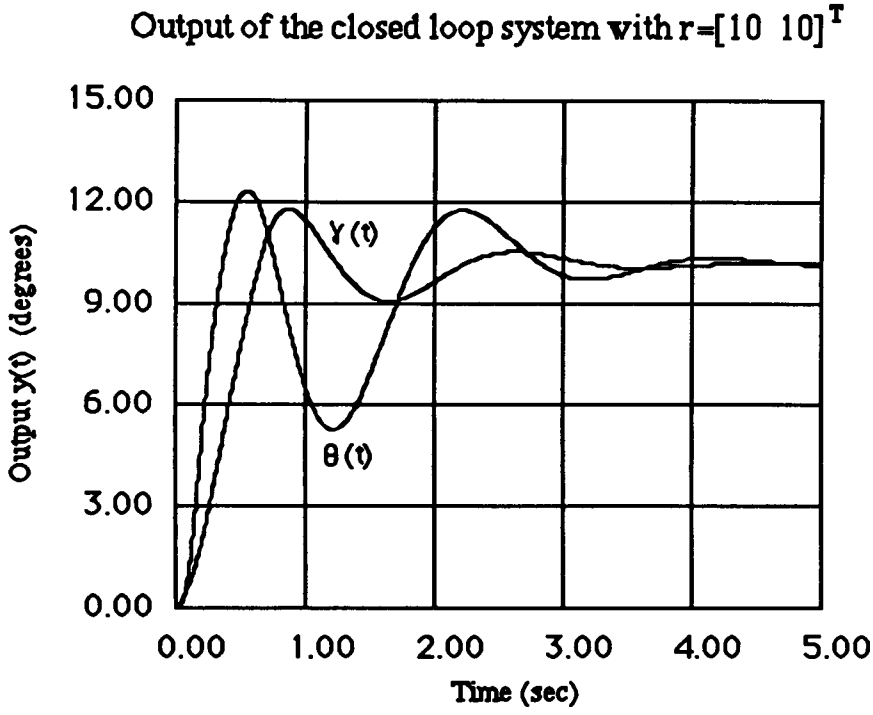

Figure 4.33: Output response for the F8 system with saturation, ($\mathbf{r} = [\ 10\ \ 10\ ]^T$).

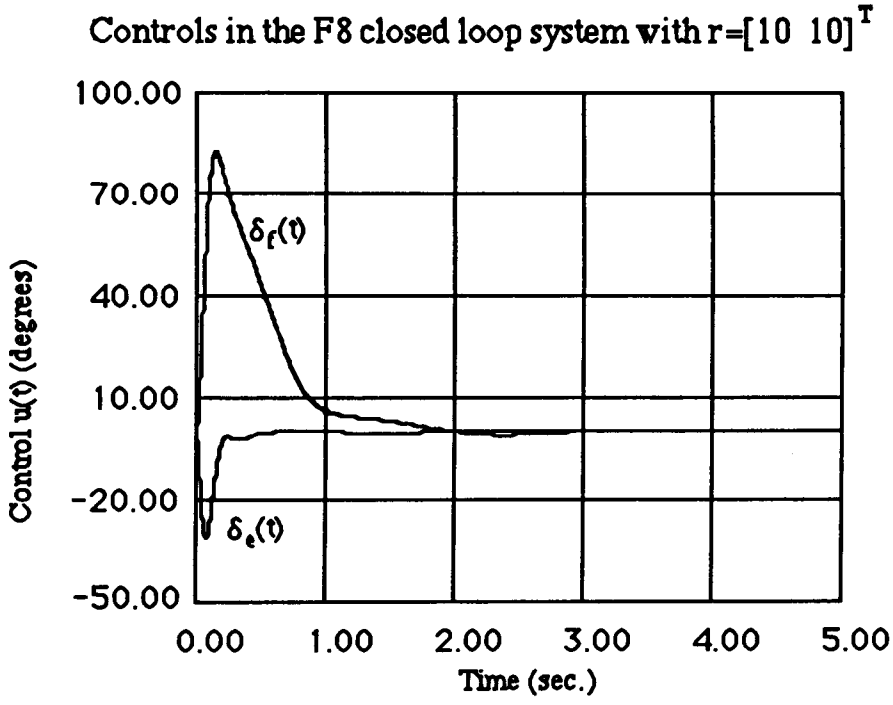

Figure 4.34: Controls in the F8 system with saturation, ($\mathbf{r} = [\ 10\ \ 10\ ]^T$).

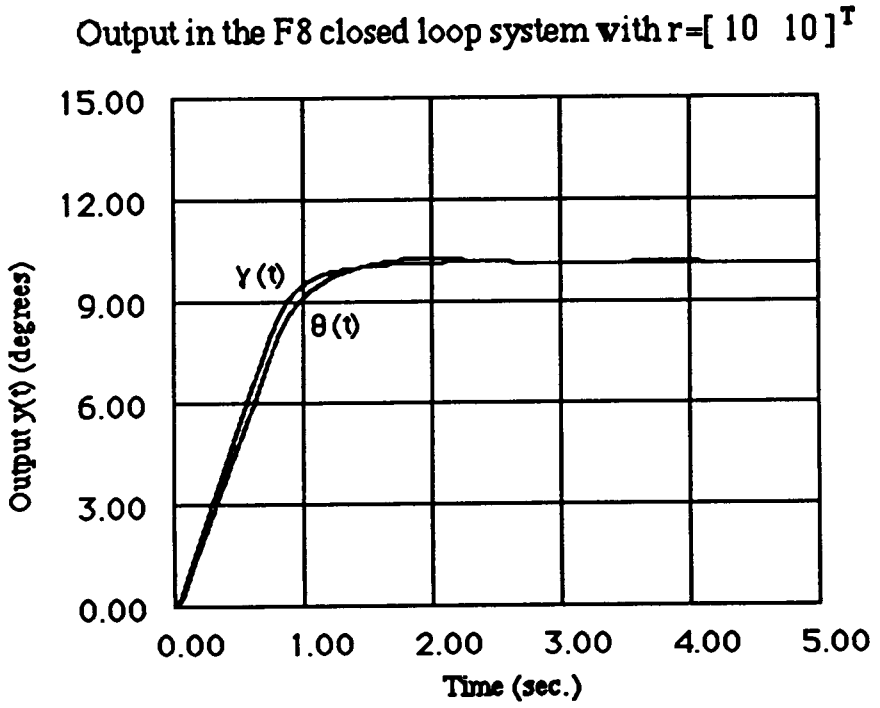

Figure 4.35: Output response of the F8 system with saturation and the EG, ($\mathbf{r} = [10 \quad 10]^T$).

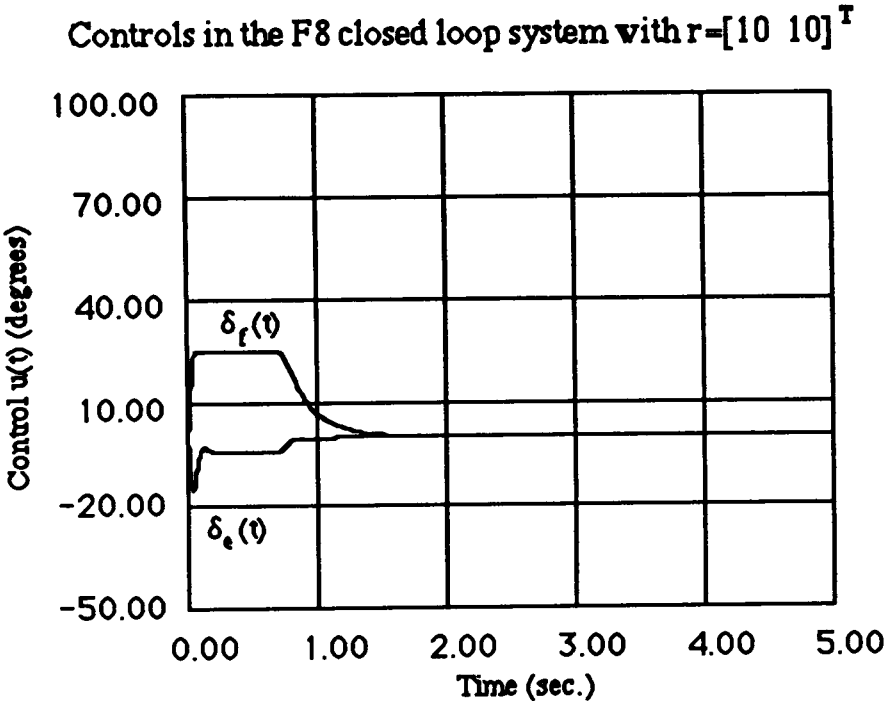

Figure 4.36: Controls in the F8 system with saturation and the EG, ($\mathbf{r} = [10 \quad 10]^T$).

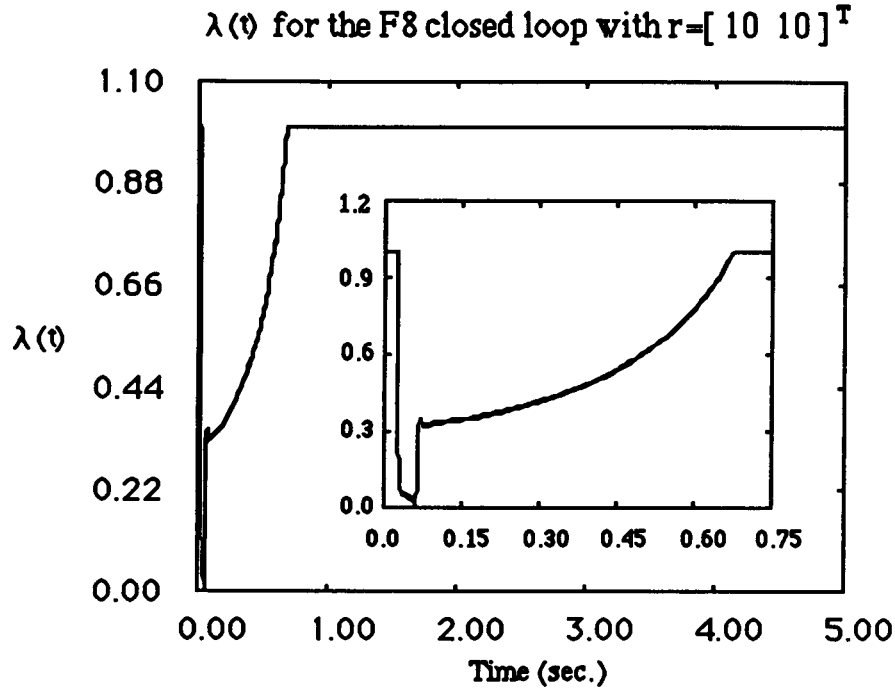

Figure 4.37: $\lambda(t)$ in the F8 system with saturation and the EG, ($\mathbf{r} = [10 \quad 10]^T$).
Insert: Blowup with $0 \leq t \leq .75$ sec.

A second simulation was performed with the F8 feedback system with the references being $\mathbf{r} = [\,0 \quad 5]^T$ which corresponds to a command for a constant flight path angle, keeping the fuselage pitch zero (at trim). Figures 4.38 through 4.44 show the responses obtained from this simulation. Similar conclusions can be made from this set of simulations regarding the benefits of the EG operator. The EG operator eliminates windup problems and makes the outputs mimic those of the purely linear design (compare figures 4.38 and 4.42).

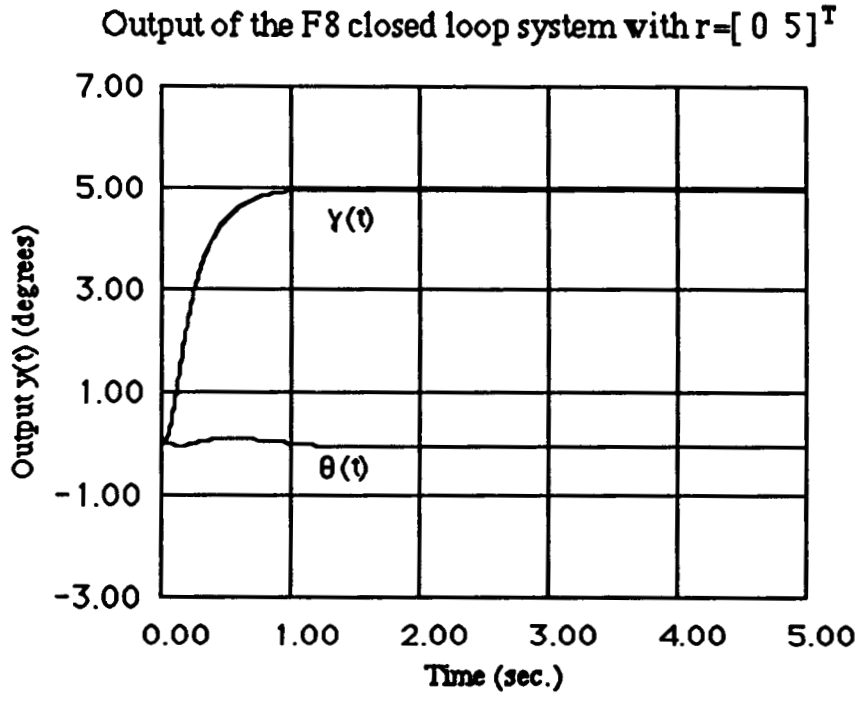

Figure 4.38: Output response for the F8 linear system, ($\mathbf{r} = [0 \quad 5]^T$).

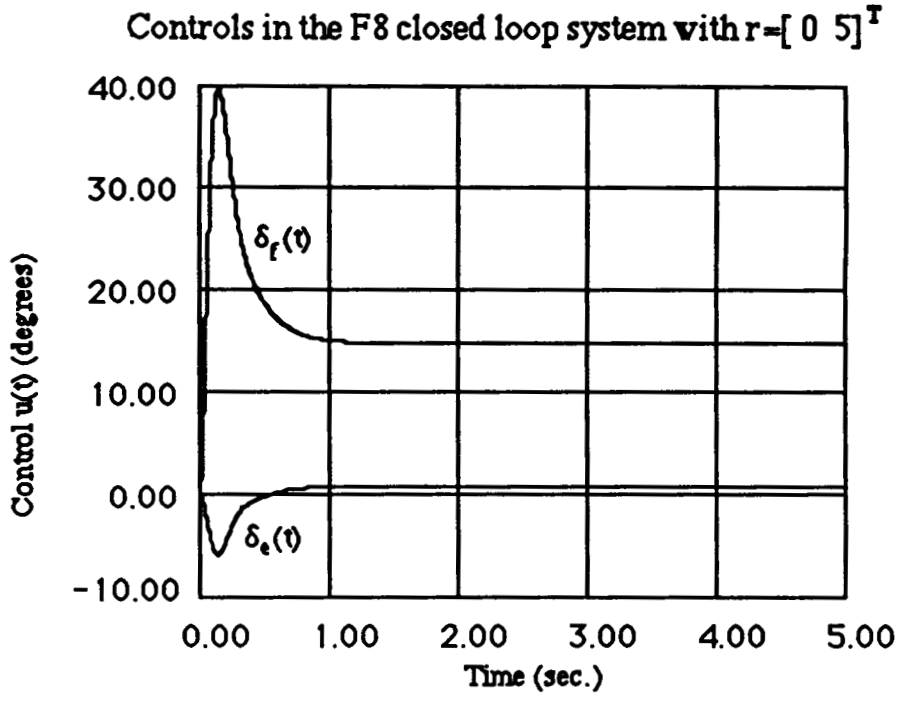

Figure 4.39: Controls in the F8 linear system, ($\mathbf{r} = [0 \quad 5]^T$).

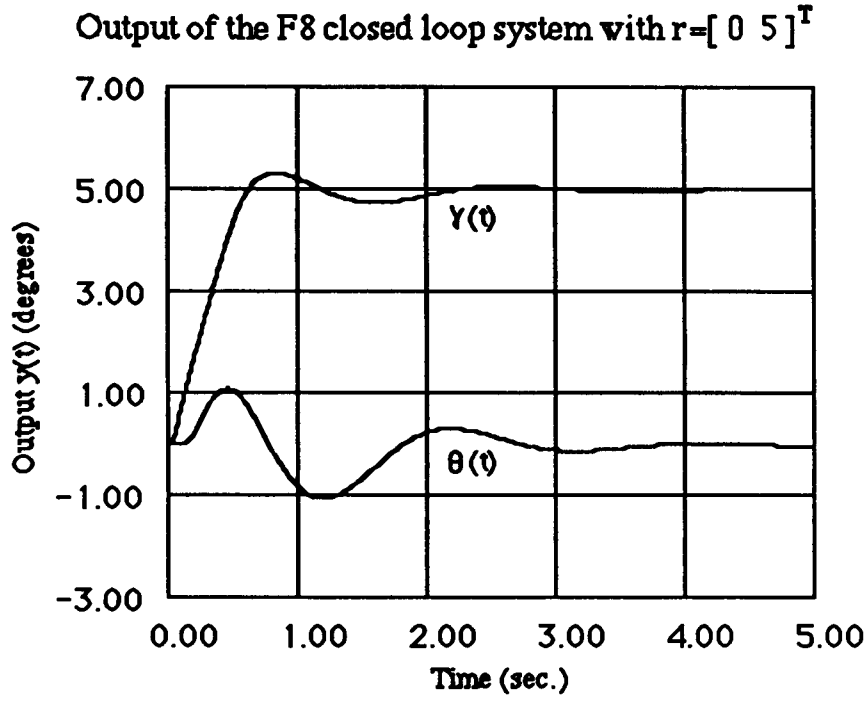

Figure 4.40: Output response for the F8 system with saturation, ($\mathbf{r} = [0 \quad 5]^T$).

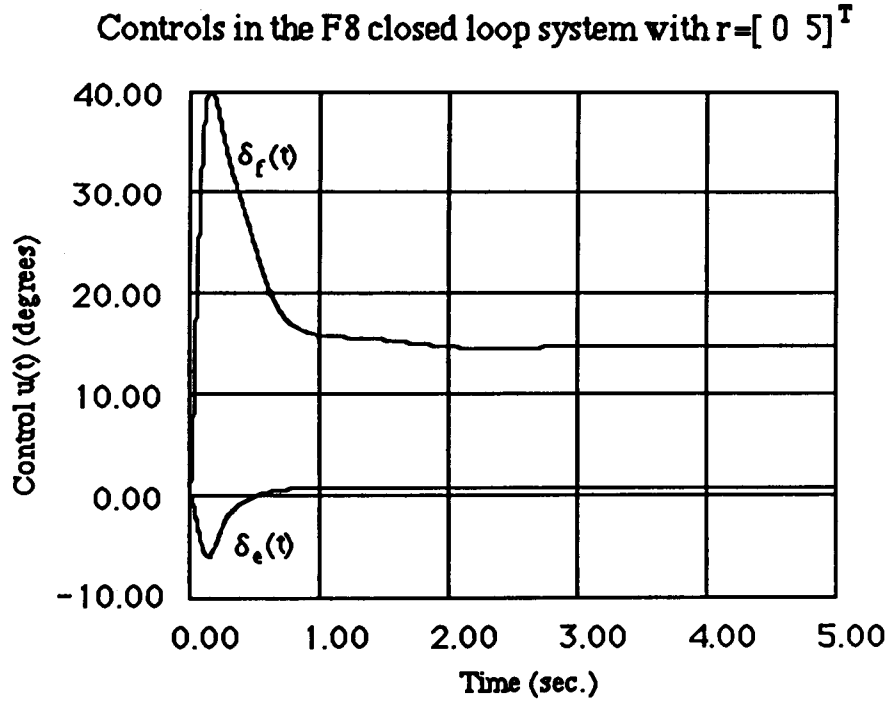

Figure 4.41: Controls in the F8 system with saturation, ($\mathbf{r} = [0 \quad 5]^T$).

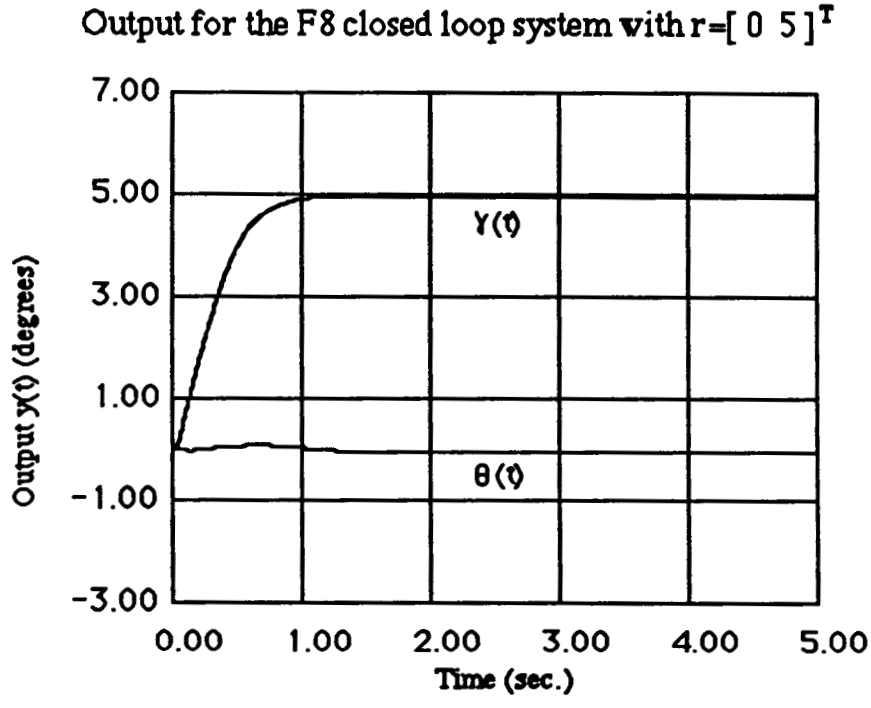

Figure 4.42: Output response for the F8 system with saturation and the EG, ($r = [0 \quad 5]^T$).

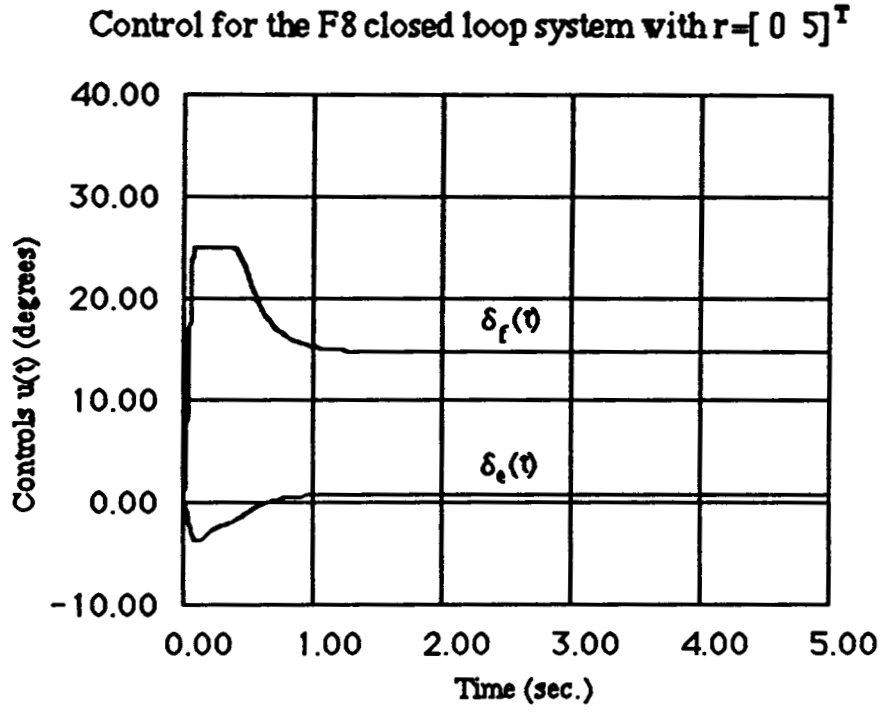

Figure 4.43: Controls in the F8 system with saturation and the EG, ($r = [0 \quad 5]^T$).

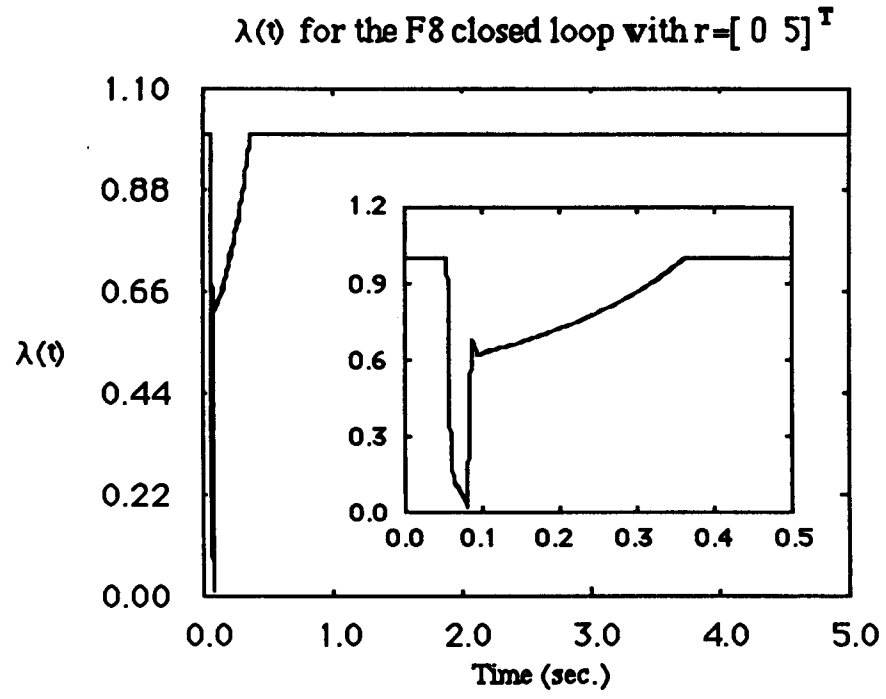

Figure 4.44: $\lambda(t)$ in the F8 system with saturation and the EG, ($r = [0 \quad 5]^T$).
Insert : Blowup with $0 \leq t \leq .5$ sec.

4.3 Concluding Remarks

In this chapter a new design methodology, the EG operator, has been introduced and illustrated for plants with multiple control magnitude saturations. The new control structure is useful for control systems with stable open loop plants and neutrally stable compensators.

The controllers that arise from the new methodology never cause the controls signals to saturate and, consequently, integrator windups are not possible. In addition, the proper direction of the controls (altered by saturation) is restored with the new controller. These desirable properties hold for any reference and input or output disturbance signal.

The new design methodology was demonstrated for an academic example and for a model of the F8 aircraft. In both cases, the control systems had the properties promised by the

methodology and the performance of the designs was substantially improved, compared with the uncompensated control system with multiple saturations.

CHAPTER 5
CONTROL STRUCTURE WITH THE OPERATOR RG

5.1 Introduction

In this section we introduce two new control structures for plants with saturating actuators. The first control structure includes a Rate Governor (RG) operator (i.e. a time-varying rate) at the reference signals. This new controller can be used for any stable linear closed loop system. An analysis of the effects of the RG operator on the closed loop system will be performed. A second control structure includes both the EG and RG operators and it can be used for any linear feedback system with a neutrally stable linear compensator.

In both the control structures the idea is to keep the system linear when the references and/or the disturbances are "small". The operators RG and/or EG will ensure that for "large" exogenous signals the control signals never saturate.

The new control structures have inherent properties (BIBO stability, no integrator windups etc.) which will be discussed and demonstrated via a simulation of the unstable F16 aircraft.

5.2 Description of the Control Structure with the Operator RG

The control structure with the operator EG, described in chapter 4, can be applied to modify linear control systems with stable plants and neutrally stable compensators. The structure cannot be used for feedback systems with unstable plants or unstable compensators. Thus, a new design procedure is needed to handle these systems. A proposed structure is shown in figure 5.1 where a Reference Governor will mask out "large" references so they will not enter into the closed loop system. Choosing the Reference governor appropriately one can

ensure that the controls never saturate so that the feedback system operates linearly.

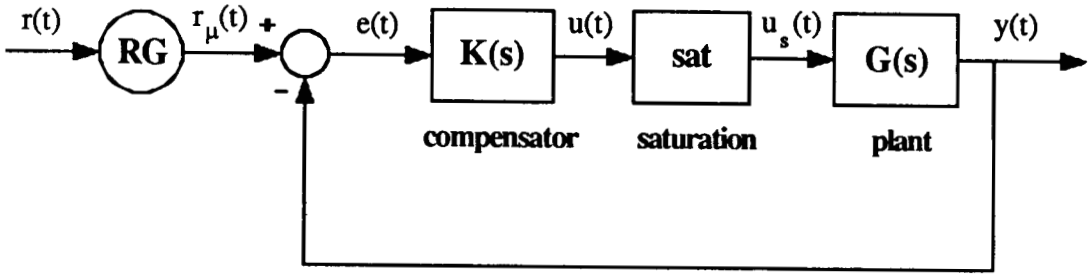

Figure 5.1: Control structure with the RG operator

To facilitate our discussion let us assume the following models for the systems shown in figure 5.1.

Plant model:

$$\dot{\mathbf{x}}(t) = \mathbf{A}\mathbf{x}(t) + \mathbf{B}\mathbf{u}_s(t) \tag{5.1}$$

$$\mathbf{y}(t) = \mathbf{C}\mathbf{x}(t) \tag{5.2}$$

Compensator model:

$$\dot{\mathbf{x}}_c(t) = \mathbf{A}_c\mathbf{x}_c(t) + \mathbf{B}_c\mathbf{e}(t) \tag{5.3}$$

$$\mathbf{u}(t) = \mathbf{C}_c\mathbf{x}_c(t) \tag{5.4}$$

$$\mathbf{e}(t) = \mathbf{r}_\mu(t) - \mathbf{y}(t) \tag{5.5}$$

Saturation model:

$$\mathbf{u}_s(t) = \text{sat}(\mathbf{u}(t)) \tag{5.6}$$

where $\mathbf{r}(t)$ are the reference signals, $\mathbf{y}(t)$ are the output signals, $\mathbf{u}(t)$ are the control signals generated by the compensator, $\mathbf{u}_s(t)$ are the saturated (output of the saturation) control signals.

In addition, consider the linear closed loop system (i.e the system without the saturation)

with the controls as output and assume the following representation

$$\dot{\mathbf{x}}_{cl}(t) = \mathbf{A}_{cl}\,\mathbf{x}_{cl}(t) + \mathbf{B}_{cl}\mathbf{r}(t) \tag{5.7}$$

$$\mathbf{u}(t) = \mathbf{C}_{cl}\,\mathbf{x}_{cl}(t) \tag{5.8}$$

where $\mathbf{x}_{cl} = \begin{bmatrix} \mathbf{x}_c \\ \\ \mathbf{x} \end{bmatrix}$

$$\mathbf{A}_{cl} = \begin{bmatrix} \mathbf{A}_c & -\mathbf{B}_c\mathbf{C} \\ \mathbf{B}\mathbf{C}_c & \mathbf{A} \end{bmatrix} \qquad \mathbf{B}_{cl} = \begin{bmatrix} \mathbf{B}_c \\ \\ \mathbf{0} \end{bmatrix} \qquad \mathbf{C}_{cl} = \begin{bmatrix} \mathbf{C}_c & \mathbf{0} \end{bmatrix}$$

Observing closely the closed loop representation, eqs. (5.7)-(5.8), one may think that the time-varying gain $\lambda(t)$ can be used as a Reference Governor. This is reasonable because the system (5.7)-(5.8) is linear, its input is the reference signal $\mathbf{r}(t)$ and its output is the control signal $\mathbf{u}(t)$. Therefore, the time-varying gain $\lambda(t)$ can be used to modify the references so that the controls never saturate.

Although the above reasoning is true, the resulting control system would be very conservative in the following sense. The states of the closed loop system, and thus the outputs, cannot reach "large" values to track analogous "large" references because if the references are reduced suddenly, the controls will saturate. For example, assume the case where a step reference of $\mathbf{r}$ is to be followed; also assume that the required linear controls, to track $\mathbf{r}$, exceed their limits for some time, and that their steady state value are within the saturation limits. If it was possible, with $\lambda(t)$, to track such reference without saturating, the following would be

true. At steady state, one could change the reference from **r** to **0** and $\lambda(t)$ would not modify the reference signal, consequently the controls would saturate. The construction of $\lambda(t)$ guarantees that the controls never saturate so the system would not be able to follow the "large" reference **r** and instead it would follow a reference smaller in magnitude.

The objective of any control system is to keep the tracking error **e**(t) "small", therefore in the Error Governor case the time-varying gain $\lambda(t)$ can be used without any problems. In addition to the magnitude of the references, the RG operator should be able to modify the rate as well. In such a case, possible reductions in the references would not cause any problems because the rate of the reduction could be modified.

Following the discussion of section 3.4 one can inject a time varying rate $\mu(t)$ at the inputs of a linear time invariant system and the outputs of that system will remain bounded. Consider the closed loop system (5.7)-(5.8) and assume that a time-varying rate (5.9)-(5.11) is introduced at the references as shown in figure 5.2

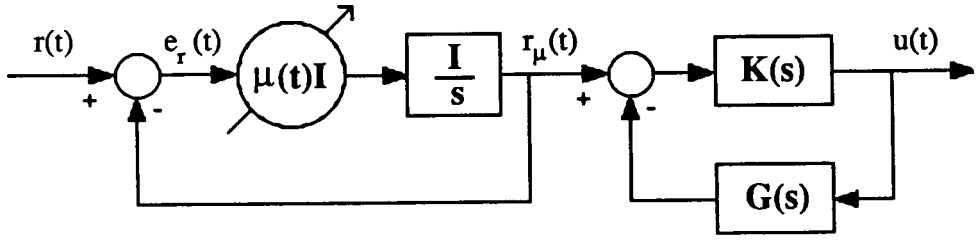

Figure 5.2: The basic system for calculating $\mu(t)$.

$$\dot{\mathbf{z}}(t) = \mu(t)\mathbf{e}_r(t) \tag{5.9}$$

$$\mathbf{e}_r(t) = \mathbf{r}(t) - \mathbf{r}_\mu(t) \tag{5.10}$$

$$\mathbf{r}_\mu(t) = \mathbf{z}(t) \tag{5.11}$$

As in section 3.4, the time varying gain $\mu(t)$ will be chosen so that if **r**(t) is small enough

never to cause control saturation then $\mathbf{r}(t) = \mathbf{r}_\mu(t)$, in contrast, if $\mathbf{r}(t)$ is large, then $\mu(t)$ will limit the references so that the controls will remain bounded. We now combine the dynamics of the rate limiter (5.9)-(5.11) with the dynamics of the closed loop system (5.7)-(5.8) to obtain an augmented system

$$\dot{\mathbf{x}}_a(t) = \mathbf{A}_a\mathbf{x}_a(t)+\mathbf{B}_a\mu(t)\mathbf{e}_r(t) \tag{5.12}$$

$$\mathbf{u}(t) = \mathbf{C}_a\mathbf{x}_a(t) \tag{5.13}$$

where

$$\mathbf{x}_a(t) = \begin{bmatrix} \mathbf{z}(t) \\ \mathbf{x}_{cl}(t) \end{bmatrix} \qquad \mathbf{A}_a = \begin{bmatrix} \mathbf{0} & \mathbf{0} \\ \mathbf{B}_{cl} & \mathbf{A}_{cl} \end{bmatrix} \qquad \mathbf{B}_a = \begin{bmatrix} \mathbf{I} \\ \mathbf{0} \end{bmatrix} \qquad \mathbf{C}_a = \begin{bmatrix} \mathbf{0} & \mathbf{C}_{cl} \end{bmatrix}$$

The objective here is to construct $\mu(t)$, $0 \le \mu(t) \le \infty$, in such a way so that for any error $\mathbf{e}_r(t)$ the controls $\mathbf{u}(t)$ never saturates. This is similar to designing a time-varying rate so that the output of a linear system remains bounded (section 3.4). At first, a function $g(\mathbf{x})$ and a set $\mathbf{B}_{A,C}$ have to be defined. The symbols $g(\mathbf{x})$ and $\mathbf{B}_{A,C}$ should be thought as generic symbols and, when they are used, they are always defined to avoid confusion.

$$g(\mathbf{x}_{a0}): \quad g(\mathbf{x}_{a0}) = \|\mathbf{u}(t)\|_\infty \tag{5.14}$$

where

$$\dot{\mathbf{x}}_a(t) = \mathbf{A}_a\mathbf{x}_a(t); \qquad \mathbf{x}_a(0) = \mathbf{x}_{a0} \tag{5.15}$$

$$\mathbf{u}(t) = \mathbf{C}_a\mathbf{x}_a(t) \tag{5.16}$$

$$\mathbf{B}_{A,C} = \{\ \mathbf{x}:\ g(\mathbf{x}) \le 1\ \} \tag{5.17}$$

For the function $g(\mathbf{x})$ to be finite the linear system in eq. (5.15) has to be **neutrally stable**. This is always true for any compensator and any plant provided that the linear closed

loop system is stable. Even if the plant is unstable the compensator has been designed to stabilize it and the system (5.15) is always neutrally stable. Therefore, the Reference Governor can be used in all cases as shown in table 3.1. With g(x) neutrally stable, as in section 3.4, the construction of $\mu(t)$ is given by:

Construction of $\mu(t)$:

For every time t choose $\mu(t)$ as follows

a) if $\mathbf{x}_a(t) \in \text{Int}\mathbf{B}_{A,C}$ then $\mu(t) = \infty$ which implies that $\mathbf{r}(t) = \mathbf{r}_\mu(t)$ (5.18)

b) if $\mathbf{x}_a(t) \in \text{Bd}\mathbf{B}_{A,C}$ then choose the largest $\mu(t)$ such that (5.19)

$$0 \le \mu(t) \le \infty$$

$$\lim_{\varepsilon \to 0} \sup \frac{g\left(\mathbf{x}_a(t)+\varepsilon[\mathbf{A}_a\mathbf{x}_a(t)+\mathbf{B}_a\mu(t)\mathbf{e}_r(t)]\right) - g\left(\mathbf{x}_a(t)\right)}{\varepsilon} \le 0 \qquad (5.20)$$

or for the points where g(x) is differentiable choose $\mu(t)$ such that

$$0 \le \mu(t) \le \infty \qquad (5.21)$$

$$Dg(\mathbf{x}_a(t))[\mathbf{A}_a\mathbf{x}_a(t)+\mathbf{B}_a\mu(t)\mathbf{e}_r(t)] \le 0 \quad \forall\, t > 0 \qquad (5.22)$$

where $Dg(\mathbf{x}_a(t))$ is the Jacobian matrix of $g(\mathbf{x}_a(t))$ as in definition 3.2.

c) if $\mathbf{x}_a(t) \notin \mathbf{B}_{A,C}$ then choose $\mu(t)$, $0 \le \mu(t) \le \infty$ such that the expression (5.20) is minimum.

The closed loop system with the RG operator (shown in figure 5.3) has the following good properties.

a) **The controls in the closed loop system will never exceed the limits of the saturation** and thus the direction of the control vector is not affected by the saturation. Hence, any inversion of the plant by the compensator is not prevented.

b) **Integrators or slow dynamics in the compensator do not windup.**

The main disadvantage of this method is that the construction of $\mu(t)$ requires the measurement of the plant states. More research is needed to assess if estimates of the states can be used to approximate the real $\mu(t)$. The computational requirements for the operator RG are larger that the ones for the operator EG. This is so because $\lambda(t)$ is computed using the compensator states while $\mu(t)$ is computed using both the states of the plant and the compensator. In section 5.2.2 the computation requirements for $\mu(t)$ will be discussed in detail.

As it was stated previously, this control structure can be used for any plant and any compensator as long as the linear closed loop system is stable (true for all sensible control systems). Because it is more difficult to compute $\mu(t)$ than $\lambda(t)$, it is recommended to use the control structure with the operator RG in feedback system with unstable plants and/or unstable compensator only.

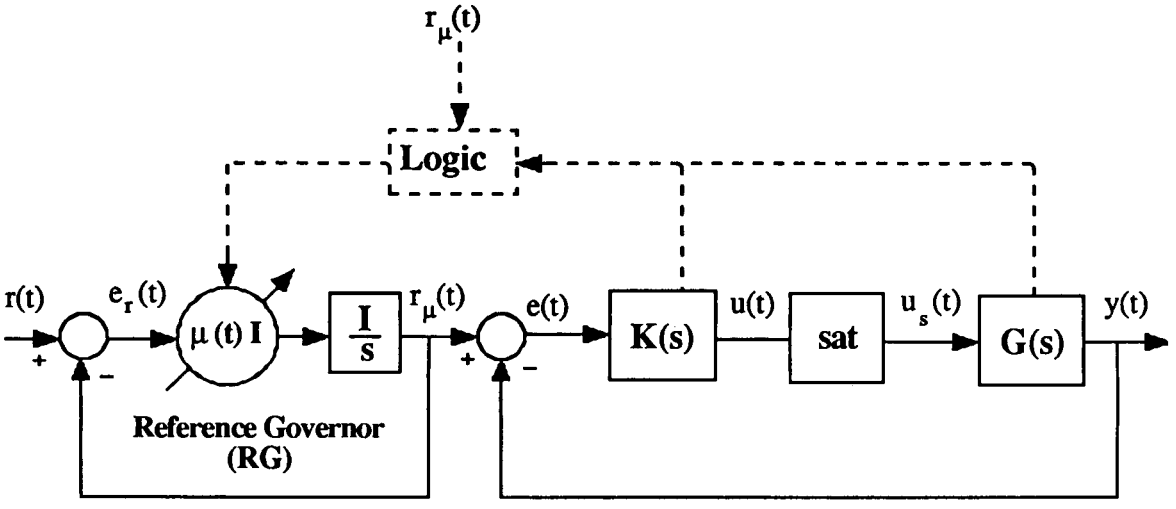

Figure 5.3: Control structure with the operator RG.

5.2.1 Stability Analysis for the Control Structure With the RG

The simple closed loop system form $\mathbf{r}(t)$ to $\mathbf{r}_\mu(t)$ (which is part of figure 5.3) is given by

the following:

$$\dot{\mathbf{z}}(t) = \mu(t)(\mathbf{r}(t) - \mathbf{z}(t)) \tag{5.23}$$

$$\mathbf{r}_\mu(t) = \mathbf{z}(t) \tag{5.24}$$

The system (5.23)-(5.24) is a BIBO stable system, i.e. for bounded $\mathbf{r}(t)$ the signal $\mathbf{r}_\mu(t)$ is also bounded. This can be shown formally by using Lyapunov stability theory with a Lyapunov function of $V = \mathbf{z}^T(t)\mathbf{z}(t)$ where $\dot{V} = 2\mu(t)\mathbf{z}^T(t)(\mathbf{r}(t) - \mathbf{z}(t))$. If $\mathbf{r}(t)$ is bounded the function $\dot{V}$ is negative definite for large $\mathbf{z}(t)$ and thus, $\mathbf{z}(t)$ will be bounded.

With the RG operator the controls never saturate so the system from $\mathbf{r}_\mu(t)$ to $\mathbf{y}(t)$ (which is part of figure 5.3) is a linear system; it is also assumed to be stable since one of the purposes of $\mathbf{K}(s)$ is to stabilize the linear feedback system. As a result, the control system from $\mathbf{r}(t)$ to $\mathbf{y}(t)$ is BIBO stable. This is an important fact because when the open loop plant is unstable the linear control system in the present of saturation may not be BIBO stable for all reference signals.

Since the RG operator is outside of the closed loop system, when disturbances are present one cannot guarantee that the control will not saturate. In fact, there always exists a disturbance that will cause saturation and instability. The stability theory described in chapter 2 will now be used to show the trade-offs between "good" command following and "good" disturbance rejection. Figure 5.4 show the closed loop system with the RG operator and output disturbances. The following analysis was done only for output disturbances, similar analysis can be performed for other type of disturbances as well.

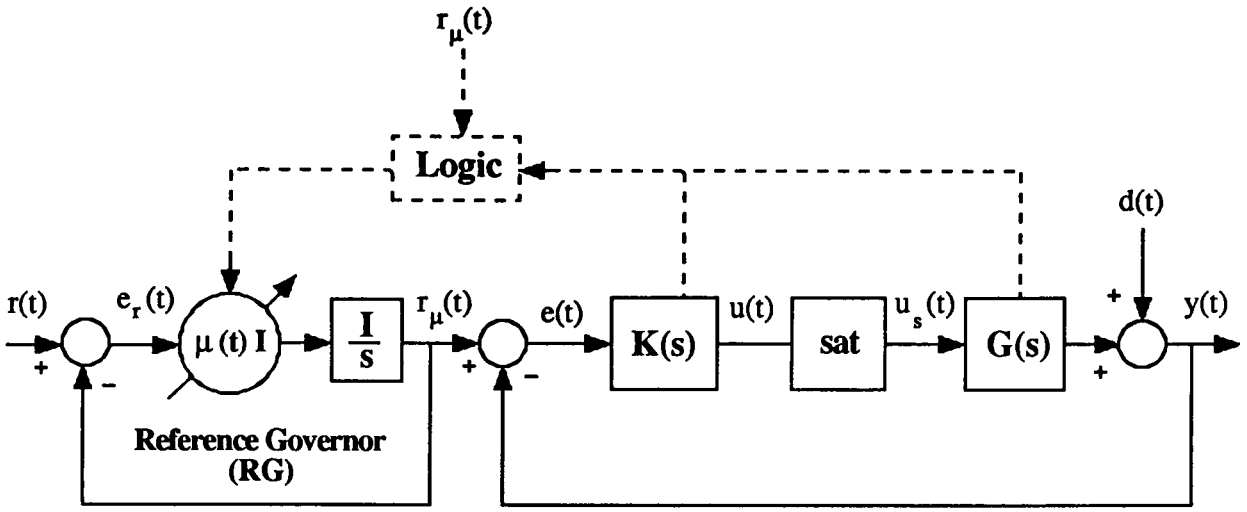

Figure 5.4: Control structure with the operator RG and output disturbances.

It is clear that if $\mathbf{r}(t)$ is chosen so that the controls will reach the saturation limits, then there is a disturbance with $\|\mathbf{d}(t)\|_\infty < \varepsilon$, $\forall \varepsilon > 0$ such that the controls will exceed the limits of the saturation. To avoid that, one can introduce an artificial saturation level $\mathbf{s} = [\, s_1 \quad s_m]^T$ with $s_i < 1$ and choose $\mu(t)$ so that the references will never cause the controls of the system to exceed the artificial saturation limit $\mathbf{s}$. Then L_∞ bounds can be defined, as we shall do in theorem 5.1, for the disturbances so that if the disturbances do not violate those L_∞ bounds the controls will always remain within the real saturation limits.

In effect, the controls action can be used, partly, to track commands ($\|u_i(t)\|_\infty \le s_i$) and, partly, to reject disturbances ($\|u_i(t)\|_\infty \le 1\text{-}s_i$). The artificial saturation $\mathbf{s}$ is "reserving" part of the control action for command following and the rest of the control action is used for disturbance rejection. In theorem 5.1 the relationship (trade-offs) between $\mathbf{s}$ and the L_∞ bound on the disturbances that can be rejected will be given.

To ensure that only part of the control is used for command following the operator RG can be used to guarantee that $\|u_i(t)\|_\infty \le s_i$. The computation of $\mu(t)$ for this case is similar to the case where the saturation limit is 1. For example, in the computation of $\mu(t)$ one could scale the

compensator so that the control saturation limits instead of s they would be 1. In the implementation, by rescaling the compensator, the actual saturation levels will be s again.

Theorem 5.1:

If the RG operator is used in any feedback system so that the controls ($\|u_i(t)\|_\infty \le s_i$), for some vector s the following is true. With zero initial conditions, the closed loop system with the RG operator will have bounded controls ($\|u(t)_\infty \le 1$) and bounded outputs for any reference and for output disturbances that satisfy the following condition.

$$\begin{bmatrix} s_1 \\ \cdots \\ s_m \end{bmatrix} + \begin{bmatrix} \|h_{11}\|_1 \ldots . \|h_{1m}\|_1 \\ \ldots\ldots\ldots\ldots \\ \|h_{m1}\|_1 \ldots . \|h_{mm}\|_1 \end{bmatrix} \begin{bmatrix} \|d_1\|_\infty \\ \ldots \\ \|d_m\|_\infty \end{bmatrix} \le \begin{bmatrix} 1 \\ \ldots \\ 1 \end{bmatrix} \tag{5.25}$$

where h_{ij} is impulse response of the ij^{th} element of the following transfer function matrix

$$\mathbf{H}(s) = [\mathbf{I} + \mathbf{K}(s)\mathbf{G}(s)]^{-1}\mathbf{K}(s) \tag{5.26}$$

Proof:

$$u(t) = \begin{bmatrix} \sum_{j=1}^{m} \int_0^t h_{1j}(t-\tau) r_{\mu 1}(\tau)\, d\tau \\ \ldots\ldots\ldots\ldots\ldots \\ \sum_{j=1}^{m} \int_0^t h_{mj}(t-\tau) r_{\mu j}(\tau)\, d\tau \end{bmatrix} + \begin{bmatrix} \sum_{j=1}^{m} \int_0^t h_{1j}(t-\tau) d_j(\tau) \\ \ldots\ldots\ldots\ldots\ldots \\ \sum_{j=1}^{m} \int_0^t h_{mj}(t-\tau) d_j(\tau) \end{bmatrix} \tag{5.27}$$

By following similar manipulations as the ones for the proof of Theorem 2.1 one can obtain the following

$$\|u_i(t)\|_\infty \le \sum_{j=1}^{m} \|h_{ij}\|_1 \, \|r_{\mu j}\|_\infty + \sum_{j=1}^{m} \|h_{ij}\|_1 \, \|d_j\|_\infty \tag{5.28}$$

Since $\mathbf{r}_\mu(t)$ is chosen so that the controls $\mathbf{u}(t)$ will never exceed the artificial limit $\mathbf{s}$ the following is true.

$$\|u_i(t)\|_\infty \le \sum_{j=1}^{m} \|h_{ij}\|_1 \, \|d_j\|_\infty + s_i \tag{5.29}$$

For the controls to remain bounded ($\|\mathbf{u}(t)\|_\infty \le 1$) the following has to be true.

$$\|u_i(t)\|_\infty \le \sum_{j=1}^{m} \|h_{ij}\|_1 \, \|d_j\|_\infty + s_i \le 1 \tag{5.30}$$

then eq. (5.30) is a compact version of eq. (5.25).

////

From the previous discussion theorem 5.1 can be used to illustrate the trade-offs between "good" command following and "good" disturbance rejection. There are two ways to use theorem 5.1

(a) If we know upper bounds on the output disturbances that exist in the operating

environment of the control system, the following is true; one can compute the artificial saturation s so that all possible disturbances will be rejected. These upper bounds usually come from experimental data and the specific operating environment of the system. Then the vector s is computed by the following:

$$\begin{bmatrix} s_1 \\ \cdots \\ s_m \end{bmatrix} \leq - \begin{bmatrix} \|h_{11}\|_1 \ldots . \|h_{1m}\|_1 \\ \ldots\ldots\ldots\ldots \\ \|h_{m1}\|_1 \ldots . \|h_{mm}\|_1 \end{bmatrix} \begin{bmatrix} \|d_1\|_\infty \\ \ldots \\ \|d_m\|_\infty \end{bmatrix} + \begin{bmatrix} 1 \\ \ldots \\ 1 \end{bmatrix} \tag{5.31}$$

An operator RG will be included in the control system to guarantee that the references will never cause the controls to exceed the artificial saturation s. In this context, if s_i, for some i, is negative then there exists a disturbance that will cause the system to saturate even if $\mathbf{r}(t) = 0$ for all t. If s_i is positive, for all i, then there is a disturbance ($d_j(t) = \|d_j(t)\|_\infty \text{sign}(h_{ij})$, for some i) with magnitude within the specified upper bounds and some reference, to cause the controls to reach the limits of the real saturation (±1). In that sense theorem 5.1 is not conservative.

(b) If the disturbances are not known then the control designer has to define the artificial saturation s. The value of s should be specified so that with, $\|u(t)\|_\infty \leq s$, there is "enough" control action for the system to perform (command following) well. One can compute s by using experimental data, the specifications of the control system, and the specific application. For example, if we have a stable plant $G^{-1}(s)$, where $G^{-1}(0)$ exists, and it is desired to track command with steady state value of r then $s = G^{-1}(0)r$. With the value of s one can compute an upper bound for the disturbances that will never cause saturation (±1) as follows:

$$\begin{bmatrix} \|h_{11}\|_1 & \cdots & \|h_{1m}\|_1 \\ \cdots & \cdots & \cdots \\ \|h_{m1}\|_1 & \cdots & \|h_{mm}\|_1 \end{bmatrix} \begin{bmatrix} \|d_1\|_\infty \\ \cdots \\ \|d_m\|_\infty \end{bmatrix} \leq \begin{bmatrix} 1 \\ \cdots \\ 1 \end{bmatrix} - \begin{bmatrix} s_1 \\ \cdots \\ s_m \end{bmatrix} \tag{5.32}$$

From theorem 5.1 (expression 5.25) is evident that the smaller the disturbances (in the operating environment of the system) the better the command following. More research is needed to find out if the vector **s** can be time varying so as it adapts to changes in the operating environment of the system. For example, if larger disturbances are present for some period of time it may be possible to decrease the value of **s** for that period and allow the controller to reject larger disturbances.

In addition to disturbances, modelling errors can cause the feedback system to saturate and thus degrade the performance or even to drive the system unstable. At this point, it is not clear how to define a class of modelling errors so that the closed loop system with the RG operator will remain stable in the presence of those modelling errors. But one can extent the idea for handling the disturbances to the case where modelling errors are present. To be more specific, one can adjust the artificial saturation levels s_i's to lower levels; at the expense of command following the stability robustness of the control system will increase. Engineering intuition and simulations have to be used to find the exact level of the s_i's and the modelling errors that can be handled.

Remember that with the EG operator for stable "true" plants and/or stable unmodelled dynamics stability (finite gain) robustness was guaranteed. That is another reason (in addition to the complexity of RG) to use the EG operator instead of the RG operator for control systems with stable plants and neutrally stable compensators.

5.2.2 Computation of the Operator RG

The computation of the RG operator can be implemented with similar techniques as the ones used to implement the operator EG (in section 4.2.2). The only difference is that the augmented system (5.12)-(5.13) is used for the computations instead of the compensator. Therefore, the state vector of the augmented system $\mathbf{x}_a(t)$ is used instead of just the compensator state vector $\mathbf{x}_c(t)$ and the reference $\mathbf{r}(t)$ is used instead of the error $\mathbf{e}(t)$.

For the RG operator the states of the compensator and the states of the plant have to be measured. It may be possible to use state estimates of the plant to compute an approximate $\mu(t)$ and more research is needed in this area to find the effects of the estimates on the computation of the operator $\mu(t)$.

For the simulations in this chapter the computations were performed on-line in the Macintosh 512K.

5.2.3 Simulation of the F16 Aircraft

As it was described previously the introduction of the saturation in the a closed loop system when the open loop plant is unstable can

(a) cause instability of the closed loop system

(b) cause integrator windups

(c) alter the directions of the controls and thus affect the performance of the system.

The purpose of the next example is to illustrate these problems and to show how the new control design method solves these problems.

Consider a model of the AFTI-16 (Advanced Fighter Technology Integration) aircraft, which is a modified F-16 aircraft. The following linear time invariant model is an approximation of the aircraft longitudinal dynamics at 3,000 ft altitude and .6 Mach velocity [43].

$$\dot{\mathbf{x}}(t) = \begin{bmatrix} -.0151 & -60.5651 & 0 & -32.174 \\ -.0001 & -1.3411 & .9929 & 0 \\ .00018 & 43.2541 & -.86939 & 0 \\ 0 & 0 & 1 & 0 \end{bmatrix} \mathbf{x}(t) + \begin{bmatrix} -2.516 & -13.136 \\ -.1689 & -.2514 \\ -17.251 & -1.5766 \\ 0 & 0 \end{bmatrix} \mathbf{u}_s(t) \tag{5.33}$$

$$\mathbf{y}(t) = \begin{bmatrix} 0 & 1 & 0 & 0 \\ 0 & 0 & 0 & 1 \end{bmatrix} \mathbf{x}(t) \tag{5.34}$$

and in compact form

$$\dot{\mathbf{x}}(t) = \mathbf{A}\mathbf{x}(t) + \mathbf{B}\mathbf{u}_s(t) \tag{5.35}$$

$$\mathbf{y}(t) = \mathbf{C}\mathbf{x}(t) \tag{5.36}$$

where

$$\mathbf{x}(t) = \begin{bmatrix} u(t) & \text{forward velocity (ft/sec)} \\ \alpha(t) & \text{angle of attack (deg)} \\ q(t) & \text{pitch rate (deg/sec)} \\ \theta(t) & \text{pitch angle (deg)} \end{bmatrix} \tag{5.37}$$

$$\mathbf{u}(t) = \begin{bmatrix} \delta_e(t) & \text{elevator angle (deg)} & \text{limit at } 25^\circ \\ \delta_f(t) & \text{flaperon angle (deg)} & \text{limit at } 25^\circ \end{bmatrix} \tag{5.38}$$

$$\mathbf{y}(t) = \begin{bmatrix} \alpha(t) & \text{angle of attack (deg)} \\ \theta(t) & \text{pitch angle (deg)} \end{bmatrix} \tag{5.39}$$

As shown in Table 5.1 the model has three unstable poles, one stable one and one minimum phase transmission zero. Figure 5.5 shows the singular values of the F16 linear model. Assume that we wish to design a closed loop system so that the F16 follows angle of attack and pitch attitude with zero steady state error required for step commands.

Table 5.1 Poles and zeros of the F16 model

Poles

Real	Imaginary	Magnitude	Damping
7.5054E-03	6.8019E-02	6.8432E-02	-1.0968E-01
7.5054E-03	-6.8019E-02	6.8432E-02	-1.0968E-01
5.4533E+00	0.0000E-01	5.4533E+00	-1.0000E+00
-7.6638E+00	0.0000E-01	7.6638E+00	1.0000E+00

Zeros

Real	Imaginary	Magnitude	Damping
-5.4188E-01	0.0000E-01	5.4188E-01	1.0000E+00
3 more infinite			

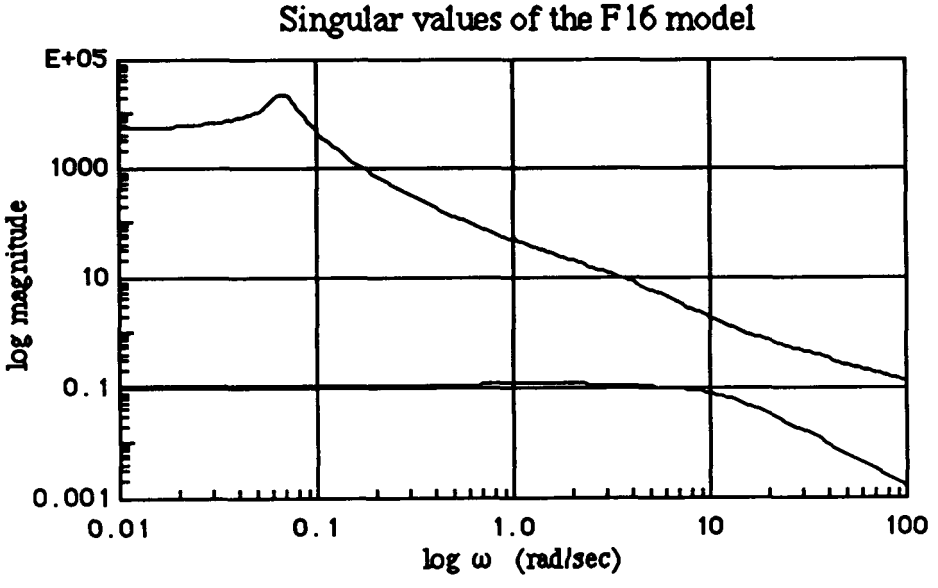

Figure 5.5: Singular values of the F16 model.

Linear control theory will be used to design the closed loop system, then the linear design

will be modified as indicated in section 5.2 with a time varying rate $\mu(t)$. Finally, simulations will be performed to assess the benefits of the new design methodology.

To obtain the linear closed loop system, integrators have to be added at the controls; and the augmented system is given by the following

$$\dot{\mathbf{x}}_a(t) = \mathbf{A}_a\mathbf{x}_a(t) + \mathbf{B}_a\mathbf{u}_a(t) \tag{5.40}$$

$$\mathbf{y}(t) = \mathbf{C}_a\mathbf{x}_a(t) \tag{5.41}$$

$$\mathbf{u}(t) = \frac{\mathbf{I}}{s}\mathbf{u}_a(t) \tag{5.42}$$

where

$$\mathbf{A}_a = \begin{bmatrix} \mathbf{0} & \mathbf{0} \\ \mathbf{B} & \mathbf{A} \end{bmatrix} \qquad \mathbf{B}_a = \begin{bmatrix} \mathbf{I} \\ \mathbf{0} \end{bmatrix} \qquad \mathbf{C}_a = \begin{bmatrix} \mathbf{0} & \mathbf{C} \end{bmatrix}$$

A linear compensator was designed for the augmented system to control the angle of attack and the pitch angle tracking errors. The LQG/LTR methodology was used to design the compensator, whose numerical specification is as follows:

$$\mathbf{K}(s) = \mathbf{G}[\, s\mathbf{I} - \mathbf{A}_a - \mathbf{B}_a\mathbf{G} - \mathbf{H}\mathbf{C}_a\,]^{-1}\,\mathbf{H} \tag{5.43}$$

$$\mathbf{K}_a(s) = \frac{\mathbf{I}}{s}\,\mathbf{K}(s) \tag{5.44}$$

where

$$H = \begin{bmatrix} 1.6144 & -2.5463 \\ -7.1687 & 7.5901 \\ -15.808 & -149.5065 \\ 5.924 & 5.1557 \\ 37.0141 & 40.7261 \\ 5.1557 & 7.4747 \end{bmatrix} \qquad G = \begin{bmatrix} 56.3 & 8.37 & .0014 & -535.6 & -88.67 & -908.22 \\ 8.37 & 19.2 & .0115 & -791.35 & -12.96 & 418.46 \end{bmatrix}$$

Table 5.2 shows the poles and transmission zeros of the compensator. Note that the compensator partially inverts the stable part of the open loop plant. To be more specific, the compensator cancels the stable pole and the minimum phase transmission zero of the plant.

Table 5.2 Poles and zeros of the F16 linear compensator

Poles

Real	Imaginary	Magnitude	Damping
-5.4188E-01	0.0000E-01	5.4188E-01	1.0000E+00
-1.3184E+01	2.3468E+01	2.6918E+01	4.8980E-01
-1.3184E+01	-2.3468E+01	2.6918E+01	4.8980E-01
-2.9587E+01	0.0000E-01	2.9587E+01	1.0000E+00
-9.7553E+01	9.7639E+01	1.3802E+02	7.0680E-01
-9.7553E+01	-9.7639E+01	1.3802E+02	7.0680E-01

Zeros

Real	Imaginary	Magnitude	Damping
-5.4485E-01	0.0000E-01	5.4485E-01	1.0000E+00
-4.9996E+00	1.6683E+00	5.2706E+00	9.4858E-01
-4.9996E+00	-1.6683E+00	5.2706E+00	9.4858E-01
-7.2543E+00	0.0000E-01	7.2543E+00	1.0000E+00
2 more infinite			

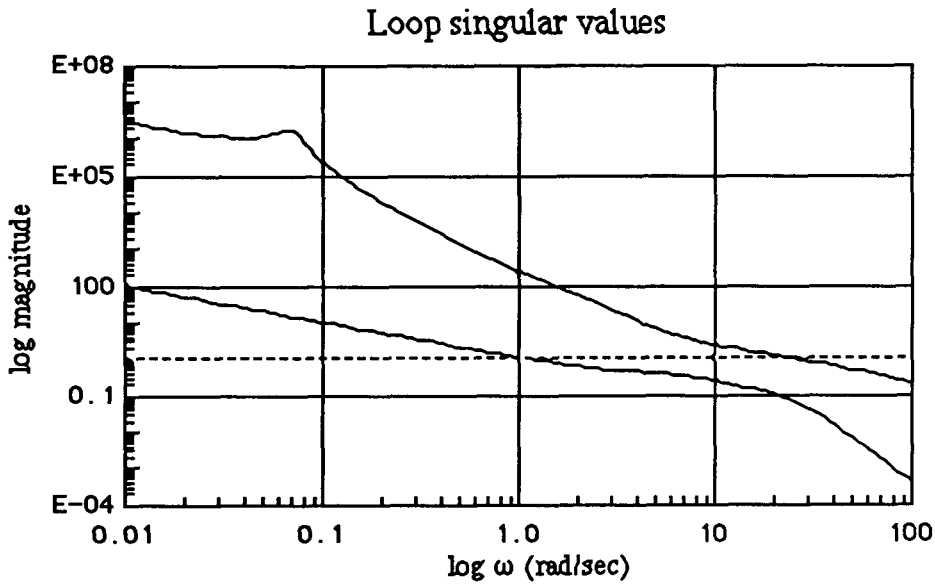

Figure 5.6: Singular values of the loop transfer function in the F16 closed loop system.

Figure 5.6 shows the singular values of the loop transfer function matrix **G**(s)**K**(s) of the linear control system. It is assumed that the **G**(s)**K**(s) loop is the desired forward loop transfer matrix. If it is not, then the linear compensator has to be redesigned. Figure 5.7 shows the control feedback system with the RG operator.

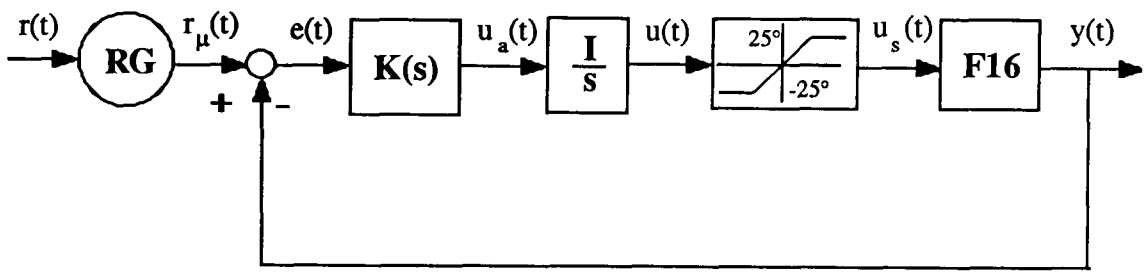

Figure 5.7: Closed loop system for the F16 example with RG.

We now deal with a multivariable control system for an unstable open loop plant with integrators and a saturation element in the forward loop. Without the RG operator the control system is expected to have the following problems (a) for certain references $\mathbf{r}(t)$ the outputs $\mathbf{y}(t)$ will be unbounded, (b) integrator windups may be present, and (c) the saturation can alter the direction of the controls and thus degrade the transient performance of the system.

Three types of simulation were performed for the closed loop system shown in figure 5.7. These different types of simulation are the following:

1) The first simulation is for the *linear system.* Again we assume that the compensator $\mathbf{K}(s)$ we designed yields desirable linear responses.
2) In the second simulation the saturation element is added to the linear system, $\mathbf{u}_s(t) = \text{sat}(\mathbf{u}(t))$, without any other modifications. This simulation is referred to as the simulation for the *system with saturation.*
3) In the third simulation $\mathbf{u}_s(t) = \text{sat}(\mathbf{u}(t))$, and $\mu(t)$ is computed entirely on-line by the method given in section 5.2.2. The simulation was performed in a Macintosh 512K and it required approximately 15-16 hours. This simulation is referred to as the simulation of the *system with saturation and the RG.*

At first, the linear system was simulated for $\mathbf{r} = [\,0 \quad 10]^T$ corresponding to a 10° pitch angle with zero (trim) angle of attack. Figures 5.8 and 5.9 show the output and control responses of the linear system. Note that the controls have "impulsive" action at the beginning and they exceed by far the 25° limits so saturation is expected. Also note that the maximum flaperon control value is approximately 83°.

We remark that the quality of the linear output transients (figure 5.8) are not particularly "nice" due to the overshoots present. However, for the sake of comparisons that follow we shall assume that they represent desirable shapes.

Figures 5.10 and 5.11 show the output and control responses of the system with

saturation. The closed loop system for the reference input $\mathbf{r} = [\,0 \quad 10]^T$ is unstable. Note that, in general, when the open loop system is unstable and saturation at the controls is present the resulting control system is only locally stable.

Figures 5.12 and 5.13 show the output and control responses of the system with saturation and the RG operator. The stability of the closed loop control system is recovered and the shape of the transient response is similar (but slower, as expected) to the linear response. Compare figures 5.8 and 5.12; they are almost identical !!!. Also, the controls $\mathbf{u}(t)$ never exceed the saturation limits, as guaranteed by the design methodology.

Figure 5.14 show the modified reference $r_{m2}(t)$. Since the first reference is zero the $r_{m1}(t)$ is zero $\forall t$ and it was not plotted. Note that the $r_{m2}(t)$, commanded pitch attitude, starts at $\approx 3^\circ$ and ramps up to the desired steady state value of 10°. The reason that the $r_{m2}(t)$ is initially $\approx 3^\circ$ is because the linear system with an $r_{m2}(t)$ of $\approx 3^\circ$ will have controls with maximum at $\approx 25^\circ$ (remember that with an $r_{m2}(t)$ of $\approx 10^\circ$ the controls had a maximum value of $\approx 83^\circ$). Then as the outputs follow the modified references the $\mathbf{r}_\mu(t)$ approaches $\mathbf{r}(t)$ in such a way that the controls will never exceed the saturation limits.

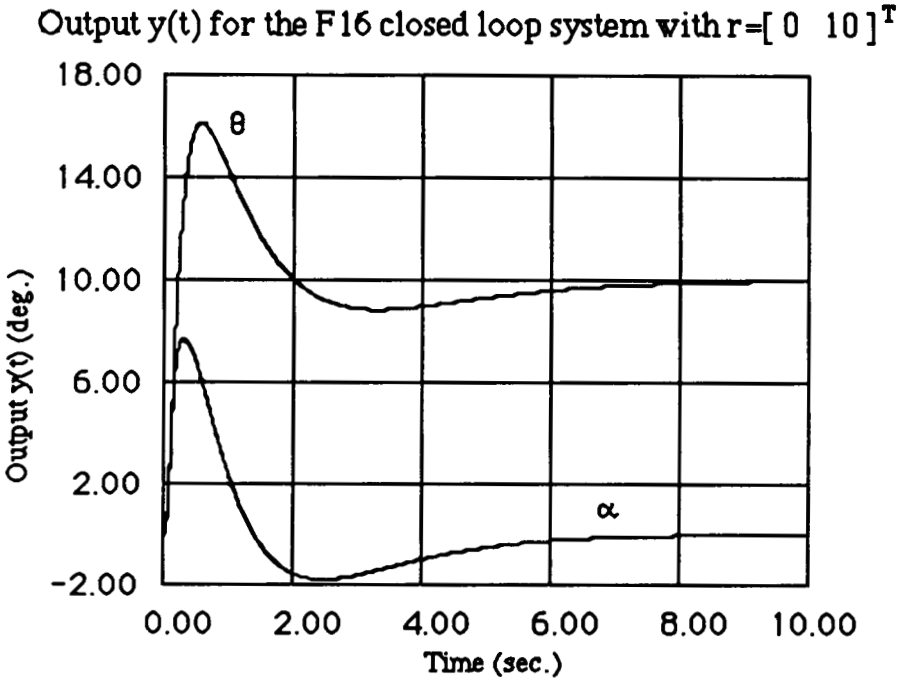

Figure 5.8: Output response of the F16 linear system, ($\mathbf{r} = [0 \quad 10]^T$).

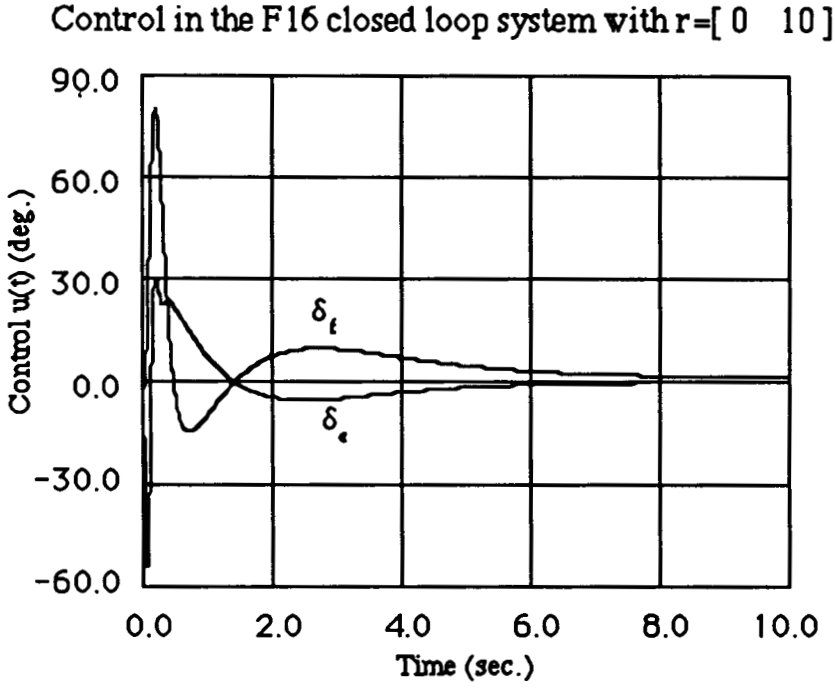

Figure 5.9: Controls in the F16 linear system, ($\mathbf{r} = [0 \quad 10]^T$).

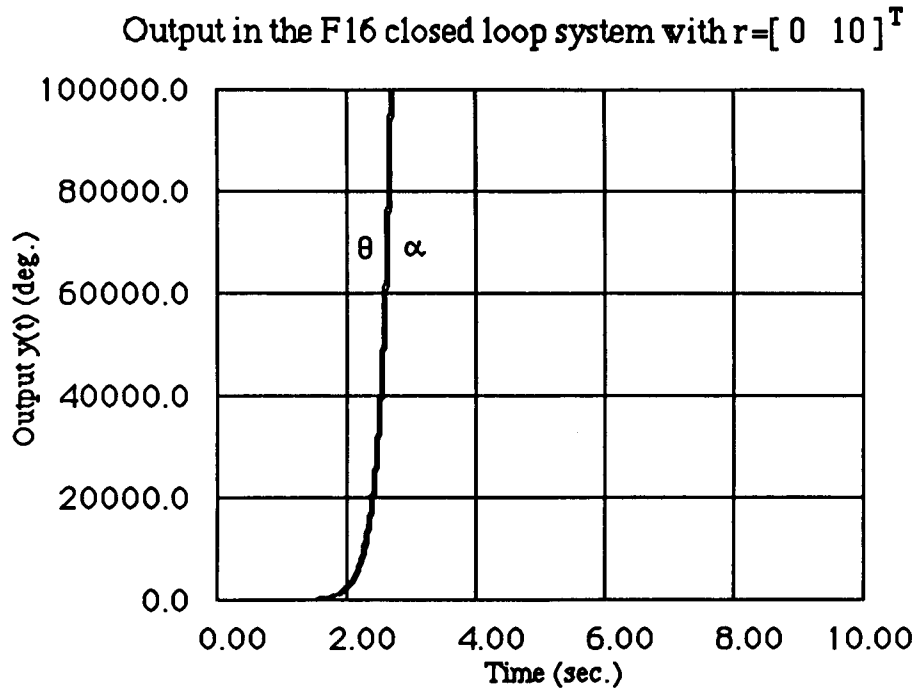

Figure 5.10: Output response of the F16 system with saturation, ($\mathbf{r} = [0 \quad 10]^T$).

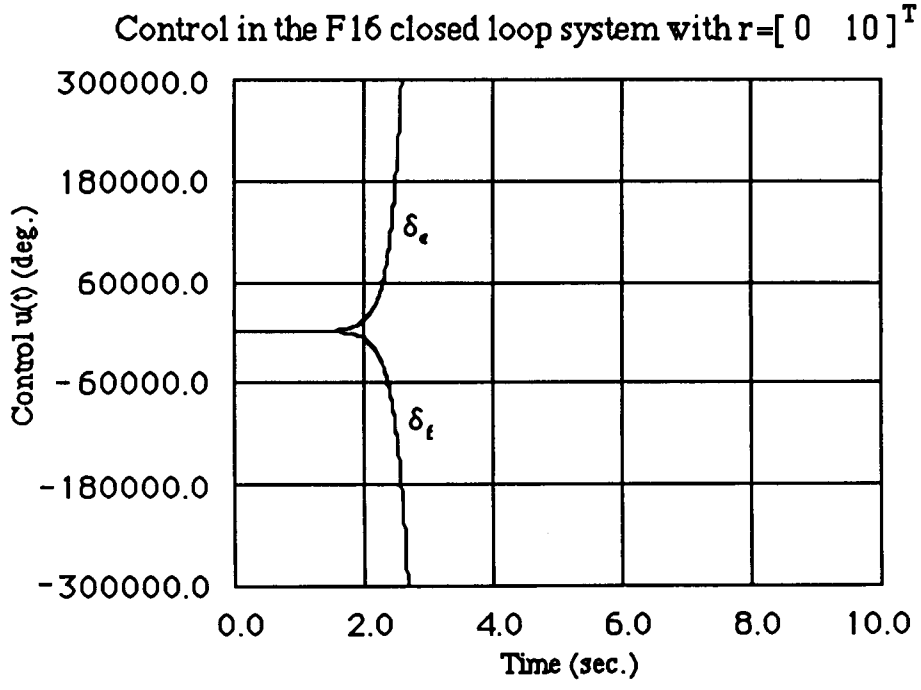

Figure 5.11: Controls in the F16 system with saturation, ($\mathbf{r} = [0 \quad 10]^T$).

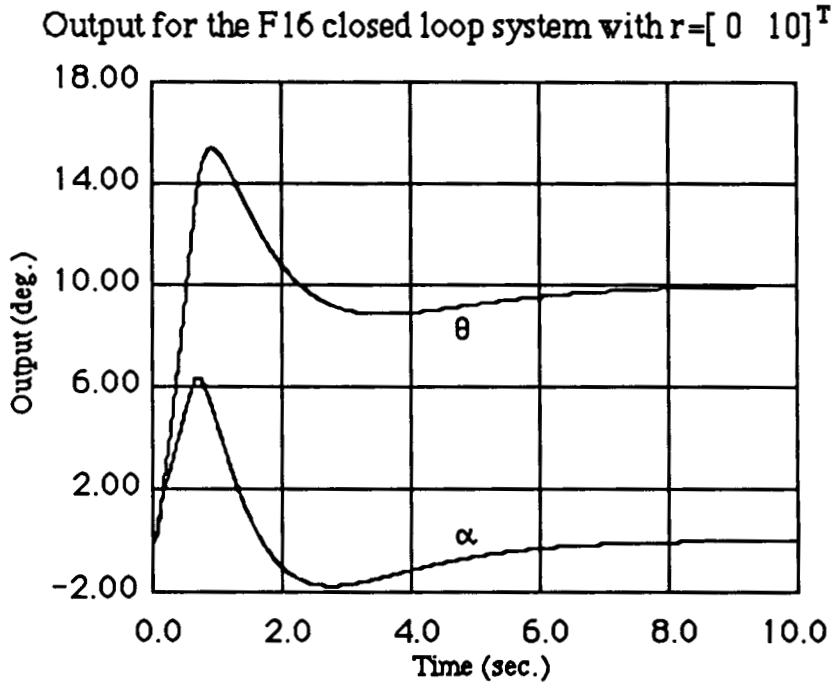

Figure 5.12: Output response for the F16 system with saturation and the RG, ($\mathbf{r} = [0 \quad 10]^T$).

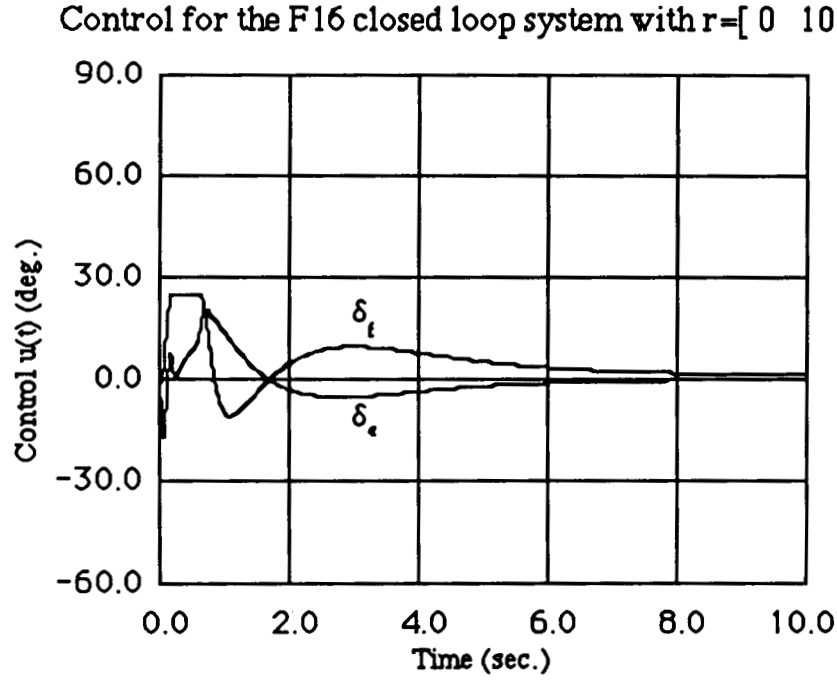

Figure 5.13: Controls in the F16 system with saturation and the RG, ($\mathbf{r} = [0 \quad 10]^T$).

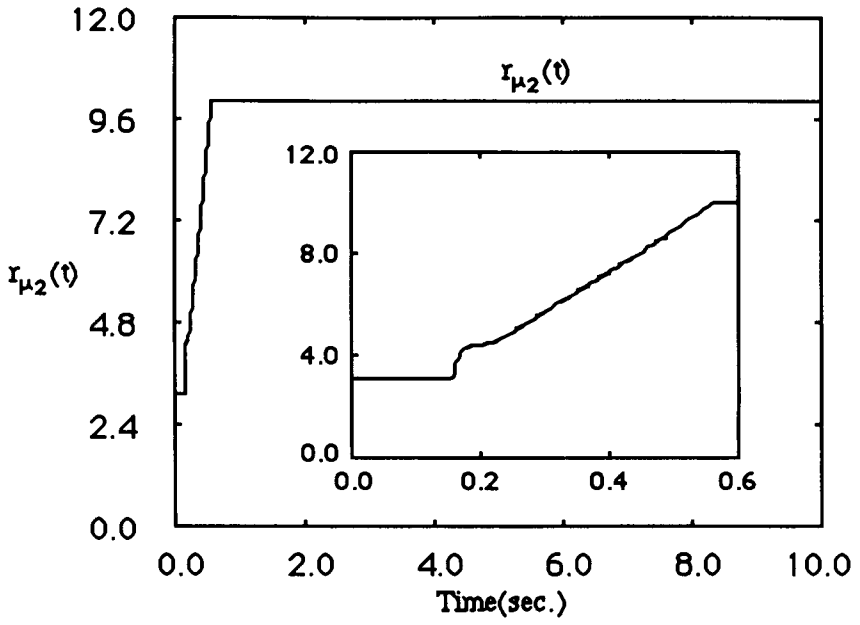

Figure 5.14: $r_{\mu 2}(t)$, the commanded pitch, in the F16 system with saturation and the RG, ($\mathbf{r} = [0 \quad 10]^T$). Blowup: Blowup with $0 \leq t \leq .6$.

A second simulation was performed for the same system with reference $\mathbf{r} = [\ 2.5 \quad 2.5\ ]^T$. Now we are commanding simultaneously 2.5° angle of attack and pitch. Figures 5.15 and 5.16 show the output and control responses of the linear system. Again the controls exceed the limits of 25° and saturation is expected.

Figures 5.17 and 5.18 show the response of the system with saturation from the output response one can see that the integrators windup although, now, the closed loop system is stable. In addition, the direction of the outputs is not similar to the direction of the outputs in the linear system and thus the control system does not behave as it was designed to behave.

Figures 5.19 and 5.20 show the output and control response of the system with saturation and the RG. The controls never exceed the limits of the saturation and thus integrator windups are not present. The output response verify the absence of integrator windups. The output response is slower because of the limited controls but the direction of the outputs is similar to that of the linear system. Figure 5.21 show the modified reference $\mathbf{r}_\mu(t)$.

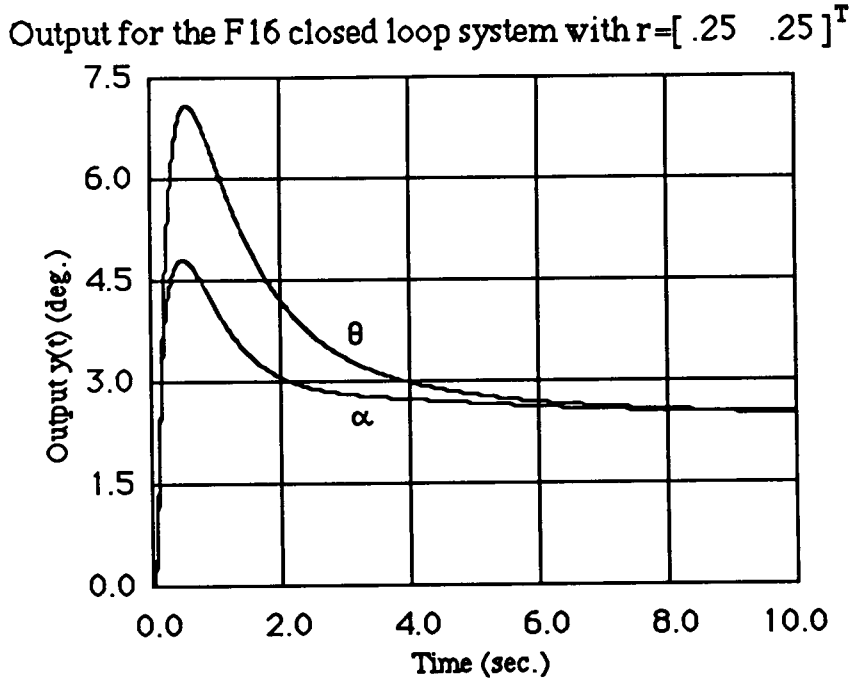

Figure 5.15: Output response for the F16 linear system, ($\mathbf{r} = [2.5 \quad 2.5]^T$).

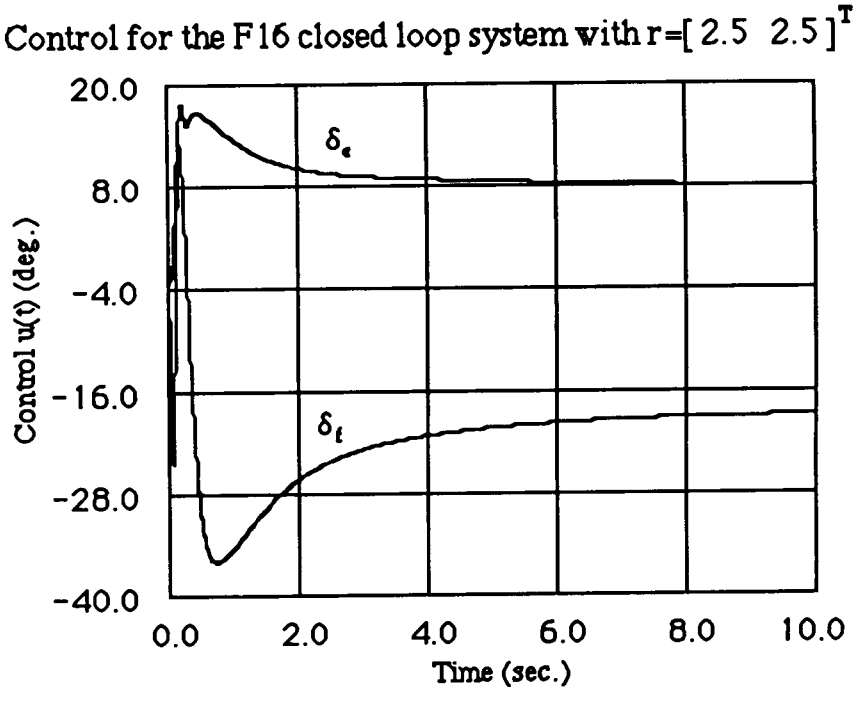

Figure 5.16: Controls in the F16 linear system, ($\mathbf{r} = [2.5 \quad 2.5]^T$).

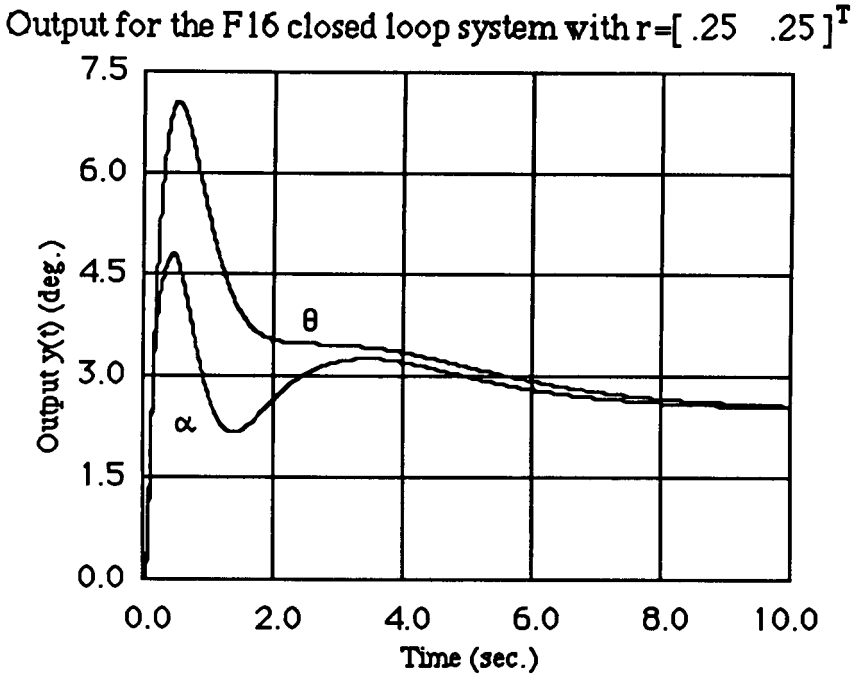

Figure 5.17: Output response for the F16 system with saturation, ($\mathbf{r} = [2.5 \quad 2.5]^T$).

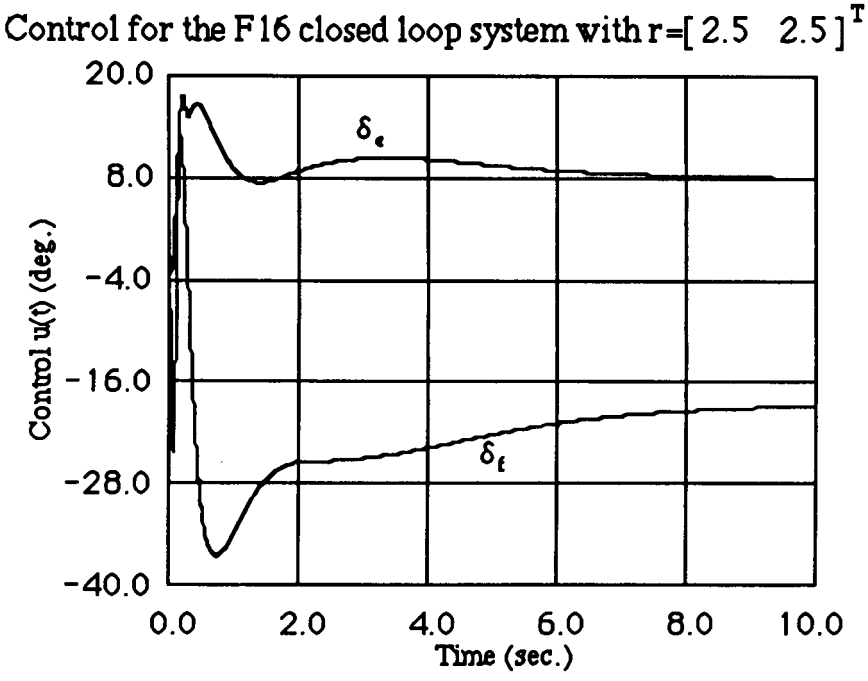

Figure 5.18: Controls in the F16 system with saturation, ($\mathbf{r} = [2.5 \quad 2.5]^T$).

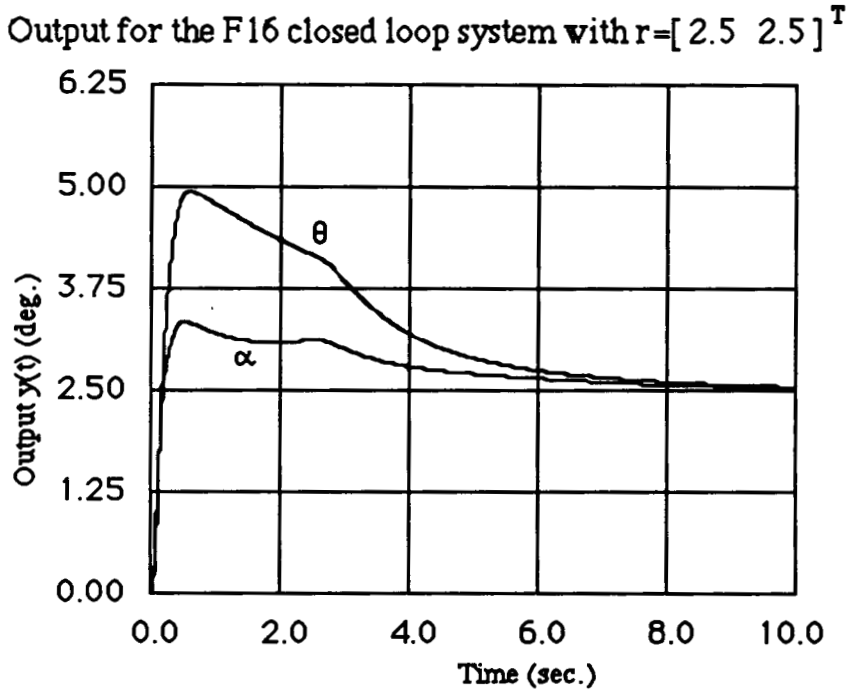

Figure 5.19: Output response for the F16 system with saturation and the RG, ($\mathbf{r} = [2.5 \quad 2.5]^T$).

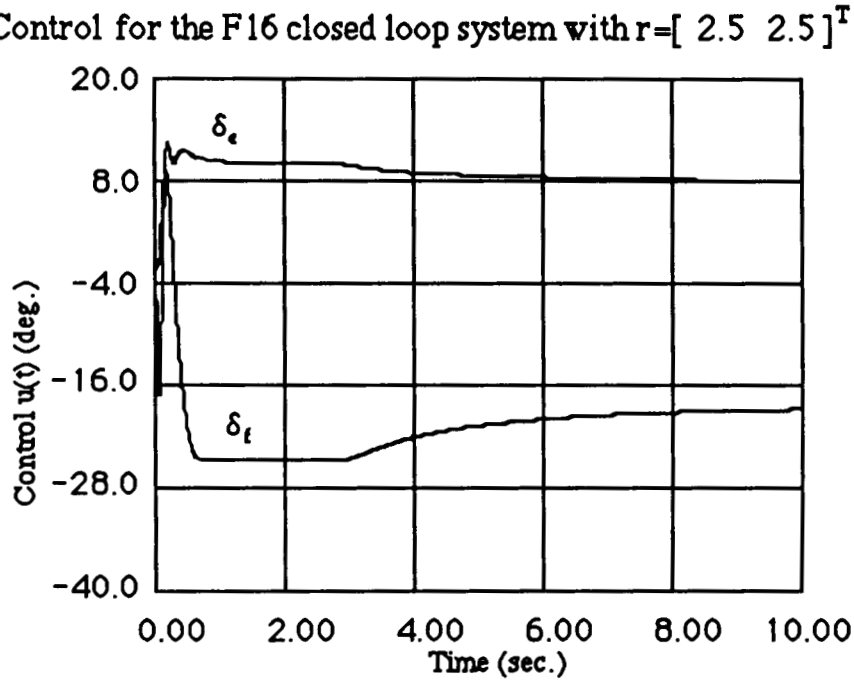

Figure 5.20: Controls in the F16 system with saturation and the RG, ($\mathbf{r} = [2.5 \quad 2.5]^T$).

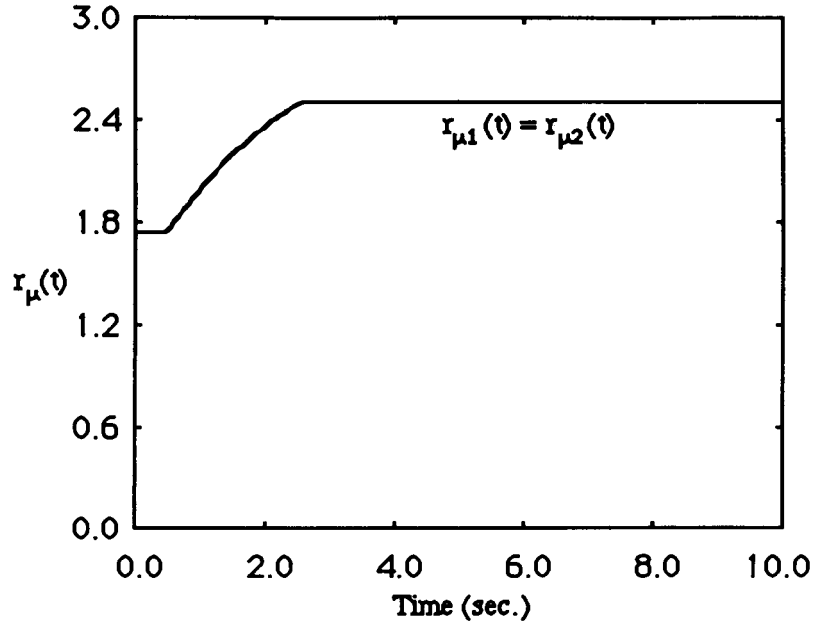

Figure 5.21: $\mathbf{r}_\mu(t)$ in the F16 system with saturation and the RG, ($\mathbf{r} = [2.5 \quad 2.5]^T$).

Another simulation was performed to demonstrate the preservation of the closed loop stability and the fact the controls will not saturate ("good" performance) for a certain class of disturbances, as it was described in section 5.2.1. An artificial saturation limit $s_1 = s_2 = 20°$ was introduced; the underline assumption here is that 20° of control action is enough for command following. It was found by using theorem 5.1 that for any reference $\mathbf{r}(t)$ and for output disturbances of the form $\mathbf{d}(t) = [d_1(t) \quad 0]^T$ the controls will never exceed the saturation limits of 25° and stability will be preserved for $\|d_1(t)\|_\infty \leq .5$. The simulation was performed for the step reference $\mathbf{r} = [\,0 \quad 5]^T$ and a step output disturbance of $\mathbf{d} = [.5 \quad 0]^T$ which was present for $t \geq .5$ sec.

Figures 5.22 and 5.23 show the output and the control responses of the system with saturation and the RG. Note that system remained stable and the disturbances are rejected as it was expected. The controls exceed the 20° limit (the artificial saturation) but they do not exceed the 25° limit (the real saturation). Figure 5.24 show the modified references for this simulation.

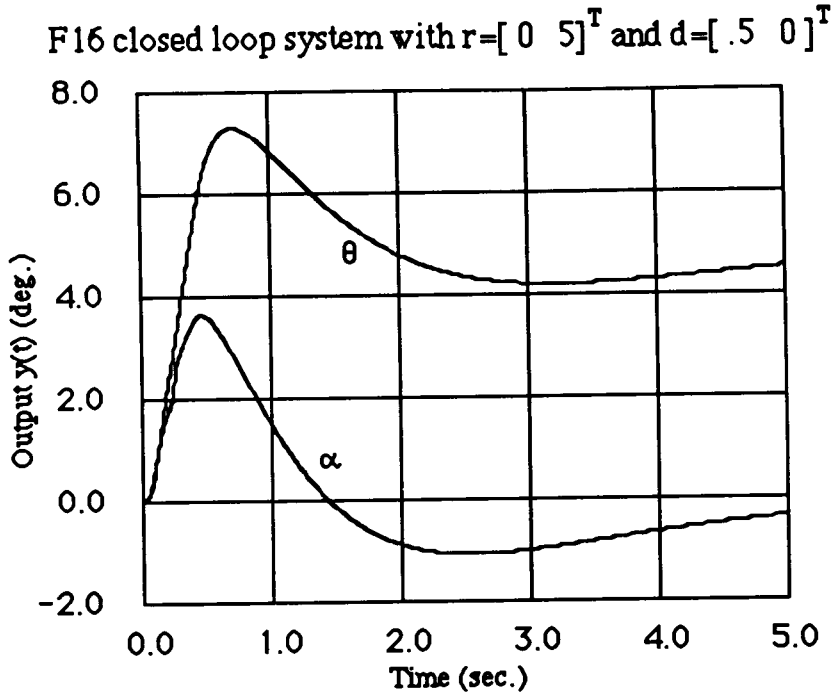

Figure 5.22 : Output response for the F16 system with saturation and the RG, ($\mathbf{r} = [0 \quad 5]^T$, $\mathbf{d} = [.5 \quad 0]^T$).

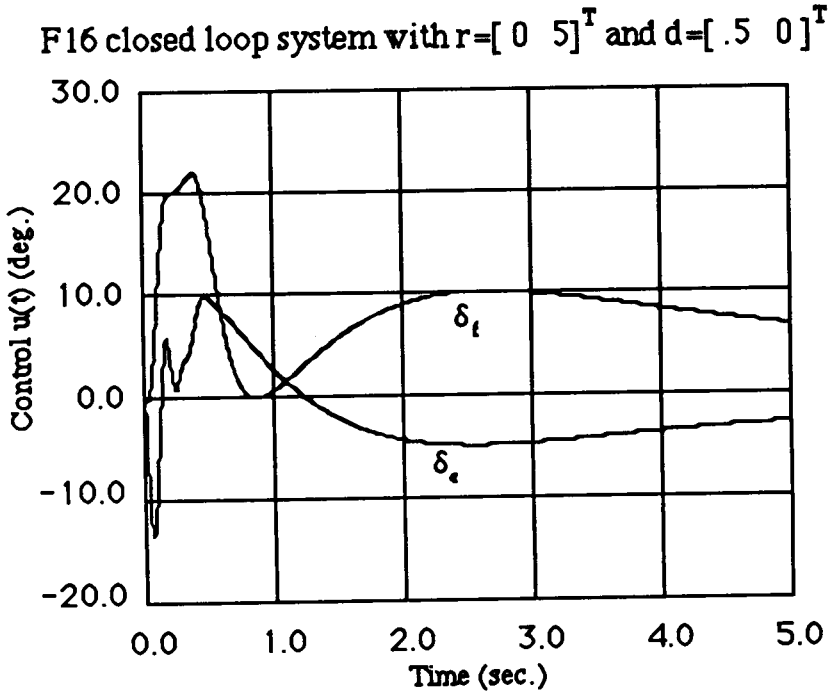

Figure 5.23: Controls in the F16 system with saturation and the RG, ($\mathbf{r} = [0 \quad 5]^T$, $\mathbf{d} = [.5 \quad 0]^T$).

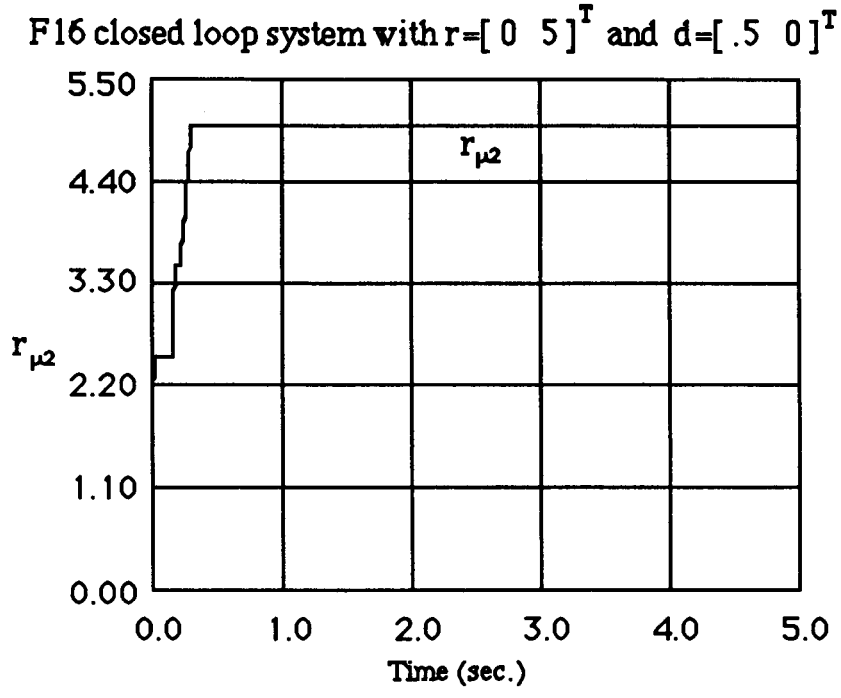

Figure 5.24: $\mathbf{r}_\mu(t)$ in the F16 system with saturation and the RG, ($\mathbf{r} = [0 \quad 5]^T$, $\mathbf{d} = [.5 \quad 0]^T$).

5.3 Control Structure with the Operators EG and RG

In section 5.2 a control structure with the RG operator has been described to be used in feedback systems with plants that are open loop unstable. The control structure is such that for any references and for all disturbances in an L_∞ set the controls of the closed loop system will not saturate. Consequently, the closed loop system remains linear, integrator windups never occur, bounded outputs are guaranteed, and the directions of the controls are not changed by the saturation.

The operation of the closed loop system is linear by the construction of the RG operator. Since the disturbances enter the system at points inside the closed loop one may be able to reject larger disturbances if the operator EG is added at the error signal. If the EG operator is

beneficial to include to the control structure or not **depends on the specific application** and the kind of disturbances which are present as we shall see in section 5.3.2.

5.3.1 Description of the Control Structure with the Operators EG and RG

If the plant in the control system is stable the EG operator is sufficient to ensure that the controls do not saturate for any reference, disturbance and modelling error (see section 4.2). Therefore, the RG operator is not needed. The control structure with the operators EG and RG is useful only for control systems with **unstable plants and neutrally stable compensators.** In this section the discussion will be centered around unstable plants and figure 5.25 show the control structure with the operators EG and RG. The models of the **G**(s), and **K**(s) systems in figure 5.25 are given in eqs. (5.1)-(5.5).

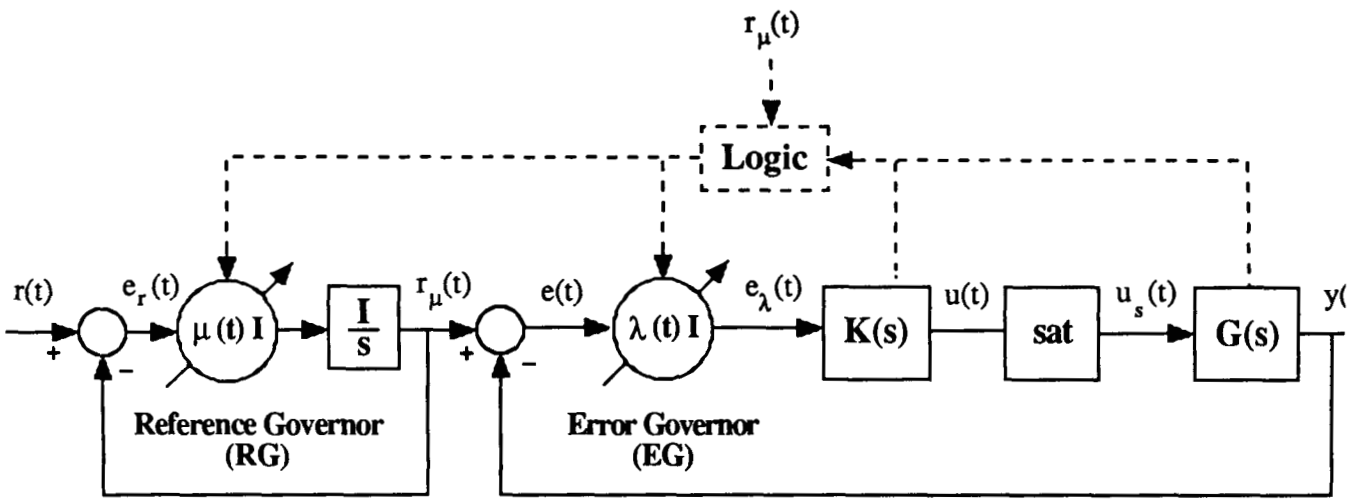

Figure 5.25: Control structure with the operator EG & RG.

Since the plant **G**(s) is open loop unstable one cannot guarantee BIBO stability with $\lambda(t)$ varying from zero to one ($0 \le \lambda(t) \le 1$). Note that if $\lambda(t) = 0$ for a finite time, the system is

running open loop, and will exhibit the instabilities of the plant.

The time-varying gain $\lambda(t)$ can be thought as a sector nonlinearity (see eq. 2.2) belonging in a sector $[1,\lambda_0]$ where λ_0 is a design parameter. The first priority for choosing λ_0 is to guarantee closed loop stability. The multiloop circle criterion (eq. (2.5), is used to define a sector $[1,\lambda_0]$, $\lambda_0 \le \lambda(t) \le 1$, such that for any nonlinear gain in the sector the closed loop system is stable. Eventually, we will ensure that the controls do not saturate so for the definition of λ_0 the saturation element in figure 5.25 will be ignored. In this case, to apply the multicircle criterion one has to compute $C_i = (1 + \lambda_0)/2$, $R_i = (1 - \lambda_0)/2$, $\mathbf{T}(s) = \mathbf{G}(s)\mathbf{K}(s)$ and then substitute these in eq. (2.5). One can search now for a λ_0, $0 \le \lambda_0 \le 1$, such that the eq. (2.5) is satisfied.

At this point we have shown that if the controls do not saturate one can choose any time-varying gain $\lambda(t)$, $\lambda_0 \le \lambda(t) \le 1$, and the closed loop system will be stable. The next step is to ensure that the controls will never saturate so that the stability argument (given above) is valid and so that the performance of the system will not degrade because of saturations. As shown in sections 4.2 and 5.2 one can design the EG and RG operators to do exactly that. The construction of $\lambda(t)$, given in chapter 4 has to be modified a little as we show in the sequel. A function $g(\mathbf{x})$ and a set $\mathbf{B}_{A,C}$ are needed for the computation of $\lambda(t)$ and they are defined as follows:

$$g(\mathbf{x_0}):\ g(\mathbf{x_0}) = \|\mathbf{u}(t)\|_\infty \tag{5.45}$$

where

$$\dot{\mathbf{x}}_c(t) = \mathbf{A}_c\mathbf{x}_c(t); \qquad \mathbf{x}_c(0)=\mathbf{x_0} \tag{5.46}$$

$$\mathbf{u}(t) = \mathbf{C}_c\mathbf{x}_c(t) \tag{5.47}$$

$$\mathbf{B}_{A,C} = \{\mathbf{x}:\ g(\mathbf{x}) \le 1\} \tag{5.48}$$

For $g(\mathbf{x})$ to be finite, for all $\mathbf{x}$, the compensator has to be neutrally stable. Therefore, the

control structure with the operators EG and RG should be used only for feedback systems with neutrally stable compensators. Then the construction of $\lambda(t)$ is given by the following

Construction of $\lambda(t)$:

For every time t choose $\lambda(t)$ as follows

a) if $\mathbf{x}_c(t) \in \text{Int}\mathbf{B}_{A,C}$ then $\lambda(t) = 1$ (5.49)

b) if $\mathbf{x}_c(t) \in \text{Bd}\mathbf{B}_{A,C}$ then choose the largest $\lambda(t)$ such that (5.50)

$$\lambda_0 \le \lambda(t) \le 1 \tag{5.51}$$

$$\lim_{\varepsilon \to 0} \sup \frac{g\left(\mathbf{x}_c(t)+\varepsilon[\mathbf{A}_c\mathbf{x}_c(t)+\mathbf{B}_c\lambda(t)\mathbf{e}(t)]\right) - g\left(\mathbf{x}_c(t)\right)}{\varepsilon} \le 0 \tag{5.52}$$

or for the points where $g(\mathbf{x})$ is differentiable choose the largest $\lambda(t)$ such that

$$\lambda_0 \le \lambda(t) \le 1 \tag{5.53}$$

$$Dg(\mathbf{x}_c(t))[\mathbf{A}\mathbf{x}_c(t)+\mathbf{B}\lambda(t)\mathbf{e}(t)] \le 0 \tag{5.54}$$

c) if $\mathbf{x}_c(t) \notin \mathbf{B}_{A,C}$ then choose $\lambda(t) = \lambda_0$.

The $\lambda(t)$ alone does not guarantee to keep the controls bounded for any reference, this is true because $\lambda(t)$ is chosen in the set $\lambda_0 \le \lambda(t) \le 1$. For this reason we introduce the RG operator at the reference signals and the time varying rate $\mu(t)$ will guarantee that the references will not cause the controls to saturate. To construct $\mu(t)$ we assume $\lambda(t) = 1$ and we follow the discussion in section 5.2. In order not to confuse the notation the function and the set needed for the construction of $\mu(t)$ will be called $\mathbf{B'}_{A,C}$ and $g'(\mathbf{x})$ and they are defined as follows:

$$g'(\mathbf{x}_{a0}): \quad g'(\mathbf{x}_{a0}) = \|\mathbf{u}(t)\|_\infty \tag{5.55}$$

where

$$\dot{\mathbf{x}}_a(t) = \mathbf{A}_a\mathbf{x}_a(t); \qquad \mathbf{x}_a(0) = \mathbf{x}_{a0} \tag{5.56}$$

$$\mathbf{u}(t) = \mathbf{C}_a\mathbf{x}_a(t) \tag{5.57}$$

$$\mathbf{B'}_{A,C} = \{\ \mathbf{x}:\ g'(\mathbf{x}) \le 1\ \} \tag{5.58}$$

where $\mathbf{x}_a$, $\mathbf{A}_a$, $\mathbf{C}_a$ are defined in eqs. (5.12)-(5.13).

For the function g'(x) to exist the system (5.56)-(5.57) has to be neutrally stable and as it was described, for the system (5.15)-(5.16), this is always true. Then the construction of $\mu(t)$ follows:

Construction of $\mu(t)$:

For every time t choose $\mu(t)$ as follows

a) if $\mathbf{x}_a(t) \in \text{Int}\mathbf{B'}_{A,C}$ then $\mu(t) = \infty$ which implies that $\mathbf{r}(t) = \mathbf{r}_\mu(t)$ (5.59)

b) if $\mathbf{x}_a(t) \in \text{Bd}\mathbf{B'}_{A,C}$ then choose the largest $\mu(t)$ such that (5.60)

$$0 \le \mu(t) \le \infty$$

$$\lim_{\varepsilon \to 0} \sup \frac{g'\left(\mathbf{x}_a(t)+\varepsilon[\mathbf{A}_a\mathbf{x}_a(t)+\mathbf{B}_a\mu(t)\mathbf{e}_r(t)]\right) - g'\left(\mathbf{x}_a(t)\right)}{\varepsilon} \le 0 \tag{5.61}$$

or for the points where g'(x) is differentiable choose the largest $\mu(t)$ such that

$$0 \le \mu(t) \le \infty \tag{5.62}$$

$$Dg'(\mathbf{x}_a(t))[\mathbf{A}_a\mathbf{x}_a(t) + \mathbf{B}_a\mu(t)\mathbf{e}_r(t)] \le 0 \quad \forall t > 0 \tag{5.63}$$

c) if $\mathbf{x}_a(t) \notin \mathbf{B'}_{A,C}$ then choose $\mu(t) = 0$.

From the construction of $\lambda(t)$ and $\mu(t)$ it is clear that if disturbances are not present then $\lambda(t) = 1$, for all t, because $\mu(t)$ is sufficient to guarantee that the controls will never saturate. So $\lambda(t)$ is a gain that is activated only if the disturbances are in such direction so that they can cause saturation in the controls. It should be pointed out that since the gain $\lambda(t)$ has a lower bound λ_0 there are always large disturbances that will cause saturation. In the next section with

the stability analysis of this structure, the trade-offs between disturbance rejection and command following will be introduced. The implementation (realization) of the operators EG and RG is described in sections 4.2.2 and 5.2.2 and will not be repeated.

5.3.2 Stability Analysis of the Control Structure with the Operators EG and RG

If the controls do not saturate with the construction of $\lambda(t)$ as described in the previous section, the constant λ_0 was chosen (using the multicircle stability theory) to ensure closed loop stability. As a result, closed stability is guaranteed for any reference and in the absence of disturbances. This is true because if disturbances are not present then $\lambda(t) = 1$, $\forall t$, and the control structure with EG and RG is the same as the control structure with only RG (see section 5.2) where BIBO stability was ensured

In the presence of disturbances one has to introduce an artificial level of saturation **s** ($\mathbf{s} = [\, s_1 \ldots s_m]^T$) as was discussed in section 5.2.1. The EG and RG operator can be chosen so that for any reference **r**(t) the controls will not exceed the artificial saturation **s**, ($\|u_i(t)\|_\infty \le s_i$). Consequently, there will be some control action "reserved" for disturbance rejection ($\|u_i(t)\|_\infty \le s_i$).

Theorem 5.2:

If the RG and EG operator are used in any feedback system so that the controls ($\|u_i(t)\|_\infty \le s_i$), for some vector **s**, the following is true. With zero initial conditions, the closed loop system with the EG and the RG operator and $\lambda_0 \le \lambda(t) \le 1$ will have bounded controls ($\|\mathbf{u}(t)\|_\infty \le 1$) and bounded outputs for any reference and for output disturbances disturbances that satisfy the following condition.

$$\begin{bmatrix} s_1 \\ \cdot\cdot \\ s_m \end{bmatrix} + \begin{bmatrix} \|h_{11}\|_1 \cdots \|h_{1m}\|_1 \\ \cdots\cdots\cdots \\ \|h_{m1}\|_1 \cdots \|h_{mm}\|_1 \end{bmatrix} \begin{bmatrix} \|d_1\|_\infty \\ \cdot\cdot \\ \|d_m\|_\infty \end{bmatrix} \leq \begin{bmatrix} 1 \\ \cdot\cdot \\ 1 \end{bmatrix} \tag{5.64}$$

where

h_{ij} is impulse response of the ij^{th} element of the following transfer function matrix

$$\mathbf{H}(s) = [I+\lambda_0\mathbf{K}(s)\mathbf{G}(s)]^{-1}\lambda_0\mathbf{K}(s) \tag{5.65}$$

Proof:

The proof of this theorem is very similar to the proof of Theorem 5.1 and is therefore omitted.

////

Theorem 5.2 is almost identical to theorem 5.1. The only difference is in eq. (5.65) where the **H**(s) transfer function is computed with the gain λ_0 in the loop. Theorem 5.2 defines the trade-offs between command following and disturbance rejection as theorem 5.1 did for the control structure with operator RG. In fact with the new **H**(s), eqs. (5.31) and (5.32) can be used to compute the artificial saturation **s**, knowing the maximum bounds of the disturbances ($\|d_j\|_\infty$, for all j), and vice-versa.

At the beginning of section 5.3 we claimed that the usefulness of the control structure with the operators EG and RG **depends on the specific application**; with theorem 5.2 one can quantify that dependence. As specified previously, the constant λ_0 is a design parameter that is chosen by using the multicircle stability criterion, in fact, more than one gain λ_0 may exist such that stability is preserved. It is not known yet if the control loop with the

reduced gain $\lambda(t)$ ($\lambda_0 \leq \lambda(t) \leq 1$, $\lambda_0 \leq 1$) performs better, i.e. rejects larger disturbances, than the nominal loop ($\lambda_0 = 1$); or it may be so that from the many λ_0 gains, that guarantee stability, one is better than the others for performance. In the sequel theorem 5.1 will be used to choose one of those λ_0 gains or to keep $\lambda_0 = 1$.

If upper bounds ($\|d_j\|_\infty$) on the disturbances are known then the idea is to use different λ_0's (including $\lambda_0 = 1$) in eq. (5.65) and with theorem 5.2 to compute the corresponding vectors s. Then choose the λ_0 that gives the best artificial saturation s. Remember that if s is larger, more control action is allocated for command following.

Similarly, if upper bounds for the disturbances are not known then for a specific vector s and different values of λ_0 one can compute the corresponding upper bounds on the disturbances from theorem 5.2. Then one can choose the λ_0 that gives the best disturbance rejection (rejection of larger disturbances).

Because all the signals are vectors it may be true that by choosing a λ_0 that increase the disturbance rejection or command following for a specific disturbance direction or command you make things worst for another directions. That is why the usefulness of the operator EG depends on the specific control system (dependence due to **H**(s)), the specifications. and the direction of the disturbances.

5.3.3 Simulation

The F16 system that was described in section 5.2.3 will be simulated with the operators EG & RG.

It should pointed out that if disturbances are not present then $\lambda(t) = 1$, for all t, because the RG operator will limit the references and the control will never saturate. Such simulations have been done in section 5.2. Here, only the response to disturbances will be considered.

First, by using the multiloop circle criterion as was discussed in section 5.3.1, it can be found that the closed loop system remains stable if any sector nonlinearity, which belong in a

sector [1,.7], is added at the error signal. This implies that one can choose $\lambda_0 = .7$ for the construction of the EG operator. It should pointed out that there are other sectors that the gain $\lambda(t)$ can belong in and stability will be preserved. The objective here is not to find the best λ_0 but rather to show how the control structure with operators EG and RG can improve the disturbance rejection properties of the control system if it is compared with the control structure with only the operator RG.

A simulation was performed for a step reference $\mathbf{r} = [\,0 \quad 5]^T$ and a step output disturbance of $\mathbf{d} = [.5 \quad 0]^T$ which was present for $t \geq .5$ sec. These conditions are the same as those in the simulation given in section 5.2 (figures 5.22 and 5.23). Again the artificial saturation limit was assumed to be $s_1 = s_2 = 20°$.

Figures 5.26 and 5.27 show the output and the control responses of the system with saturation and the EG & RG. The disturbance is rejected and the controls do not exceed the 20° limit (the artificial saturation) where in the previous case (figures 5.22 and 5.23) the controls exceeded the 20° limit. Thus it is evident that with the introduction of the EG one can reject larger disturbances of the type $\mathbf{d}(t) = [d_1(t) \quad 0]^T$. This may not be true for disturbances in all directions as indicated in section 5.3.2. Figures 5.28 and 5.29 show the modified references and the $\lambda(t)$ used for this simulation.

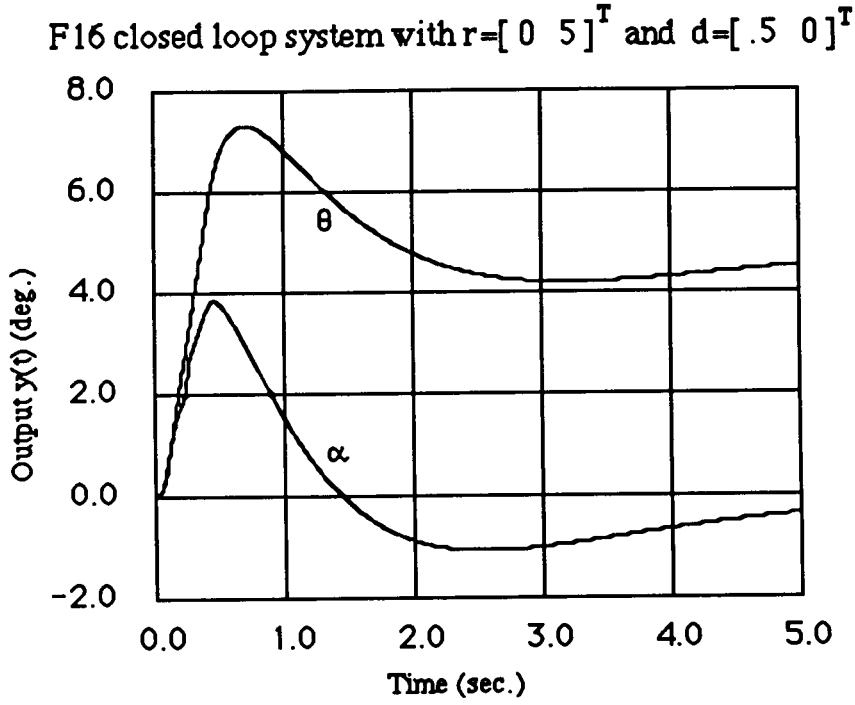

Figure 5.26: Output response for the F16 system with saturation and the EG & RG, ($\mathbf{r} = [0\ 5]^T$, $\mathbf{d} = [.5\ 0]^T$).

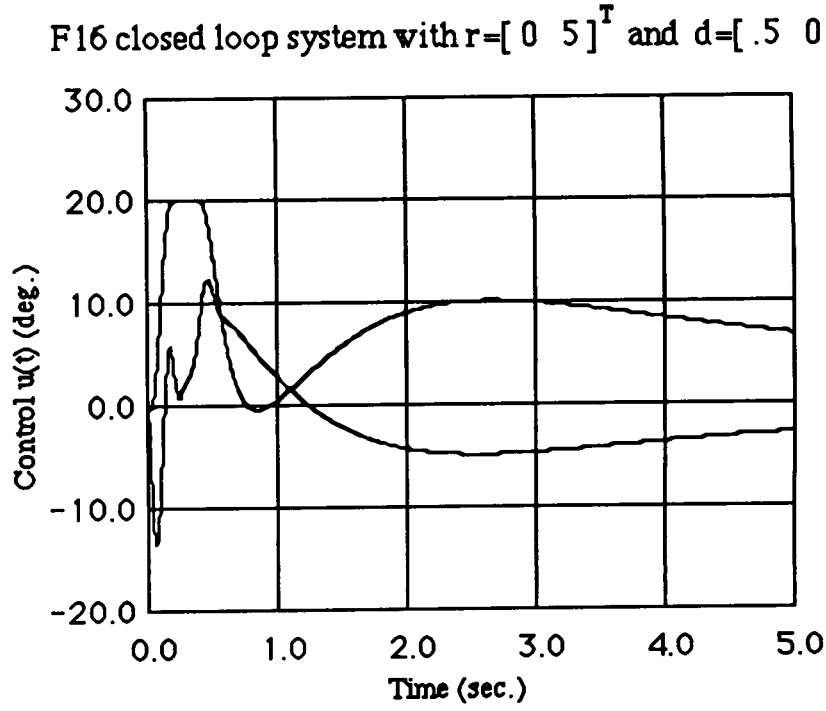

Figure 5.27: Controls in the F16 system with saturation and the EG & RG, ($\mathbf{r} = [0\ 5]^T$, $\mathbf{d} = [.5\ 0]^T$).

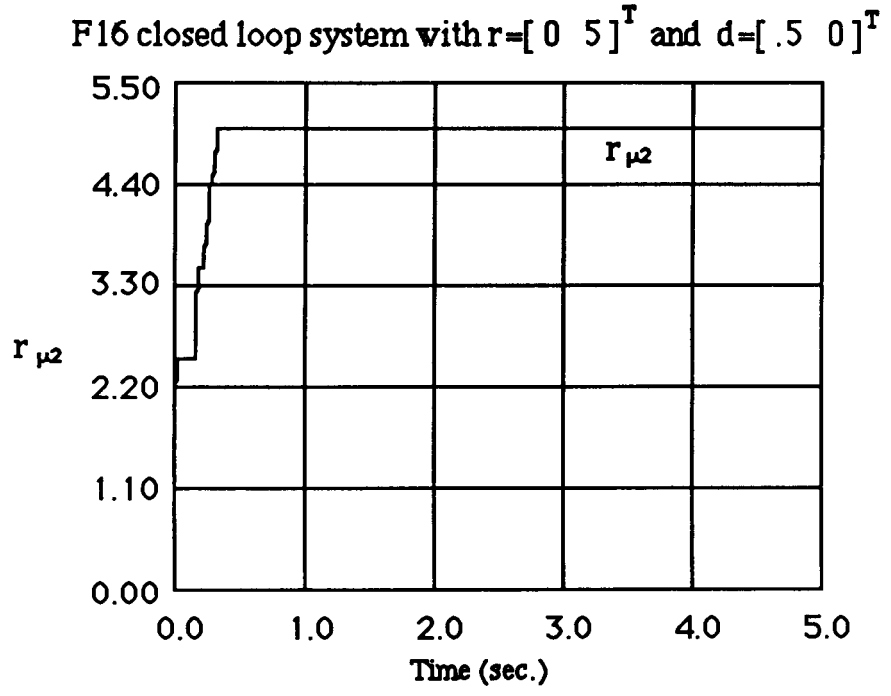

Figure 5.28: $r_{\mu 2}(t)$ the F16 system with saturation and the EG & RG, ($\mathbf{r} = [0\ \ 5]^T$, $\mathbf{d} = [.5\ \ 0]^T$).

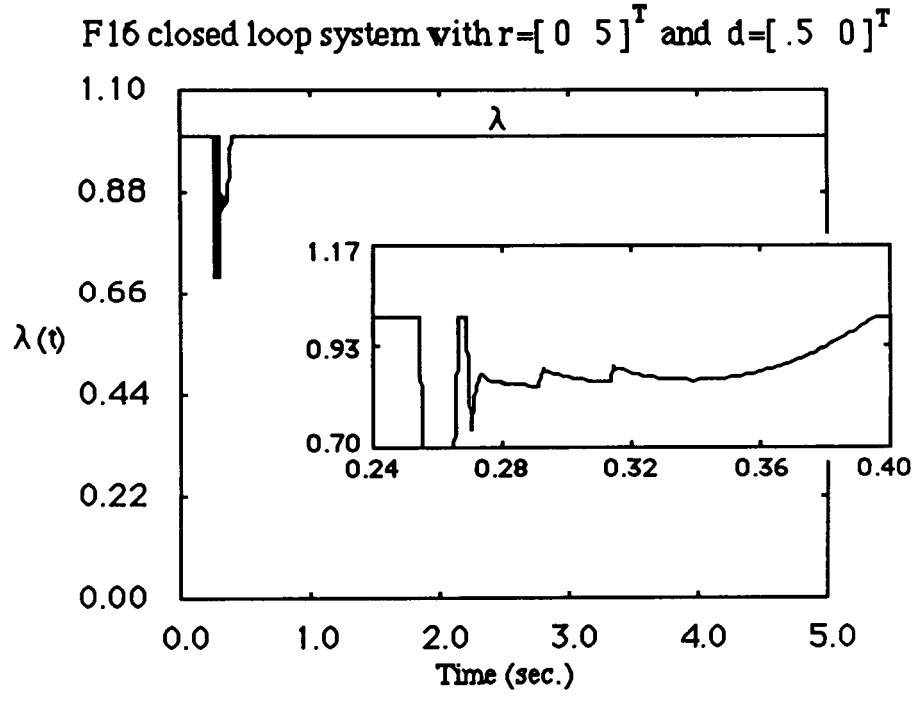

Figure 5.29: $\lambda(t)$ the F16 system with saturation and the EG & RG, ($\mathbf{r} = [0\ \ 5]^T$, $\mathbf{d} = [.5\ \ 0]^T$). Blowup: with $.24 \le t \le .4$.

5.4 Concluding Remarks

In this chapter it has been shown how that the operator RG can be used to design control systems for plants with multiple saturations. The operator RG preprocesses the reference signals in such a way so that the references never cause the controls in the closed loop system to saturate. Typically, sudden large step commands are translated by the RG operator into slower commands, they look like ramps, so as to allow the limited controls not only to stabilize the system but also to eventually track the reference. Thus the signals in the closed loop system remain bounded for any reference and if integrators are present in the loop they never windup. The control structure with the operator RG can be used in any stable linear feedback system.

In addition, we have shown how to define input and output disturbance sets so that, if the disturbances belong to these sets, then the outputs of the system remain bounded. With this new design methodology one can distribute the control action among rejecting disturbances and following references as it is needed for specific applications.

Finally, another control structure combining the operators EG and RG was introduced. This control structure can be used in feedback systems with neutrally stable compensators. The set of disturbances that are rejected can be potentially larger and thus better control systems can be designed.

The control systems that arise from the new design methodology were used in a simulation for the unstable F16 aircraft model and the advantages of the new controllers were demonstrated.

CHAPTER 6
COMPARISONS

6.1 Introduction

As mentioned previously, prior to the results in this thesis, there did not exist a general and systematic way for designing control systems for plants with multiple saturations. Current SISO control systems include special logic, in addition to the linear controllers, that try to deal with the integrator windup problem.

One can try to extend these SISO techniques to multivariable control systems. In this chapter some integrator antiwindup circuits, which are direct extensions of the SISO techniques, will be presented. As one may suspect these extensions are not expected to work as well for MIMO systems as they do for SISO systems; this is true because the directions of the signals in MIMO systems are also important. But for specific examples they may be successful and since they are simple to implement they may be preferred over our new design methodology presented in chapters 4 and 5.

In this chapter comparisons will be given between the new control design methodology and the conventional antiwindup circuits. These comparisons will be performed for two specific examples: An other academic example with peculiar directional properties, due to Doyle et al [30], and the F8 aircraft which we described in chapter 4.

As we demonstrated, in MIMO systems, in addition to the integrator windup problem, the alteration of the direction of the controls by the saturations can cause problems (see academic example #1 in chapter 4). At present there does not exist a design technique which addresses this directionality problem; hence, comparisons with our design method cannot be performed.

6.2 Comparison of Our Design Methodology with Conventional Antiwindup Designs

In order to compare the conventional antiwindup control design methods with the methodology described in chapters 4 and 5 (the EG and RG operators) two examples will be used. The first example (referred to as academic example #2) was introduced in [30] and it is defined as follows:

Plant dynamics:

$$\mathbf{P}(s) = \frac{4(0.1+s)}{s}\,\mathbf{R}^{-1} \quad \text{and} \quad \mathbf{R}=\begin{bmatrix} 4 & 5 \\ 3 & 4 \end{bmatrix} \tag{6.1}$$

Compensator dynamics:

$$\mathbf{K}(s) = \frac{1}{4(0.1+s)}\mathbf{R} \tag{6.2}$$

Form the compensator structure it is evident that the compensator is a partial inverse of the plant. Since the compensator has "slow dynamics", windups are to be expected whenever the controls are saturated. Figure 6.1 shows the closed loop system with the plant, the compensator and the saturation element. The saturation has limits of ± 1 in each control u_i.

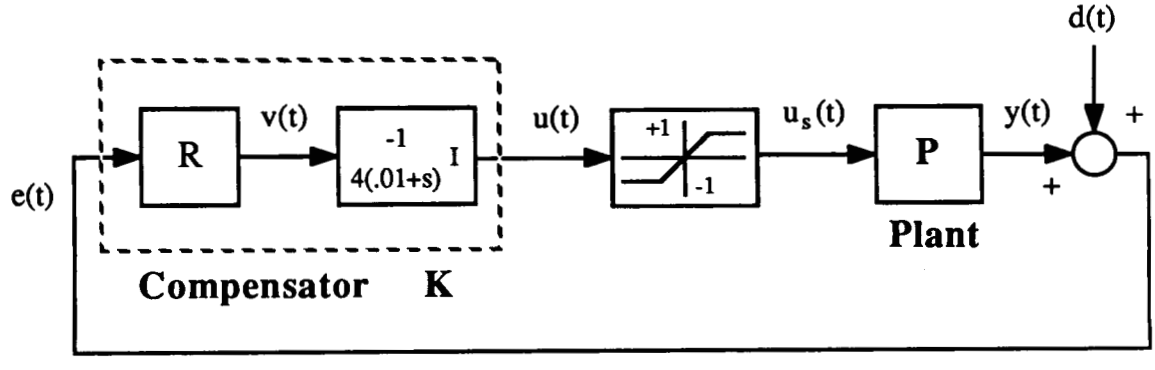

Figure 6.1: Closed loop system for the academic example #2.

Using the academic example #2 the following five different simulations were performed for the constant disturbance vector $\mathbf{d}(t) = [.61 \quad .79]^T$.

(1) The closed loop system was simulated without the saturation (i.e. $\mathbf{u}(t) = \mathbf{u_s}(t)$). This simulation is referred as the simulation for the *linear system.* As before, we view the response of the linear system as the desired one and the objective is to mimic, to the extend posssible, the linear response when the multiple saturations are introduced.

(2) The closed loop system was simulated with the saturation as shown in figure 6.1. This simulation is referred as the simulation for the *system with saturation.*

(3) The closed loop system was simulated with the saturation and a conventional antiwindup strategy (CAW). In this case, the CAW modifies the compensator's slow dynamics when saturation occurs so that the compensator states will never have values larger than the saturation limits. In refernce to figure 6.1, the inputs to the slow compensator dynamics are modified in the following way

$$\text{CAW:} \qquad \mathbf{v}(t) = \mathbf{Re}(t) + 100(\mathbf{u}(t) - \mathbf{u_s}(t)) \tag{6.3}$$

The problem with this CAW strategy is that the different control channels do not communicate so that if one control u_i saturates, then the corresponding v_i is modified and the v_j's ($i \neq j$) do not change. Consequently, the direction of the controls is modified and in MIMO system this can cause performance problems (as we have observed several times before). This simulation is referred to as the *system with saturation and CAW.*

(4) The closed loop system was simulated with the saturation and modified conventional antiwindup (MAW) strategies. The MAW used modifies the compensator's slow dynamics when saturation occurs so that the compensator states will never have values larger than the saturation limits. The difference here is that when a control channel u_i saturates, all the other control channels are also modified. The inputs to the slow compensator dynamics in figure 6.1 are changed in the following way

MAW: $\mathbf{v}(t) = \mathbf{Re}(t) + \alpha \mathbf{u}(t)$ (6.4)

where $$\alpha = \begin{cases} 0 & \text{for } \|u\|_\infty \leq 1-\varepsilon \\ 10 & \text{for } \|u\|_\infty > 1-\varepsilon \end{cases} \quad (6.5)$$

This simulation is referred as the simulation of the *system with saturation and MAW.*

(5) The last simulation was performed with the EG operator as specified in chapter 4. This simulation is referred as the simulation of the *system with saturation and the EG.*

Simulations (1) through (4) can be also found in [30]; they are duplicated so that they can be compared to simulation (5).

Figures 6.2 and 6.3 show the output and control responses of the linear system. The compensator partially inverts the plant and the open loop system becomes an integrator. The responses verify that. Note that the controls exceed the saturation limits (±1).

Figures 6.4 and 6.5 show the output and control responses of the system with saturation. Because of the peculiar directional properties of the plant, when the controls saturate the output response deteriorates dramatically.

Figures 6.6 and 6.7 show output and control responses of the system with saturation and CAW. The controls stay within the bounds of the saturation but because the CAW feedback loop operates in a "SISO fashion" the response in figure 6.6 is still terrible. The windup problem seems to be corrected but the directions of the control seem to be wrong. As was remarked above, each control when it saturates, activates a feedback loop without communicating with the other control channel. Again, it is obvious that directions of the controls are important in MIMO systems.

Figures 6.8 and 6.9 illustrate the outputs and the control responses of the system with saturation and MAW. The responses mimic the linear ones (they are slower as expected);

Compare figures 6.2 and 6.8. The directional problem is corrected because when saturation in one of the channels occurs the feedback loop is activated for all the channels. The directionality of the controls is preserved and thus the integrator windups and the control directional problems are corrected.

Figures 6.10 and 6.11 show the output and control responses of the system with saturation and the EG operator. The responses here are identical to the ones when the MAW strategy was used. The EG operator preserves the inversion of the plant by the compensator and the control directions are not altered. Figure 6.12 show the $\lambda(t)$ for the EG operator that was used in this simulation.

This set of simulations show the potential pitfalls of adapting "good" SISO strategies to MIMO systems. By being clever one may find "good" MIMO strategies (the MAW) which have less computational complexity as compared with our EG operator approach. On the other hand, they are not systematic and each design must be individually developed, adapted, and tuned.

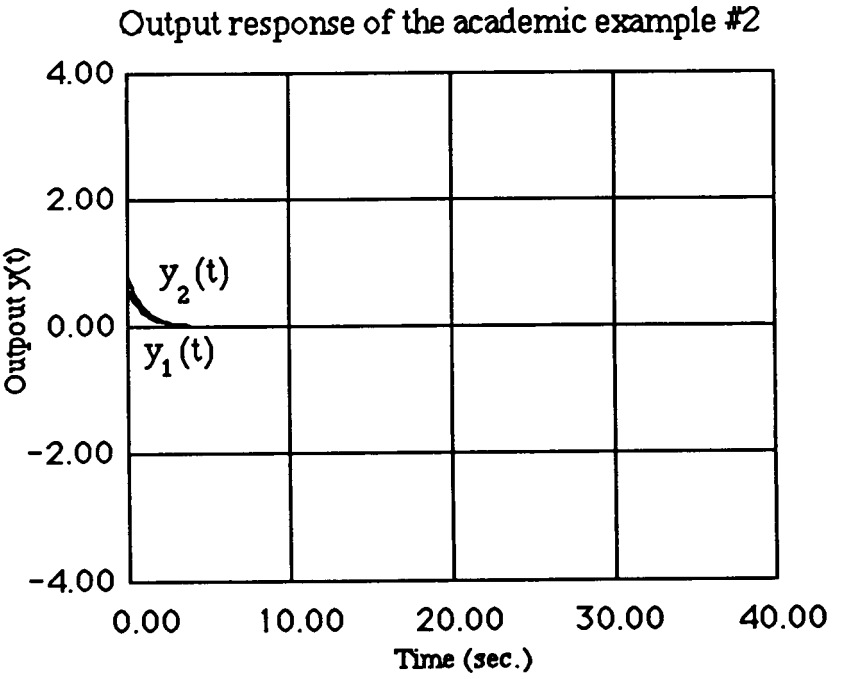

Figure 6.2: Output response for the linear system.

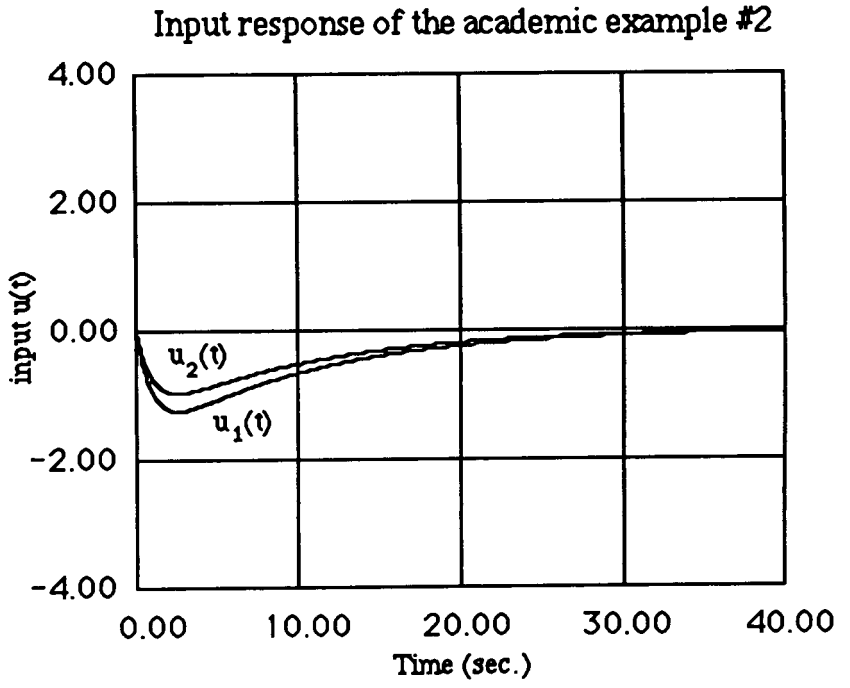

Figure 6.3: Controls in the linear system.

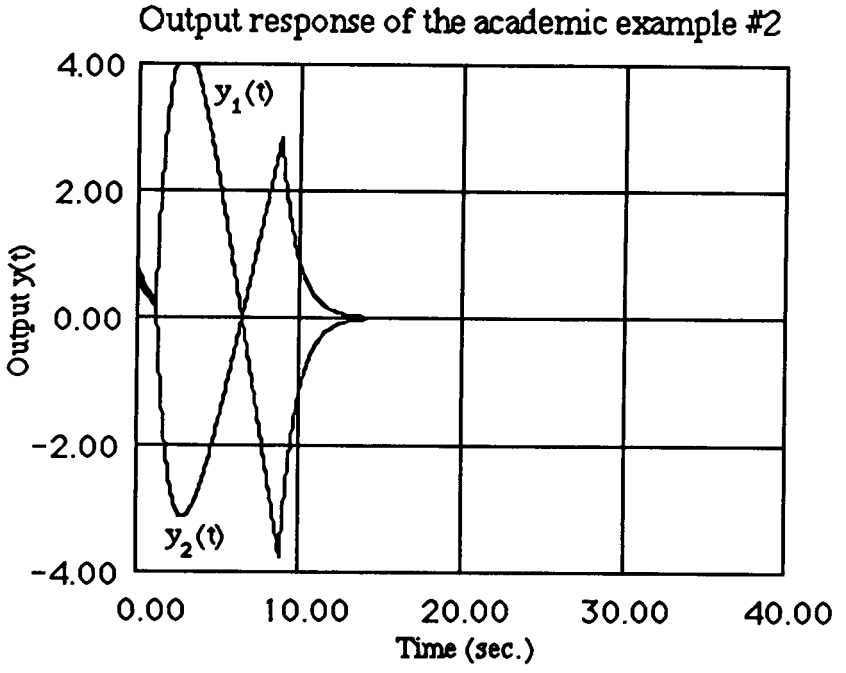

Figure 6.4: Output response for the system with saturation.

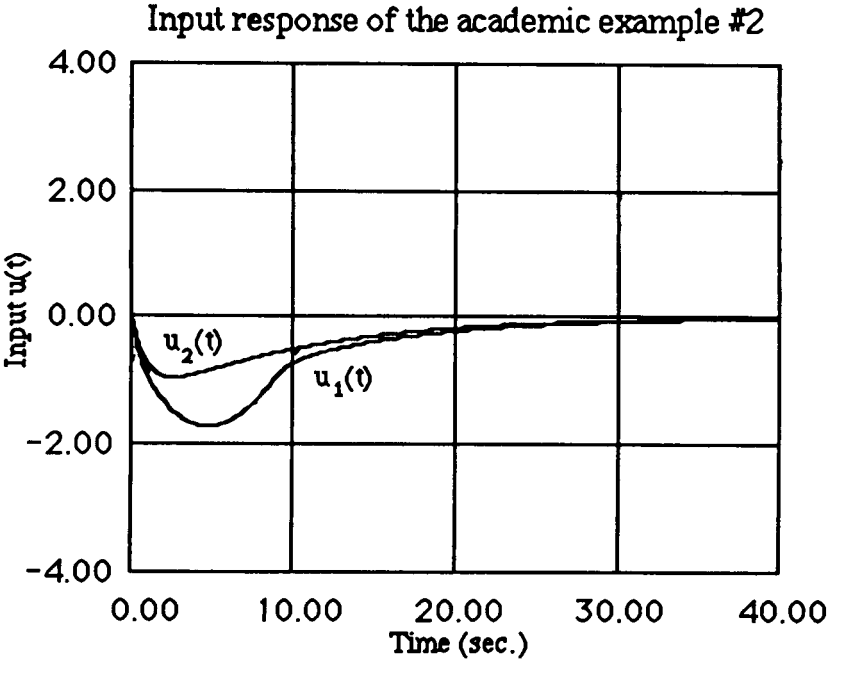

Figure 6.5: Controls in the system with saturation.

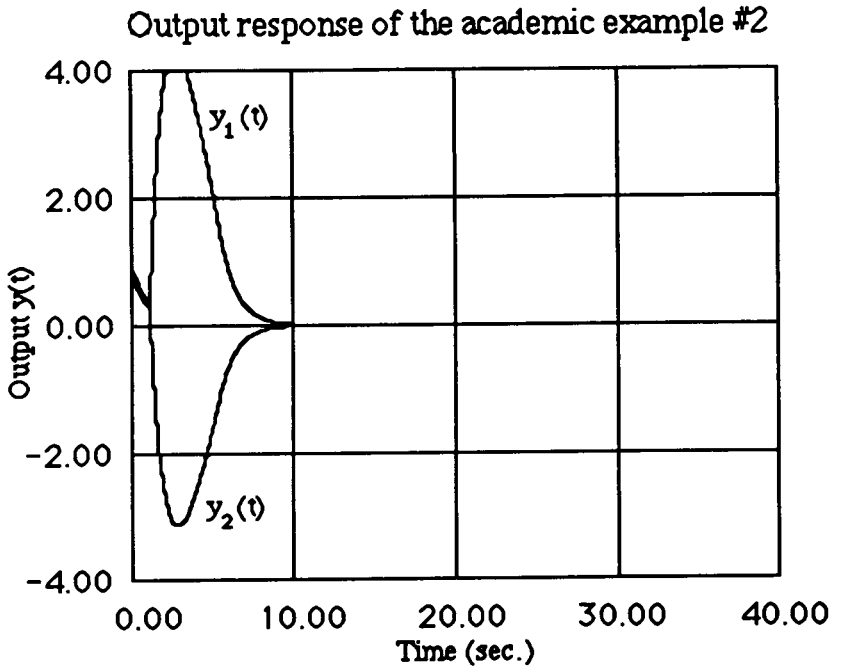

Figure 6.6: Output response for the system with saturation and CAW.

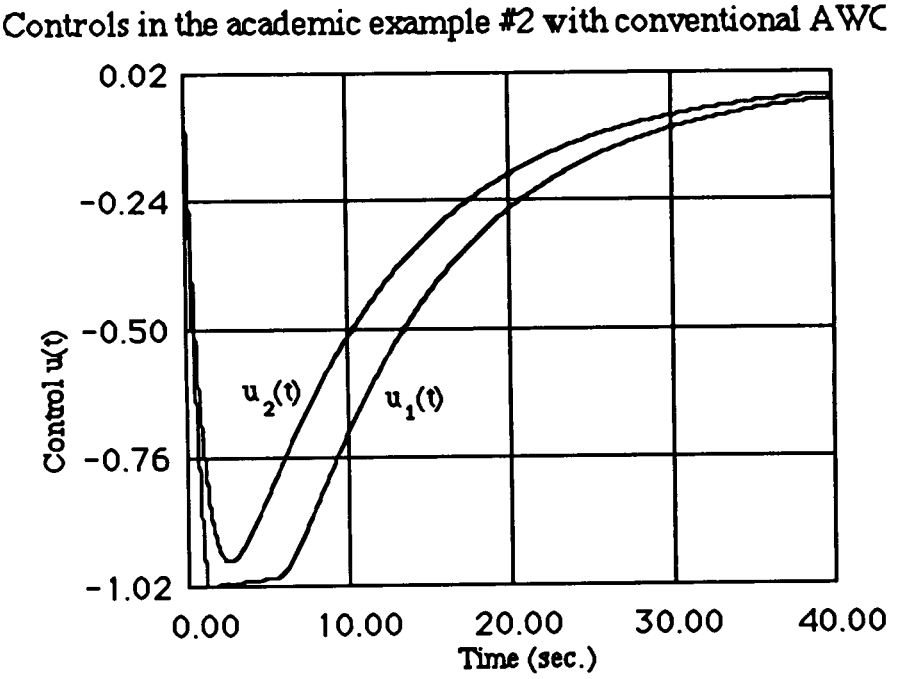

Figure 6.7: Controls in the system with saturation and CAW.

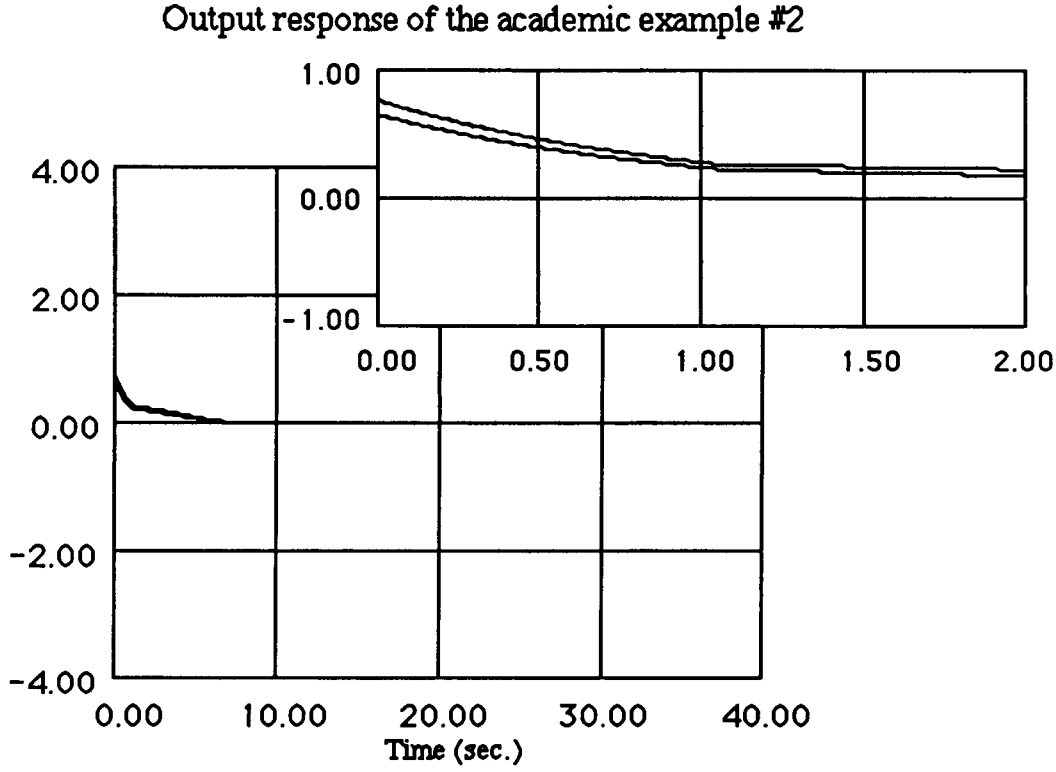

Figure 6.8: Output response for the system with saturation and MAW. Blowup: Outputs for 0-2 sec.

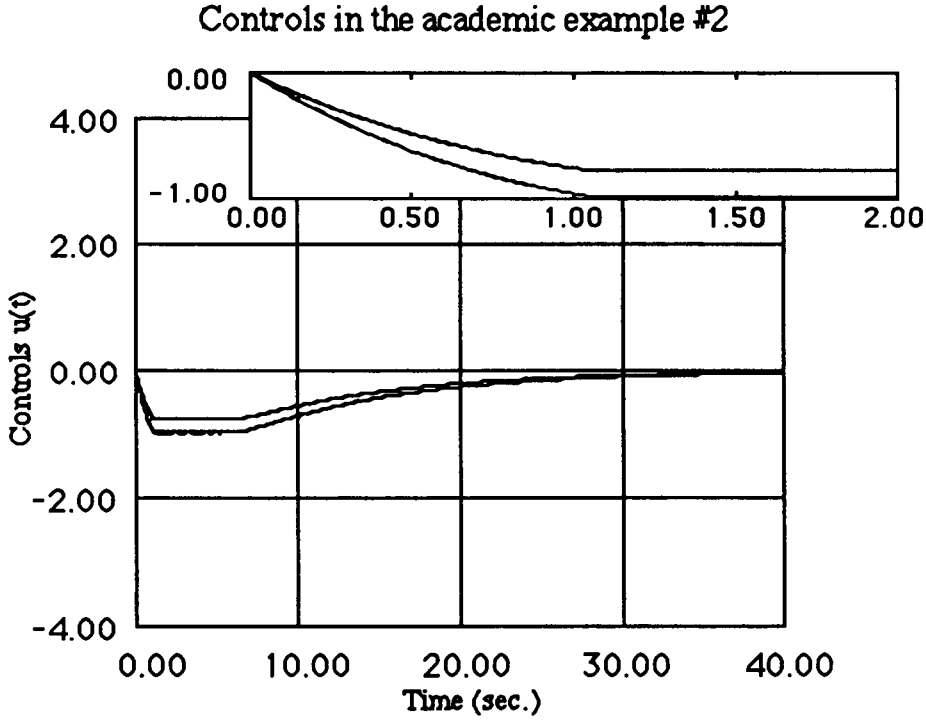

Figure 6.9: Controls for the system with saturation and MAW. Blowup: Controls for 0-2sec.

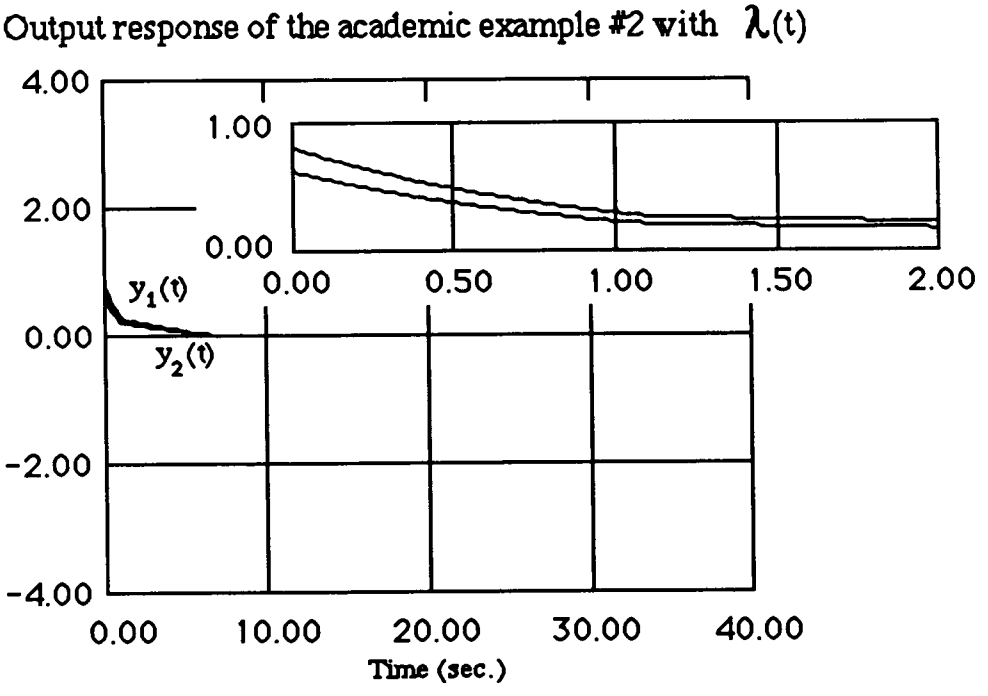

Figure 6.10: Output response for the system with saturation and the EG.

Blowup: Outputs for 0-2 sec.

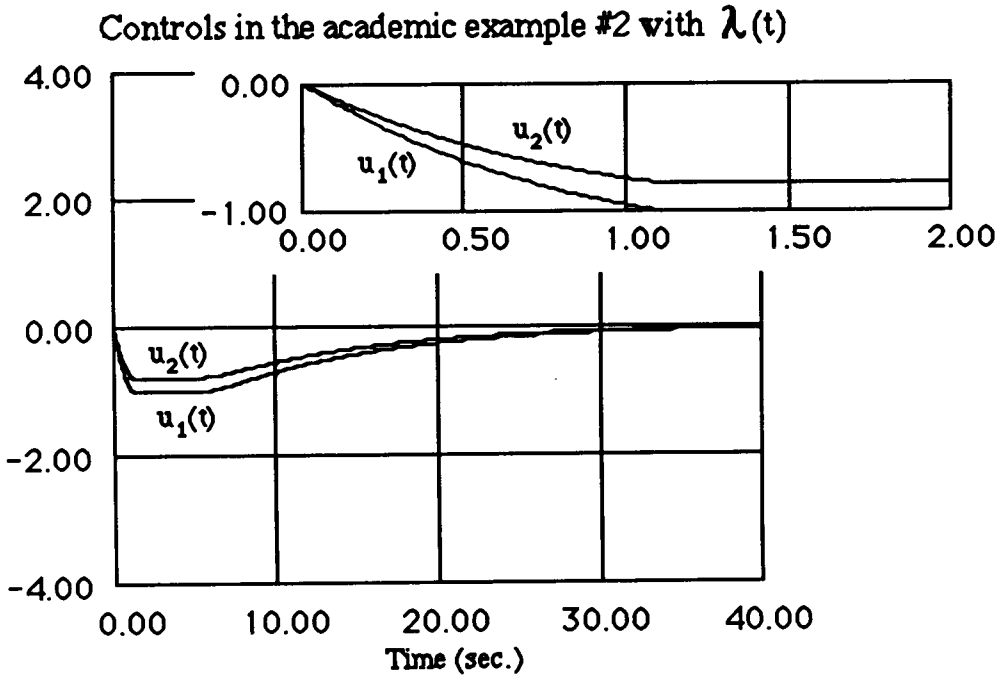

Figure 6.11: Controls in the system with saturation and the EG.

Blowup: Controls for 0-2 sec.

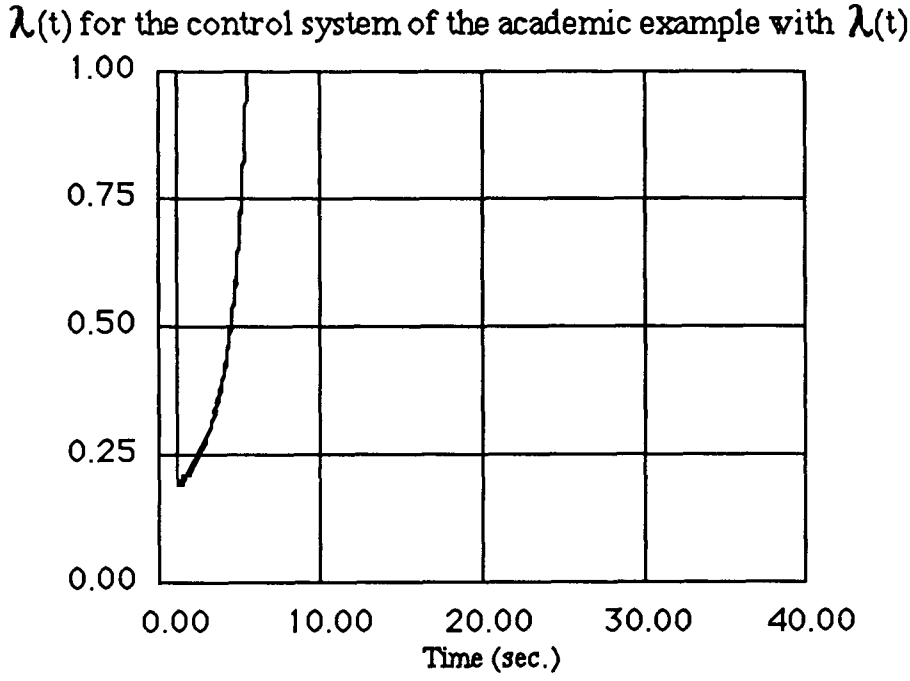

Figure 6.12: λ(t) for the system with saturation and the EG.

Another set of simulations was performed for the F8 aircraft closed loop system, which was described in chapter 4. The closed loop system is shown in figure 6.13. Simulations with the CAW, MAW and the EG operator were performed for this control system. The simulations for the linear system and the system with saturation are shown in chapter 4 (see figures 4.31, 4.32, 4.33, and 4.34).

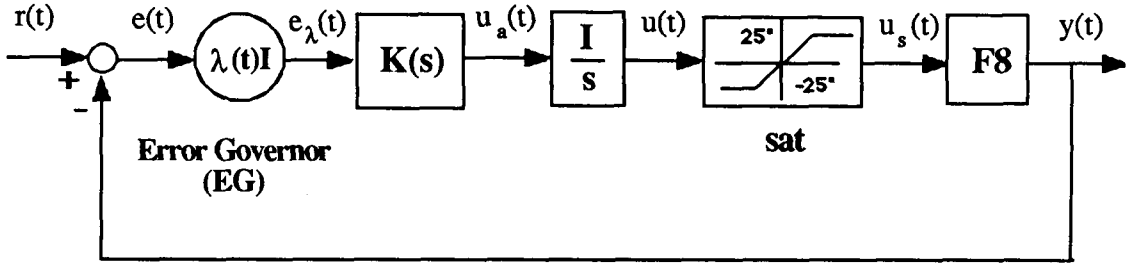

Figure 6.13: The closed loop system for the F8 aircraft.

Three new simulations were performed for this system as follows:

(1) The closed loop system was simulated with the saturation and modified antiwindup (MAW) strategies. The difference here is that whenever one control channel u_i saturates all the other control channels are modified. The inputs to the integrators are changed in the following way (see figure 6.13).

$$\text{MAW:} \quad \mathbf{u_a = Ke + \alpha u} \tag{6.6}$$

$$\text{where} \quad \alpha = \begin{cases} 0 & \text{for} \quad \|u\|_\infty \leq 1-\varepsilon \\ 100 & \text{for} \quad \|u\|_\infty > 1-\varepsilon \end{cases} \tag{6.7}$$

The MAW does not guarantee any more that the controls will not saturate, because the compensator dynamics are ignored in the antiwindup strategy. This is why the computations are very simple. This simulation is referred to as the simulation of the *system with saturation and MAW*.

(2) In this simulation, in addition to MAW the control direction will also be preserved by limiting the control magnitude. We wanted to see if the control direction preservation provides any advantages, at least, in this example. The following operation on the controls will be introduced

$$\mathbf{u' = [I/s]u_a} \tag{6.8}$$

$$\mathbf{u(t) = \beta u'} \tag{6.9}$$

where

$$\beta = \begin{cases} 1 & \text{for} \quad \|u'\|_\infty \le 25 \\ \dfrac{1}{\|u'\|_\infty} 25 & \text{for} \quad \|u'\|_\infty > 25 \end{cases} \tag{6.10}$$

The controls will now always remain within the saturation limits, and thus the direction of the control vector will be preserved. Note that the gain β does not commute with the compensator $\mathbf{K}$ (i.e. $\mathbf{G\beta K} \neq \mathbf{GK\beta}$) and, consequently, if the linear compensator inverts or partially inverts the linear plant, then the inversion operation will be disturbed by the gain β. This simulation is referred as the simulation with *saturation, MAW and control direction preservation (CDP).*

(3) The last simulation was performed with the EG operator, as specified in chapter 4. This simulation is referred as the simulation of *the system with saturation and the EG.*

Figures 6.14 and 6.15 show the output and control responses of the system with saturation and MAW to the constant reference $\mathbf{r} = [\ 10 \quad 10]^T$. One can see that the responses are better than the ones obtained when no antiwindup strategy was used (shown in figure 4.33). The direction of the output response is not exactly similar to the linear one (shown in figure 4.31). The small problem in the direction of the outputs is caused because the controls saturate for a small period of time.

Figures 6.16 and 6.17 show the output and control responses of the system with saturation, MAW and CDP. At least for this example, the control direction preservation does not seem to offer any advantage. Instead it appears that the output response deteriorates (compare figures 6.16 and 6.14).

Figures 6.18 and 6.19 show the output and control responses of the system with saturation and the EG. The benefit of the EG operator is obvious and the nonlinear response mimics the linear one. Note that the controls never saturate. Comparison of figures 6.18, 6.16 and 6.14 demonstrate the superiority of the EG operator design; note, however, that it requires much more (off-line and on-line) computation than the other designs.

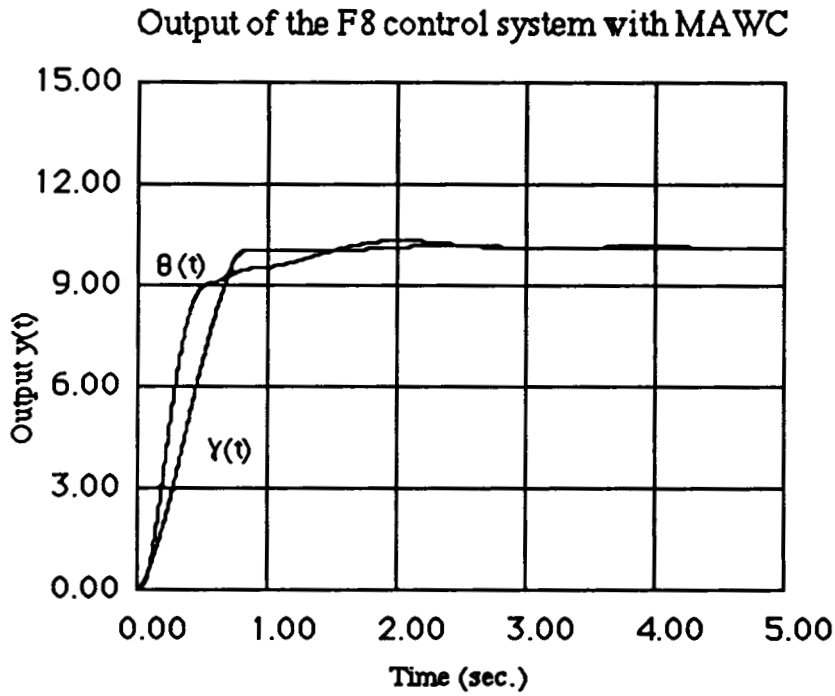

Figure 6.14: Output response for the F8 system with saturation and MAW, ($\mathbf{r} = [10 \quad 10]^T$).

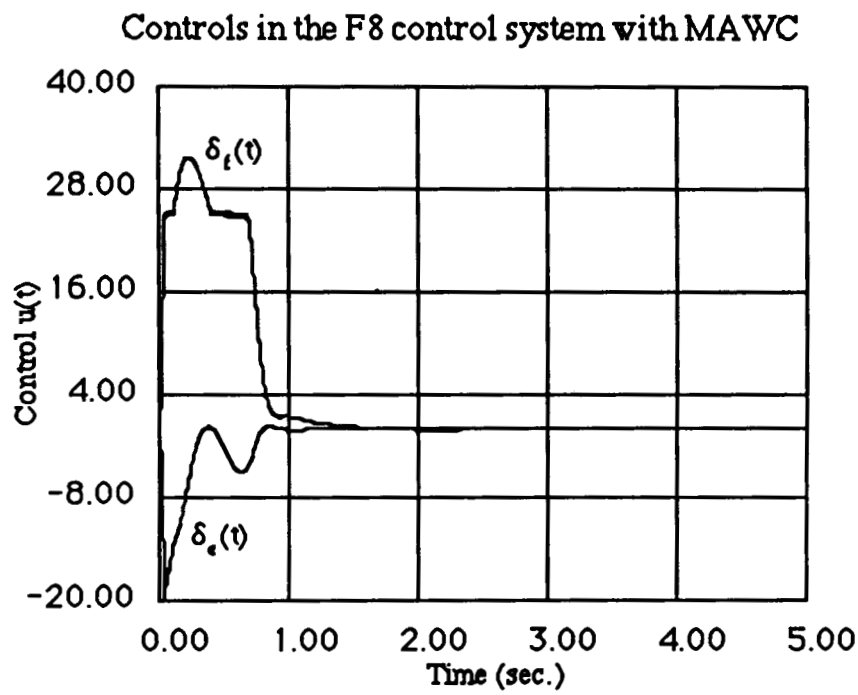

Figure 6.15: Controls in the F8 system with saturation and MAW, ($\mathbf{r} = [10 \quad 10]^T$).

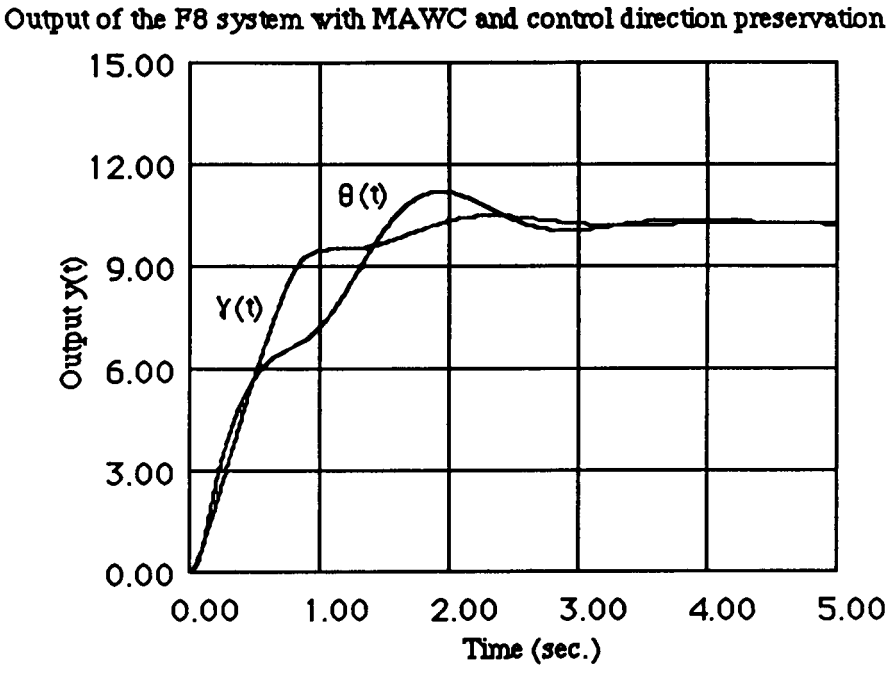

Figure 6.16: Output response for the F8 system with saturation, MAW and CDP, ($\mathbf{r} = [10 \quad 10]^T$).

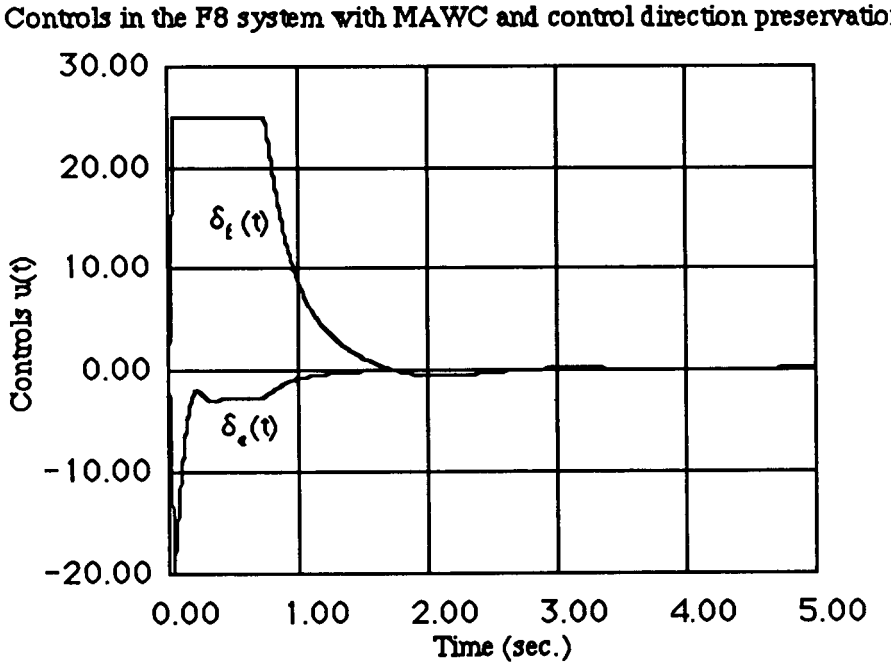

Figure 6.17: Controls in the F8 system with saturation, MAW and CDP, ($\mathbf{r} = [10 \quad 10]^T$).

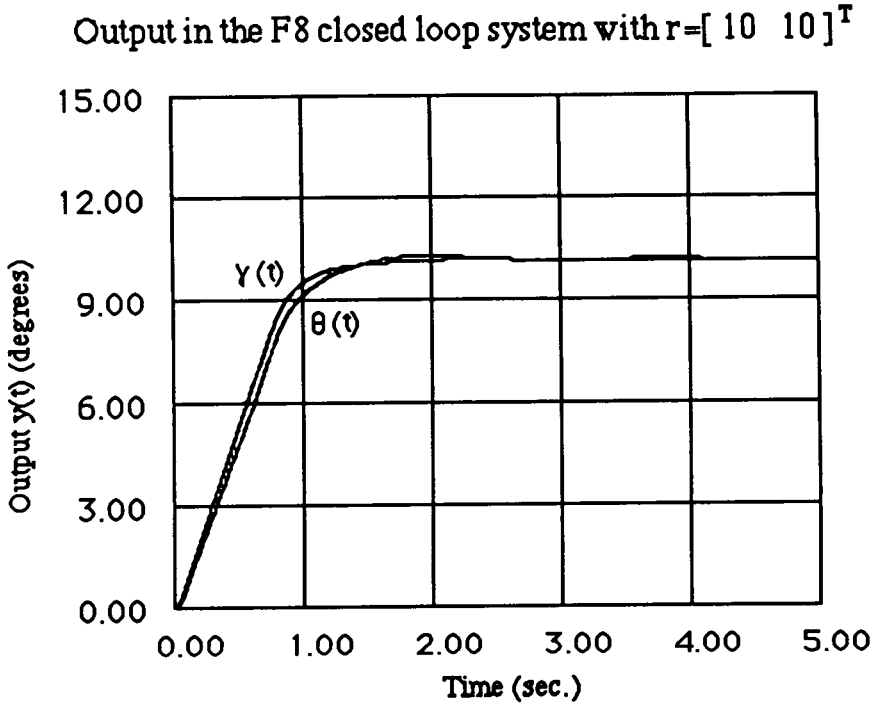

Figure 6.18: Output response for the F8 system with saturation and the EG, ($\mathbf{r} = [10 \quad 10]^T$).

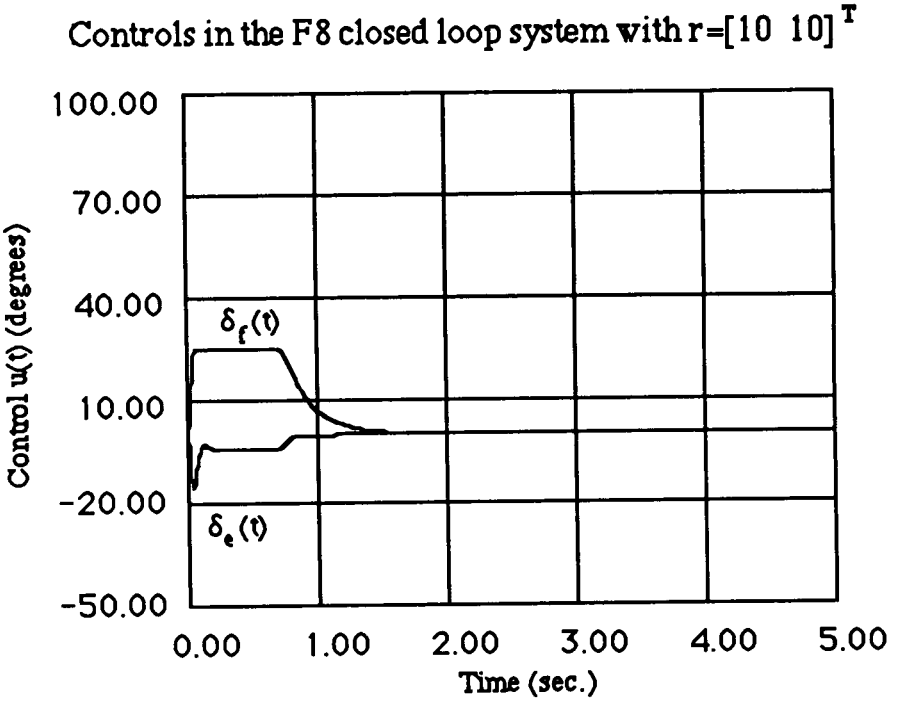

Figure 6.19: Outputs in the F8 system with saturation and the EG, ($\mathbf{r} = [10 \quad 10]^T$).

In the simulations above, it was found that some simple "fixes" led to reasonable output performance. However, we can never be sure that the same ad-hoc "fixes" will continue to work well for other reference inputs and/or disturbances.

Three more simulations were performed for the same system but for a different reference input ($\mathbf{r} = [20 \quad 20]^T$). The reason for doing these additional simulations is to find out how the references can affect the output and control responses since the closed loop system is nonlinear.

Figures 6.20 and 6.21 show the output and control responses of the system with saturation and MAW. One can see that integrator windups are now dominantly present in addition to the alteration of the control direction. The reason is that the compensator states are not included in the antiwindup strategy and nothing explicitly prevents them from windup. It is not clear how one would design MAW for the compensator, since the compensator is a highly coupled MIMO system.

Figures 6.22 and 6.23 show the output and control response of the system with saturation, MAW and CDP. Now the output responses seem to be improved (minor direction problems still exist) and the integrator windups are not very large.

Figures 6.24 and 6.25 show the output and control response of the system with saturation and the EG. The responses mimic the ones of the linear system, as our systematic methodology guarantees.

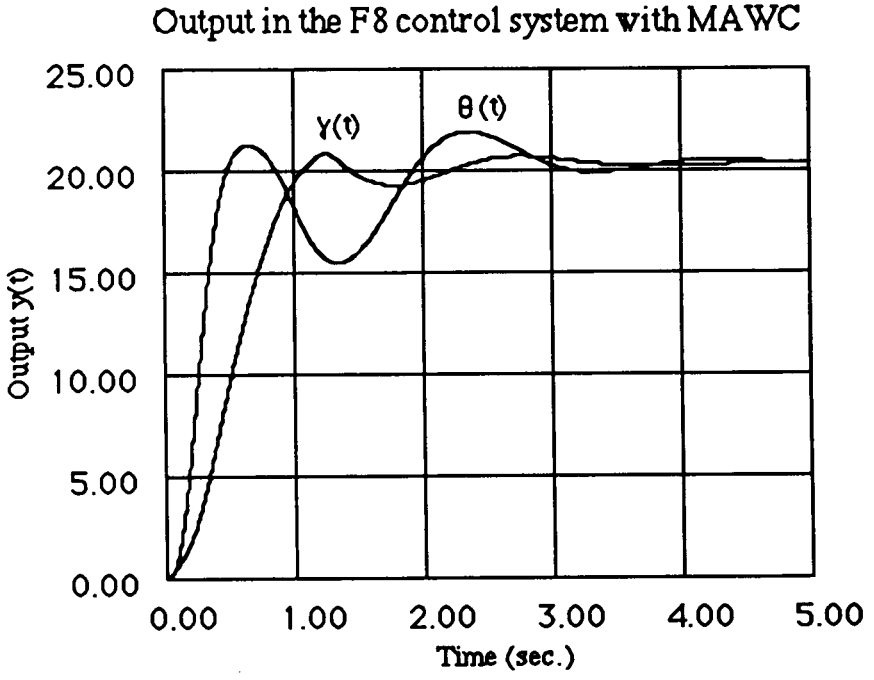

Figure 6.20: Output response for the F8 system with saturation and MAW, ($\mathbf{r} = [20 \quad 20]^T$).

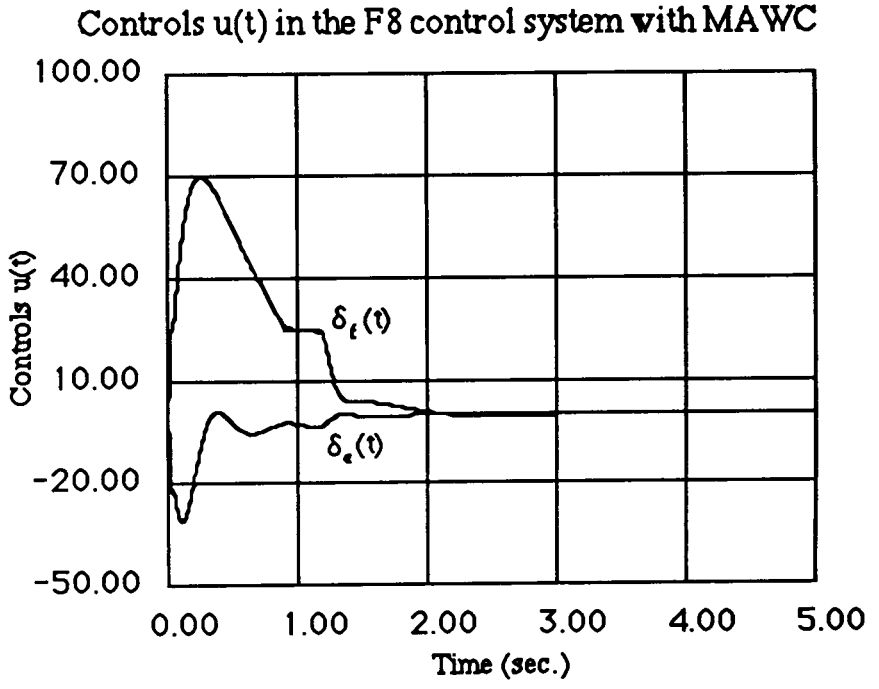

Figure 6.21: Controls in the F8 system with saturation and MAW, ($\mathbf{r} = [20 \quad 20]^T$).

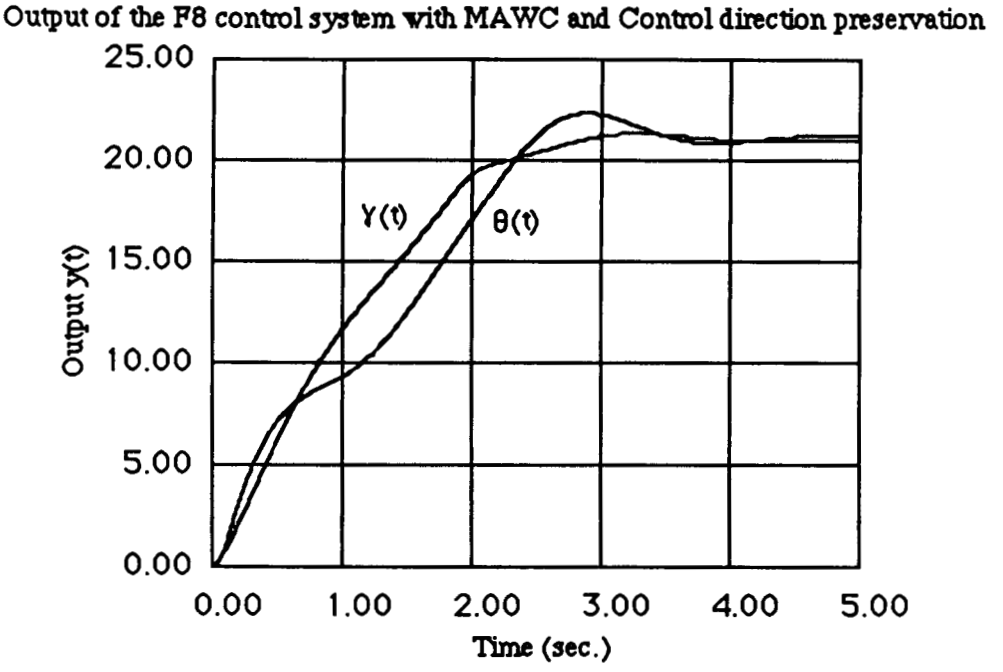

Figure 6.22: Output response for the F8 system with saturation, MAW and CDP, ($\mathbf{r} = [20 \quad 20]^T$).

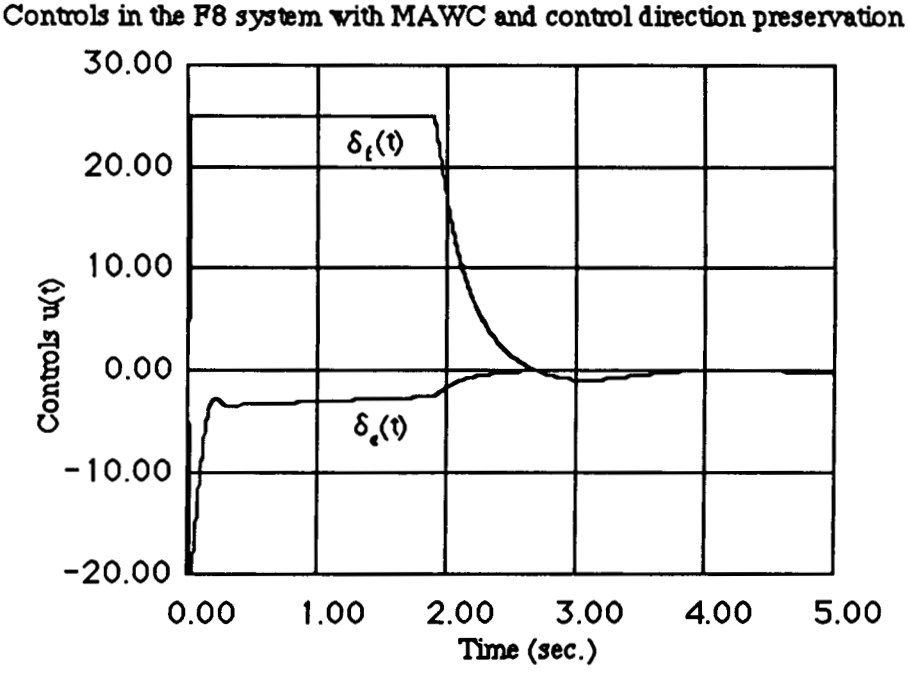

Figure 6.23: Controls in the F8 system with saturation, MAW and CDP, ($\mathbf{r} = [20 \quad 20]^T$).

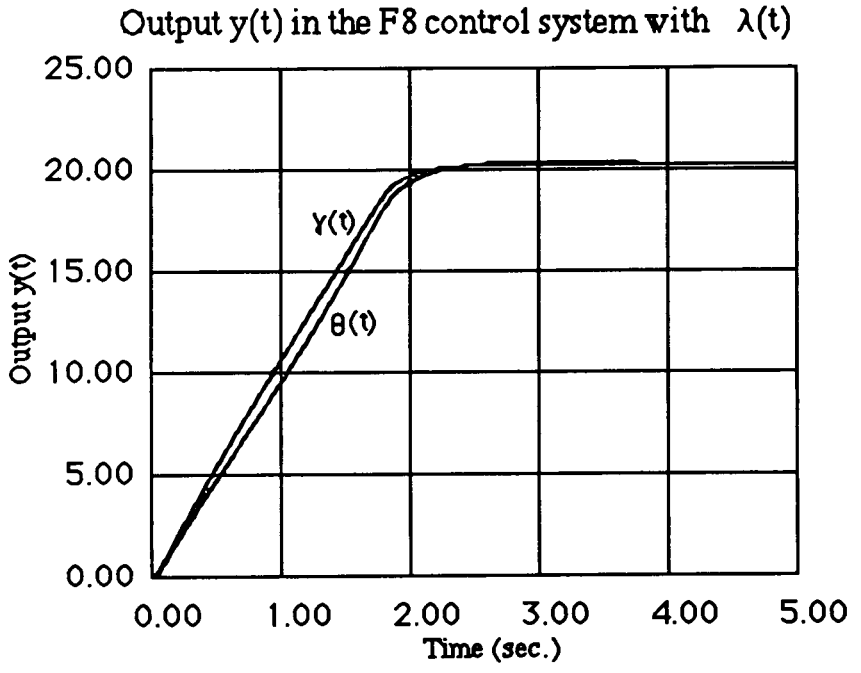

Figure 6.24: Output response of the F8 system with saturation and the EG, ($\mathbf{r} = [20 \quad 20]^T$).

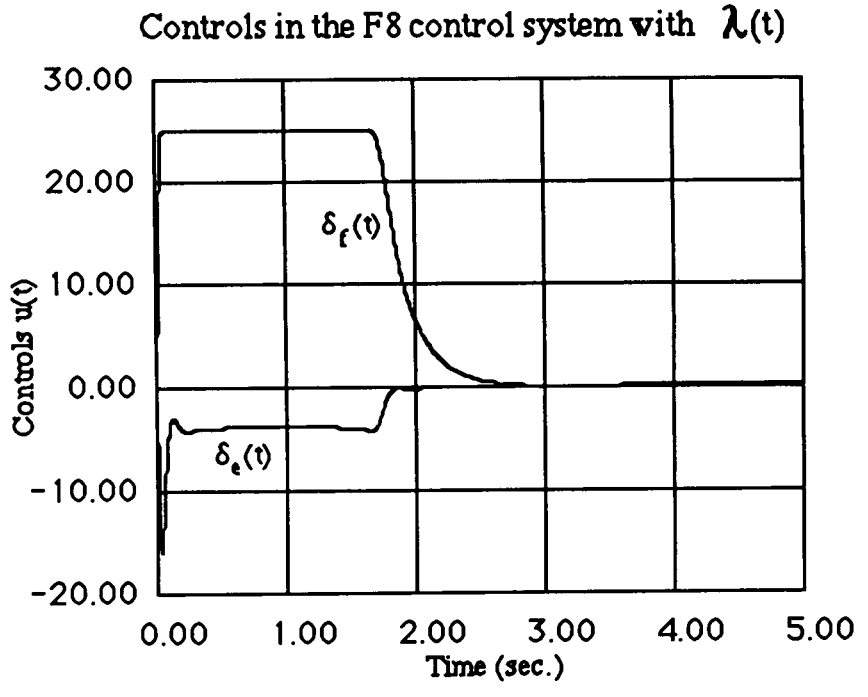

Figure 6.25: Controls in the F8 system with saturation and the EG, ($\mathbf{r} = [20 \quad 20]^T$).

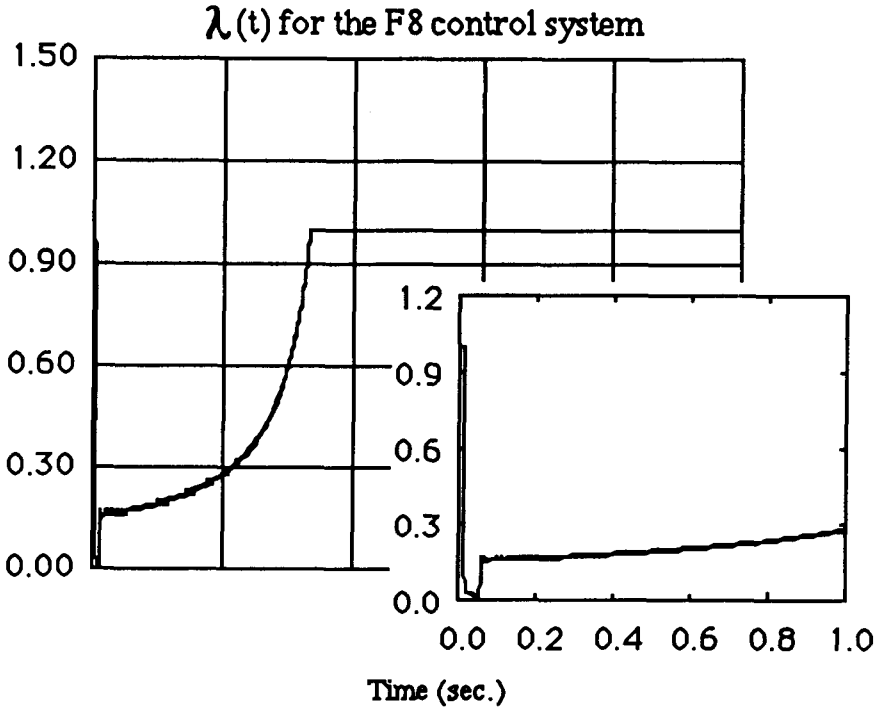

Figure 6.26: $\lambda(t)$ for the F8 system with saturation and the EG, ($\mathbf{r} = [20 \quad 20]^T$). Blowup: $\lambda(t)$ for 0-1sec.

6.3 Concluding Remarks

In this chapter we compared via simulations our new design methodology with extensions of conventional SISO antiwindup circuits to MIMO systems. The comparisons were performed for two examples. In both cases it was shown that our design methodology performs consistently better.

The extension of the SISO antiwindup circuits to MIMO systems is not simple and, in general, it is not known if such extensions are possible. For simple control systems, the conventional antiwindup circuits may work and eliminate or partially eliminate integrator windups. In contrast the new design methodology introduced in chapters 4 and 5 is general and eliminates windups completely. The price that one has to pay for using the new design methodology is that the off-line computation for high dimentional controllers is extensive.

For MIMO control systems the conventional antiwindup strategies do not solve the control directionality problem i.e. the alteration of the control vector direction. Additional logic may have to be introduced to fix up that problem.

In summary, for a specific control system conventional antiwindup strategies should be considered as they may solve the problem of integrator windups. If this is the case, since the conventional antiwindup strategies are simple to implement, they should be used. If for the specific control system the conventional antiwindup strategies do not solve the problem, then the new design methodology, proposed in this thesis, should be used.

CHAPTER 7
RATE SATURATION, RATE/MAGNITUDE SATURATION AND STATE LIMITERS

7.1 Introduction

Magnitude saturation of the control signals is a commonplace nonlinear phenomenon that the control system designer must address. However, in addition to magnitude saturation, the control system designer must also deal with rate saturation (often combined with magnitude saturation), and with the problem of enforcing specific limits upon the magnitude of certain critical state variables (often for safety reasons). For example, in aircraft problems we may wish to limit the angle of attack so as to prevent stall; in turbofan engines one may wish to limit certain turbine temperatures to avoid damage.

In this chapter it will be shown how the techniques developed in chapters 3 to 5 can be extended for the design of MIMO control systems with rate saturation, rate and magnitude saturation and state limiters.

The idea here is to design a linear compensator for the linearized plant and then by operating on the error and/or the references to modify the controls so that the closed loop system will have "nice" properties.

Three very common cases will be considered in this chapter. The first case is the case where the control's *rate is bounded*, the second case is the case where the controls *magnitude and rate are bounded*, and the third case is the case where certain *states* of the plant should remain *bounded.*

In this chapter, a way of modifying the references and/or the error signals with the EG and the RG operator will be introduced so that the controls or certain states will not violate their

predefined bounds. The methods used are similar to the ones described in chapters 4 and 5 with minor modifications for each of three cases. Even though it may seem repetitious, for completeness, the construction of the EG and RG operators will be stated again. But for details that are omitted here one should refer to Chapters 3, 4 and 5.

7.2 Rate Saturation

In this section systems with control rate saturation will be investigated. Consider a closed loop system which consists of a plant, a compensator and a rate saturation at the plant input as shown in figure 7.1.

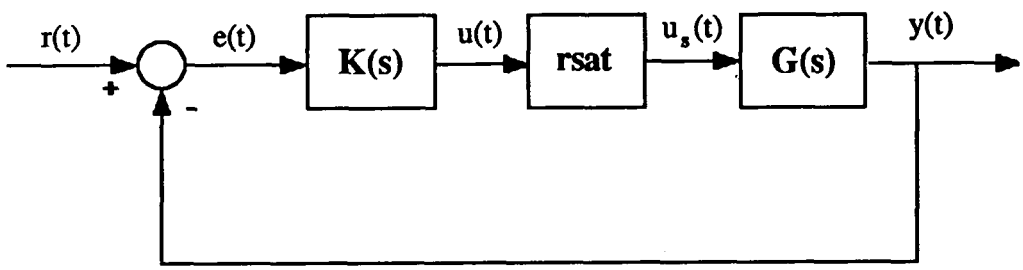

Figure 7.1: Closed loop system with rate saturation

The plant model is given by the following state space representation

$$\dot{\mathbf{x}}(t) = \mathbf{A}\mathbf{x}(t) + \mathbf{B}\mathbf{u}_s(t) \tag{7.1}$$

$$\mathbf{y}(t) = \mathbf{C}\mathbf{x}(t) \tag{7.2}$$

The compensator generates $\mathbf{u}(t)$ from $\mathbf{e}(t)$ and is given by the following state space representation

$$\dot{\mathbf{x}}_c(t) = \mathbf{A}_c\mathbf{x}_c(t) + \mathbf{B}_c\mathbf{e}(t) \tag{7.3}$$

$$\mathbf{u}(t) = \mathbf{C}_c\mathbf{x}_c(t) \tag{7.4}$$

$$\mathbf{e}(t) = \mathbf{r}(t) - \mathbf{y}(t) \tag{7.5}$$

where $\mathbf{r}(t)$ is the reference and $\mathbf{y}(t)$ is the output vector.

The rate saturation is modelled with a simple closed loop model given by

$$\dot{\mathbf{u}}_s(t) = \text{sat}(\mathbf{u}(t) - \mathbf{u}_s(t)) \tag{7.6}$$

where $\mathbf{u}(t)$ are the commanded control signals, $\mathbf{u}_s(t)$ are the actual (output of the rate saturation) controls driving the plant with $\mathbf{u}(t) = [\, u_1(t) , \ldots , u_m(t)]^T$, $\mathbf{u}_s(t) = [\, u_{s1}(t) , \ldots , u_{sm}(t)]^T$ and

$$\text{sat}(u_i(t) - u_{si}(t)) = \begin{cases} \dfrac{1}{k} & u_i(t) - u_{si}(t) \geq \dfrac{1}{k} \\ u_i(t) - u_{si}(t) & -\dfrac{1}{k} \leq u_i(t) - u_{si}(t) \leq \dfrac{1}{k} \\ -\dfrac{1}{k} & u_i(t) - u_{si}(t) \leq -\dfrac{1}{k} \end{cases} \tag{7.7}$$

and in compact form

$$\mathbf{u}_s(t) = \text{rsat}(\mathbf{u}(t)) \tag{7.8}$$

In eq. (7.7) the value of k can be chosen to be "large enough" so that when the saturation is used in the linear region the $\mathbf{u}(t)$ will be approximately equal to $\mathbf{u}_s(t)$. The model of the rate

saturation is shown in figure 7.2.

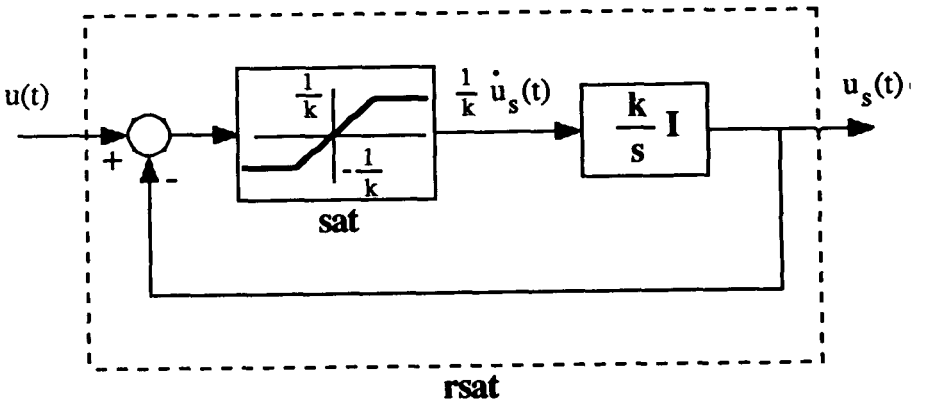

Figure 7.2: Model of the rate saturation

Note that the rate saturation cannot be modelled simply as $\dot{\mathbf{u}}_s(t) = \text{sat}(\dot{\mathbf{u}}(t))$ because at steady state the $\mathbf{u}_s(t)$ and $\mathbf{u}(t)$ signals can differ. For example, consider the case where u(t) is ramp with slope 1 from t = 0 to t = 1 and the rate saturation is 1/2. In that case the steady state value of u(t) is 1 and the steady state value of $u_s(t)$ is 1/2. Figure 7.3 shows the u(t) signal with the signal $u_s'(t)$ when $\dot{u}_s'(t) = \text{sat}(\dot{u}(t))$ and the signal $u_s''(t)$ when $\dot{u}_s''(t)$ is computed from eqs. (7.6)-(7.8).

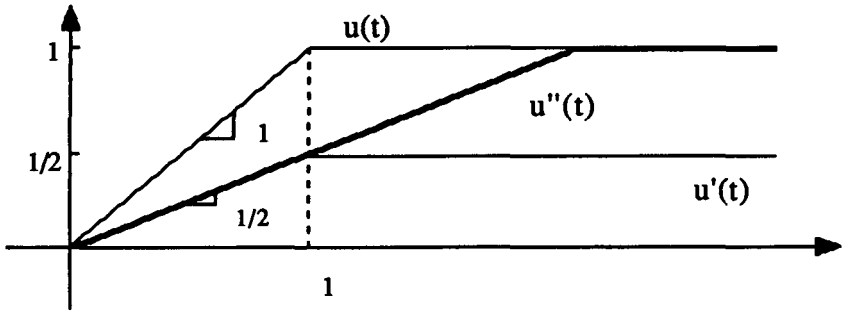

Figure 7.3: A sample u(t) signal and the outputs u'(t) and u"(t) from two different rate saturation models.

Thinking in a similar manner as for the magnitude saturation the idea is to modify the references error $\mathbf{e}(t)$ to $\mathbf{e}_\lambda(t)$ and/or $\mathbf{r}(t)$ to $\mathbf{r}_\mu(t)$ by the EG and/or the RG operators only when conditions exist so that the control rate $\dot{\mathbf{u}}(t)$ will saturate. The modification has to be carried out in such a way that any current or future references will never cause the control rates to saturate.

In sections 7.2.1 and 7.2.3 two different control structures for plants with rate saturation are given. The two different control structures are with the EG or the RG operators. Table 7.1 shows the application of the two control structures depending the stability of the plant and the compensator.

Table 7.1: Applications of the control system with the EG and/or RG operators for plants with rate saturation

	Neutrally stable compensator	Unstable compensator
Stable plant	Control structure with EG Control structure with RG Control structure with RG and EG	Control structure with RG
Unstable plant	Control structure with RG Control structure with RG and EG	Control structure with RG

7.2.1 Control Structure with EG for Plants with Rate Saturation

The control structure that will be introduced in this section is similar to the control structure with the operator EG (see section 4.3). This control structure is useful for stable plants with neutrally stable compensators. A time varying gain $\lambda(t)$ (EG operator) will be introduced at the error signal $\mathbf{e}(t)$ so that the controls will never saturate. The control rate $\dot{\mathbf{u}}(t)$ with the EG operator is given by

$$\dot{\mathbf{x}}_c(t) = \mathbf{A}_c\mathbf{x}_c(t) + \mathbf{B}_c\lambda(t)\mathbf{e}(t) \tag{7.9}$$

$$\mathbf{u}(t) = \mathbf{C}_c\mathbf{x}_c(t) \tag{7.10}$$

$$\dot{\mathbf{u}}(t) = \mathbf{C}_c\mathbf{A}_c\mathbf{x}_c(t) + \mathbf{C}_c\mathbf{B}_c\lambda(t)\mathbf{e}(t) \tag{7.11}$$

The eqs. (7.9)-(7.11) are to be interpreted as a dynamic system with states $\mathbf{x_c}(t)$, input $\lambda(t)\mathbf{e}(t)$ and output $\dot{\mathbf{u}}(t)$. Note that there is a feedforward term $\mathbf{C_cB_c}$ from the inputs $\lambda(t)\mathbf{e}(t)$ to the outputs $\dot{\mathbf{u}}(t)$. The objective here is to construct $\lambda(t)$ in such a way so that for any error $\mathbf{e}(t)$ the control rate $\dot{\mathbf{u}}(t)$ never saturates. This is similar to designing a time-varying gain so that the output of a linear system remains bounded (section 3.3). By following the discussion in section 3.3 one can construct $\lambda(t)$ to achieve the objective. At first, a function $g'(\mathbf{x})$ and a set $\mathbf{R_{A,C}}$ have to be defined

$$g'(\mathbf{x_0}): \quad g'(\mathbf{x_0}) = \|\dot{\mathbf{u}}(t)\|_\infty \tag{7.12}$$

where

$$\dot{\mathbf{x}}(t) = \mathbf{A_c}\mathbf{x}(t); \qquad \mathbf{x}(0) = \mathbf{x_0} \tag{7.13}$$

$$\dot{\mathbf{u}}(t) = \mathbf{C_cA_c}\mathbf{x}(t) \tag{7.14}$$

$$\mathbf{R_{A,C}} = \{\, \mathbf{x}: g'(\mathbf{x}) \le 1 \,\} \tag{7.15}$$

For the function $g'(\mathbf{x})$ to be finite the compensator (eqs. (7.3)-(7.5)) has to be neutrally stable. That is why the Error Governor is to be used only for neutrally stable compensators as shown in table 7.1. As in section 3.3 the construction of $\lambda(t)$ is given by

Construction of $\lambda(t)$ for the system with a feedforward term:

For every time t choose $\lambda(t)$ as follows

a)The largest $\lambda(t)$ such that $\|\mathbf{C_c A_c x_c}(t) + \mathbf{C_c B_c}\lambda(t)\mathbf{e}(t)\|_\infty \le 1$

b) if $\mathbf{x_c}(t) \in \mathrm{Bd}\mathbf{R_{A,C}}$ then choose the largest $\lambda(t)$ such that (7.16)

$$0 \le \lambda(t) \le 1 \tag{7.17}$$

$$\limsup_{\varepsilon \to 0} \frac{g'(\mathbf{x_c}(t) + \varepsilon[\mathbf{A_c x_c}(t) + \mathbf{B_c}\lambda(t)\mathbf{e}(t)]) - g'(\mathbf{x_c}(t))}{\varepsilon} \le 0 \tag{7.18}$$

or for the points where $g(\mathbf{x_c})$ is differentiable choose the largest $\lambda(t)$ such that

$$0 \le \lambda(t) \le 1 \tag{7.19}$$

$$Dg'(\mathbf{x_c}(t))[\mathbf{A_c x_c}(t) + \mathbf{B_c}\lambda(t)\mathbf{e}(t)] \le 0 \quad \forall t>0 \tag{7.20}$$

where $Dg'(\mathbf{x_c}(t))$ is the Jacobian matrix of $g'(\mathbf{x_c}(t))$ as it is given in definition 3.2.

c) if $\mathbf{x_c}(t) \notin \mathbf{R_{A,C}}$ then choose $\lambda(t)$, $0 \le \lambda(t) \le 1$ such that the expression in (7.18) is minimum.

The control structure with the EG operator for plants with rate saturation presented here is similar and therefore has similar properties as the control structure with the EG operator for plants with magnitude saturations presented in chapter 4. In most applications the control rate saturation is present in addition to the control magnitude saturation and section 7.3.1 introduces a control structure with the EG operator for plants with both control magnitude and rate saturations.

7.2.2 Academic Example

Consider the following system which is the compensator for the academic example #1

defined in section 4.2.3.

$$\dot{\mathbf{x}}(t) = \begin{bmatrix} -2.6093 & 1.4180 \\ -7.1476 & 1.5213 \end{bmatrix} \mathbf{x}(t) + \begin{bmatrix} -29.8308 & 2.989 \\ -68.7543 & 10.8387 \end{bmatrix} \mathbf{e}(t) \qquad (7.21)$$

$$\mathbf{u}(t) = \begin{bmatrix} -1 & 1 \\ 2 & -1 \end{bmatrix} \mathbf{x}(t) \qquad (7.22)$$

Assume that in the academic example #1 it is desired to have $\|\dot{\mathbf{u}}(t)\|_\infty \leq 2.5$ for every t and e(t). To use the control structure with the EG operator one has to modify e(t) to $\lambda(t)e(t)$. The computation of $\lambda(t)$ requires the calculation of the $\mathbf{R}_{A,C}$ set.

$$g'(\mathbf{x}_0): \mathbb{R}^2 \rightarrow \mathbb{R}, \quad g'(\mathbf{x}_0) = \|\dot{\mathbf{u}}(\mathbf{x}_0,t)\|_\infty \qquad (7.23)$$

$$\mathbf{R}_{A,C} = \{ \mathbf{x} \in \mathbb{R}^2 : g'(\mathbf{x}) \leq 2.5 \} \qquad (7.24)$$

The computation of the EG operator for this case is the same as the one given in section 4.2. In summary, one has to compute the $\mathbf{R}_{A,C}$, from the $\mathbf{R}_{A,C}$ set one can construct the function g'(x) since g'(x) is a cone and the $\mathbf{R}_{A,C}$ set is the intersection of the cone with the g'(x) = 2.5 hyperplane. By knowing g(x) and the $\mathbf{R}_{A,C}$ set one can construct $\lambda(t)$ as it is shown in sections 3.3 and 4.2.

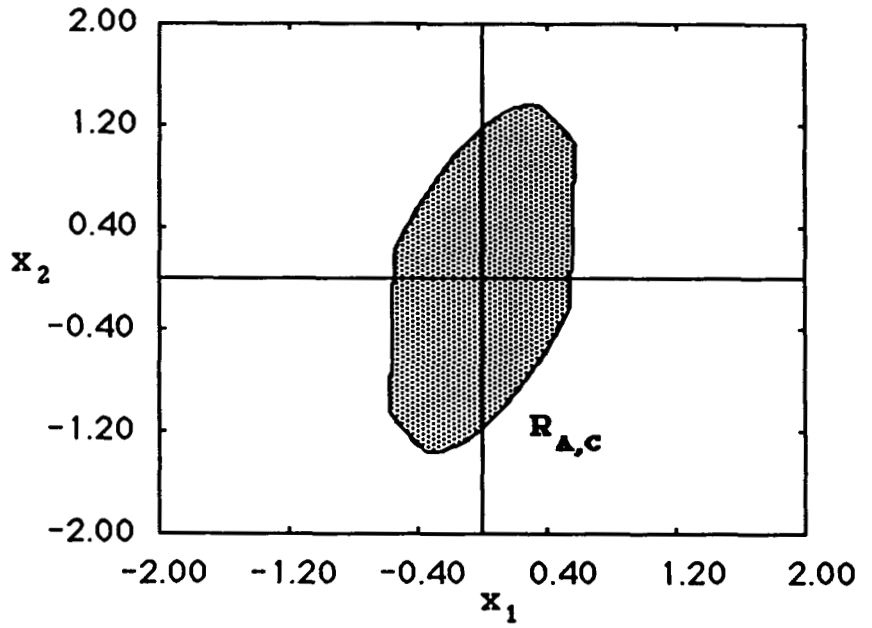

Figure 7.4: The $\mathbf{R}_{A,C}$ set for the academic example #1.

Figure 7.4 shows the set $\mathbf{R}_{A,C}$. Note the symmetry with respect to the origin, the convexity and the fact that the set is bounded because all the modes of the system are observable. This set will be used in the sequel in (section 7.3) to design a compensator that will insure that the magnitude and the rate of the controls remain bounded.

7.2.3 Control Structure with RG for Plants with Rate Saturation

In analogy to chapter 3 and 5, a time varying rate $\mu(t)$ will be introduced at the reference signal $\mathbf{r}(t)$ so that the controls of the plant will never exceed their rate limits as shown in figure 7.5. The RG operator is a time-varying rate limiter on the references where $\mu(t)$ is a time-varying gain, $0 \leq \mu(t) \leq \infty$.

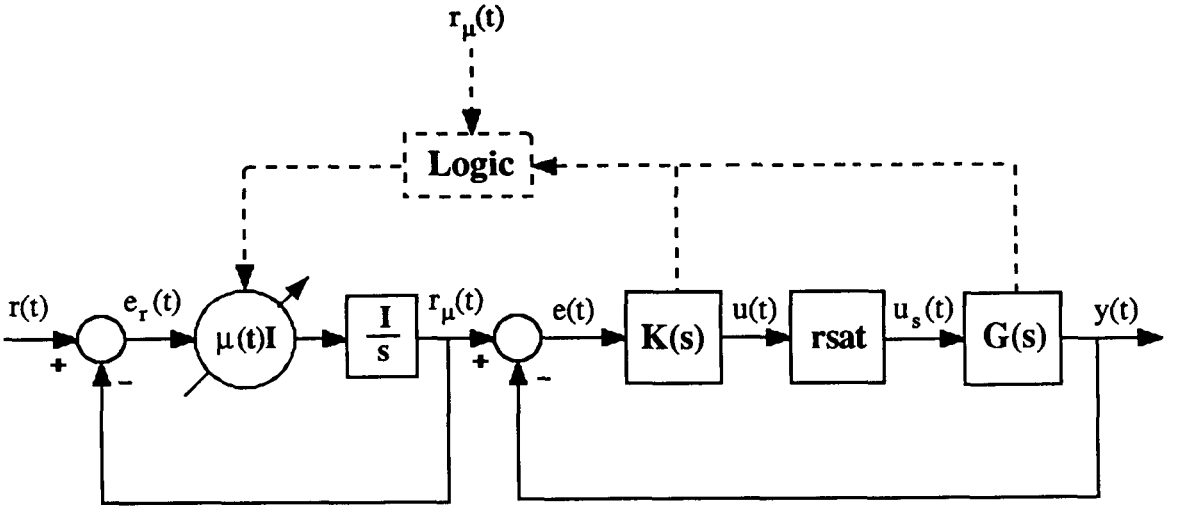

Figure 7.5: Control structure with the RG operator for plants with rate saturation.

The plant and the compensator dynamics in figure 7.5 are described in eqs. (7.1)-(7.5). Assuming that the states of the integrators in the time varying rate are $\mathbf{z}(t)$ then the time varying rate at the references can be described by the following

$$\dot{\mathbf{z}}(t) = \mu(t)\mathbf{e}_r(t) \tag{7.25}$$

$$\mathbf{e}_r(t) = \mathbf{r}(t) - \mathbf{r}_\mu(t) \tag{7.26}$$

$$\mathbf{r}_\mu(t) = \mathbf{z}(t) \tag{7.27}$$

As in chapter 5, the time varying gain $\mu(t)$ will be chosen so that if $\mathbf{r}(t)$ is small enough never to cause saturation of the rate of the controls then $\mathbf{r}(t) = \mathbf{r}_\mu(t)$ and if $\mathbf{r}(t)$ is large enough to cause saturation of the rate of the controls then $\mu(t)$ will limit the references so that the rate of the controls will remain bounded. Consider the linear closed loop system (i.e the system without rate saturation) and assume the following representation

$$\dot{x}_{cl}(t) = A_{cl}\, x_{cl}(t) + B_{cl} r_{\mu}(t) \tag{7.28}$$

$$u(t) = C_{cl}\, x_{cl}(t) \tag{7.29}$$

$$\dot{u}(t) = C_{cl}A_{cl}\, x_{cl}(t) + C_{cl}B_{cl} r_{\mu}(t)$$

where $$x_{cl} = \begin{bmatrix} x_c \\ \\ x \end{bmatrix}$$

$$A_{cl} = \begin{bmatrix} A_c & -B_cC \\ BC_c & A \end{bmatrix} \qquad B_{cl} = \begin{bmatrix} B_c \\ \\ 0 \end{bmatrix} \qquad C_{cl} = \begin{bmatrix} C_c & 0 \end{bmatrix}$$

Then one can combine the dynamics of the rate limiter (7.22)-(7.24) with the dynamics of the closed loop system (7.25)-(7.26) to obtain an augmented system

$$\dot{x}_a(t) = A_a x_a(t) + B_a \mu(t) e_r(t) \tag{7.30}$$

$$\dot{u}(t) = C_a x_a(t) \tag{7.31}$$

where

$$x_a(t) = \begin{bmatrix} z(t) \\ x_{cl}(t) \end{bmatrix} \qquad A_a = \begin{bmatrix} 0 & 0 \\ B_{cl} & A_{cl} \end{bmatrix} \qquad B_a = \begin{bmatrix} I \\ 0 \end{bmatrix} \qquad C_a = \begin{bmatrix} C_{cl}B_{cl} & C_{cl} \end{bmatrix}$$

The objective here is to construct $\mu(t)$, $0 \le \mu(t) \le \infty$, in such a way so that for any error

$e_r(t)$ the control rate $\dot{u}(t)$ never saturates. This is similar to designing a time-varying rate so that the output of a linear system remains bounded (section 3.4). At first, a function $g'(x)$ and a set $R_{A,C}$ have to be defined. The symbols $g'(x)$ and $R_{A,C}$ should be thought as generic symbols and when they are used they are always defined to avoid confusion.

$$g'(x_{a0}): \quad g'(x_{a0}) = \|\dot{u}(t)\|_\infty \tag{7.32}$$

where

$$\dot{x}_a(t) = A_a x_a(t); \qquad x_a(0) = x_{a0} \tag{7.33}$$

$$\dot{u}(t) = C_a x_a(t) \tag{7.34}$$

$$R_{A,C} = \{ x: \ g'(x) \le 1 \} \tag{7.35}$$

For the function $g'(x)$ to be finite the linear system in eq. (7.33) has to be neutrally stable. This is always true for any compensator and any plant provided that the linear closed loop system (the system in figure 7.1 without the saturation) is stable. Therefore, the Reference Governor can be used in all cases as shown in table 7.1. As in section 3.3 the construction of $\mu(t)$ is given by

Construction of $\mu(t)$:

For every time t choose $\mu(t)$ as follows

a) if $x_a(t) \in \text{Int}\mathbf{R}_{A,C}$ then $\mu(t) = \infty$ which implies that $r(t) = r_\mu(t)$ (7.36)

b) if $x_a(t) \in \text{Bd}\mathbf{R}_{A,C}$ then choose the largest $\mu(t)$ such that (7.37)

$$0 \le \mu(t) \le \infty$$

$$\lim_{\varepsilon \to 0} \sup \frac{g'\left(x_a(t)+\varepsilon[A_a x_a(t)+B_a \mu(t) e_r(t)]\right) - g'\left(x_a(t)\right)}{\varepsilon} \le 0 \qquad (7.38)$$

or for the points where $g'(x)$ is differentiable choose the largest $\mu(t)$ such that

$$0 \le \mu(t) \le \infty \qquad (7.39)$$

$$Dg'(x_a(t))[A_a x_a(t)+B_a \mu(t) e_r(t)] \le 0 \quad \forall\, t > 0 \qquad (7.40)$$

where $Dg'(x_a(t))$ is the Jacobian matrix of $g'(x_a(t))$ as in definition 3.2.

c) if $x_a(t) \notin \mathbf{R}_{A,C}$ then choose $\mu(t)$, $0 \le \mu(t) \le \infty$ such that the expression (7.38) is minimum.

Because the control structure given above is similar to the control structure introduced in chapter 5 both structure have the same properties. More specifically, the control rate remains bounded and as a consequence, integrator windups and the control direction do not cause any problems in the performance of the system. As it was described in chapter 5 the states of the plant have to be measured for the realization of the RG operator and the off-line computational requirements can be severe if the state dimension of the plant and the compensator is large.

With the rate saturation problem transformed to fit the magnitude saturation problem it is obvious how the control structure with the EG and RG operators can be used to deal with rate saturations as it was discussed in section 5.3.1 (Description of the Control Structure with The Operators EG and RG).

7.3 Rate/Magnitude Saturation

Assume that a given closed loop system consists of a plant, a compensator, a magnitude saturation nonlinearity (sat), and a rate saturation nonlinearity (rsat) as shown in Figure 7.6. The saturation elements (sat, rsat) have been defined in eqs. (2.1) and (7.6).

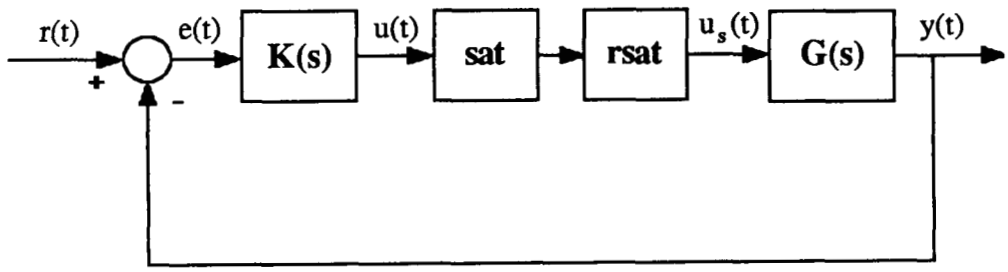

Figure 7.6: Closed loop system with rate and magnitude saturation

The following models for the plant and the compensator can be assumed

Plant model:

$$\dot{\mathbf{x}}(t) = \mathbf{A}\mathbf{x}(t) + \mathbf{B}\mathbf{u}_s(t) \tag{7.41}$$

$$\mathbf{y}(t) = \mathbf{C}\mathbf{x}(t) \tag{7.42}$$

Compensator model:

$$\dot{\mathbf{x}}_c(t) = \mathbf{A}_c\mathbf{x}_c(t) + \mathbf{B}_c\mathbf{e}(t) \tag{7.43}$$

$$\mathbf{u}(t) = \mathbf{C}_c\mathbf{x}_c(t) \tag{7.44}$$

$$\mathbf{e}(t) = \mathbf{r}(t) - \mathbf{y}(t) \tag{7.45}$$

Saturation model:

$$\mathbf{u}_s(t) = \text{rsat}(\text{sat}(\mathbf{u}(t))) \tag{7.46}$$

7.3.1 Control Structure with EG for Plants with Rate and Magnitude Saturation

The problem here is to keep the control magnitude and rate bounded. The idea is to modify the error $\mathbf{e}(t)$ to $\mathbf{e}_\lambda(t)$ only when the references are large enough and the controls $\mathbf{u}(t)$ will saturate either in magnitude or rate. The modification has to be accomplished in such a way that any current or future references will never cause the system to saturate. The operator EG has to be introduced as part of the compensator. The modified compensator is defined as follows.

$$\dot{\mathbf{x}}_c(t) = \mathbf{A}_c\mathbf{x}_c(t) + \mathbf{B}_c\lambda(t)\mathbf{e}(t) \tag{7.47}$$

$$\mathbf{u}(t) = \mathbf{C}_c\mathbf{x}_c(t) \tag{7.48}$$

$$\dot{\mathbf{u}}(t) = \mathbf{C}_c\mathbf{A}_c\mathbf{x}_c(t) + \mathbf{C}_c\mathbf{B}_c\lambda(t)\mathbf{e}(t) \tag{7.49}$$

In chapter 4 it was described how one can introduce the operator EG such that the magnitude of the controls remain bounded. That was done by defining a function $g(\mathbf{x})$ and a set $\mathbf{B}_{A,C}$ and by constructing a time varying gain, call it $\lambda_1(t)$, such that the states of the compensator remained in the $\mathbf{B}_{A,C}$ set for any reference.

In section 7.2.1 it was described how one can introduce the operator EG such that the rate of the controls remain bounded when the open loop plant is stable. That was done by

defining a function g'(x) and a set $\mathbf{R}_{A,C}$ and by constructing a time varying rate, call it $\lambda_2(t)$, such that the states of the compensator remained in the $\mathbf{R}_{A,C}$ set for any reference.

Since the problem here is to keep both the magnitude and rate bounded one can choose $\lambda(t)$ in eqs. (7.47)-(7.49) as the minimum of $\lambda_1(t)$ and $\lambda_2(t)$ and that will prevent the controls of saturating both in magnitude and rate. To do this, one has to compute, at every time t_0, both $\lambda_1(t)$ and $\lambda_2(t)$ (in addition to the fact that both the $\mathbf{B}_{A,C}$ and $\mathbf{R}_{A,C}$ sets have to be precomputed and stored during the operation of the system). Another way of computing the $\lambda(t)$ is to define another set $\mathbf{S}_{A,C}$

$$\mathbf{S}_{A,C} = \mathbf{B}_{A,C} \cap \mathbf{R}_{A,C} \tag{7.50}$$

Then one can use the $\mathbf{S}_{A,C}$ set in the implementation of $\lambda(t)$ in section 4.2.2. To be more specific in the construction of $\lambda(t)$ in section 4.2.2 the $\mathbf{S}_{A,C}$ set can be used instead of the $\mathbf{B}_{A,C}$ set. The function g(x) can be computed by constructing the cone g(x) with the set $\mathbf{S}_{A,C}$ being the set of points where $g(x) \geq 1$. Since the $\mathbf{S}_{A,C}$ is the intersection of both $\mathbf{B}_{A,C}$ and $\mathbf{R}_{A,C}$ the compensator and plant states will remain in both $\mathbf{B}_{A,C}$ and $\mathbf{R}_{A,C}$ for all t, and the controls will never saturate in either magnitude and rate.

7.3.2 Academic Example

Consider the academic example given in section 3.3 and section 7.2. The $\mathbf{B}_{A,C}$ set has been calculated in section 3.3 and the set $\mathbf{R}_{A,C}$ was calculated in section 7.2. Figure 7.7 shows both $\mathbf{B}_{A,C}$ and $\mathbf{R}_{A,C}$ sets and their intersection $\mathbf{S}_{A,C}$. The $\mathbf{S}_{A,C}$ set will be used to modify the compensator when both control magnitude and rate saturations are present.

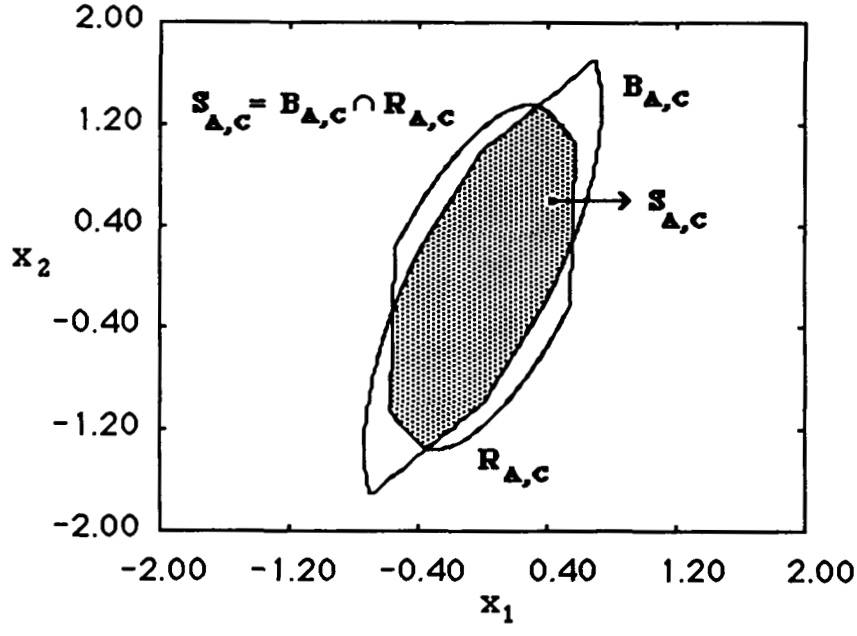

Figure 7.7: The $S_{A,C}$ set for the academic example.

7.3.3 Simulation of the Academic Example

Four distinct type of simulations were performed. These simulations correspond to the *linear system*, to *the system with magnitude saturation*, to *the system with rate and magnitude saturation* and to *the system with rate, magnitude saturation and the EG operator.*

All the computations were performed in the Macintosh 512K and the calculation of the EG operator required approximately 15-16 hours. The first simulation was performed with reference $\mathbf{r} = [.22 \quad .22]^T$. The magnitude saturation is assumed to be ±1 and the rate saturation is assumed to be ±2.5

Figure 7.8 show the state trajectory of the compensator states for the linear system. Note that the state trajectory does not remain in the $S_{A,C} = R_{A,C} \cap B_{A,C}$; therefore, the potential exists for saturating in both rate and magnitude.

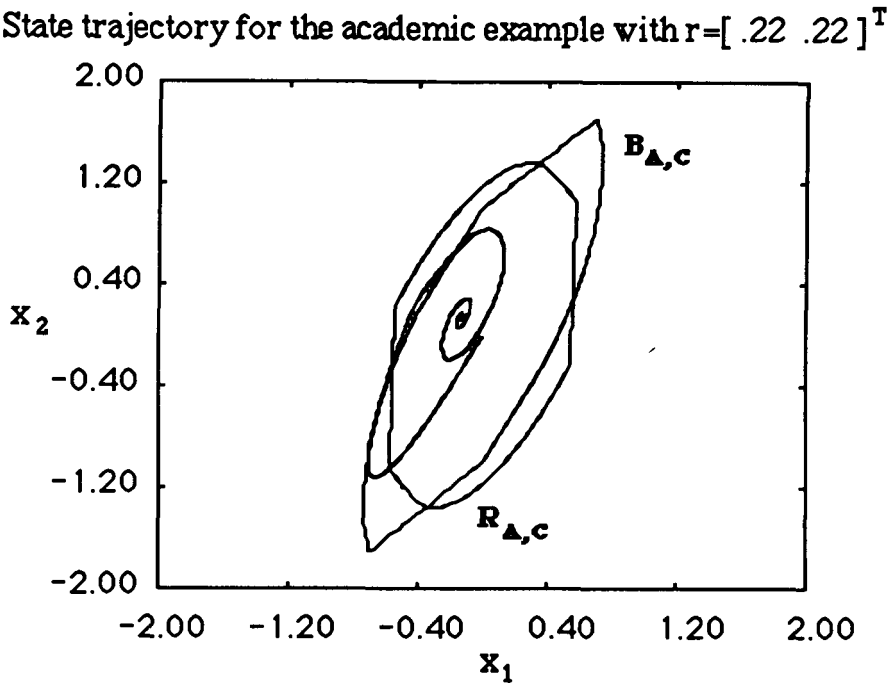

Figure 7.8: State trajectory of the linear closed loop system with reference $\mathbf{r} = [\ .22\quad .22]^T$

Figures 7.9 and 7.10 show the output and control responses for the linear system. The controls violate the ±1 limits and the rate of the controls exceed the ±2.5 limits. The linear response is assumed to be the desired one.

Figures 7.11 and 7.12 show the output and control responses of the system with magnitude saturation. One can see that the output response has significantly deteriorated even for a small amount of saturation (≈1.1).

Figures 7.13 and 7.14 show the output and control response of the system with both magnitude and rate saturation. The response of the system has now completely deteriorated in both the controls and the outputs.

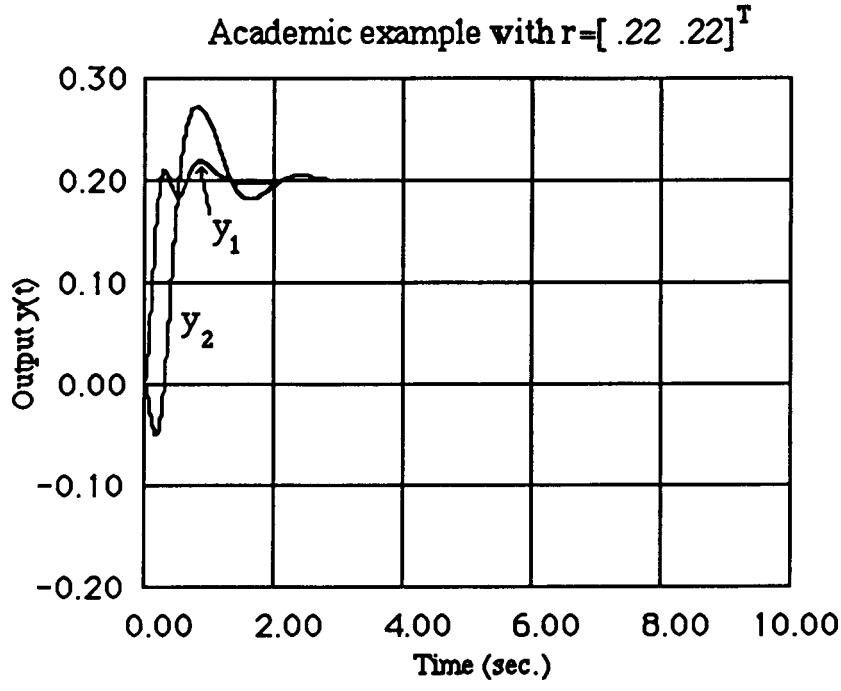

Figure 7.9: Output of the linear system, ($\mathbf{r} = [\ .22\quad .22]^T$)

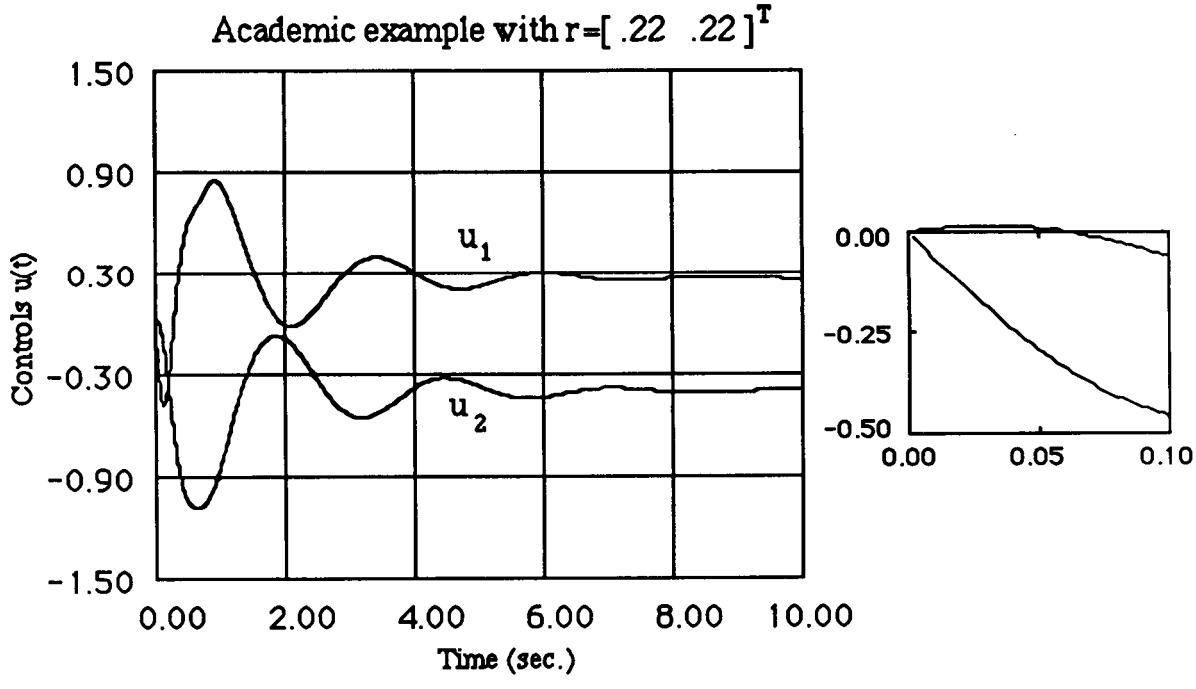

Figure 7.10: Control of the linear system with reference ($\mathbf{r} = [\ .22\quad .22]^T$)
Insert: Blowup with $0 < t < .1$ sec

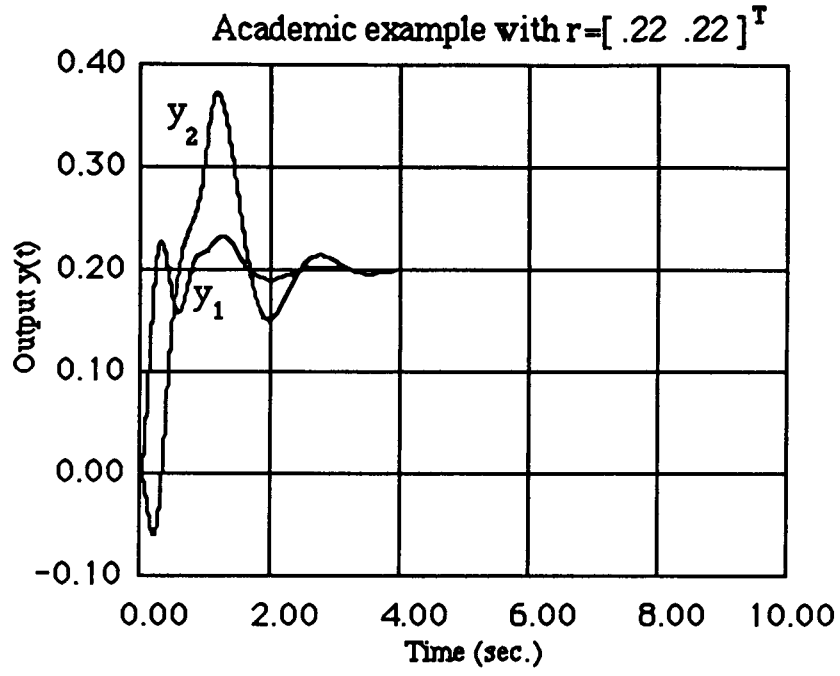

Figure 7.11: Output of the system with control magnitude saturation, without control rate saturation and with reference ($\mathbf{r} = [\ .22\ \ .22]^T$)

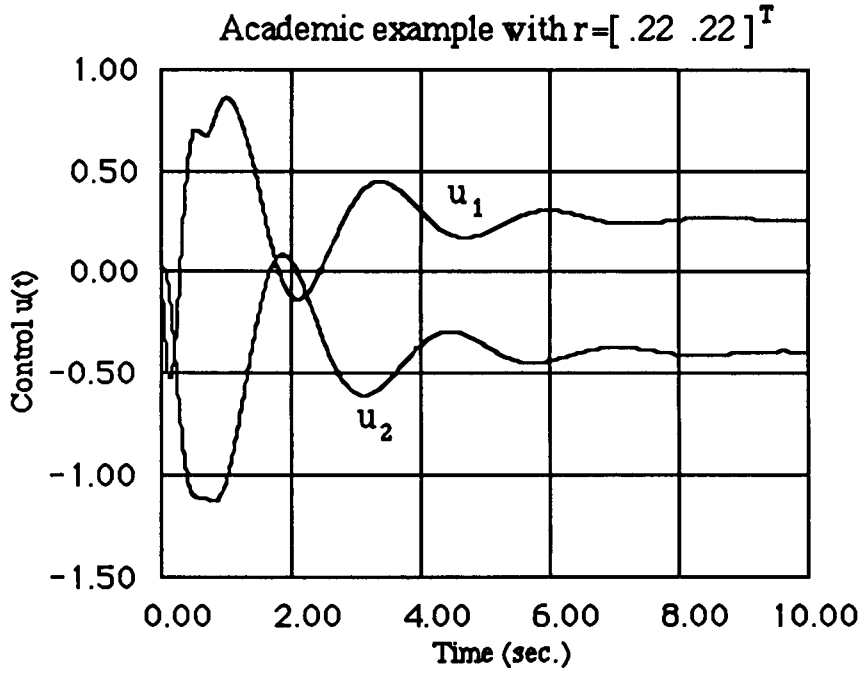

Figure 7.12: Control of the system with control magnitude saturation, without control rate saturation and with reference ($\mathbf{r} = [\ .22\ \ .22]^T$)

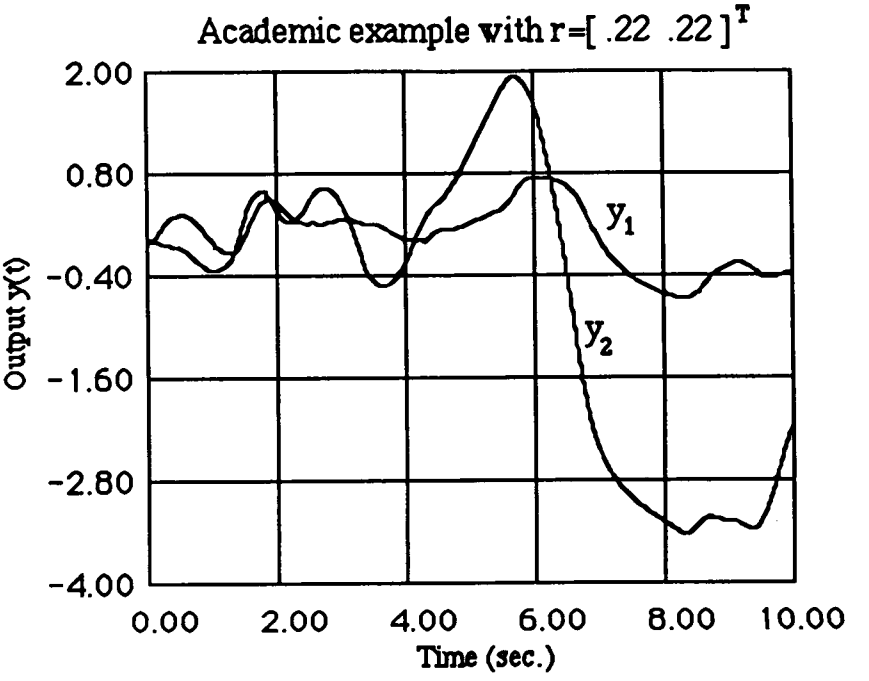

Figure 7.13: Output of the system with control magnitude and rate saturation, ($\mathbf{r} = [\ .22\ \ .22]^T$)

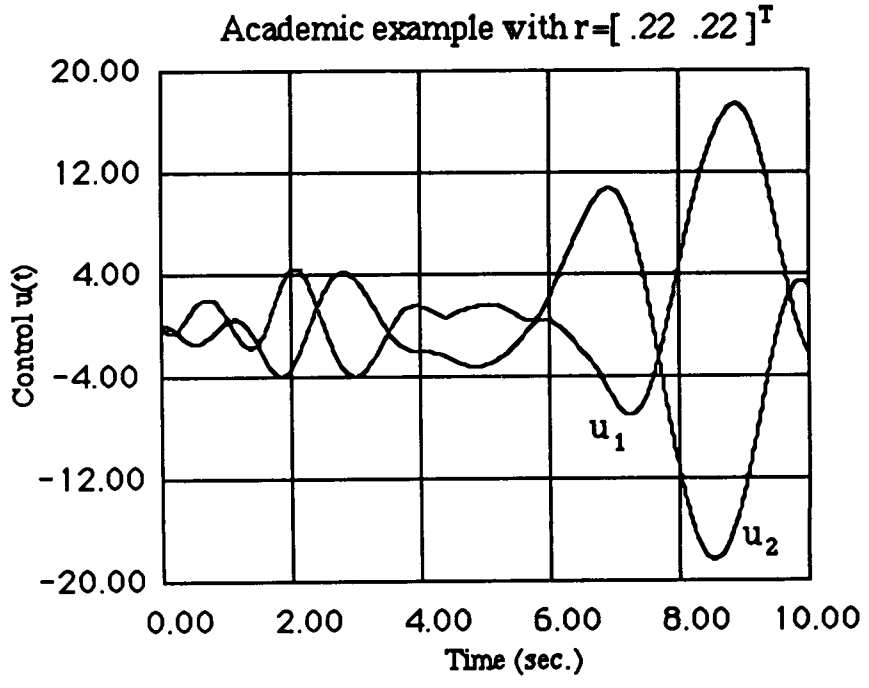

Figure 7.14: Control in the system with control magnitude and rate saturation, ($\mathbf{r} = [\ .22\ \ .22]^T$)

Figure 7.15 show the state trajectory of the system with magnitude and rate saturation and the EG operator. Note that the state trajectory of the compensator does remain in $\mathbf{S}_{A,C}$ for all t and so neither magnitude nor rate saturation will occur.

Figures 7.16 and 7.17 show the output and control response of the system with the EG operator. Note that the output direction is similar to the linear response (figure 7.9) and that the controls remain within the limits of the magnitude and rate saturation.

Figure 7.18 show the $\lambda(t)$ required for this simulation. One can see that the $\lambda(t)$ starts at a value less than 1 since the controls at the beginning would exceed the rate saturation limit then gradually $\lambda(t)$ increases to 1, then the states of the compensator reach the boundary of the $\mathbf{R}_{A,C}$ set and $\lambda(t)$ is decreased. Note that $\lambda(t)$ is also decreased drastically again at $\approx$.6 sec, because the states of the compensator reach the boundary of the $\mathbf{B}_{A,C}$ set.

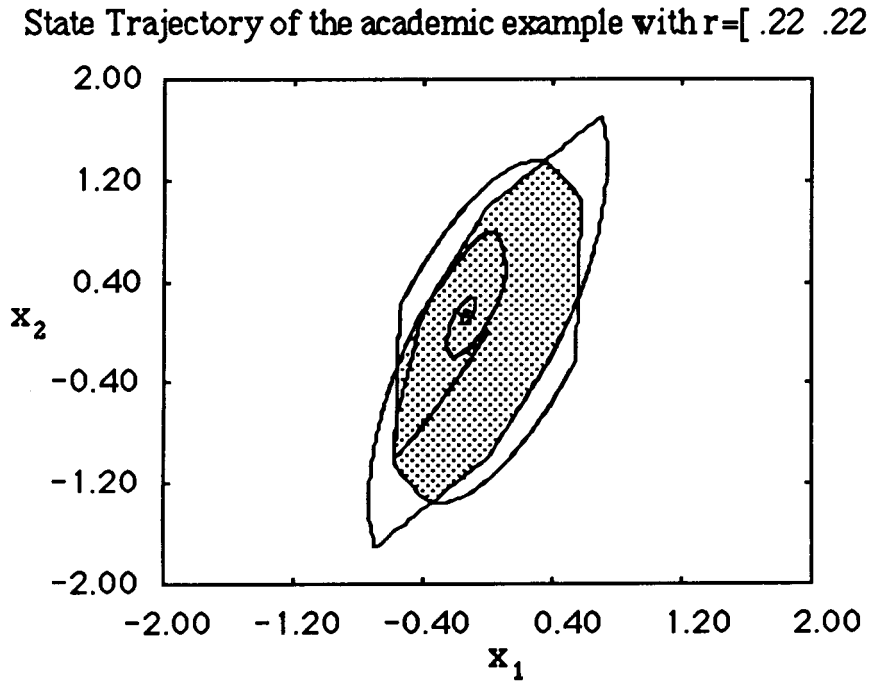

Figure 7.15: State trajectory of the system with control magnitude /rate saturation and the EG, ($\mathbf{r} = [\ .22\ \ .22]^T$)

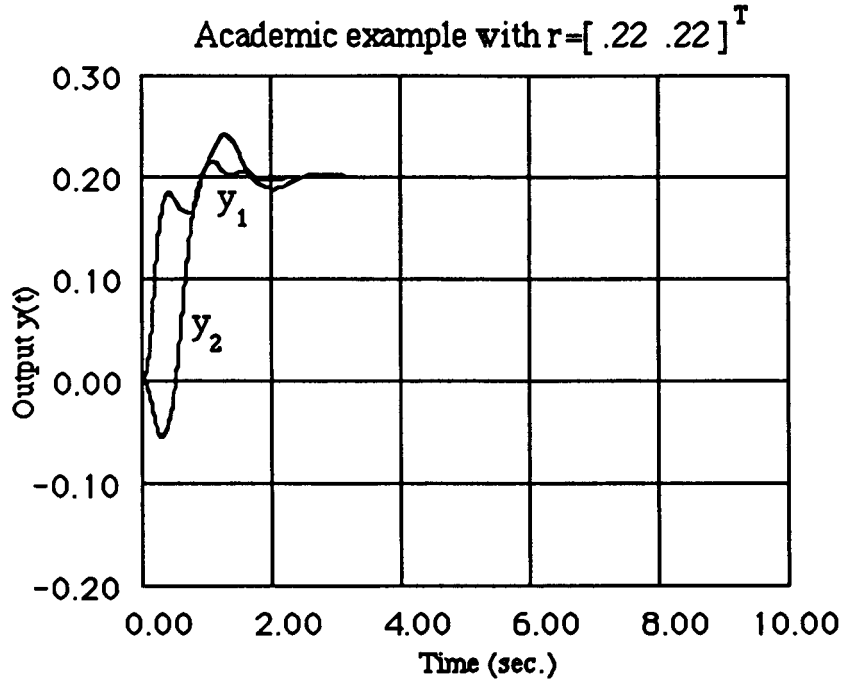

Figure 7.16: Output of the system with magnitude/rate saturation and the EG, ($\mathbf{r} = [22 \quad .22]^T$).

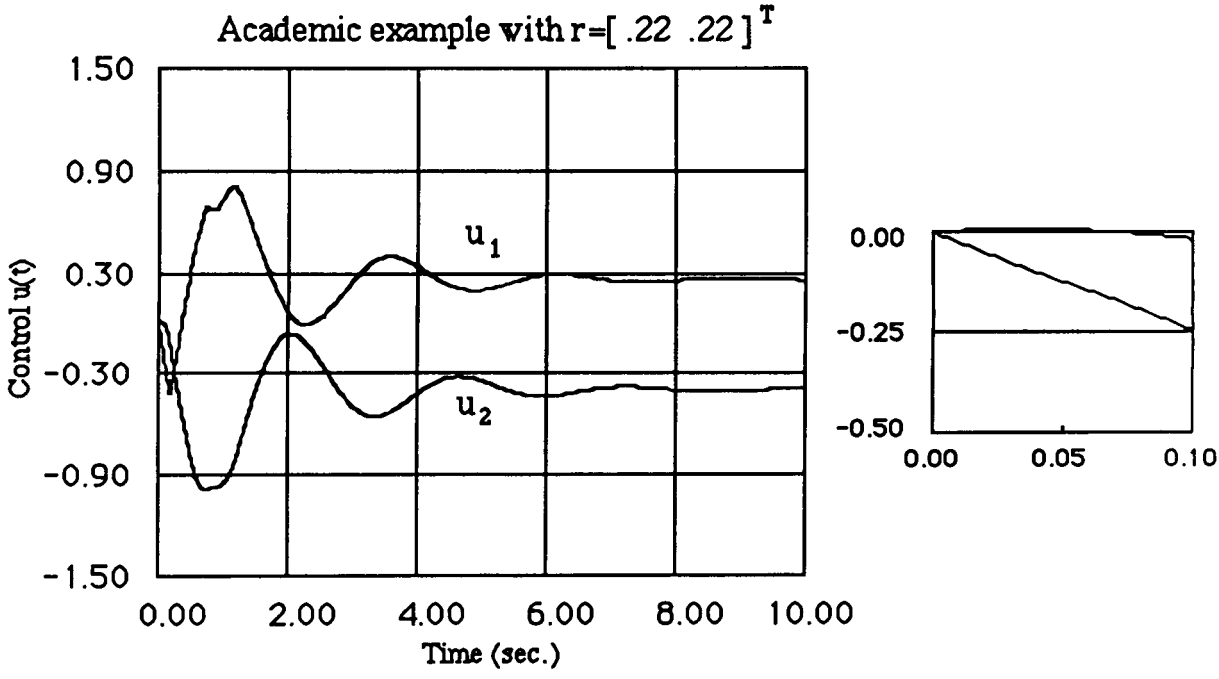

Figure 7.17: Controls in the system with magnitude/rate saturation and the EG, ($\mathbf{r} = [\ .22 \quad .22]^T$). Insert: Blowup of $0 < t < .1$ sec

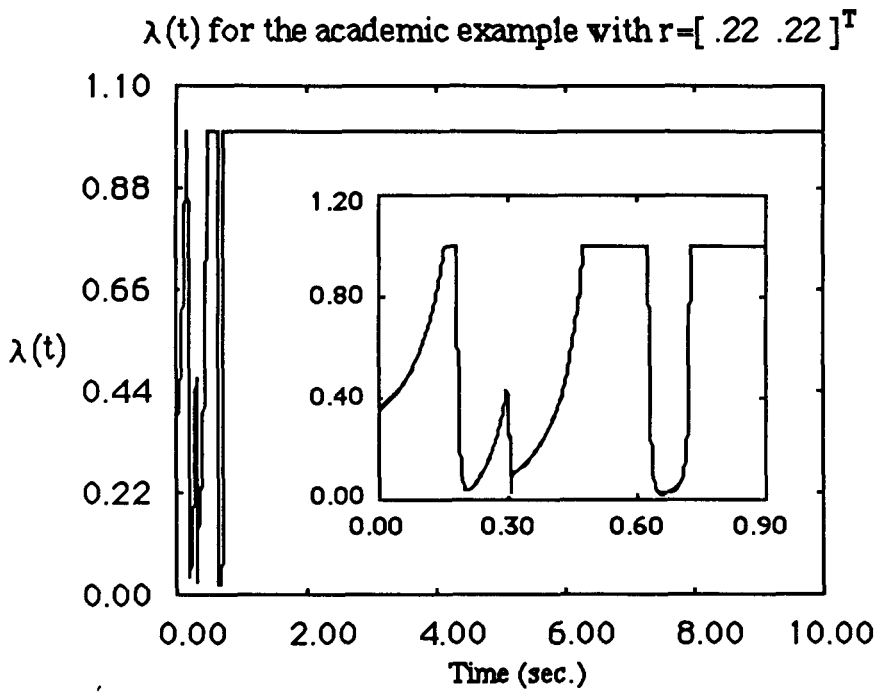

Figure 7.18: λ(t) of the system with magnitude/rate saturation and the EG, ($\mathbf{r} = [\ .22 \quad .22]^T$). Insert: Blowup $0 \leq t \leq .9$ sec.

Another set of simulations was performed with the reference being $\mathbf{r} = [\ 0 \quad 2.5]^T$. The observations that one can make from this simulation results (figures 7.19-7.28) are similar to the ones made from the previous simulation. The magnitude saturation affects negatively the desired linear response of the system and when the magnitude saturation is combined with the rate saturation then the performance of the system deteriorates dramatically. The error governor (EG) seems to fix all problems.

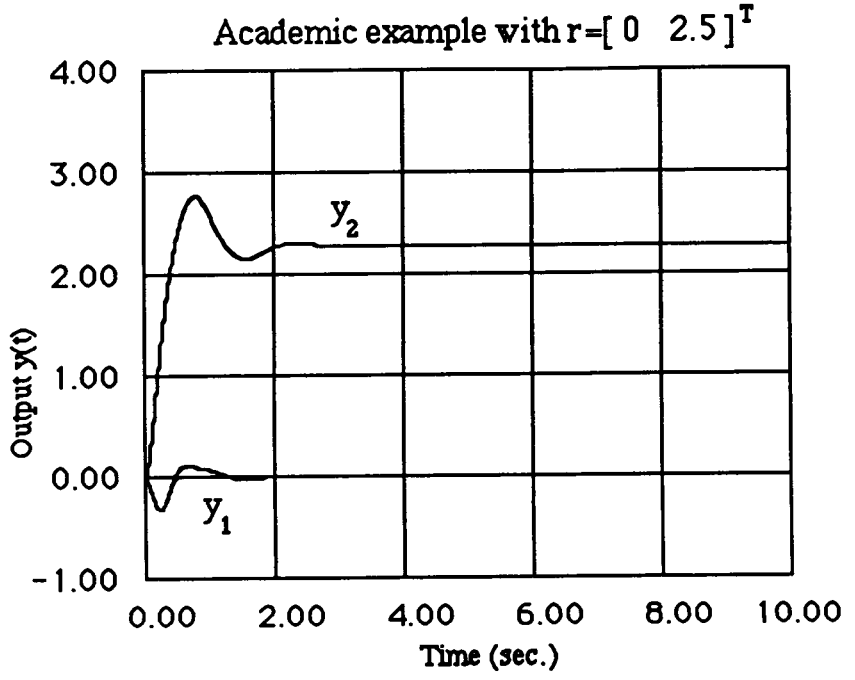

Figure 7.19: Output of the linear system, ($\mathbf{r} = [\,0 \quad 2.5]^T$).

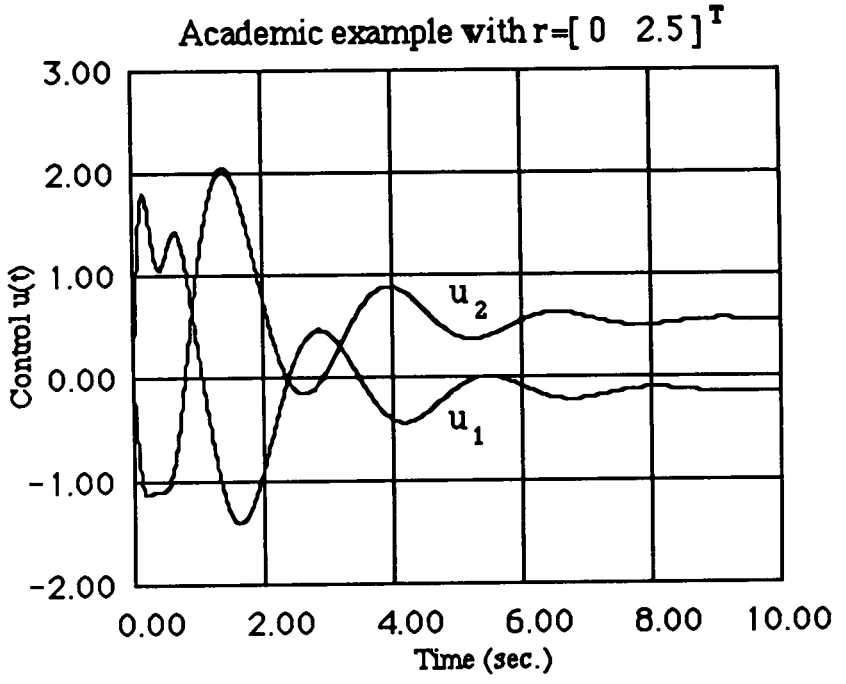

Figure 7.20: Controls in the linear system, ($\mathbf{r} = [\,0 \quad 2.5]^T$).
Insert: Blowup with $0 < t < .1$ sec

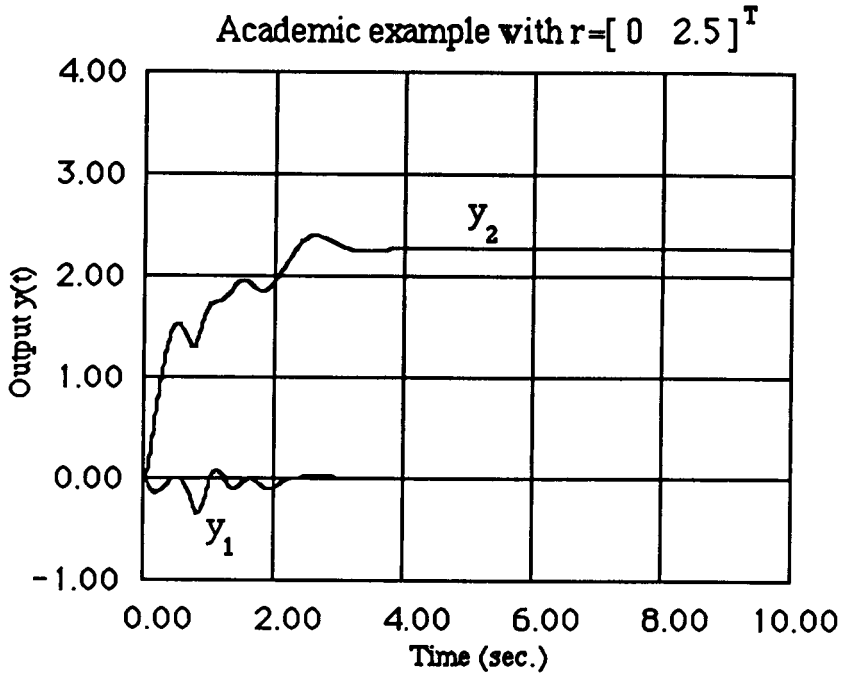

Figure 7.21: Output of the system with only magnitude saturation, ($\mathbf{r} = [\,0 \quad 2.5]^T$).

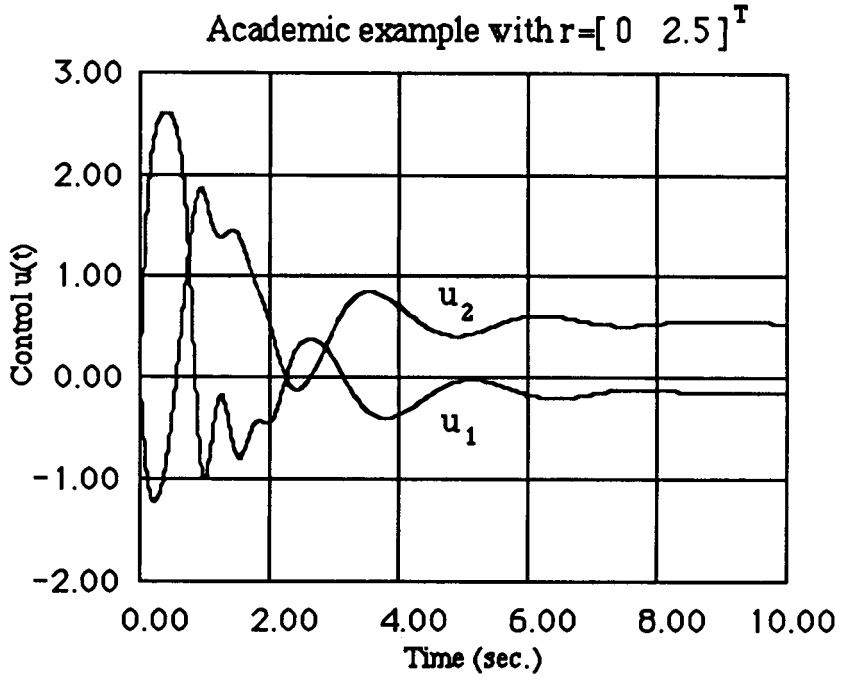

Figure 7.22: Controls in the system with only magnitude saturation, ($\mathbf{r} = [\,0 \quad 2.5]^T$).

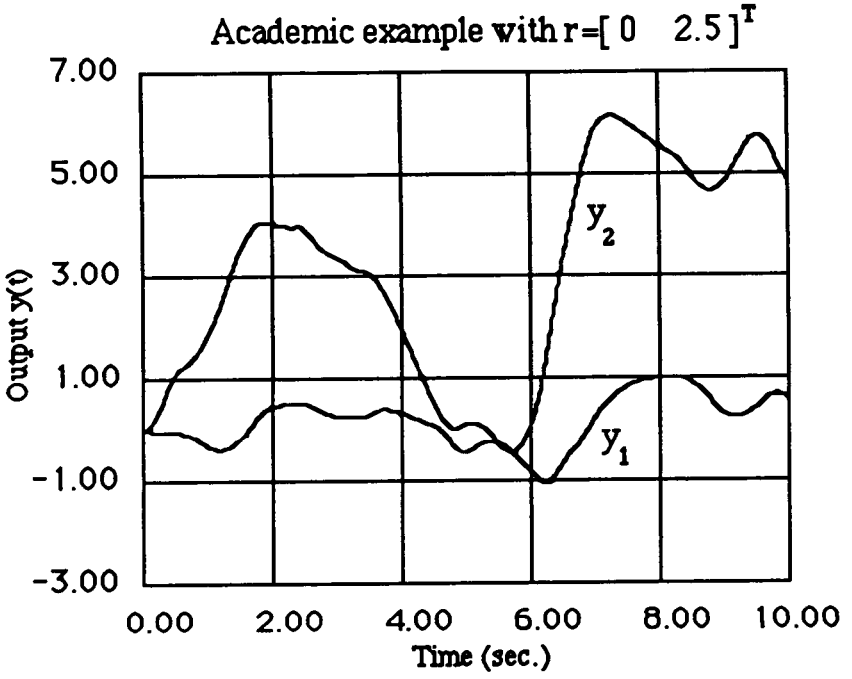

Figure 7.23: Output of the system with magnitude/rate saturation, ($\mathbf{r} = [\,0 \quad 2.5\,]^T$).

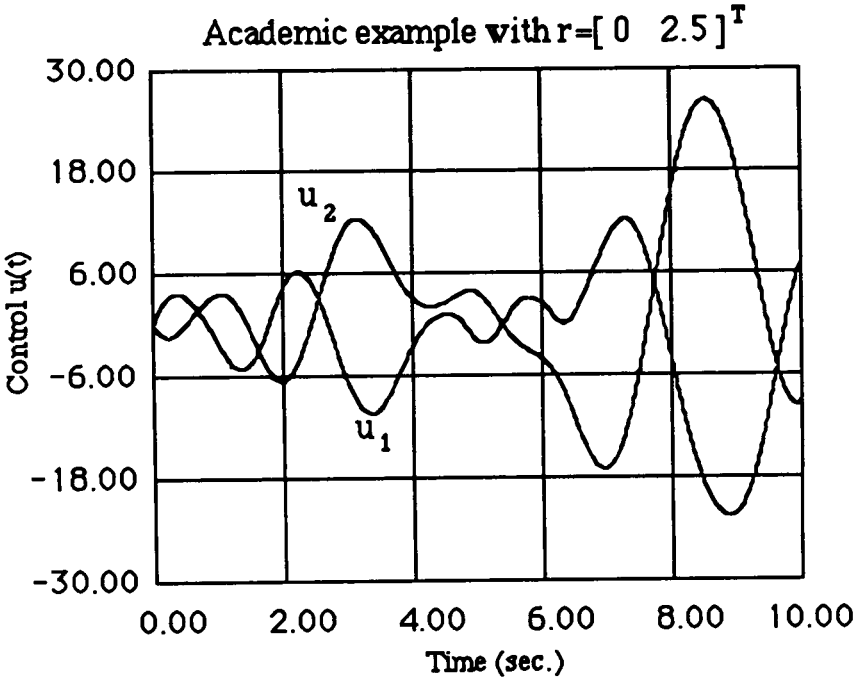

Figure 7.24: Controls in the system with magnitude/rate saturation, ($\mathbf{r} = [\,0 \quad 2.5]^T$).

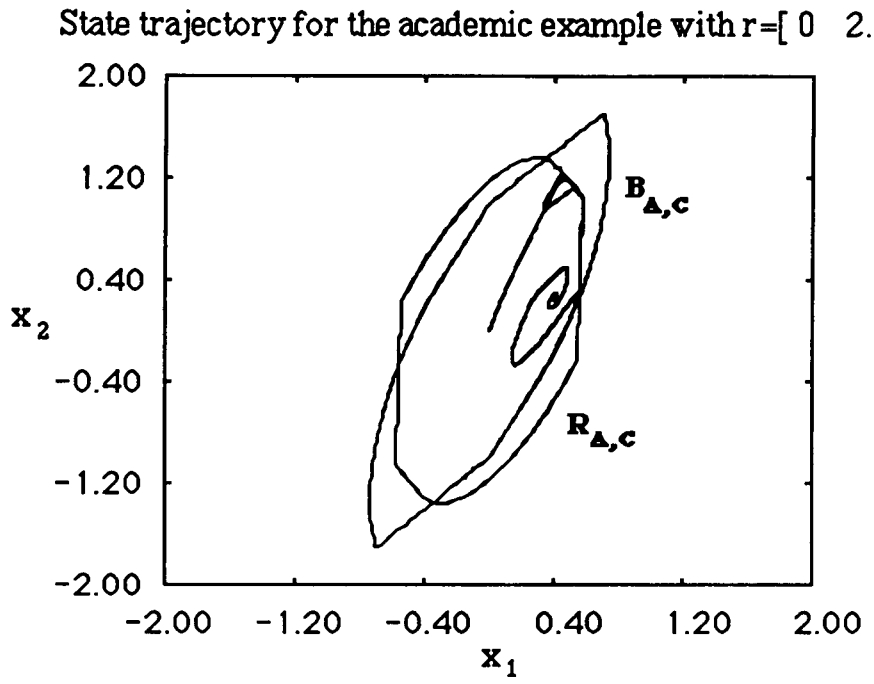

Figure 7.25: State trajectory of the compensator state in the system with magnitude/rate saturation and the EG ($\mathbf{r} = [\,0 \quad 2.5]^T$).

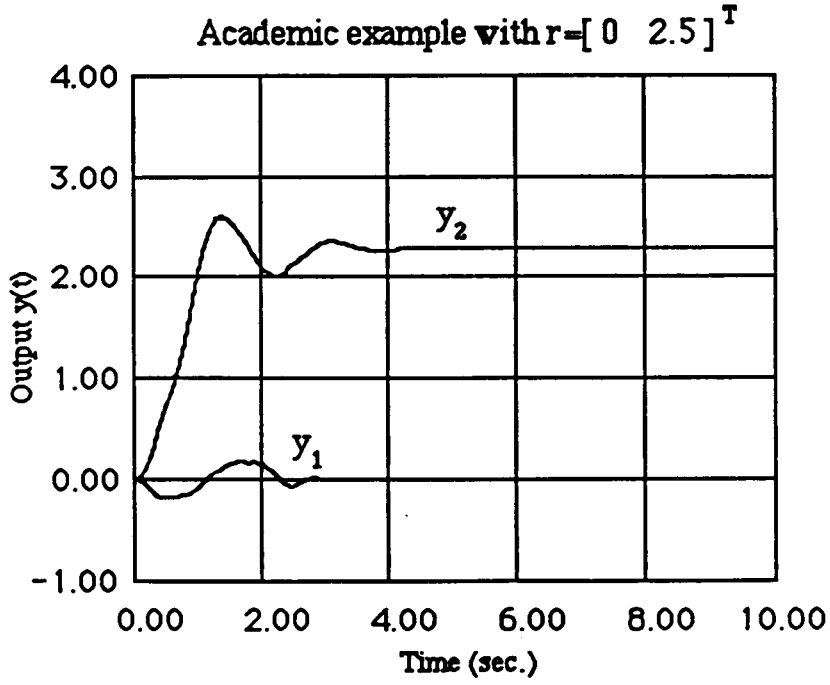

Figure 7.26: Output of the system with magnitude/rate saturation and the EG, ($\mathbf{r} = [\,0 \quad 2.5\,]^T$).

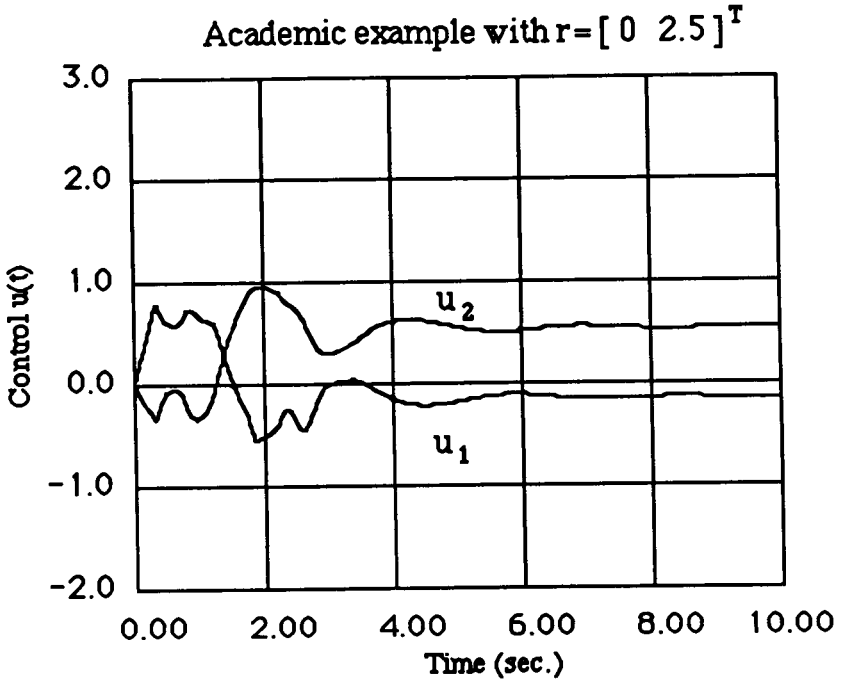

Figure 7.27: Controls in the system with magnitude/rate saturation and the EG, ($\mathbf{r} = [\,0 \quad 2.5\,]^T$).

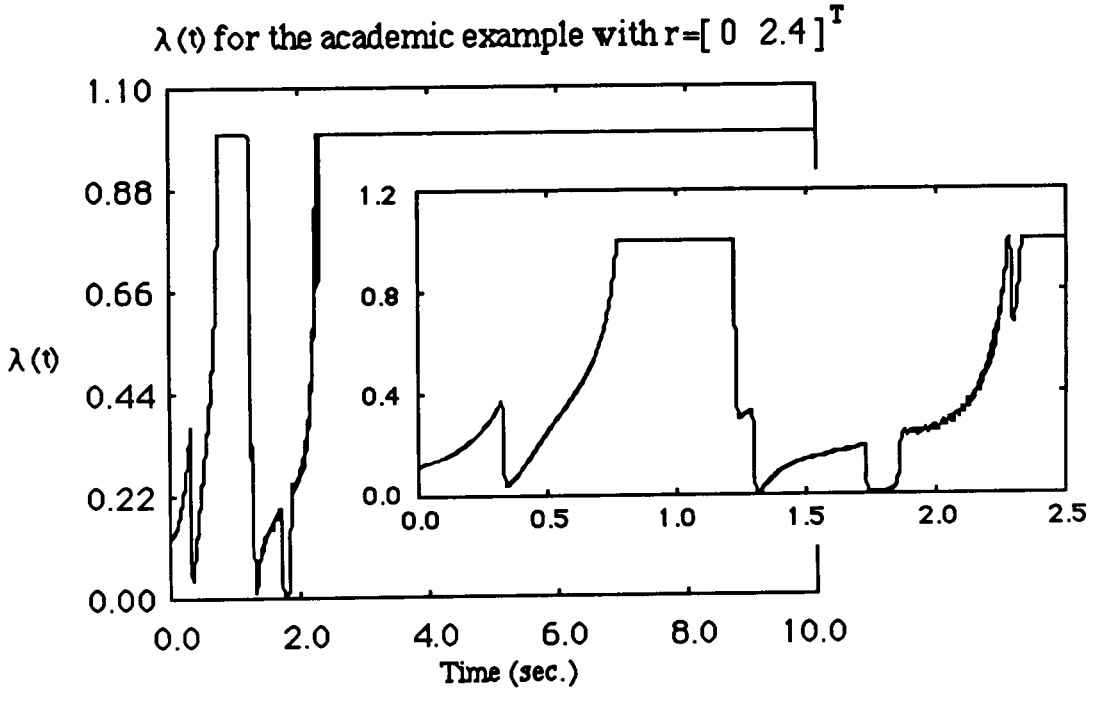

Figure 7.28: $\lambda(t)$ of the system with magnitude/rate saturation and the EG, ($\mathbf{r} = [\,0 \quad 2.5\,]^T$).

7.3.4 Control Structure with RG for Plants with Rate and Position Saturation

The problem here is to keep the control magnitude and rate bounded. The idea is to modify the references $\mathbf{r}(t)$ to $\mathbf{r}_\mu(t)$ only when the references are large enough and the controls $\mathbf{u}(t)$ will saturate either in magnitude or rate. The modification has to be in such a way that any current or future references will never cause the system to saturate. The operator RG has to be introduced and it is defined in the following

$$\dot{\mathbf{z}}(t) = \mu(t)\mathbf{e}_r(t) \tag{7.51}$$

$$\mathbf{e}_r(t) = \mathbf{r}(t) - \mathbf{r}_\mu(t) \tag{7.52}$$

$$\mathbf{r}_\mu(t) = \mathbf{z}(t) \tag{7.53}$$

In chapter 5 it was described how one can introduce the operator RG such that the magnitude of the controls remain bounded. That was done by defining a function $g(\mathbf{x})$ and a set $\mathbf{B}_{A,C}$ and by constructing a time varying rate, call it $\mu_1(t)$, such that the states of the compensator remained in the $\mathbf{B}_{A,C}$ set for any reference.

In section 7.2.3 it was described how one can introduce the operator RG such that the rate of the controls remain bounded when the open loop plant is unstable. That was done by defining a function $g'(\mathbf{x})$ and a set $\mathbf{R}_{A,C}$ and by constructing a time varying rate, call it $\mu_2(t)$, such that the states of the compensator remained in the $\mathbf{R}_{A,C}$ set for any reference.

Since the problem here is to keep both the magnitude and rate bounded, one can choose $\mu(t)$ in eq. (7.52) as the minimum of $\mu_1(t)$ and $\mu_2(t)$ and that will prevent the controls of saturating both in magnitude and rate. Doing that one has to compute at every time t_0 both $\mu_1(t)$ and $\mu_2(t)$, in addition to the fact that both $\mathbf{B}_{A,C}$ and $\mathbf{R}_{A,C}$ has to be stored during the operation of the system.

Another way of computing $\mu(t)$ is to define another set $\mathbf{S}_{A,C}$

$$\mathbf{S}_{A,C} = \mathbf{B}_{A,C} \cap \mathbf{R}_{A,C} \tag{7.54}$$

Then one can use the $\mathbf{S}_{A,C}$ set in the construction of $\mu(t)$ in section 5.2.2. Because the $\mathbf{R}_{A,C}$ is the intersection of both $\mathbf{R}_{A,C}$ and $\mathbf{R}_{A,C}$ the compensator and plant states will remain in both $\mathbf{R}_{A,C}$ and $\mathbf{R}_{A,C}$, for all t.

7.4 Limits on State Variables

In many cases it is desired that a subset of states of the plant remain bounded, ie. limited in magnitude, perhaps for safety reasons. In this section the EG and RG operators will be used to insure that under any reference and disturbance or class of disturbances certain states of the plant remain bounded.

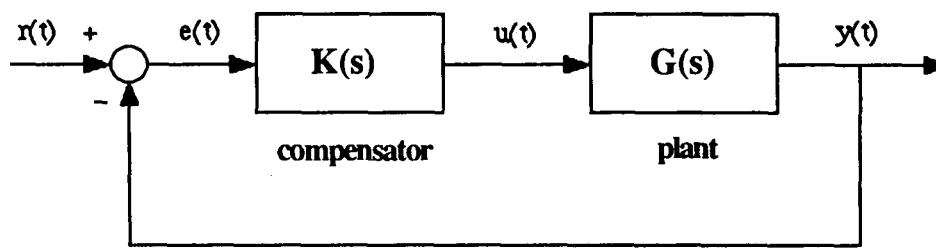

Figure 7.29: The linear closed loop system

Figure 7.29 shows the closed loop system with the plant and a linear compensator. The plant model and the compensator model are given by:

Plant: $$\dot{\mathbf{x}}(t) = \mathbf{A}\mathbf{x}(t) + \mathbf{B}\mathbf{u}(t) \tag{7.55}$$

$$\mathbf{y}(t) = \mathbf{C}\mathbf{x}(t) \tag{7.56}$$

Compensator:

$$\dot{\mathbf{x}}_c(t) = \mathbf{A}_c\mathbf{x}_c(t) + \mathbf{B}_c\mathbf{e}(t) \tag{7.57}$$

$$\mathbf{u}(t) = \mathbf{C}_c\mathbf{x}_c(t) \tag{7.58}$$

$$\mathbf{e}(t) = \mathbf{r}(t) - \mathbf{y}(t) \tag{7.59}$$

where $\mathbf{r}(t)$ is the reference and $\mathbf{y}(t)$ is the output vector.

Also assume that the state space representation of the loop transfer function $\mathbf{G}(s)\mathbf{K}(s)$ is given by

$$\dot{\mathbf{x}}_l(t) = \mathbf{A}_l\mathbf{x}_l(t) + \mathbf{B}_l\mathbf{e}(t) \tag{7.60}$$

$$\mathbf{y}(t) = \mathbf{C}_l\mathbf{x}_l(t) \tag{7.61}$$

where

$$\mathbf{x}_l(t) = \begin{bmatrix} \mathbf{x}_c(t) \\ \mathbf{x}(t) \end{bmatrix} \quad \mathbf{A}_l = \begin{bmatrix} \mathbf{A}_c & \mathbf{0} \\ \mathbf{B}\mathbf{C}_c & \mathbf{A} \end{bmatrix} \quad \mathbf{B}_l = \begin{bmatrix} \mathbf{B}_c \\ \mathbf{0} \end{bmatrix} \quad \mathbf{C}_l = \begin{bmatrix} \mathbf{0} & \mathbf{C} \end{bmatrix}$$

Let $\mathbf{x}_b(t)$ denote the vector of states that should remain bounded, and assume that the limits for the states are ± 1 ($\|\mathbf{x}_b(t)\|_\infty \leq 1$). Typically, $\mathbf{x}_b(t)$ will be a subset of the entire plant state vector $\mathbf{x}(t)$.

$$\mathbf{x}(t) = \begin{bmatrix} \mathbf{x}_b(t) \\ \mathbf{x}_r(t) \end{bmatrix} \tag{7.62}$$

The objective now is by introducing the EG and RG operators to prevent the $\mathbf{x_b}(t)$ states of exceeding their limits. In sections 7.4.1 and 7.4.2 two control structures with the EG and RG operators will be given (similar to the ones for the control rate and control magnitude saturations). Table 7.2 shows potential applications for these two structures.

Table 7.2: Applications of the control structures with RG and EG operators for plants with state limiters

Neutrally stable G(s)K(s)	**Unstable G(s)K(s)**
Control structure with EG Control structure with RG Control structure with EG and RG	Control structure with RG

7.4.1 Control Structure with EG for Plants with Limits on the State Variables

A time varying gain $\lambda(t)$ will be introduced at the error signal $\mathbf{e}(t)$ so that the states $\mathbf{x_b}(t)$ of the plant will never exceed their limits. Consider the state space representation of the loop transfer function and define as an output the state variables that have to remain bounded $\mathbf{x_b}(t)$.

$$\dot{\mathbf{x}}_l(t) = \mathbf{A}_l\mathbf{x}_l(t) + \mathbf{B}_l\lambda(t)\mathbf{e}(t) \quad (7.63)$$

$$\mathbf{x_b}(t) = \mathbf{C_b}\mathbf{x}_l(t) \quad (7.64)$$

where

$$\mathbf{x}_I(t) = \begin{bmatrix} \mathbf{x}_c(t) \\ \mathbf{x}_b(t) \\ \mathbf{x}_r(t) \end{bmatrix} \qquad \mathbf{C}_b = \begin{bmatrix} \mathbf{0} & \mathbf{I} & \mathbf{0} \end{bmatrix}$$

One should consider the system given in eqs. (7.63)-(7.64) as linear system with $\lambda(t)e(t)$ as its input, $\mathbf{x}_b(t)$ as its states and $\mathbf{x}_b(t)$ as its output. Then the goal is to choose the time-varying gain $\lambda(t)$ so that the output of the linear system $\mathbf{x}_b(t)$ remain bounded. By following the discussion in section 3.3 one can construct $\lambda(t)$ to achieve our objective. A function $g(\mathbf{x})$ and a set $\mathbf{B}_{A,C}$ have to be defined

$$g(\mathbf{x}_0): \; g(\mathbf{x}_0) = \|\mathbf{x}_b(\mathbf{x}_0,t)\|_\infty \tag{7.65}$$

where $$\dot{\mathbf{x}}_I(t) = \mathbf{A}_I\mathbf{x}_I(t); \qquad \mathbf{x}_I(0) = \mathbf{x}_0 \tag{7.66}$$

$$\mathbf{x}_b(\mathbf{x}_0,t) = \mathbf{C}_b\mathbf{x}_I(t) \tag{7.67}$$

$$\mathbf{B}_{A,C} = \{ \mathbf{x}: \; g(\mathbf{x}) \leq 1 \} \tag{7.68}$$

For the function $g(\mathbf{x})$ to be finite the loop transfer function $\mathbf{G}(s)\mathbf{K}(s)$ has to be neutrally stable. That is why the Error Governor is to be used only for neutrally stable loop transfer functions as shown in table 7.1. As in section 3.3 the construction of $\lambda(t)$ is given by

Construction of $\lambda(t)$:

For every time t choose $\lambda(t)$ as follows

a) if $\mathbf{x}_l(t) \in \mathrm{Int}\mathbf{B}_{A,C}$ then $\lambda(t) = 1$ (7.69)

b) if $\mathbf{x}_l(t) \in \mathrm{Bd}\mathbf{B}_{A,C}$ then choose the largest $\lambda(t)$ such that (7.70)

$$0 \le \lambda(t) \le 1 \tag{7.71}$$

$$\limsup_{\varepsilon \to 0} \frac{g(\mathbf{x}_l(t) + \varepsilon[\mathbf{A}_l\mathbf{x}_l(t) + \mathbf{B}_l\lambda(t)\mathbf{e}(t)]) - g(\mathbf{x}_l(t))}{\varepsilon} \le 0 \tag{7.72}$$

or for the points where $g(\mathbf{x}_l)$ is differentiable choose the largest $\lambda(t)$ such that

$$0 \le \lambda(t) \le 1 \tag{7.73}$$

$$Dg(\mathbf{x}_l(t))[\mathbf{A}_l\mathbf{x}_l(t)+\mathbf{B}_l\lambda(t)\mathbf{e}(t)] \le 0 \quad \forall t>0 \tag{7.74}$$

c) if $\mathbf{x}_l(t) \notin \mathbf{R}_{A,C}$ then choose $\lambda(t)$, $0 \le \lambda(t) \le 1$ such that the expression in (7.72) is minimum.

With the operator EG in the loop one can guarantee that the states $\mathbf{x}_b(t)$ will never violate their predefined limits. The properties and the implementation of the control system are similar to the ones for control structure described in chapter 4 (sections 4.2.1 and 4.2.2). The operator EG can be used to ensure that certain outputs of the system ($\mathbf{C}'\mathbf{x}_l(t)$) are bounded (limits on overshoots). This can be done by replacing $\mathbf{C}_b$ in eq. 7.64 and replace it with $\mathbf{C}'$ and the rest of the procedure remains the same.

It is common that in addition to the limits on the state variables, magnitude and/or rate saturations are present. The construction of the EG operator in this case follows from section 7.3.1. One can design a $\lambda_1(t)$ to handle the magnitude saturation, a $\lambda_2(t)$ to handle the rate saturation, and a $\lambda_3(t)$ to handle the limits on the states. Then the operator EG $\lambda(t) = \min(\lambda_1(t),\lambda_2(t),\lambda_3(t))$.

7.4.2 Control Structure with RG for Plants with Limits on the State Variables

A time varying rate $\mu(t)$ will be introduced at the reference signal $\mathbf{r}(t)$ so that the $\mathbf{x_b}(t)$ states will not exceed their limits as shown in figure 7.30. The RG operator is constructed in a way similar to the one given in chapters 3 and 5. Figure 7.30 shows the control structure with the RG operator.

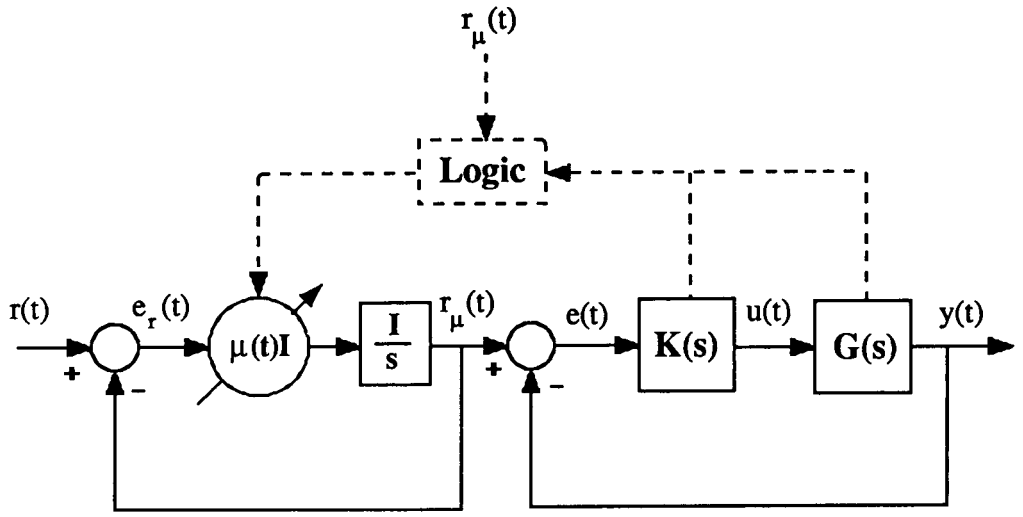

Figure 7.30: Control structure with the RG operator for plants with state limiters.

The plant and the compensator dynamics in figure 7.30 are described in eqs. (7.55)-(7.59). Assuming that the states of the integrators in the time varying rate are $\mathbf{z}(t)$ then the time varying rate at the references can be described by the following

$$\dot{\mathbf{z}}(t) = \mu(t)\mathbf{e_r}(t) \tag{7.75}$$

$$\mathbf{e_r}(t) = \mathbf{r}(t) - \mathbf{r}_\mu(t) \tag{7.76}$$

$$r_\mu(t) = z(t) \tag{7.77}$$

Following the discussion in chapter 5, consider the linear closed loop system and assume the following state space representation

$$\dot{x}_l(t) = (A_l - B_l C_l)\, x_l(t) + B_l r_\mu(t) \tag{7.78}$$

$$x_b(t) = C_b x_l(t) \tag{7.79}$$

where $x_l(t)$, A_l, B_l, C_b are the defined in eqs. (7.60), (7.61), and (7.64)

Then one can combine the dynamics of the rate limiter (7.75)-(7.77) with the dynamics of the closed loop system (7.78)-(7.79) to obtain the following augmented system

$$\dot{x}_a(t) = A_a x_a(t) + B_a \mu(t) e_r(t) \tag{7.80}$$

$$\dot{u}(t) = C_a x_a(t) \tag{7.81}$$

where

$$x_a(t) = \begin{bmatrix} z(t) \\ x_l(t) \end{bmatrix} \qquad A_a = \begin{bmatrix} 0 & 0 \\ B_l & A_l \end{bmatrix} \qquad B_a = \begin{bmatrix} I \\ 0 \end{bmatrix} \qquad C_a = \begin{bmatrix} 0 & C_b \end{bmatrix}$$

To construct $\mu(t)$ one has to define a function $g(x)$ and a set $B_{A,C}$ as follows

$$g(x_{a0}): \quad g(x_{a0}) = \|x_b(t)\|_\infty \tag{7.82}$$

where $$\dot{x}_a(t) = A_a x_a(t); \qquad x_a(0) = x_{a0} \tag{7.83}$$

$$\mathbf{x}_b(t) = \mathbf{C}_a\mathbf{x}_a(t) \tag{7.84}$$

$$\mathbf{B}_{A,C} = \{\ \mathbf{x}:\ g(\mathbf{x}) \le 1\ \} \tag{7.85}$$

For the function g(x) to be finite the augmented system has to be neutrally stable. As discussed in section 5.2 this is always true even if the plant is unstable.

Construction of $\mu(t)$:

For every time t choose $\mu(t)$ as follows

a) if $\mathbf{x}_a(t) \in \mathrm{Int}\mathbf{B}_{A,C}$ then $\mu(t) = \infty$ which implies that $\mathbf{r}(t) = \mathbf{r}_\mu(t)$ (7.86)

b) if $\mathbf{x}_a(t) \in \mathrm{Bd}\mathbf{B}_{A,C}$ then choose the largest $\mu(t)$ such that (7.87)

$$0 \le \mu(t) \le \infty$$

$$\lim_{\varepsilon \to 0} \sup \frac{g\left(\mathbf{x}_a(t)+\varepsilon[\mathbf{A}_a\mathbf{x}_a(t)+\mathbf{B}_a\mu(t)\mathbf{e}_r(t)]\right) - g\left(\mathbf{x}_a(t)\right)}{\varepsilon} \le 0 \tag{7.88}$$

or for the points where g(x) is differentiable choose the largest $\mu(t)$ such that

$$0 \le \mu(t) \le \infty \tag{7.89}$$

$$Dg(\mathbf{x}_a(t))[\mathbf{A}_a\mathbf{x}_a(t)+\mathbf{B}_a\mu(t)\mathbf{e}_r(t)] \le 0 \quad \forall\ t > 0 \tag{7.90}$$

where $Dg(\mathbf{x}_a(t))$ is the Jacobian matrix of $g(\mathbf{x}_a(t))$ as in definition 3.2.

c) if $\mathbf{x}_a(t) \notin \mathbf{R}_{A,C}$ then choose $\mu(t)$, $0 \le \mu(t) \le \infty$ such that the expression (7.88) is minimum.

The implementation of this control structure is similar to the one given for the control structure with the operator RG. The states $\mathbf{x}_b(t)$ do not exceed their limits for any reference r(t). The stability analysis and the analysis of the disturbance rejection for the control system

described above are analogous to the ones given in section 5.2.1. It easy to see how one could combine the operators EG and RG to obtain a control structure similar to the one described in section 5.3.1. In this case of course the objective would be to prevent the $\mathbf{x_b}(t)$ states from violating their limits.

7.5 Concluding Remarks

In this chapter it has been shown that the operators EG and RG can be used to design control systems when the controls saturate in magnitude and/or rate and when it is desired to keep certain states of the plant bounded. The techniques used to design the control system are similar to the ones used when only magnitude saturation is present.

Also it has been shown how to design control systems when combinations of rate and magnitude saturation are present. In a similar manner one can design control systems when in addition to magnitude and rate saturations certain states of the plant are not to exceed specific limits.

With operators EG and RG if integrators are present in the control system the integrators never windup. Also the nonlinear response is similar, to the extent possible, to the linear one. The simulations in this chapter verify the expected behavior of the control system.

CHAPTER 8
CONCLUSIONS AND SUGGESTIONS FOR FUTURE RESEARCH

8.1 Conclusion

Saturations exist in almost every physical system. In this thesis, the effects of multiple saturations present in a closed loop control system were studied extensively. The multiple saturations can include limits on the control magnitudes, limits on the control rate and/or limits on certain states of the plant.

In the presence of saturations the stability and performance of a linear control system can suffer. For example, a linear control system that is closed loop stable can become unstable when saturations are present for certain references and disturbances. Saturations can also affect the performance of the control system by introducing reset windups and by changing the direction of the control signal. Large overshoots and oscillatory outputs are the consequence.

The control literature reflects that a significant amount of effort has gone into finding solutions for the reset windup problem in SISO systems. This has resulted in many heuristic reset antiwindup strategies which have proved successful when used in SISO systems. Of course, problems due to saturations are amplified in the MIMO case. However, there has been no systematic method for designing MIMO control systems in the presence of multiple saturations.

In this thesis a new systematic control design methodology has been introduced for systems with multiple saturations. The methodology can be applied to stable and unstable open loop plants with magnitude and/or rate control saturations and to systems in which state limits are desired. The study was done in two parts, the analysis part and the design part.

In the analysis part, a new stability result was derived which allows the designer to

specify the sizes of the exogenous disturbances and/or references so that the closed loop system remains stable. In the analysis part it was also discussed how saturations can affect negatively the performance of the nonlinear system and new performance criteria were introduced for judging the quality of these designs.

In the design part, a systematic methodology was introduced for the design of control systems with multiple saturations. The idea was to introduce a supervisor loop; and when the references and/or disturbances are "small" enough so as not to cause saturations, the system operates linearly as designed. When the signals are large enough to cause saturations, then the control law is modified in such a way to preserve, to the extent possible, the behavior of the linear control design.

The main benefits of the methodology are that it leads to controllers with the following properties:

(a) The signals that the modified compensator produces never cause saturation.

(b) Possible integrators or slow dynamics in the compensator never windup.

(c) The closed loop system has inherent stability properties.

(d) The on-line computation required to implement the control system is feasible.

The main disadvantage of the methodology is the off-line computational requirements for high dimensional systems.

These properties were demonstrated in numerous simulations which included models of the F8 aircraft (stable), the F16 aircraft (unstable) and an academic example. In addition, the methodology was contrasted against extensions of SISO reset antiwindup strategies to MIMO systems. The advantages of the new design methodology were clearly demonstrated.

8.2 Future Research Directions

The extensions of this research lie primarily in the areas of implementation and applications

of the new design methodology.

At first, the new design methodology should be applied to a few realistic examples to access the benefits and the drawbacks of the resulting controllers. Applications of systems with multiple saturations include: aerospace systems, undersea vehicles, nuclear reactors, process control systems etc. For example in the case of nuclear reactors, the absolute necessity of keeping the states of the reactor bounded makes the use of the new design methodology appealing.

For control systems with compensators that have large number of states, the calculation of the function $g(\mathbf{x})$ (chapter 3) can be computationaly demanding. More research is needed to define new and more efficient ways of computing and approximating the function $g(\mathbf{x})$. In addition, the effects of an approximate $g(\mathbf{x})$ on the performance of the control system has to be further examined.

For open loop unstable plants the new control design methodology requires the measurement of the states of the plant. It may be possible to estimate these states, and use these estimates for computing $\mu(t)$, instead of the real state measurement. A new study is needed to determine the effects of the state estimator on the computation of $\mu(t)$, and the effects of this approximation on the performance of the control system. In addition, more research is needed to determine precisely the effects of unmodelled dynamics and/or modelling errors on the computation and performance of the Reference Governor (RG).

Finally, the use of the Error Governor and the Reference Governor can be expanded to shape the response of a control system. For example, one could use the EG and/or RG to modify and shape the overshoot of a control system. Further research in this area will determine all such potential uses of the EG and RG operators.

REFERENCES

[1] M. Athans, "6.233-6.234 Class Notes", M.I.T., Fall 1986-Spring 1987, Cambridge, MA.

[2] J.C. Doyle and G. Stein, " Multivariable Feedback Design: Concepts for a Classical/Modern Synthesis", IEEE Transactions on Automatic Control, Vol. AC-26, No. 1, February 1981, pp. 4-16.

[3] G. Stein and M. Athans,"The LQG/LTR Procedure for Multivariable Feedback Control Design", IEEE Transactions on Automatic Control, Vol. AC-32, No. 2, February 1987, pp. 105-114.

[4] H. Kwakernaak and R. Sivan, " The Maximally Achievable Accuracy of Linear Optimal Regulators and Linear Optimal Filters", IEEE Transactions on Automatic Control, Vol. AC-17, No. 1, February 1972, pp. 79-86.

[5] H. Kwakernaak and R. Sivan, *Linear Optimal Control Systems*, New York, Wiley-Interscience, 1972.

[6] B.A. Francis, *A Course in H_∞ Control Theory*, Lecture Notes in Control and Information Sciences, Springer-Verlag, Berlin, 1987.

[7] J.A. Mette, "Multivariable Control of a Submarine Using the LQG/LTR Method", S.M. Thesis, M.I.T., Cambridge, MA, 1985.

[8] A.A. Rodriguez and M. Athans, " Multivariable Control of a Twin Lift Helicopter System Using the LQG/LTR Design Methodology", Proceedings of the American Control Conference, Seattle, WA, 1986, pp. 1325-1332.

[9] G.D. Hanson and R.F. Stengel, "Effects of Displacement and Rate Saturation on the Control of Statically Unstable Aircraft", AIAA Journal of Guidance, Control and Dynamics, Vol.7, No 2, March-April 1984, pp. 197-205.

[10] P.C. Shivastava, "Stability Regions of Relaxed Static Stability Aircraft under Control Saturation Constraints", Ph.D. Thesis, Princeton University, Dept. of Mechanical and Aerospace Engineering, MAE-1747-T, 1986.

[11] G. Zames," On the Input-Output Stability of Time-Varying Nonlinear Feedback Systems. Part-I: Conditions Derived Using Concepts of Loop Gain, Conicity, and Positivity ", IEEE Transactions on Automatic Control, Vol. AC-11, No. 2, April 1966, pp. 228-238.

[12] G. Zames, " On the Input-Output Stability of Time-Varying Nonlinear Feedback Systems. Part-II: Conditions Involving Circles in the Frequency Plane and Sector Nonlinearities", IEEE Transactions on Automatic Control, Vol. AC-11, No. 3, July 1966, pp. 465-476.

[13] J.C.Willems , *The Analysis of Feedback Systems*, The M.I.T. Press, Cambridge MA, 1971.

[14] M. Vidyasagar, *Nonlinear System Analysis*, Prentice-Hall, New Jersey, 1978.

[15] M. G. Safonov and M. Athans," A Multiloop Generalization on the Circle Stability Criterion for Stability",IEEE Transactions on Automatic Control,Vol. AC-26,No. 2, April 1981, pp. 415-422.

[16] K. S. Narendra, " Stability of nonlinear systems", Nonlinear Systems Analysis, Vol. 1, Fundamental Principles, The American Society of Mechanical Engineers, New York, 1978.

[17] N. Rouche, P. Habets and M Laloy, *Stability Theory by Lyapunov's Direct Method*, New York, Springer-Verlag, 1977.

[18] M. Athans, P.L. Falb, *Optimal Control*, New York, McGraw-Hill, 1966.

[19] C.A. Harvey, " On Feedback Systems Possessing Integrity With Respect to Actuators Outages", Proceedings of the ONR/MIT Workshop on Resent Developments in the Robustness Theory of Multivariable Systems, LIDS-R-954, M.I.T., Cambridge, MA, April 25-27, 1979.

[20] P. Molander and J.C. Willems, " Robustness Results For State Feedback Regulators", Proceedings of the ONR/MIT Workshop on Resent Developments in the Robustness Theory of Multivariable Systems, LIDS-R-954, M.I.T., Cambridge, MA, April 25-27, 1979.

[21] A. Weinreb and A.E. Bryson," Optimal Control of Systems with Hard Control Bounds" IEEE Transactions on Automatic Control, Vol. AC-30, No. 11, November 1985, pp. 1135-1138.

[22] S.M. Joshi, "Stability of Multiloop LQ Requlators with Nonlinearities: II-Regions of Ultimate Boundedness", IEEE Transactions on Automatic Control, Vol. AC-31, No. 4, April 1986, pp. 367-370.

[23] I. Horowitz, "Feedback Systems with Rate and Amplitude Limiting", Int. J. Control, Vol. 40, No. 6, 1984, pp. 1215-1229.

[24] H.W. Thomas, D.J. Sandoz and M. Thomson, " New desaturation strategy for digital PID controlers", IEE Proceedings, Vol. 130, Pt. D, No. 4, July 1983, pp.113.

[25] P. Gutman and P. Hagander, " A New Design of Constrained Controllers for Linear Systems", IEEE Transactions on Automatic Control, Vol. AC-30, No. 1, January 1985, pp. 22-33.

[26] A. H. Glattfelder and W. Scaufelberger," Stability Analysis Of Single Loop Control Systems with Saturation and Antireset-Windup Circuits", IEEE Transactions on Automatic Control, Vol. AC-28, No. 12, December 1983, pp. 1074-1081.

[27] R. Hanus, " A New Technique for Preventing Windup Nuisances", Proc. IFIP Conf. on Auto. for Safety in Shipping and Offshore Petrol. Operations, 1980, pp. 221-224.

[28] N.J. Krikelis, "State Feedback Integral Control with 'Intelligent' Integrators", Int. J. Control, Vol. 32, No. 3, 1980, pp. 465-473.

[29] P. Kapasouris and M. Athans, " Multivariable Control Systems with Saturating Actuators Antireset Windup Strategies", Proceedings of the American Control Conference, Boston, MA, 1985, pp. 1579-1584.

[30] J.C. Doyle, R.S. Smith and D.F. Enns, " Control of Plants with Input Saturation Nonlinearities", Proceedings of the American Control Conference, Minneapolis, MN, 1987, pp. 1034-1039.

[31] M.G. Safonov, "Robustness and Stability Aspects of Stochastic Multivariable Feedback System Design", Ph.D. Thesis, ESL-R-763, M.I.T., Cambridge, MA, 1977.

[32] D.B. Grunberg, "A Methodology for Designing Robust Multivariable Nonlinear Control Systems", Ph.D. Thesis, LIDS-TH-1609, M.I.T., Cambridge, MA, 1986.

[33] *Nonlinear Systems Analysis and Synthesis: Volume 2- Techniques and Applications*, The American Society of Mechanical Engineers, New York, 1980.

[34] J.E. Gibson, *Nonlinear Automatic Control*, McGraw-Hill, New York, 1963.

[35] C.A. Desoer and M. Vidyasagar, *Feedback Systems: Input-Output Properties* , New York, Academic, 1985.

[36] C.T. Chen, *Introduction to Linear Systems Theory*, Holt, Rinehart and Winston, Inc., New York, 1970.

[37] M.W. Hirsch and S. Smale, *Differential Equations, Dynamical Systems, and Linear Algebra*, New York, Academic Press, 1974.

[38] R.R. Goldberg, *Methods of Real Analysis*, New York, John Wiley & Sons, 1976.

[39] H.L. Royden, *Real Analysis*, New York, MacMillan, 1968.

[40] W. Rudin, *Functional Analysis*, New York, McGraw-Hill, 1973.

[41] C. DeBoor, *A Practical Guide to Splines*, New York, Springer - Verlag, 1980.

[42] G.G. Lorentz, C.K. Chui, L.L. Schumaker, *Approximation Theory III*, Academic Press Inc., New York, 1976.

[43] D. Brett Ridgely, "Use of Entire Eigenstructure Assignment with High-Gain Error-Actuated Flight Control Systems", S.M. Thesis, AFIT/GAE/AA81D-24, Air Force Institute of Technology, Wright-Patterson Air Force Base, Ohio, December 1981.